Water, carbon, and nutrient cycles in terrestrial groundwater-dependent ecosystems of drylands:

Ziziphus lotus' shrublands as case study

María Trinidad Torres García

PhD Thesis — March 2022

UNIVERSIDAD DE ALMERÍA

Water, carbon, and nutrient cycles in terrestrial groundwater-dependent ecosystems of drylands: *Ziziphus lotus'* shrublands as case study

Los ciclos del agua, el carbono y los nutrientes en ecosistemas terrestres dependientes de agua subterránea de zonas áridas: los matorrales de *Ziziphus lotus* como caso de estudio

Memoria presentada por
María Trinidad Torres García
para optar al Grado de Doctor en Ciencias Aplicadas al Medio Ambiente por la
Universidad de Almería

Esta tesis ha sido dirigida por Javier Cabello Piñar, Profesor Titular del Departamento de Biología y Geología de la Universidad de Almería y director del Centro Andaluz para la Evaluación y Seguimiento del Cambio Global (CAESCG) y por María Jacoba Salinas Bonillo, Profesora Titular del Departamento Biología y Geología de la Universidad de Almería y secretaria del CAESCG

Vº Bº Director   Vº Bº Directora

Javier Cabello Piñar   Mª Jacoba Salinas Bonillo

Marzo 2022

A mis padres,

A Manu

El árbol es luz condensada,

agua erguida, tierra que aspira a volar.

Joaquin Araujo

Hay una linde en el silencio que rompe el azar.

Sí, el árbol al caer solo en el bosque tiene sonoridad.

Raul de Tapia

Herbario Sonoro

AGRADECIMIENTOS

juntos, con estos grandes amigos y compañeros, y nuestras familias, podremos con lo que se presente. Gracias a todos por esta emocionante etapa. Vamos a por la siguiente.

TABLE OF CONTENTS

LIST OF FIGURES

CHAPTER II. Squandering water in drylands: the water-use strategy of the phreatophyte Ziziphus lotus in a groundwater-dependent ecosystem

CHAPTER III. A multiple-trait analysis of ecohydrological acclimatisation in a dryland phreatophytic shrub

CHAPTER IV. Decoupled soil biological activity and vegetation dynamics in a groundwater-dependent ecosystem in drylands

4.   GENERAL DISCUSSION

LIST OF TABLES

3.   RESULTS

CHAPTER I. Modular growth and functional heterophylly of the phreatophyte Ziziphus lotus: A trait-based study

CHAPTER III. A multiple-trait analysis of ecohydrological acclimatisation in a dryland phreatophytic shrub

CHAPTER IV. Decoupled soil biological activity and vegetation dynamics in a groundwater-dependent ecosystem in drylands

ABBREVIATIONS, ACRONYMS, AND SYMBOLS

A	Photosynthetic rate	$\mu mol\ m^{-2}\ s^{-1}$
AIC	Akaike information criterion	
ANCOVA	Analysis of covariance	
ANOVA	Analysis of variance	
C	Carbon	
Ca	Atmospheric CO_2 concentration	
Ci	CO_2 concentration inside leaf air spaces	$\mu mol\ mol^{-1}$
C_{mic}	Microbial biomass carbon	$mg\ kg^{-1}\ soil$
C:N	Ratio Carbon:Nitrongen	
CO_2	Carbon dioxide	
CO_2 efflux	Carbon dioxide efflux from the soil	$\mu mol\ m^{-2}\ s^{-1}$
DTGW	Depth to groundwater	m
E	Transpiration rate	$mmol\ m^{-2}\ s^{-1}$
eC	Electrical conductivity (salinity)	$mS\ cm^{-1}$
GDE	Groundwater-dependent ecosystem	
g_s	stomatal conductance	$mol\ m^{-2}\ s^{-1}$
Hv	Huber value	
IRGA	Infrared gas analyzer	
LMM	Lineal mixed effect model	
N	Nitrogen	
NDVI	Normalized difference vegetation index	
NO_3^-	Nitrate ion	$mg\ kg^{-1}\ soil$
NO_2^-	Nitrite ion	$mg\ kg^{-1}\ soil$
N_{tot}	Total nitrogen	$g\ kg^{-1}\ soil$
P	Precipitation	mm
PAR	Photosynthetically active radiation	$\mu mol\ mol-1$
PO_4^{3-}	Phosphate ion	$mg\ kg-1\ soil$
REML	Restricted maximum likelihood	
Rs	Soil respiration	$\mu mol\ CO_2\ m^{-2}\ s^{-1}$
SEM	Scanning Electron Microscope	

SLA	Specific leaf area	$cm^2\ g^{-1}$
Soil Temp.	Soil temperature	℃
SO_4^{2-}	Sulfate ion	$mg\ kg^{-1}$ soil
SOM	Soil organic matter	%
SPI	Stomata pore index	
SWC	Soil water content	%
Tair	Air temperature	℃
T_{GW}	Groundwater temperature	℃
TOC	Total organic carbon	$g\ kg^{-1}$ soil
VPD	Vapor pressure deficit	kPa
WEOC	Water extractable organic carbon	$g\ kg^{-1}$ soil
WUEi	Intrinsic water-use-efficiency	$\mu mol\ CO_2\ mol^{-1}\ H_2O$
$\delta^2 H$	Stable hydrogen isotope (deuterium)	‰
$\delta^{18}O$	Stable oxygen isotope	‰
$\Delta^{13}C$	Leaf carbon isotope discrimination	‰
$\Delta\Psi_{max}$	Maximum range of daily leaf water potential	MPa
Ψ_{md}	Midday water pontential	MPa
Ψ_{pd}	Predawn water pontential	MPa

ABSTRACT

Terrestrial groundwater-dependent ecosystems (GDEs) rely on groundwater to maintain their structure, composition, and functions. In drylands, where water is the most limiting ecological factor, such ecosystems have a unique role for biodiversity and human well-being, given they use an inaccessible source of water for most plants. Climate change, groundwater depletion and pollution, and land-use changes might be reducing water availability for these ecosystems, jeopardizing their ability to provide ecosystem functions and services. Understanding the ecological processes underlying plant water use, carbon and nutrient uptake, and soil-plant interactions in these ecosystems is critical for sustainable groundwater management, biodiversity conservation, and climate change adaptation in drylands.

The primary goal of this thesis is to investigate the functioning of a terrestrial GDE from Mediterranean arid regions and its phreatophytic vegetation to: (1) understand its contribution to the water, carbon, and nutrient cycles, and (2) provide scientific evidence to managers and policymakers policymakers who must deal with the sustainable management of groundwater and ensure GDEs' contributions to people in the face of global change. To do this, I focused on *Ziziphus lotus* (L.) Lam. (Rhamnaceae), a long-lived, winter deciduous, and deep-rooted phreatophyte that significantly modifies the arid landscape conditions, creating a GDE considered as a priority habitat for conservation in Europe. The general hypothesis is that spatiotemporal variations in groundwater availability and climate variability can alter the functioning of this GDE. I used the coastal plain of the Cabo de Gata-Níjar Natural Park (Spain) as a study area since it provides a spatial gradient in the depth-to-groundwater (DTGW) to test this hypothesis. I developed four studies that address spatiotemporal variations in processes related to water, carbon, and nutrient cycles at different structural levels, from leaves and individuals to vegetation patches.

Chapter I focused on plant morpho-functional and physiological traits to identify growth patterns at the individual level and temporal variations throughout the growing season. I described *Z. lotus'* growth pattern as the repetition of modular units composed by shoots (short and long) and branches (flowering and plagiotropic) with differentiated

functions. Related to the branches, I identified morpho-functionally distinct leaves (i.e., heterophylly) with different water-use patterns. Both modular growth and heterophylly might contribute to prioritizing resource investment in particular functions over time, either for reproduction (in spring when plants might obtain water and nutrients from the topsoil layer) or growth (throughout the growing season).

The focus of **Chapter II** was to assess two main aspects related to the water-use strategy of *Z. lotus*: the source of water and its transport regulation through the plant. I used stable isotopes (δ^2H, δ^{18}O, and Δ^{13}C), stem water potentials, leaf gas-exchange measurements, and leaf nutrient concentrations to uncover the partial groundwater dependency and anisohydric stomatal regulation of *Z. lotus* across the spatial DTGW gradient. Nevertheless, as DTGW increased, I found that *Z. lotus* (1) decreased groundwater use and (2) reduced water loss through transpiration while increasing water-use efficiency (i.e., less extreme anisohydric behaviour). I also detected a physiological threshold at 13 − 14 m, indicating the maximum groundwater depth for better functioning.

Chapter III introduced the temporal variability defined by seasonal climatic conditions (e.g., the atmospheric evaporative demand) to identify plant ecophysiological thresholds with a trait-based analysis. I found that some traits were more affected by high DTGW and groundwater salinity (e.g., low photosynthetic rate and stomatal conductance, and high Huber value [ratio between sapwood cross-sectional area to leaf area]). In contrast, other traits were more related to seasonal variations in atmospheric conditions (e.g., high transpiration and more negative predawn and midday water potential in summer). This study confirmed spatial ecophysiological thresholds (Chapter II) that depend on groundwater characteristics (i.e., difficulties to obtain groundwater at high depths [> 14 m] and salinity levels). Additionally, the analysis identified new temporal thresholds related to atmospheric evaporative demand that indicated significantly lower vapor pressure deficit and water stress in spring than in summer.

In **Chapter IV**, I considered the heterogeneous spatial distribution of vegetation in drylands to study soil-plants interactions. I assessed the spatiotemporal coupling between vegetation functioning and soil biological activity and its relationship with soil quality (soil properties and nutrient availability), mineralization rates, and water availability in patches

of *Z. lotus*. I found that soil and vegetation showed a decoupled activity. Whereas soil respiration and mineralization processes promptly responded to rainfall pulses, vegetation activity was overall decoupled from precipitation. The presence of phreatophytes enhanced soil quality and soil biological activity, thereby promoting fertile islands in drylands.

In general, the GDE dominated by *Z. lotus* contributes to enhancing the primary productivity of drylands through its phreatophytic nature, which increases transpiration, carbon assimilation, soil activity, and mineralization processes, fostering nutrient cycling. However, these processes and GDEs are threatened by groundwater overexploitation, climate change effects, and land use changes due to: (1) the dependence of phreatophytes on groundwater (DTGW threshold for better functioning up to 14 m); (2) the necessity of soil water (mostly from precipitation) for nutrient uptake, reproductive investment, and soil microbial activation; and (3) the importance of every single long-lived plant to maintain ecosystem functioning.

RESUMEN

Los ecosistemas terrestres dependientes de agua subterránea (por sus siglas en inglés GDEs) dependen de esta fuente de agua para mantener su estructura, composición y funcionamiento. En zonas áridas, donde el agua es el factor ecológico más limitante, estos ecosistemas tienen un papel fundamental para la biodiversidad y el bienestar humano debido a que utilizan una fuente de agua inaccesible para muchas plantas. El cambio climático, la disminución del agua subterránea y su contaminación, y los cambios de uso del suelo podrían estar reduciendo el agua disponible para los GDEs, amenazando su capacidad de proveer funciones y servicios ecosistémicos. Entender los procesos ecológicos subyacentes al uso del agua de las plantas, la obtención de carbono y nutrientes, y las interacciones suelo-planta en estos ecosistemas es esencial para la gestión sostenible del agua subterránea, la conservación de la biodiversidad y la adaptación al cambio climático en zonas áridas.

El objetivo principal de esta tesis es investigar el funcionamiento de un GDE terrestre de zonas áridas mediterráneas y a su vegetación freatófita para: (1) entender su contribución en los ciclos del agua, carbono y nutrientes y (2) proporcionar evidencia científica a gestores y legisladores que tienen que lidiar con la gestión sostenible del agua subterránea y asegurar las contribuciones de los GDE a la sociedad ante el cambio global. Para ello, me centré en el arbusto *Ziziphus lotus* (L.) Lam. (Rhamnaceae), un freatófito longevo, caducifolio, y con un sistema radicular profundo, que modifica de forma significativa las condiciones áridas del paisaje, creando un GDE considerado como hábitat prioritario de conservación en Europa. La hipótesis general es que las variaciones espaciotemporales en la disponibilidad de agua subterránea y la variabilidad climática pueden alterar el funcionamiento del GDE. La llanura costera del parque natural de Cabo de Gata-Níjar (España) ha sido una zona de estudi idónea para confirmar esta hipótesis ya que proporciona un gradiente espacial de profundidad al agua subterránea (DTGW). Desarrollé cuatro estudios que abordan variaciones espaciotemporales en procesos relacionados con los ciclos del agua, el carbono y los nutrientes a diferentes niveles estructurales, desde las hojas y los individuos, hasta los parches de vegetación.

El **Capítulo I** se centra en el estudio de características morfo-funcionales y fisiológicas de las plantas para identificar patrones de crecimiento a nivel individual y variaciones temporales a lo largo de la estación de crecimiento. Describí el patrón de crecimiento de *Z. lotus* como la repetición de unidades modulares compuestas de brotes (cortos y largos) y ramas (floríferas y plagiotrópicas) con diferentes funciones. En relación a las ramas, identifiqué hojas morfo-funcionalmente distintas (i.e., heterofilia) con diferentes patrones de uso del agua. Tanto el crecimiento modular como la heterofilia podrían contribuir a priorizar la inversión de recursos en funciones concretas en el tiempo, tanto para reproducción (en primavera cuando las plantas obtendrían el agua y los nutrientes de las capas superiores del suelo) o para crecimiento (a lo largo de la estación de crecimiento).

El objetivo del **Capítulo II** fue evaluar dos aspectos principales relacionados con la estrategia en el uso del agua de *Z. lotus*: la fuente de agua y la regulación de su transporte a través de la planta. Utilicé isótopos estables (δ^2H, δ^{18}O y Δ^{13}C), potenciales hídricos, medidas de intercambio gaseoso y concentraciones de nutrientes en las hojas para descubrir la dependencia parcial del agua subterránea y la regulación estomática anisohídrica de *Z. lotus* a través del gradiente de profundidad al agua subterránea. Sin embargo, con el aumento de la profundidad, encontré que *Z. lotus* (1) disminuyó la cantidad de agua subterránea obtenida y (2) redujo la pérdida de agua a través de la transpiración mientras que aumentaba su eficiencia (i.e., un comportamiento anisohídrico menos extremo). También detecté un umbral ecofisiológico a 13 – 14 m que indica la máxima profundidad de agua subterránea para un mejor funcionamiento.

El **Capítulo III** introdujo la variabilidad temporal definida por las condiciones climáticas estacionales (p. ej., la demanda evapotranspirativa de la atmósfera) con el objetivo de identificar umbrales ecofisiológicos através de un análisis basado en características de la planta. Encontré que algunas características estaban más afectadas por una mayor profundidad al agua subterránea y salinidad (p. ej., bajo ratio fotosintético y conductancia estomática, y alto Huber value [relación entre el área transversal de la albura y el área foliar]). Por el contrario, otras características estuvieron más relacionadas con las variaciones estacionales en las condiciones atmosféricas (p. ej., transpiración alta y potenciales hídricos antes del amanecer y a medio día más negativos en verano). Este estudio confirmó los umbrales espaciales ecofisiológicos (Capítulo II) que dependen de las

características del agua subterránea (i.e., las dificultades para obtener agua subterránea a elevada profundidad [> 14 m] y niveles de salinidad). Además, el análisis identificó nuevos umbrales temporales relacionados con la demanda evapotranspirativa de la atmósfera que indican de forma significativa un menor déficit de presión de vapor y estrés hídrico en primavera que en verano.

En el **Capítulo IV** consideré la distribución espacial heterogénea de la vegetación en zonas áridas para el estudio de las interacciones suelo-planta. Evalué el acoplamiento espaciotemporal entre el funcionamiento de la vegetación y la actividad biológica del suelo y su relación con la calidad del suelo (propiedades del suelo y disponibilidad de nutrientes), las tasas de mineralización y la disponibilidad de agua en los parches de *Z. lotus*. Descrubrí que el suelo y la vegetación tenían una actividad desacoplada. Mientras que la respiración del suelo y los procesos de mineralización responden rápidamente a los pulsos de lluvia, la actividad de la vegetación estaba desacoplada de la precipitación. La presencia de freatófitos mejoró la calidad del suelo y su actividad biológica, por lo tanto, fomentando las islas de fertilidad en zonas áridas.

En general, los GDE dominados por *Z. lotus* contribuyen a mejorar la productividad primaria de zonas áridas a través de su naturaleza freatófita, lo que aumenta la transpiración, la asimilación de carbono y los procesos de mineralización, promoviendo el ciclado de nutrientes. Sin embargo, estos procesos y los GDE están amenazados por la sobreexplotación de los acuiferos, los efectos del cambio climático y los cambios de uso del suelo debido a: (1) la dependencia de los freatófitos del agua subterránea (umbral de profundidad al agua subterránea para un buen funcionamiento hasta los 14 m en *Z. lotus*); (2) la necesidad de agua en el suelo (principalmente de la precipitación) para la obtención de nutrientes, la inversión en reproducción y la activación de la microbiota del suelo; y (3) la importancia de cada planta longeva para mantener el funcionamiento del ecosistema.
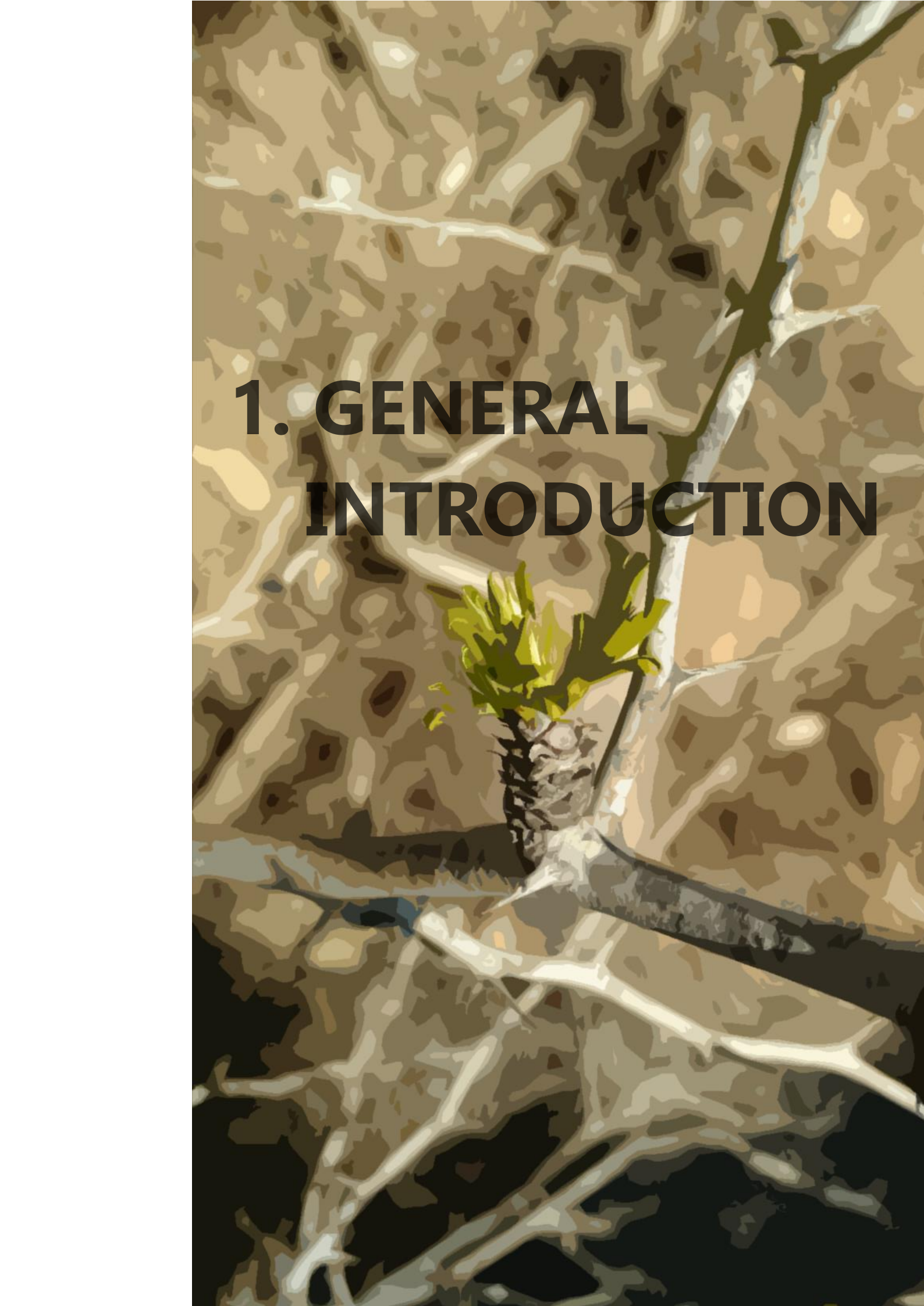
1. GENERAL INTRODUCTION

Water is the most limiting factor for global ecosystem productivity, and its availability is a major determinant of plant and biome distribution (Lambers and Oliveira, 2019). Whereas abundant and evenly distributed rainfall in the tropics promotes lush and dense forests, seasonal droughts, or reduced precipitation, drive the development of grasslands, savannas, or semi-deserts with scattered shrubs. Water availability is particularly a limiting factor in drylands – Iing hyper-arid, arid, semiarid, and dry-subhumid ecosystems – not only for its scarcity but also for its intermittence and unpredictability (D'Odorico et al., 2019). Water is also an essential resource for human life and for 38% of the total global population that inhabits these regions, covering about 41% of Earth's land surface (Reynolds et al., 2007). The climatic characteristics of drylands (lower annual precipitation than potential evapotranspiration) and the relatively low fertility of their soils limit the biota and control biogeochemical cycles (Newman et al., 2006; Maestre et al., 2012; Delgado-Baquerizo et al., 2013).

Biophysical and social characteristics make drylands highly vulnerable to global change effects, particularly, to climate change. Global drylands are expected to experience higher warming rates than more humid areas under ongoing climate change scenarios. In a scenario where global temperature increases by 2°C, drylands will suffer 3.2 – 4.0°C warming (44% more than humid areas) (Huang et al., 2017). Moreover, global warming will alter air circulation patterns globally, which will affect precipitation regime across scales, reducing rainfall amounts and promoting prolonged drought periods in many regions, as in the Mediterranean basin (Guiot and Cramer, 2016). Because of higher temperatures, precipitation regime shifts, and land-use changes, soil moisture is projected to decrease worldwide by the end of the 21st century by 5 – 15% (Dai, 2013). Coupled with the increasing demand for water for agriculture and human consumption in a more densely populated planet, dryland ecosystem integrity is severely threatened (Eamus et al., 2016).

1.1. Groundwater-dependent ecosystems in drylands

Groundwater is the largest global store of liquid freshwater, accounting for about 96% of all liquid freshwater on Earth (Shiklomanov, 1998). We can define groundwater reservoirs as the saturation zone of the regolith and its associated capillary fringe (Eamus et al., 2006). Although being hidden from view, as population's demand for water increases, the

exploitation of groundwater reserves also does, particularly in drylands (Eamus et al., 2006). In Spain, 25% of the aquifers (179 out of 729) are seriously overexploited, and the main driver is the agricultural activity, as stated by the European Commission in its Second River Basin Management Plan (European Commission, 2019). Cropland areas have remarkably increased for the last 15 years, hence water uptake for irrigation (up to 33% from 2005 to 2015) (Subsecretaría de Agricultura, Pesca y Alimentación, 2017; WWF, 2019). Moreover, more than half a million illegal boreholes are estimated to be obtaining groundwater in Spain (WWF, 2019), most in the South and East of the country (more arid regions with highly intensified cropping systems). It leads to an uncertain scenario for both population and ecosystems and to a conflict for such limited resource.

Ecosystems can use groundwater either at some successional stage of their evolution or by generations, but not necessarily rely on groundwater to survive (Dresel et al., 2010). We can classify as groundwater-dependent ecosystems (GDEs) those ecosystems that partially or totally depend on groundwater to maintain their function and community composition over generations (Smith et al., 2006). Such dependence means that variations in groundwater availability would significantly alter the ecosystem and even degrade it irreversibly (Colvin et al., 2003; Eamus et al., 2006). Thus, GDEs requires a sustainable groundwater management that can maintain the ecological structure and function of the ecosystem (Klove et al., 2014). However, managers and policymakers must face numerous challenges, beginning with the unequivocal identification and characterization of these ecosystems (Hatton and Evans 1998; Murray et al. 2006).

Groundwater-dependent ecosystems are around the globe in all climatic zones, from the northern to the southern hemisphere, although the vast majority of studies about GDEs have been developed in Australia and the United States. For example, since the early 80s, numerous authors have described the groundwater dependence of Eucalyptus (Talsma and Gardner 1986; Mensforth et al., 1994; O'Grady et al., 2006b) and *Banksia* spp. (Zencich et al., 2002; Canham et al., 2009) across Australian ecosystems, and of woody species (e.g., *Artemisia* spp., *Chrysothamnus* spp., *Prosopis* spp.) in the southwestern United States (Nichols, 1994; Naumburg et al., 2005; Wilcox et al., 2006; Patten et al., 2008; Scott et al., 2008). Riparian forests have also received much attention through the study of willows (*Salix* spp.) or paperbarks (*Malaleuca* spp.) (O'Grady et al., 2006a; Butterfield et al., 2021).

These studies used evapotranspiration measurements, leaf and soil water potential, or stable isotopes (δ^2H, δ^{18}O) in soil water/ groundwater/ xylem water, to assess the reliance on groundwater. More recent studies have incorporated remote sensing techniques to identify and monitor GDEs (Smith et al., 2006; Dresel et al., 2010; Barron et al., 2014; Gou et al., 2015; Guirado et al., 2018). However, some biases exist when assessing plant groundwater use related to vegetation density, seasonality, or GDE class (Gou et al., 2015).

During the last decades, numerous attempts have been made to provide a generalizable classification of GDEs. Most of these are based on geographic settings and are designed for a specific region (e.g., Hatton and Evans, 1998 for Australia, and Colvin et al., 2007 for South Africa). Eamus et al. (2006) developed a more useful classification for management based upon the type of groundwater dependency and the communities that constitute them. This classification recognizes three classes of GDEs: (1) aquifer and cave ecosystems with stygofauna living in the groundwater, (2) ecosystems that depend on the surface expression of groundwater (e.g., wetlands or riparian forests), and (3) ecosystems that depend on the subsurface expression of groundwater (e.g., terrestrial vegetation).

Terrestrial GDEs and phreatophytic vegetation

When referring to GDEs, most research has focused on wetlands, where groundwater contribution is recognizable, or riparian ecosystems (e.g., O'Grady et al., 2006b in Northern Australia (the Daly River); González et al., 2012 in Spain (the Ebro River); and Butterfield et al., 2021 in the Western United States) where groundwater discharge dominates river baseflow (Hatton and Evans 1998). However, the study of terrestrial GDEs is more challenging than most ecosystems listed above because the most common access for plants to groundwater is via the capillary fringe (i.e., the unsaturated zone above the water table) and the development of deep-root systems (Eamus et al., 2006). These roots can reach more than 50 meters depth in *Prosopis glandulosa* Torr., 30 – 60 meters in some Acacia species of South Africa (Colvin et al., 2007), and up to 60 meters in shrubs of *Ziziphus lotus* (L.) Lam. (Le Houérou, 2006). Despite having deep roots, we still need to confirm the species' connection to groundwater in these terrestrial ecosystems.

Plants that invest in deep roots to access more stable water sources are called phreatophytes or well-plants (Meinzer, 1927). Phreatophytes can show different levels of

reliance on groundwater, ranging from complete dependence (obligate) to occasional supplementary use (facultative) (Hatton and Evans, 1998). Obligate phreatophytes depend on groundwater for survival, even though they can use groundwater discontinuously (Eamus et al., 2006). Facultative phreatophytes, on the contrary, only uptake a small proportion of groundwater, although it is still essential for long-term survival and the maintenance of ecosystem structure and function (Hultine et al., 2020). Facultative species can be connected to groundwater throughout their life span or can be disconnected for decades until the water table level rises, extracting water from the vadose zone of the soil profile (Hultine et al., 2020).

Besides the degree of dependency, understanding the response of the vegetation to variations in groundwater availability is essential for managing GDEs (Murray et al., 2003). Such variations, either increasing or decreasing groundwater, can cause positive or negative effects on vegetation depending on the interaction between biotic and abiotic factors (Naumburg et al., 2005). Whereas declining water tables can result in water stress for most of the vegetation in drylands, it can also benefit those ecosystems with saline soils that increase the soil volume available for leaching. Likewise, rising water tables can saturate the rooting zone and drive anaerobic processes (Naumburg et al., 2005). Knowing the degree of groundwater dependency of the vegetation, the groundwater regime required to the persistence of the GDE, the safe limits to change in groundwater regime, and the traits that better describe the ecosystem functioning are among the major steps towards the sustainable management of GDEs (Eamus et al., 2006). This knowledge will pave the way for the maintenance of the ecological structure and function of GDEs (Klove et al., 2014) that will ensure the contributions of this ecosystem to people.

1.2. Nature's contributions to people in GDEs

Nature contributes to human wellbeing through biodiversity and ecosystem functions and services (IPBES, 2019). Many of these contributions are mediated by water since it is a crucial driver for ecological processes (Sun et al., 2017; Jobbagy et al., 2021). GDEs maintain specific functions in drylands, having a pivotal role in dryland productivity and global carbon I cycles (Poulter et al., 2014). Dryland phreatophytes decouple the ecosystem's primary productivity from precipitation when connected to groundwater (Hultine et al.,

2020), promoting evapotranspiration and increasing structural complexity and floristic diversity (O' Grady et al. 2007). The development of deep roots can also influence soil moisture, soil stability and C sequestration (Funk et al., 2016). Thus, GDEs contribute to regional climate regulation, water filtration, erosion control, soil formation, nutrient cycling, habitat provision, biodiversity maintenance, genetic resources, and recreation (Eamus et al., 2005; O'Grady et al., 2002, 2006a, 2006b; Klove et al., 2011). Most of these contributions cannot be fully replaced or are irreplaceable if ecosystems continue to be altered (IPBES, 2019).

In drylands, people's dependence on nature's resources such as freshwater becomes even more evident, hence the connection between the social and ecological system (Hough et al., 2018). However, anthropogenically-induced activities such as groundwater overexploitation or land-use changes can lead to environmental changes. Consequently, they can dramatically alter ecosystem structure, composition, and ecological processes (e.g., biogeochemical cycles, evapotranspiration), fostering the decline of nature's contributions to human wellbeing (Vitousek et al. 1997; Sun et al., 2017, Fig. 1). Throughout this PhD thesis, I considered addressing ecological processes, understood at the scale of organism or between organisms, since ecosystem functions cover a broader scale than that of individuals or vegetation patches.
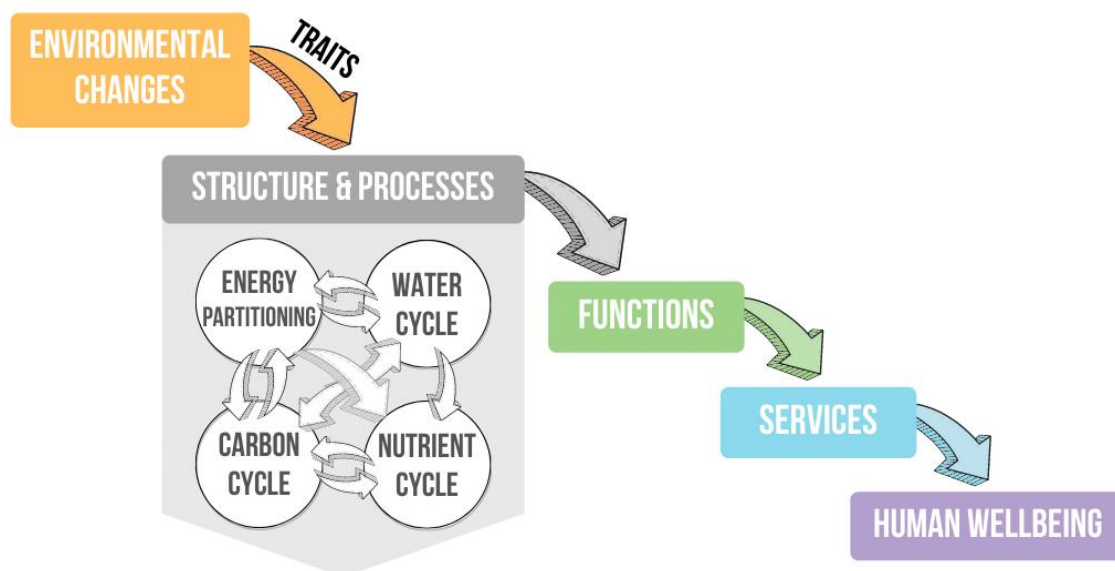
Figure 1. Ecosystem services cascade (modified from Haines-Young and Potschin, 2013) and interconnections between **ecological process bundles** that underlie **ecosystem functions** (modified from Sun et al., 2017).

1.3.   Relevant processes for this thesis

Ecological processes related to energy, water, carbon, and nutrient cycling are closely coupled (Fig. 1), and their interconnection forms the basis for the functioning of the ecosystems and the delivery of services (Burkhard and Maes, 2017; Sun et al. 2017). Through this thesis, I assessed different ecological processes driven by phreatophytes that include water and nutrient uptake, C assimilation and growth, water loss, soil biological activity and mineralization (Fig. 2).

The energy partitioning directly affects the water cycle through its relationship with evapotranspiration (Sun et al., 2017). Solar radiation and global surface temperature drive the water cycle through the vertical transfer of water from the biosphere and the soil to the atmosphere (Hartzell, 2019). The driving force of this movement is a pressure gradient developed first by roots to obtain water from the soil and second, by the transpirative demand of the atmosphere (i.e., vapor pressure deficit, VPD) to foster plant water loss (transpiration) throughout the stomata (Lombardini and Rossi, 2019). The movement of water along the soil-plant-atmosphere continuum (SPAC) depends on water availability but also on soil properties, temperature, and transpiration rates. Thus, in dryland ecosystems, the gradient in water potential through the SPAC is larger because of the low soil water content and great temperature and VPD.

In this general scenario, some plants can regulate the water loss via the stomata and keep water potentials within adequate physiologically bounds (Martínez-Vilalta and García-Forner, 2017). These species defined as isohydric avoid cavitation of xylem vessels in detriment of C assimilation (Tyree and Zimmerman, 2002). Contrary, anisohydric plants have higher resistance to cavitation and limited capacity to maintain stable water potentials, reaching higher absolute values (Lombardini and Rossi, 2019). The threshold of xylem pressure for cavitation depends on the species and the anatomical traits of the xylem such as the diameter (Sperry and Tyree, 1988). Nevertheless, cavitation can also occur in roots exposed to soil droughts, representing a strategy of allowing cavitation in some roots to prevent it in the stems (Lombardini and Rossi, 2019).
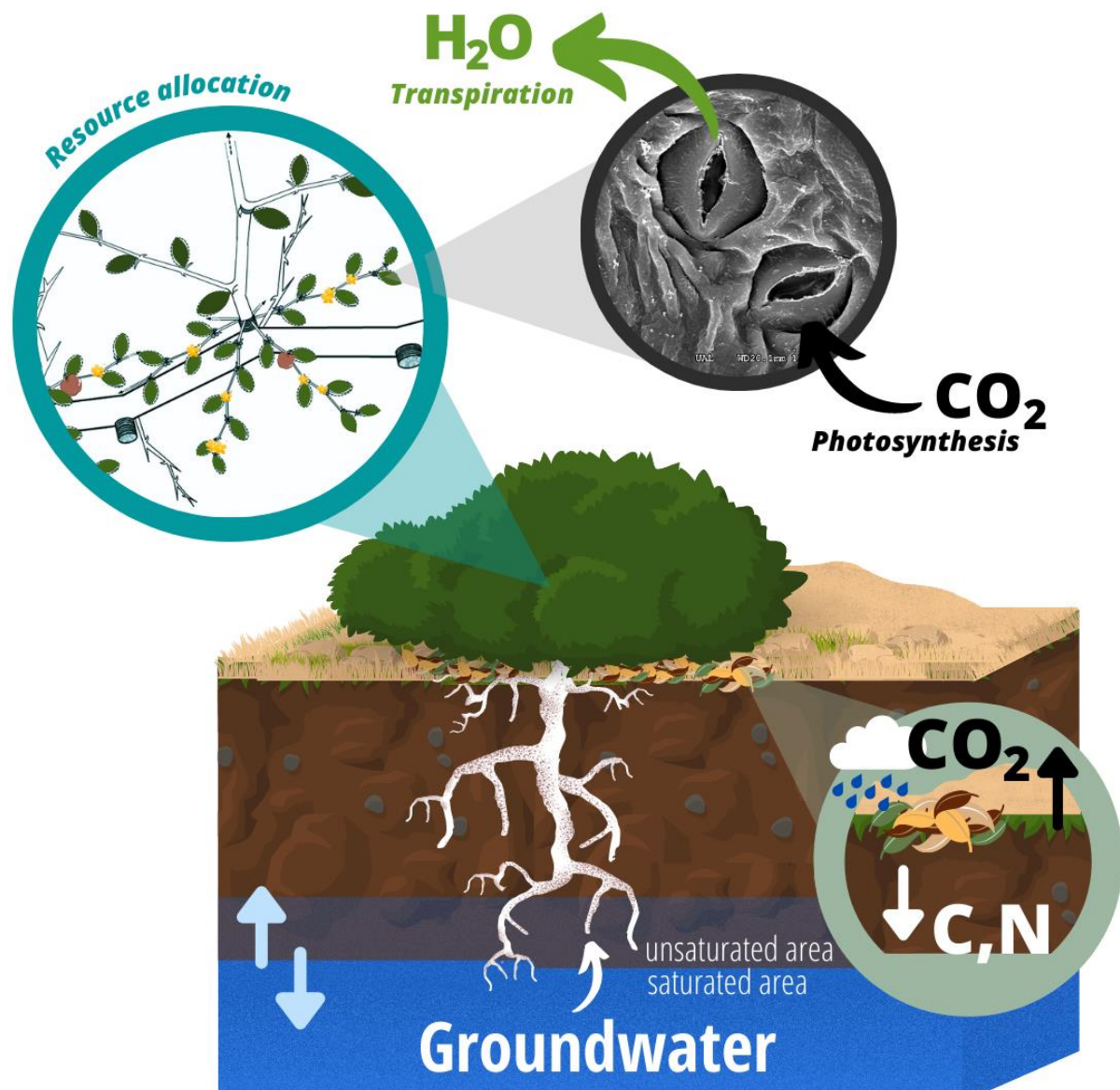
Figure 2. Processes of a groundwater-dependent ecosystem. Groundwater, which can fluctuate due to spatiotemporal variations, is **uptaken** by plant roots, from either the saturated zone or the unsaturated intermediate vadose area. Water moves upwards following a water potential gradient and is lost through **transpiration** by stomata: the gateway between the biosphere and the atmosphere for gas exchange. Atmospheric CO_2 is assimilated by stomata through **photosynthesis.** Part of the C assimilated by the plants is allocated either to grow or to reproduce (i.e., flowering and fruiting), and ultimately transferred to the soil as litter, where **mineralization** processes take place (heterotrophic respiration and nutrient release).

Plants assimilate carbon from the atmosphere by stomata through photosynthesis, a process limited by resource availability and climate. Nutrients such as nitrogen and phosphorus, water availability, CO_2 concentration, atmosphere temperature, and light intensity are important factors determining photosynthetic rates (Sardans and Peñuelas,

2013). Particularly, phosphorus is required in photosynthesis for adenosine triphosphate (ATP) whereas nitrogen is needed to synthesize Rubisco enzymes (Schlesinger and Bernhardt, 2020). Moreover, the amount of atmospheric CO_2 that diffuses into the plant leaves is determined by stomatal conductance (i.e., the stomatal aperture), which will depend partially on light and water availability. In fact, water is the most limiting resource of photosynthetic processes in drylands for most species (Eamus et al., 2016), although for phreatophytes, leaf nutrient accumulation is also decisive to face future scenarios of global warming (Querejeta et al., 2021).

Nutrient acquisition depends on soil water availability, since nutrients move towards absorptive roots by diffusion and mass flow, and upwards throughout the plant by water potential deficit (Schlesinger et al., 2016). In drylands, the ability of plants to obtain nutrients, which typically accumulates in the topsoil layer (Jobbagy and Jackson, 2001), is reduced to periods of high soil moisture (Querejeta et al., 2021) when they take advantage to grow (Ryel et al., 2008). Nevertheless, some species are winter deciduous, and the period of high resource acquisition (water and nutrients) coincides with soil drought. This is the case of some phreatophytes with dimorphic root systems, which can use topsoil water during wetter periods, and increase groundwater use during drought (Ehleringer et al., 1991, Ryel et al., 2008). Therefore, phreatophytes can experience a vertical decoupling between water and nutrients that can reduce cumulative nutrient uptake, limit C assimilation (Querejeta et al., 2021), and even diminish litter quality (Salazar-Tortosa et al., 2018).

Part of the C assimilated by the plants is allocated to growth and developmental processes (i.e., flowering, fruiting), and ultimately transferred to the soil as litter, where it becomes part of the soil organic matter (SOM) (Manzoni et al., 2019). The cycling of organic C in soils requires the breakdown of complex SOM compounds by enzymatic reactions that release simpler compounds used by soil microorganisms. Further microbial metabolic reactions release nutrients transformed into mineral forms (e.g., NH_4^+, NO_3^-, PO_4^-) that are available to be uptake by plants (Rumpel and Chabbi, 2019). These reactions also produce CO_2, which is partially retained in the soil biomass, and partially lost into the atmosphere through heterotrophic respiration (Schlesinger and Andrews, 2000). However, SOM breakdown can be constrained by physical and chemical processes (e.g., occlusion in

microaggregates and adsorption to clay) that limit microbial access to it and lead to the stabilization of soil organic C. Moreover, as soil dries, the transport rate of SOM is reduced, relying on diffusion processes to supply resources (Schimel and Schaeffer, 2012). Thus, water availability tightly controls soil biogeochemical cycles in drylands (Manzoni et al., 2019).

Rainfall fluctuations act as drivers of the soil-plant system, causing temporal variability in drylands where the intermittent nature of precipitation promotes pulses in the ecosystem (Noy-Meir, 1973; Austin et al., 2004; Manzoni et al., 2019). Reduced soil moisture inhibits microbial processes (Sardans et al., 2008), but also decreases microbial biomass and activity (Delgado-Baquerizo et al., 2013). Since plant nutrient uptake is restricted under soil moisture limitations, NO_3^- and labile organic matter accumulates in the soil (Austin et al., 2004). When water availability increases, mainly after prolonged droughts, the stimulation of C and N mineralization occurs, and net C is immediately released through soil respiration, that encompasses both autotrophic (i.e., plant roots and rhizosphere) and heterotrophic respiration (microbial communities) (Birch, 1959; Austin et al., 2004). Moreover, the spatial distribution of vegetation in patches leads to uneven distribution of resources, and the development of "fertile islands" in drylands (Reynolds et al., 1999). Whereas C, nutrients, and water mostly accumulate under vegetation canopy, the intermediate bare soils usually show resource limitation and also reduced microbial activity (Gallardo and Schlesinger, 1992). Due to the complexities derived from these interconnections in the soil-plant system, predicting how and to what extent an environmental change will alter the functioning of a GDE, and then the provision of services, remains a major challenge.

1.4.   Objectives

The primary aim of this thesis is to investigate the functioning of a terrestrial groundwater-dependent ecosystem (GDE) of Mediterranean arid regions and its phreatophytic vegetation to (1) understand its contribution in the water, carbon, and nutrient cycles, and (2) provide scientific evidence to managers and policymakers who have to deal with the sustainable management of groundwater and the conservation of the ecosystems in the face of global change. I focused on *Ziziphus lotus* (L.) Lam., a long-lived, winter deciduous shrub well adapted to arid conditions. It can develop deep roots (up to 60 m, Le Houérou, 2006) to reach groundwater sources (Tirado, 2009), thus it is considered a phreatophyte driving one of the few terrestrial GDEs in European drylands (Guirado et al., 2018).

Using *Z. lotus* and the ecosystem that constitutes in drylands as a case study, the specific objectives of this thesis were:

1. Identify growth patterns and differences in plant morpho-functional traits to understand the ecological strategies and adaptations of *Z. lotus* throughout the growing season.

2. Assess the degree of dependency, the patterns of groundwater use, and the mechanism that regulates water transport through the plant.

3. Evaluate the relationship of spatiotemporal variations in groundwater characteristics (i.e., depth, salinity, temperature) and seasonal climatic conditions with the ecophysiology and possible thresholds in the functioning of *Z. lotus*.

4. Analyze the coupling between vegetation functioning and soil biological activity, and its relationship with water availability in *Z. lotus* patches.

1.5.   Scope and structure of this thesis

There is a clear need to better understand how dryland ecosystems respond to current and future climate change effects, that is, temperature increases (between 2 – 5°C for the second half of the 21st century in the Mediterranean region) (Giorgi and Lionello, 2008) and precipitation reductions with more frequent extreme events (Guiot and Cramer, 2016).

This PhD thesis is based on the hypothesis that spatial and temporal variations of water availability (mainly groundwater) alter processes related to the carbon, nutrients, and water cycles in a GDE of dryland. This might result in a reduction in the contributions of these valuable ecosystems to people. To test this hypothesis, this thesis is set in a small coastal plain in the southeast of Spain that provides a natural spatial gradient in depth-to-groundwater (DTGW), from 2 to 25 meters. The temporal variability is defined by the climatic seasonality and the fluctuations in VPD or precipitation.

This thesis encompasses 5 sections, including this **Introduction**, which provides the general background, and the objectives and hyphotheses of the study. The second section gathers the **General methodology** used along this thesis, the area and species studied, and the experimental design developed to address the objectives. The section of **Results** consists of four research-data chapters that address the four specific objectives above mentioned. These chapters embody three published articles and a prospective manuscript for acceptance.

In **Chapter I**, I analyzed *Z. lotus'* morpho-functional and physiological traits, related to resource acquisition and water loss, to identify growth patterns at the individual scale and temporal variations throughout the growing season. Particularly, I evaluated the species heterophylly (i.e., the development of morpho-functional distinct leaves) and the architectural and growth pattern to understand better the processes of carbon assimilation and resource allocation and the strategies that underlie the persistence of this long-lived species in drylands.

The focus of **Chapter II** was to define the degree of groundwater use by *Z. lotus* and its capacity to limit water loss maintaining stable water potentials (i.e., the degree of iso-/anisohydry). In this study I applied stable isotope approaches (δ^2H and δ^{18}O in xylem water, groundwater, and precipitation; and Δ^{13}C in leaves) and water potential relationships (predawn vs midday). I also analyzed foliar nutrient concentrations and gas exchange rates to evaluate plants' responses to increasing water stress provided by the spatial gradient of DTGW.

In **Chapter III**, I introduced the temporal variability defined by seasonal climatic conditions (i.e., the atmospheric evaporative demand). I developed a multiple-trait analysis to assess the spatiotemporal variability in the ecophysiology of *Z. lotus* and to identify thresholds related to groundwater availability (defined by groundwater depth and salinity) and climatic conditions (VPD).

In **Chapter IV**, I considered the heterogeneous spatial distribution of vegetation in drylands to study soil-plants interactions. I combined field measurements of soil respiration, laboratory experiments of induced respiration and mineralization, and remote sensing analysis to disentangle whether vegetation and soil biological activity dynamics are coupled in GDEs. I also assessed the relationship of soil environmental conditions and soil quality with soil biogeochemical processes, considering the heterogeneous spatial distribution of vegetation in drylands.

A brief conceptual analysis of the implications for preserving arid GDEs and their biogeochemical processes under climate change effects is shown in **Chapter IV** and extended in the **General discussion**. In this later section, I also discuss the collective outcomes of this thesis and its relevance to understand and highlight the importance of arid GDEs as essential ecosystems for water, carbon, and nutrient cycles in drylands. Finally, I provide some **General conclusions** of the achievements and main findings of this research.

References

Austin AT, Yahdjian L, Stark JM, et al (2004) Water pulses and biogeochemical cycles in arid and semiarid ecosystems. *Oecologia*, 141, 221–235.

Barron OV, Emelyanova I, Van Niel TG, et al (2014) Mapping groundwater-dependent ecosystems using remote sensing measures of vegetation and moisture dynamics: GDEs mapping using remote measures of vegetation/moisture dynamics. *Hydrol Process*, 28:372–385.

Birch H (1959) The effect of soil drying on humus decomposition and nitrogen availability. *Plant Soil*, 12, 9–31.

Burkhard B, Maes J (Eds.) (2017) *Mapping Ecosystem Services*. Pensoft Publishers, Sofia, 374 pp.

Butterfield BJ, Palmquist EC, Hultine KR (2021) Regional coordination between riparian dependence and atmospheric demand in willows (*Salix* L.) of western North America. *Divers Distrib*, 27:377–388.

De Bello F, Lavorel S, Díaz S, et al (2010) Towards an assessment of multiple ecosystem processes and services via functional traits. *Biodivers Conserv*, 19:2873–2893.

Canham CA, Froend RH, Stock WD (2009) Water stress vulnerability of four Banksia species in contrasting ecohydrological habitats on the Gnangara Mound, Western Australia. *Plant Cell Environ*, 32(1):64-72.

Colvin C, Le Maitre D, Hughes S (2003) Assessing Terrestrial Groundwater Dependent Ecosystems in South Africa. Water Research Commission, WRC Report No. 1090-2/03.

Colvin C, Le Maitre D, Saayman I, Hughes S (2007) An Introduction to Aquifer Dependent Eco systems in South Africa. Water Research Commission. WRC Report No. TT301/07.

Dai A (2013) Increasing drought under global warming in observations and models. *Nature Clim Change*, 3, 52–58.

Delgado-Baquerizo M, Maestre FT, Gallardo A, et al (2013) Decoupling of soil nutrient cycles as a function of aridity in global drylands. *Nature*, 502:672–676.

D'Odorico P, Porporato A, Wilkinson Runyan C (2019). Ecohydrology of Arid and Semiarid ecosystems: An Introduction. In: D'Odorico P, Porporato A, Wilkinson Runyan C (Eds.). *Dryland Ecohydrology*. Springer International Publishing, Cham, pp 1–27.

Dresel PE (2010) Mapping terrestrial groundwater dependent ecosystems: method development and example output. Dept. of Primary Industries, Melbourne

Eamus D, Froend R, Loomes R, et al (2006) A functional methodology for determining the groundwater regime needed to maintain the health of groundwater-dependent vegetation. *Aust J Bot*, 54:97.

Eamus D, Fu B, Springer AE, Stevens LE (2016) Groundwater Dependent Ecosystems: Classification, Identification Techniques and Threats. In: Jakeman AJ, Barreteau O, Hunt RJ, et al. (eds) *Integrated Groundwater Management*. Springer International Publishing, Cham, pp 313–346

Eamus D, Macinnis-Ng CMO, Hose GC, et al (2005) Ecosystem services: An ecophysiological examination. *Aust J Bot*, 53(1), 1-19. Aust J Bot

Ehleringer JR, Phillips SL, Schuster WSF, Sandquist DR (1991) Differential utilization of summer rains by desert plants. *Oecologia*, 88:430–434.

European Commission (2019). Commission Staff Working Document. Second River Basin Management Plans. Member State: Spain. Brussels, Belgium. Available online: https://eur-lex.europa.eu/LexUriServ/LexUriServ.do?uri=SWD:2019:0042:FIN:EN:PDF (accessed on16 September 2021).

Funk JL, Larson JE, Ames GM, et al (2017) Revisiting the H oly G rail: using plant functional traits to understand ecological processes. *Biol Rev*, 92:1156–1173.

Gallardo A, Schlesinger WH (1992) Carbon and nitrogen limitations of soil microbial biomass in desert ecosystems. *Biogeochemistry*, 18:1–17.

Giorgi F, Lionello P (2008) Climate change projections for the Mediterranean region. *Glob Planet Change,* 63: 90–104

González E, González-Sanchis M, Comín FA, Muller E (2012) Hydrologic thresholds for riparian forest conservation in a regulated large Mediterranean river. *River Res Applic*, 28:71–80.

Gou S, Gonzales S, Miller GR (2015) Mapping Potential Groundwater-Dependent Ecosystems for Sustainable Management. *Groundwater*, 53:99–110.

Guirado E, Alcaraz-Segura D, Rigol-Sánchez JP, et al (2018) Remote-sensing-derived fractures and shrub patterns to identify groundwater dependence. *Ecohydrology*, 11:e1933.

Guiot J, Cramer W (2016) Climate change: The 2015 Paris Agreement thresholds and Mediterranean basin ecosystems. *Science*, 354: 4528–4532.

Haines-Young R, Potschin M (2013) Common International Classification of Ecosystem Services (CICES): Consultation on Version 4, August-December 2012.

Hatton TJ, Evans R (1998) Dependence of ecosystems on groundwater and its significance to Australia. Vol 12/98, Occasional paper. *Land and Water Resources Research and Development Corporation*, Canberra.

Hartzell S (2019) Ecohydrology of Photosynthesis. In: D'Odorico P, Porporato A, Wilkinson Runyan C (Eds.). *Dryland Ecohydrology*. Springer International Publishing, Cham, pp 101–120.

Hough M, Pavao-Zuckerman MA, Scott CA (2018) Connecting plant traits and social perceptions in riparian systems: Ecosystem services as indicators of thresholds in social-ecohydrological systems. *J Hydrol*, 566:860–871.

Huang T, Pang Z, Liu J, et al (2017) Groundwater recharge in an arid grassland as indicated by soil chloride profile and multiple tracers. *Hydrol Process*, 31:1047–1057.

Hultine KR, Froend R, Blasini D, et al (2020) Hydraulic traits that buffer deep-rooted plants from changes in hydrology and climate. *Hydrol Process*, 34:209–222.

IPBES (2019): Summary for policymakers of the global assessment report on biodiversity and ecosystem services of the Intergovernmental Science-Policy Platform on Biodiversity and Ecosystem Service. IPBES secretariat, Bonn, Germany. 56pp.

Jobbágy E, Jackson RB (2001) The distribution of soil nutrients with depth: Global patterns and the imprint of plants. *Biogeochemistry*, 53: 51–77.

Jobbágy E, Pascual M, Barral M, et al (2021) Representación espacial de la oferta y la demanda de los servicios ecosistémicos vinculados al agua. *Ecología Austral* 31, p. 918–933.

Klove B, Ala-Aho P, Bertrand G, et al (2014) Climate change impacts on groundwater and dependent ecosystems. *J Hydrol*, 518:250–266.

Klove B, Allan A, Bertrand G, et al (2011) Groundwater Dependent Ecosystems: Part II – Ecosystem Services and Management under Risk of Climate Change and Land Use Intensification. *Environ. Sci. Policy*, 14(7), 782-793.

Lambers H, Oliveira RS (2019) Plant Physiological Ecology. Springer International Publishing, Cham.

Le Houérou, H. N. (2006) Agroforestry and silvopastoralism: The role of trees and shrubs (Trubs) in range rehabilitation and development. *Science et changements planétaires/Sécheresse* 17:343–348

Lombardini L, Rossi L (2019) Ecophysiology of Plants in Dry Environments. In: D'Odorico P, Porporato A, Wilkinson Runyan C (Eds.). *Dryland Ecohydrol*. Springer International Publishing, Cham, pp 71–100.

Maestre FT, Salguero-Gómez R, Quero JL (2012) It is getting hotter in here: determining and projecting the impacts of global environmental change on drylands. *Phil Trans R Soc B* 367:3062–3075.

Manzoni S, Ahmed, MH, Porporato A (2019) Ecohydrological and Stoichiometric Controls on Soil Carbon and Nitrogen Dynamics in Drylands. In: D'Odorico P, Porporato A, Wilkinson Runyan C (Eds.). *Dryland Ecohydrol*. Springer International Publishing, Cham, pp 279–308.

Martínez-Vilalta J, Garcia-Forner N (2017) Water potential regulation, stomatal behaviour and hydraulic transport under drought: deconstructing the iso/anisohydric concept: Deconstructing the iso/anisohydric concept. *Plant Cell Environ,* 40:962–976.

Meinzer OE (1927) Plants as indicators of groundwater. U. S. Geological Survey, Water-Supply Paper 577. U. S. Government Printing Office, Washington, D.C., USA.

Mensforth LJ, Thorburn PJ, Tyerman SD, et al (1994) Sources of water used by riparian Eucalyptus camaldulensis overlying highly saline groundwater. *Oecologia*, 100, 21–28.

Murray BR, Hose GC, Eamus D, Licari D (2006) Valuation of groundwater-dependent ecosystems: a functional methodology incorporating ecosystem services. *Aust J Bot*, 54:221.

Murray BR, Zeppel MJB, Hose GC, Eamus D (2003) Groundwater dependent ecosystems in Australia: it's more than just water for rivers. *Ecol Manag Restor*, 4, 110–113.

Naumburg E, Mata-gonzalez R, Hunter RG, et al (2005) Phreatophytic Vegetation and Groundwater Fluctuations: A Review of Current Research and Application of Ecosystem Response Modeling with an Emphasis on Great Basin Vegetation. *Environ Manag*, 35:726–740.

Newman BD, Wilcox BP, Archer SR, et al (2006) Ecohydrology of water-limited environments: A scientific vision: OPINION. *Water Resour Res*, 42.

Nichols WD (1994) Groundwater discharge by phreatophyte shrubs in the Great Basin as related to depth to groundwater. *Water Resour Res*, 30, 3265-3274.

Noy-Meir I (1973) Desert ecosystems: environment and producers. *Ann Rev Ecol Syst*, 4:25–51.

O'Grady AP, Eamus D, Cook PG, Lamontagne S (2006a) Comparative water use by the riparian trees Melaleuca argentea and Corymbia bella in the wet–dry tropics of northern Australia. *Tree Physiol*, 26(2): 219-228.

O'Grady AP, Eamus D, Cook PG, Lamontagne S (2006b) Groundwater use by riparian vegetation in the wet – dry tropics of northern Australia. *Aust J Bot*, 54:145.

O'Grady AP, Eamus D, Cook PG, et al (2002) Tree water use and sources of transpired water in riparian vegetation along the Daly River, Northern Territory. Department of the Environment, Water, Heritage and the Arts, Northern Territory Government

Patten DT, Rouse L, Stromberg JC (2008) Isolated Spring Wetlands in the Great Basin and Mojave Deserts, USA: Potential Response of Vegetation to Groundwater Withdrawal. *Environ Manage*, 41, 398–413.

Poulter B, Frank D, Ciais P, et al (2014) Contribution of semi-arid ecosystems to interannual variability of the global carbon cycle. *Nature*, 509:600–603.

Querejeta JI, Ren W, Prieto I (2021) Vertical decoupling of soil nutrients and water under climate warming reduces plant cumulative nutrient uptake, water-use efficiency and productivity. *New Phytol*, 230:1378–1393.

Reynolds JF, Smith D. Stafford M, et al (2007) Global Desertification: Building a Science for Dryland Development. *Science*, 316:847–851.

Reynolds JF, Virginia RA, Kemp PR, et al (1999) Impact of drought on desert shrubs: effects of seasonality and degree of resource island development. *Ecol Monogr*, 69:69–106.

Rumpel C, Chabbi A (2019) Chapter 1 – Plant–Soil Interactions Control CNP Coupling and Decoupling Processes in Agroecosystems with Perennial Vegetation. In: Lemaire G, Carvalho PCDF, Kronberg S, Recous S (eds) *Agroecosystem Diversity*. Academic Press, pp 3–13

Ryel RJ, Ivans CY, Peek MS, Leffler AJ (2008) Functional Differences in Soil Water Pools: a New Perspective on Plant Water Use in Water-Limited Ecosystems. *Progress in Bot*, 69, 397-422.

Salazar-Tortosa D, Castro J, Villar-Salvador P, et al (2018) The "isohydric trap": A proposed feedback between water shortage, stomatal regulation, and nutrient acquisition drives differential growth and survival of European pines under climatic dryness. *Glob Change Biol*, 24:4069–4083.

Sardans J, Peñuelas J (2013) Plant-soil interactions in Mediterranean forest and shrublands: impacts of climatic change. *Plant Soil*, 365:1–33.

Sardans J, Peñuelas J, Prieto P, Estiarte M (2008) Drought and warming induced changes in P and K concentration and accumulation in plant biomass and soil in a Mediterranean shrubland. *Plant Soil*, 306:261–271.

Schimel J, Schaeffer SM (2012) Microbial control over carbon cycling in soil. *Front Microbiol*, 3

Schlesinger WH, Andrews JA (2000) Soil respiration and the global carbon cycle. *Biogeochemistry*, 48, 7–20.

Schlesinger WH, Bernhardt ES (2020) Biogeochemistry (Fourth Edition). Academic Press.

Schlesinger WH, Dietze MC, Jackson RB, et al (2016) Forest biogeochemistry in response to drought. *Glob Change Biol*, 22: 2318–2328.

Scott RL, Cable WL, Huxman TE, et al (2008) Multiyear riparian evapotranspiration and groundwater use for a semiarid watershed. *J Arid Environ*, 72(7): 1232–1246.

Shiklomanov IA (1998) World water resources: a new appraisal and assessment for the 21st century. Paris: United Nations Educational, Scientific and Cultural Organization.

Smith PL, Williams RM, Hamilton S, Shaik M (2006) A risk-based approach to groundwater management for terrestrial groundwater dependant ecosystems. Murray Darling Basin Conference. Dept. Natural Resources NSW.

Sperry JS, Tyree MT (1988) Mechanism of water stress-induced xylem embolism. *Plant Physiol* 88:581–587.

Subsecretaría de Agricultura, Pesca y Alimentación (2017). Encuesta de Superficies y Rendimientos de Cultivos (ESYRCE). Ministerio de Agricultura, Pesca, Alimentación y Medio Ambiente.

Sun G, Hallema D, Asbjornsen H (2017) Ecohydrological processes and ecosystem services in the Anthropocene: a review. *Ecol Process*, 6:35.

Talsma T, Gardner B (1986) Soil water extraction by a mixed Eucalypt forest during a drought period. *Aust Jour Soil Res*. 24 25-32

Tirado R (2009) 5220 Matorrales arborescentes con Ziziphus (*). In VV.Aaaa., Bases ecológicas preliminares para la conservación de los tipos de hábitat de interés comunitario en España. Ministerio de Medio Ambiente, y Medio Rural y Marino. 68 p.

Tyree MY, Zimmerman MH (2002) Xylem structure and the ascent of sap. Springer, Berlin

Vitousek PM, Mooney HA, Lubchenco J, Melillo JM (1997). Human domination of Earth's ecosystems. *Science*, 277, 494–499

Wilcox BP, Owens MK, Dugas WA, et al (2006) Shrubs, streamflow, and the paradox of scale. *Hydrol Process*, 20: 3245-3259.

WWF (2019) Agua para hoy, sed para mañana. Documento de posición, 7 pp.

Zencich SJ, Froend RH, Turner JV, Gailitis V (2002) Influence of groundwater depth on the seasonal sources of water accessed by Banksia tree species on a shallow, sandy coastal aquifer. *Oecologia*, 131:8–19.

2. GENERAL METHODOLOGY

2.1. Study area: the azufaifar and *Ziziphus lotus*

This PhD thesis has been developed in the coastal plain of the Cabo de Gata-Níjar Natural Park (Almería), southeast of the Iberian Peninsula (Fig. 1) where the most extensive and best-preserved population of *Ziziphus lotus* (L.) Lam. In the European continent inhabits (Rey et al., 2018). The area known as Amoladeras-Torregarcía is located at the western end of the Natural Park, bounded by the residential area of Retamar (to the west), the AL-3115 road and areas of extensive greenhouse crops (to the northeast) and an intermittent watercourse known as Rambla Morales (to the east).

The climate is semiarid, characterized by mild temperatures and higher rates of evapotranspiration than precipitation. Particularly, mean annual temperature is 18ºC and mean rainfall is 220 mm/year, which occurs mostly in autumn and winter (Machado et al., 2011). During the study period (2017 – 2019), monthly temperatures showed on-average values, although precipitation fluctuated both monthly and yearly (Fig. 2). Whereas 2017 and 2018 were slightly dry years, 2019 was above average. In general, spring (March – April) and autumn precipitation (September – October) were more relevant than winter precipitation, which was below average throughout the study period.

The study area is located over the western part of the coastal detritic aquifer named as Hornillo-Cabo de Gata. The aquifer is bounded to the East by the volcanic uplands of the Sierra de Cabo de Gata, to the West, by the Carboneras Fault (a tectonic feature), and to the South by the Mediterranean Sea (García et al., 2004). It comprises Plio-Pleistocene conglomerates, with aeolian sands beneath it and Pliocene marine marls at the base. The geology originated from the sedimentary fill of the Bay of Almería with materials from the Sierra Alhamilla mountains (1000 m.a.s.l) and from coastal marine deposits from the Quaternary period (Vallejos et al., 2018). The main source of aquifer recharge is direct precipitation but also small inputs from nearby aquifers. However, reduced precipitation in the area and increasing groundwater overexploitation of near aquifers have contributed to diminish groundwater resources (García et al., 2004).
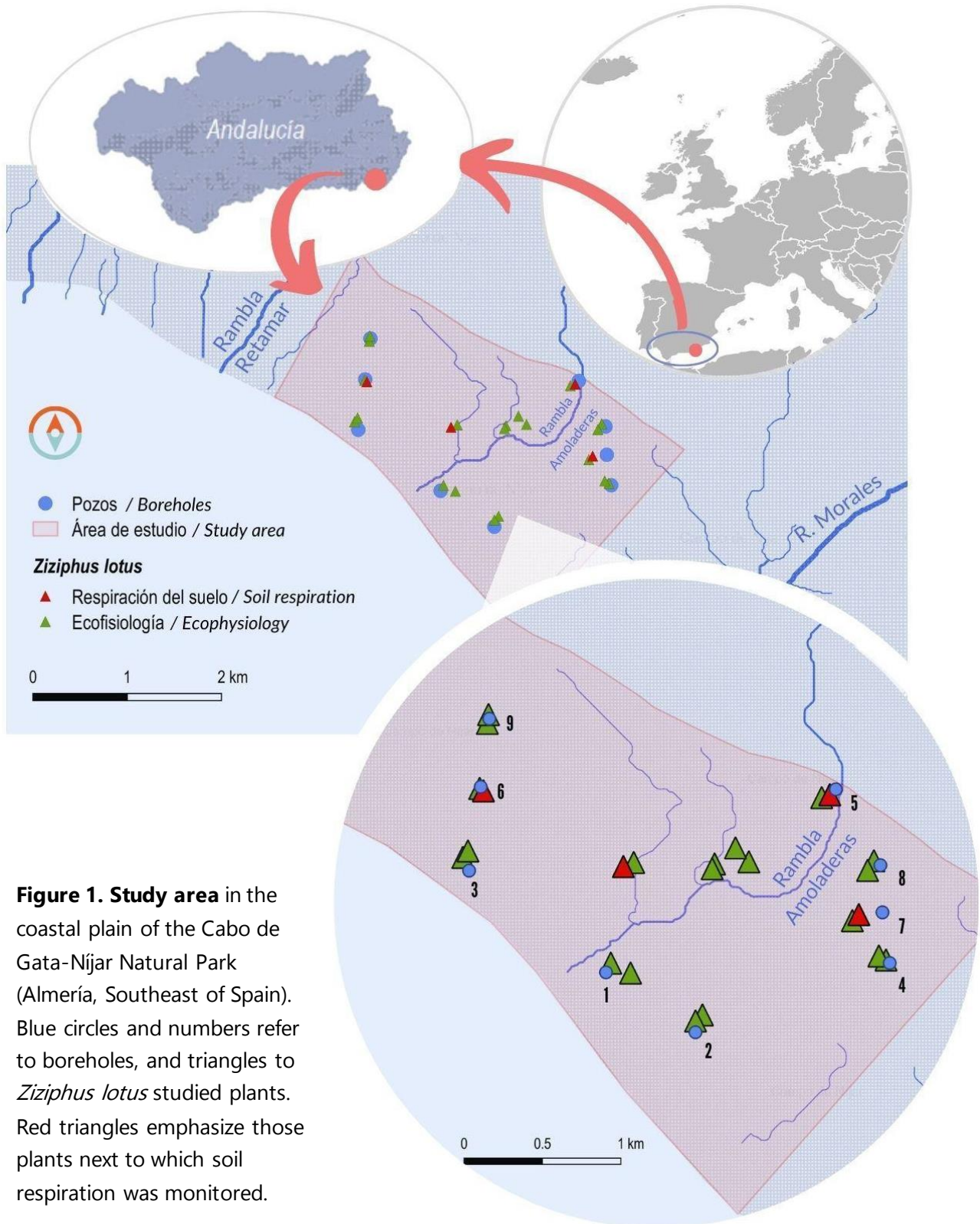
Figure 1. Study area in the coastal plain of the Cabo de Gata-Níjar Natural Park (Almería, Southeast of Spain). Blue circles and numbers refer to boreholes, and triangles to *Ziziphus lotus* studied plants. Red triangles emphasize those plants next to which soil respiration was monitored.

Z. lotus is a xerophytic shrub of the Rhamnaceae family located in coastal areas of the Mediterranean basin, especially in northern Morocco, the southeast of the Iberian Peninsula (Almeria, Murcia, and Alicante), on the islands of Sicily and Cyprus, as well as in the Near East (Sánchez-Gómez et al., 2003). It is a long-lived species (Rey et al., 2018)

considered as relict in Europe, where it reaches its northern distribution limit. The degradation and fragmentation of *Z. lotus* populations, promoted by land-use changes in favor of agriculture and urbanization, threatens the persistence of the species (Mota et al., 1996; Tirado, 2009) In addition, the scarce regeneration observed in the southeastern Iberian Peninsula increases its vulnerability (Rey et al., 2018). This is one of the reasons why "arborescent matorrals with *Ziziphus*" (5220*) are considered a priority habitat for conservation in Europe (Habitat Directive, 92/43/EEC).
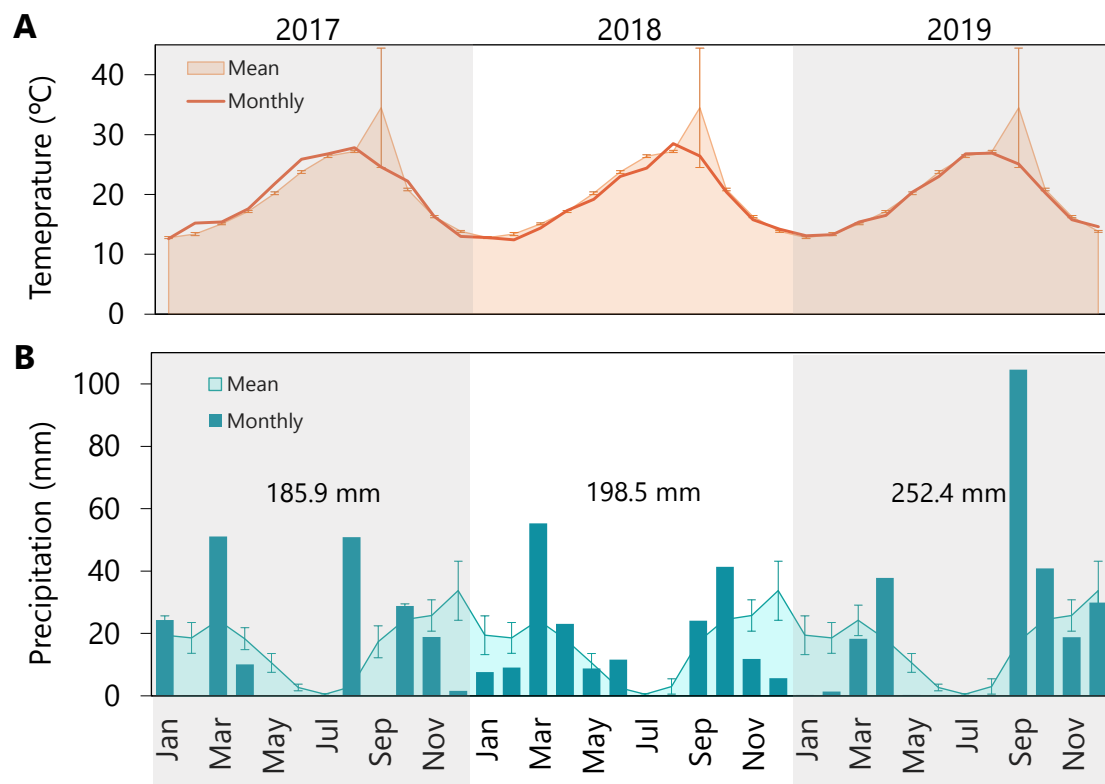
Figure 2. Mean (± SE) and monthly temperature (A) and precipitation (B) in the study area during the three sampling periods (2017 – 2019). Mean annual temperature and precipitation (from January to December) are shown. (Data from the Spanish Meteorological Agency).

Z. lotus is the ecosystem's engineering species, determining its structure and functioning. It is one of the few shrubs that constitutes an arborescent stratum in semiarid Mediterranean regions, reaching 4 meters in height and 35 m in diameter (Tirado 2009) (Fig. 3). *Z. lotus* is photosynthetically active in spring and summer (April – October), being deciduous in autumn and winter. Because of its activity and size, it is common to find smaller shrubs associated with *Z. lotus* such as *Asparagus albus* L., *A. horridus* L., *Lycium intricatum* Boiss., *Salsola oppositifolia* Desf., and *ithania frutescens* (L.) Pauquy (Tirado and

Pugnaire, 2003; Tirado, 2009). These formations or patches of vegetation can accumulate sediments under their canopy forming *nebkhas* (Tengberg et al., 1998; Lang et al., 2013): particular geomorphic structures observed under shrubs of desert or coastal areas such as *Acacia* spp., *Nitraria* spp., or *Prosopis glandulosa* Torr. (Tirado 2009, Wang et al., 2019). *Nebkhas* with large canopies can shade direct sun radiation, prevent high soil temperatures, increase soil moisture content, avoid soil erosion, and provide habitats for birds and small animals (Luo et al., 2021). Moreover, they accumulate large amounts of organic matter and nutrients contributing to the development of fertile islands in drylands (Wang et al., 2019).

Figure 3. Plants of *Ziziphus lotus* in the study area. Regular-size individual at the front and the biggest plant in the plain at the back.

2.2. Experimental design

The experimental design revolves around the groundwater-monitoring network that was established on the plain in 2019 in the context of the Life ADAPTAMED project (Fig. 1). The network consists of nine boreholes that discern between three sites in the area (east plain, west plain, and the seasonal stream that crosses it, Rambla Amoladeras). Bores also followed a spatial gradient from the coastline to the inner part of the plain, where elevation was also higher. Thus, groundwater depth was expected to be lower in bores 1, 2, and 3 than in bores 8 and 9.

Next to each borehole, two adult individuals of *Z. lotus* were selected in 2017 at a maximum distance of 200 m. Six additional individuals were selected in the intermittent stream that crosses the area (Rambla Amoladeras) to increase representativeness. In total, 24 individuals of *Z. lotus* were monitored and sampled during the development of this thesis (triangles in Fig. 1). In four of those plants (red triangles, Fig. 1) soil respiration was also assessed (see section 2.3.3).
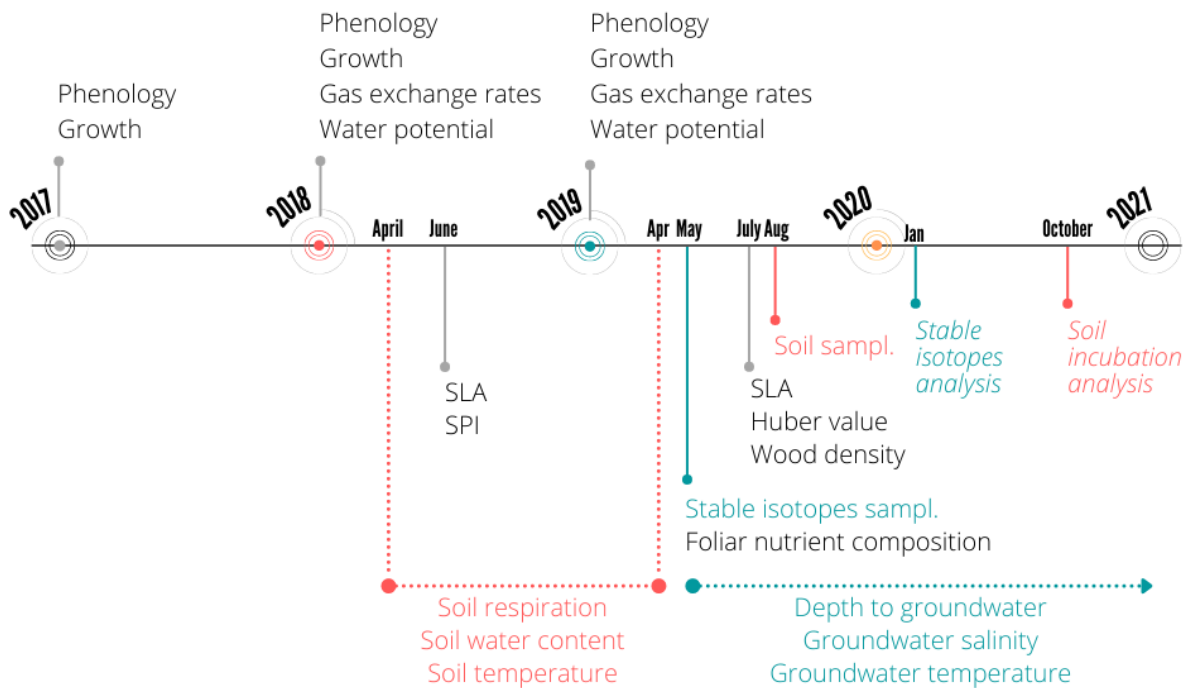
Figure 4. Timeline of sampling and analyses developed during this thesis. Colors refer to the ecosystem component (black: vegetation; red: soil; blue: groundwater). Measurements were either periodically obtained during the season (labels coming out of the year or between dotted lines), or punctually collected (coming out of a month). Laboratory analyses are shown in italic.

2.3. Sampling and analyses

Sampling was carried out from 2017 to 2019 and the last laboratory analysis was concluded in October 2020 (Fig. 4). Some of the measurements were periodically obtained during the species growing season, such as phenology and growth rate that were monitored monthly, or water potential and gas exchange rates that were assessed in three periods (May, July, September). We considered May (late-spring), July (mid-summer), and September (late-summer) as representative periods to capture the functioning of the species throughout its growing season. Other samples were obtained once per year such as leaves and stems

for foliar or isotopic analyses. Overall, sampling can be divided into three groups that correspond to three components of the ecosystem: vegetation, groundwater, and soil.

2.3.1. Plant morphology and ecophysiology throughout functional traits

Plant functional traits refer to the morphological, physiological and phenological traits of plants that have an effect on their development (Pérez-Harguindeguy et al., 2013). Functional traits have been used to understand plant responses to environmental factors and describe their life strategies (Lavorel and Garnier, 2002), but also for the study of ecosystem functioning (Mori and Niinemets, 2010), and ultimately the services it provides (De Bello et al., 2010).

Ecosystem processes are controlled by the combination of key biotic traits (De Bello et al., 2010) that reflect how ecosystems adapt or respond to the environment (Cornelissen et al., 2003). Traits can perform at different scales, from organs to ecosystems (Violle et al., 2007), and across trophic levels (e.g., plants and soil invertebrates) (De Bello et al., 2010). In this sense, traits such as specific leaf area (SLA), rooting depth, canopy/body size, and microbial diversity control processes linked to soil fertility, carbon sequestration, and water flow (De Bello et al., 2010).

Because dominant plant traits have great relevance to ecosystem processes (Diaz et al., 1998), the study of functional traits allows to scaling from individuals to ecosystems (Mori and Niinemets, 2010). For example, the density of stomata in a plant determines its water use efficiency and photosynthetic rates, contributing to biomass production and primary productivity of the ecosystem (Romermann et al., 2016). Therefore, we begin with the study of the functional traits of *Z. lotus* with the aim of understanding the functioning of the ecosystem it constitutes in drylands. The functional traits that have been analyzed in this thesis can be divided into 3 large groups according to the scale: functional traits at the leaf, stem, and whole plant level (Fig. 5). For all the traits and, because of the size of the species, sampling and monitoring was developed in different points around the outer part of the canopy (the main orientations: north, east, south, west) to cover the variability that can be derived from the environmental conditions (e.g., dominant winds (east – west) or radiation).
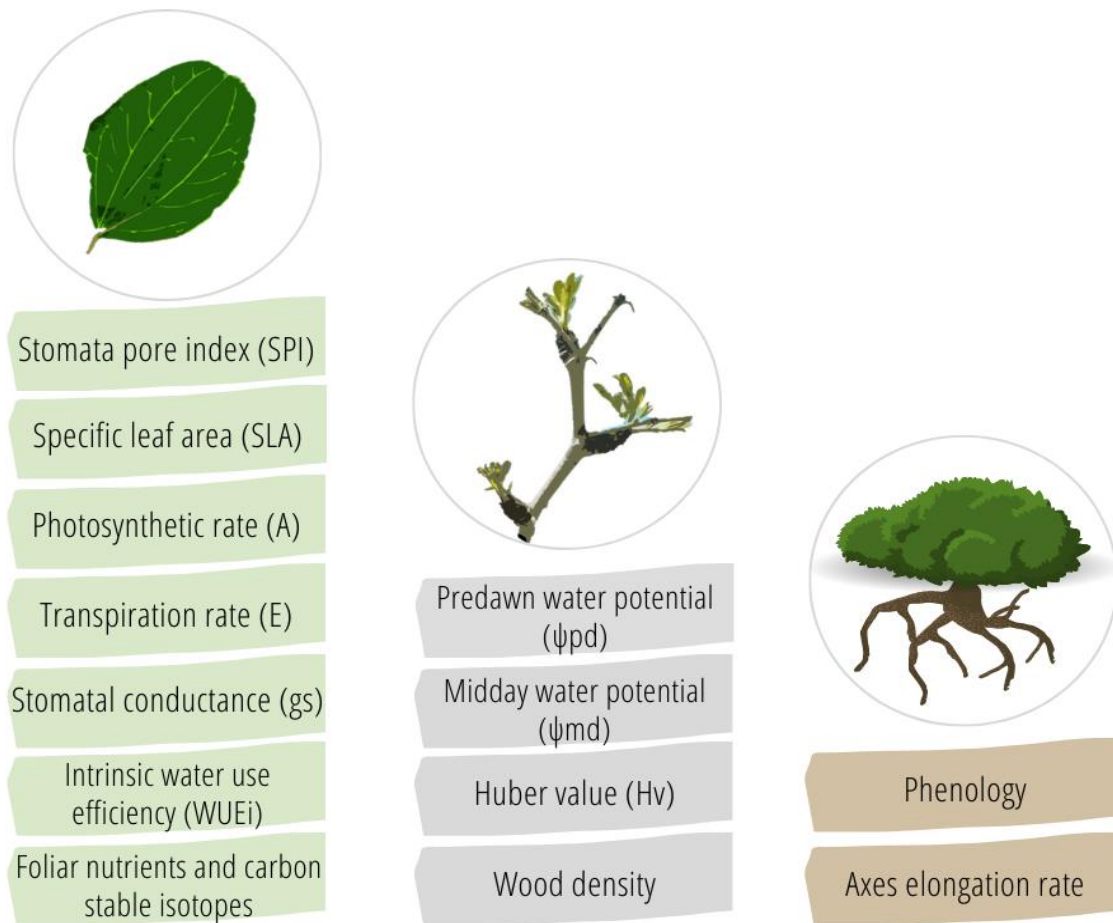
Figure 5. Plant functional traits analyzed at the leaf, stem, and whole plant level.

Leaf traits and analyses

We observed from the beginning of this thesis that *Z. lotus* developed two types of leaves emerging from different shoots. Because of that, sampling was designed to collect and analyze both kinds of leaves, either to compare between them (Chapter I) or to cover the variability of the canopy. Thus, note that the sampling number hereafter encompasses both types of leaves.

I began with the smallest part of the plant involved in gas exchanges: the stomata. **Stomata** are pores, found in the epidermis of leaves, stems, and other organs, constituted by specialized cells. They are the gateway between the biosphere and the atmosphere for gas exchange, having major implications on the global carbon and water cycles (Klein et al., 2014). To visualize stomata, we used a Scanning Electron Microscope (SEM) Hitachi S-3500N. Firstly, 10 leaves of *Z. lotus* were collected in 2018 and immediately fixed in FAA solution (40% formaldehyde: acetic acid; 50% ethanol; 2:1:10. v/v) for at least 24 hours.

Fixed leaves were stored in the solution at 4ºC until being dehydrated the day before visualization. Leaves were dehydrated throughout an ethanol series (50, 60, 70, 85 and 100%) and then critical-point dried, which is a widely used method to dry biological samples for examination with the SEM. Subsequently, pieces of leaf were stuck to an aluminum stub with double-sided graphite tape where a gold layer of approximately 20 nm was applied to give conductive properties to the samples (Fig. 6). Images from different sections of the abaxial side of the leaves were obtained and stomata were counted. The length of each guard cell was measured with a digital leaf-area meter (Windias 3.2., Cambridge, UK). Finally, the **stomatal pore index (SPI)** was calculated from the ratio of stomatal density to the square guard cell length (Sack et al., 2003).
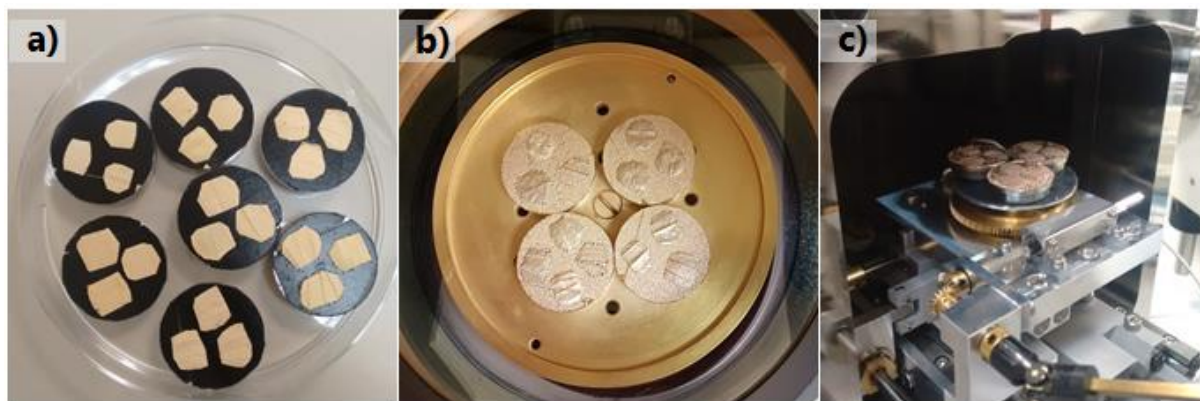
Figure 6. Sample preparation before visualizing stomata with the Scanning Electron Microscope (SEM): a) fragments of dehydrated leaves on the stubs, b) leaf samples and stubs after Au imprimation, and c) samples being introduced in the SEM.

The **specific leaf area (SLA)** was assessed in 2018 and 2019. This is a characteristic closely related to the investment and use of resources (Pérez-Harguindeguy et al., 2013). To avoid leaf dehydration, we cut four sun-exposed branches per plant, which were immediately driven to the laboratory in a portable cool-box. Once in the laboratory, we collected and scanned 80 leaves per plant (Fig. 7a). Then, these leaves were individually dried in the oven for 72 h at 60°C (Fig. 7b) and weighed with a precision balance. Single leaf area was estimated with the digital leaf-area meter. From these data, the mean SLA was calculated as the average of the ratio of leaf area (cm^2) to leaf dry weight (g).
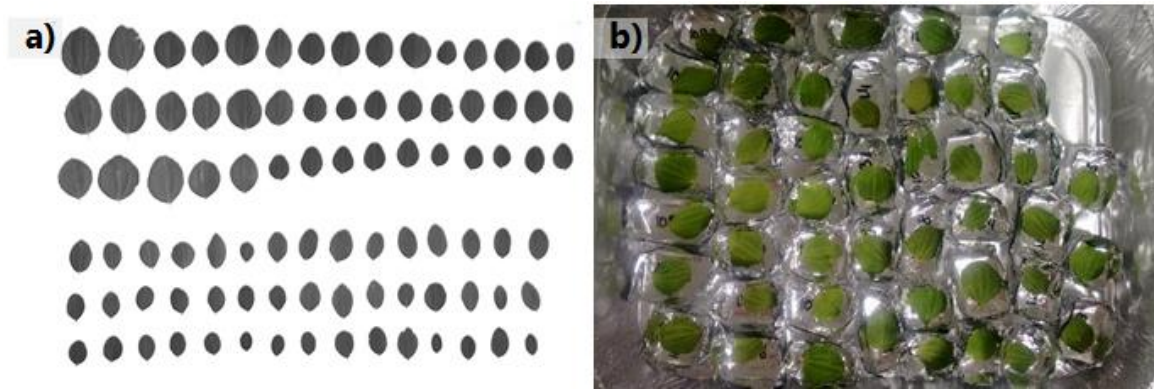
Figure 7. Specific leaf area procedure: a) scanned leaves for leaf area estimation, and b) oven-dried individual leaves to be weighed.

Instantaneous **gas exchange rates** were also estimated at the leaf level using a Li-6400XT portable infrared gas analyzer (IRGA) (LI-COR Inc., Lincoln, NE, USA). Photosynthetic rate (A), stomatal conductance (g_s), transpiration rate I, and vapor pressure deficit (VPD) were measured in 8 leaves per plant in the three sampling periods of 2018 and 2019 growing seasons (May, July, and September). The intrinsic water use efficiency (WUEi) was derived from the ratio of A to g_s. Leaves are inserted into the chamber of the IRGA where conditions were kept constant throughout: ambient temperature at 25-30°C, flow rate of 400 µmol s^{-1}, CO_2 concentration of 400 µmol mol^{-1}, and light intensity of 1800 µmol m^{-2} s^{-1}. Gas exchange measurements were obtained in different moments of the growing season to compare the functioning of the plants with time. To avoid biases, measurements were taken between 10:00 and 12:00 on sunny days.

Finally, in May 2019 we collected 30 leaves per individual to analyze nutrient concentration and **leaf carbon isotope discrimination ($\Delta^{13}C$)**. Leaves were stored in paper bags and oven-dried at 60°C for 48 h to finely ground to powder. The **concentration of nutrients** such as Na, P, K, Ca, Mg, S, Fe, Cu, and Zn were measured by inductively coupled plasma optical emission spectrometry (ICP-OES, Thermo Elemental Iris Intrepid II XDL, Franklin, MA, US) after a microwave-assisted digestion with HNO_2–H_2O_2 (4:1, v:v) in ionomica laboratory at CEBAS-CSIC (Murcia, Spain). However, foliar N concentration was analyzed by a CHNOS Elemental Analyzer (vario ISOTOPE cube, Elementar, Hanau, Germany) interfaced to an IsoPrime100 mass spectrometer (Isoprime, Cheadle, UK) in the CSIB at the University of California, Berkeley. For carbon isotope analysis a combustion module (CM) coupled to a cavity ringdown spectroscopy (CRDS) System (G2201-iAnalyzer, Picarro) was

used (see Chapter II for further details). We calculated $\Delta^{13}C$ from $\delta^{13}C$, using the following equation (Werner et al., 2012):

$$\Delta^{13}C = (\delta^{13}Ca - \delta^{13}Cp)/(1 + \delta^{13}Cp) \tag{1}$$

where $\delta^{13}Ca$ and $\delta^{13}Cp$ are the $\delta^{13}C$ values of the CO_2 in air and the plant, respectively.

Stem traits and analyses

The water potential refers to the energy to move water from the soil to the plant. At the stem level, maximum and minimum **water potentials** were obtained at midday (Ψ_{md}) and predawn (Ψ_{pd}) respectively in the three sampling periods of 2018 and 2019 growing season. Four stems per individual were excised approximately between 05:30 and 06:30 hours (1 h before sunrise) for measuring Ψ_{pd}, and between 13:30 and 14:30 hours (solar midday) for Ψ_{md}, although the period of sampling can slightly vary depending on the moment of the solar year. Stem water potential was measured in the field using a Scholander pressure chamber (SKPM1405, Skye Instruments, Powys, UK) (Fig. 8).

Figure 8. Stem water potential measurement. a) Measurement of predawn water potential, b) Scholander pressure chamber SKPM1405, and c) detail of the stem with a drop of water after exceeding its water potential.

The **Huber value (Hv)**, the ratio of sapwood cross-sectional area to mean total leaf area, refers to the investment of stem tissue per unit leaf area fed (Tyree and Ewers, 1991). In July 2019, three branches of approximately one meter were cut per plant, from which all leaves were removed. Sapwood cross-sectional area, that can be distinguished from heartwood by the color difference, was measured with a digital caliper in the base of the branch. To estimate total leaf area, all leaves of the stem were scanned with the digital leaf-

area meter (WinDIAS 3.2.). From the cut branches, wood density was also estimated as the volume of a piece of branch divided by its dry weight (after 48 h at 60ºC).

Three pieces of branch per plant were also cut and debarked in May 2019 for **isotopic analysis**. Particularly, xylem water was extracted through cryogenic vacuum distillation in the CEBAS-CSIC laboratory. The procedure consists of storing the stems at -20°C in glass vials tightly sealed by lids and wrapped with Parafilm to minimize potential evaporation. Then, the same vials were defrosted at room temperature, introduced in the vacuum system, and rapidly frosted again using liquid nitrogen for 45 minutes. Afterwards, samples were heated in vacuo (10-3 mBar) to a final temperature of 100°C for approximately 2 h, and the extracted water was cryogenically trapped using liquid nitrogen (Fig. 9).
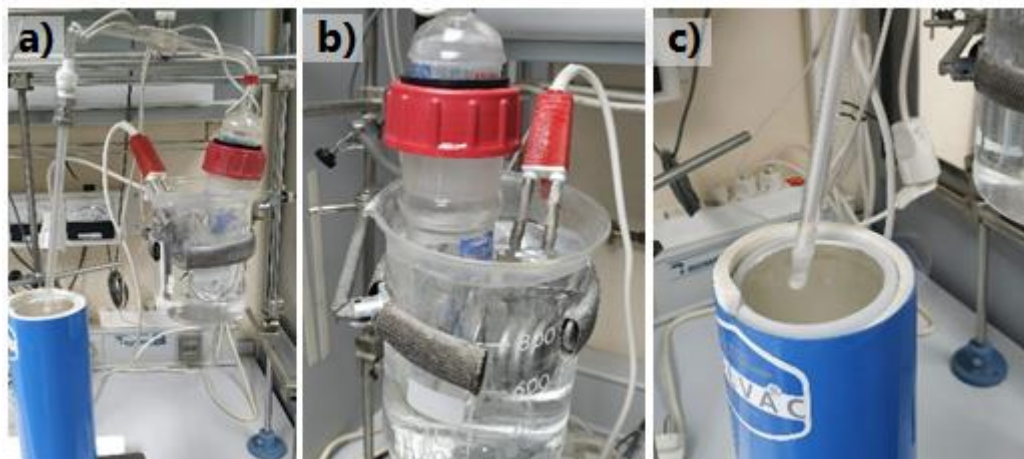
Figure 9. Cryogenic vacuum distillation system: a) complete extraction system, b) vase with samples vials being heated, c) liquid nitrogen trap for extracted water.

The water stable isotopes δ^2H and $\delta^{18}O$ were measured in xylem water, and also in groundwater and water from precipitation precipitation by cavity ringdown spectroscopy (CRDS). This technique is increasingly used for isotopic analyses since it allows the simultaneous measurement of oxygen and hydrogen isotopes with high accuracy (Martín-Gómez et al., 2015). A L2140-I Picarro water isotope analyzer was used interfaced with an A0211 high-precision vaporizer (Picarro, Santa Clara, CA, US). Potential organic contamination of plant-extracted water (i.e., combustible organic compounds such as alcohols and other volatiles) was removed from water samples using a Picarro micro-combustion module (MCM) (Brand et al., 2009; Gázquez et al., 2015). Afterwards, ChemCorrect software (Picarro) was used to confirm the effectiveness of pyrolytic catalysts.

Finally, each sample (three per plant) was injected 10 times into the vaporizer, which was heated to 110°C (see Chapter II for further details).

Whole plant traits

At the whole plant level, we monitored the **phenology** and **growth** of 24 stems per plant that were marked in 2017. These stems encompass shoots and branches with the different types of leaves (see Chapter I for further details). Phenology (i.e., duration of a stage in annual life cycle) reflects the ecological strategy of the species to deal with the timing of environmental conditions (Gorai et al., 2010). Leaf flushing, flowering, and fruiting patterns respond to environmental controls, both abiotic and biotic. In seasonal climates, whereas leaf flushing and fall are usually linked to climatic constraints such as rainfall, irradiance, temperature, and photoperiod, flowering and fruiting timing are more determined by genetic control and resource availability (Fenner, 1998). Therefore, leaf flushing, bud production, flowering, fruiting, and leaf abscission were assessed monthly from March, when incipient leaves appear, to November, when the lasting leaves fall (Fig. 10). At the end of the season, the length of the stems, either shoots or branches, was measured to estimate their elongation.
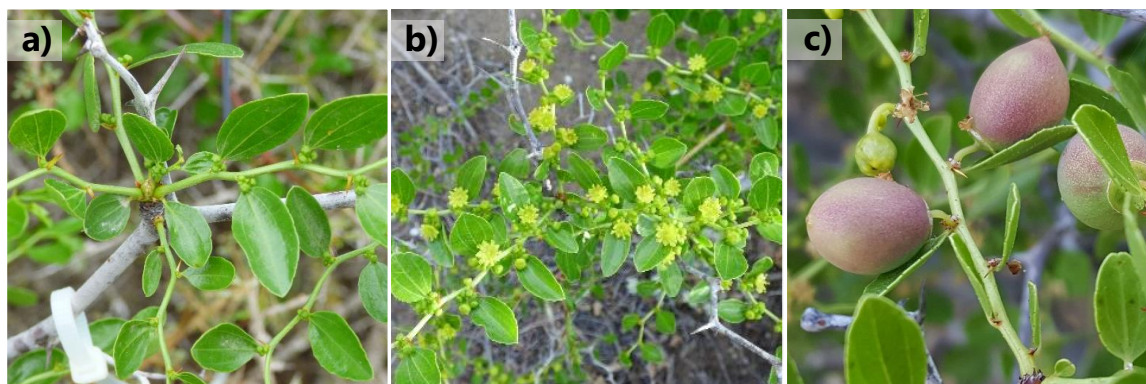
Figure 10. Examples of *Z. lotus* stems at different phenological phases: a) bud production in April, b) flowering in May, and c) fruiting in June.

2.3.2. Groundwater monitoring and sampling

In May 2019, two sensors were installed in eight of the nine boreholes to monitor groundwater level (Hobo U20 Water level logger) and quality (i.e., electrical conductivity and temperature; Hobo U24 conductivity logger). The sensors record these three parameters every 15 minutes in parallel with an atmospheric pressure sensor located in the

area that aims to correct the measurements of groundwater level (initially provided as the pressure of the column of water and air immediately above the sensor). Corrections were developed with the software HOBOware (Onset, Cape Cod, MA, USA). Periodically, manual measurements were undertaken to confirm the reliability of the data and the proper working of the sensors. Groundwater was also collected during that period for stable isotope analysis. Samples were obtained 5 meters below the water table to avoid evaporative water (Fig. 11).

Figure 11. Boreholes in the study area. a) General image, b) bore next to *Ziziphus lotus* in winter, and c) open bore to obtain groundwater measurements.

2.3.3. Soil activity and properties

Soil respiration and mineralization

Soil respiration (Rs) is a process derived from the biological activity of the soil and is expressed by the emission of CO_2. It encompasses the autotrophic respiration of plant roots and rhizosphere activity, and the heterotrophic respiration of microbial communities (Schlesinger and Andrews, 2000; Oyonarte et al., 2012). Rs is the second largest carbon flux in terrestrial ecosystems and drives the incorporation of CO_2 into the soil carbon pool (Schlesinger and Andrews, 2000). We used a manual and portable opaque soil chamber system (EGM-4, PP-systems, Hitchin, UK) to obtain monthly discrete measurement of CO_2 effluxes for 1 year (Fig. 4). The chamber was located over polyvinyl chloride collars (PVC collars, 15 cm in diameter and 7 cm in height) that were inserted 3.5 cm into the soil and placed around the four selected patches of *Z. lotus* (red triangles, Fig. 1), both under-canopy and inter-canopy (Fig. 12). Because of the low rates of Rs typical of drylands, each collar was monitored for 120 seconds, and measurements obtained every 4 seconds to

ensure reliable data. We estimated the fluxes of CO_2 from the slopes of CO_2 molar fractions of the confined air versus time, by using either linear or quadratic regression for the best regression fit (Pérez-Priego et al., 2010). Soil temperature and water content were obtained next to each collar and at the time of Rs measurement (between 11:00 and 13:00 to avoid strong diurnal fluctuations). Please, see Chapter IV for further details.

Figure 12. In situ soil respiration monitoring. a) PVC collar and thermometer inserted in bare soil (inter-canopy) and b) inserted under canopy. c) Portable opaque soil chamber system (EGM-4, PP-systems, Hitchin, UK) measuring CO_2 effluxes under canopy in winter.

We developed two mineralization experiments in the laboratory related to the microbial respiration: the estimation of microbial biomass and of carbon mineralization rates. For both experiences, three soil composite samples were collected in August 2019, right before late-summer rainfall. Soil sub-samples were sieved to 2 mm (fine-earth fraction) to remove leaf litter, but also coarse gravel. Then, samples were air-dried at 25ºC for several days and stored a 4ºC until the experiments.

The first experiment consisted of assessing microbial biomass carbon (C_{mic}) in real time through the substrate induced respiration method (SIR) defined by Anderson and Domsch (1978). The SIR method assumes that the magnitude of microbial biomass is closely related to the emission of CO_2 of such microorganisms (microbial respiration) as a consequence of the organic substrate decomposition (García et al., 2003). Such respiration can be stimulated by adding an organic substrate easy to decompose. We used a saturated glucose solution that was incorporated into 15 g of soil [12 samples x 2 sites (under- and inter-canopy) x 3 replicates] previously incubated for 24 h in glass jars with water. The glass jars with the soil samples were sealed with plastic gas-tight lids that had septum ports with

rubber septa. Soils were incubated with controlled and maintained conditions of humidity (65% of soil water holding capacity) and temperature (25ºC) for 6h. A volume of 0.5 ml of air from the sealed jars was captured to assess CO_2 concentration using an infrared CO_2 Analyser (Q-box SR1LP Soil respiration package, Qubit Systems, Canada) (Fig. 13). Then, we estimated C_{mic} according to the recalibration of West and Sparling (1986) at 25ºC (eq. 2) from the original equation of Anderson and Domsch (1978):

$$C_{mic} \text{ (µg g}^{-1}\text{soil)} = 32.8 \times (\text{µl } CO_2 \text{ g}^{-1}\text{soil h}^{-1}) + 3.7 \qquad (2)$$

Figure 13. Soil sample a) preparation, b) incubation, and c) analysis with an infrared CO_2 Analyser.

The second experiment consisted of the evaluation of soil mineralization dynamics. In this case, dry soil samples were pre-incubated for 24 h at 25ºC. Then water was added, samples were sealed, and the first measurement was obtained one hour afterwards to capture the initial pulse of CO_2. The same conditions of humidity (65% of soil water holding capacity) and temperature (25ºC) were maintained throughout the experiment. A volume of 0.5 ml of air was obtained from the sealed jars and CO_2 concentration was immediately measured with the infrared CO_2 Analyzer. After each measurement, the jars with the samples were opened to refresh the headspace with the room air and then sealed until the next day. We continued measuring CO_2 concentration every 24h for 23 days.

Soil properties analyses

Two carbon fractions were analyzed: (1) total organic carbon content (TOC) and (2) water extractable organic carbon (WEOC). TOC was estimated with the modified Walkley-Black method. This method consists of a reaction carried out with $K_2Cr_2O_7$ and H_2SO_4

(Mingorance et al., 2007). Cr_3^+ resulting from organic C oxidation was determined by spectrophotometry using a UV-spectrophotometer. WEOC was extracted following the procedure described in Embarcher et al. (2007) (Fig. 14). Briefly, 25 g of soil sample was shaken for 30 min with 10 mM $CaCl_2$ with a soil:solvent ratio of 1:2 (w/w). The solution was centrifuged for 15 min at 6000 rpm to accelerate the subsequent filtration. Then, part of the solution was desiccated, and the carbon content estimated from the residue using the modified Walkley-Black method.

Figure 14. Procedure for analyzing carbon fraction. a) Soil solution mixture, and b) filtration process, both as part of the procedure for obtaining water extractable organic carbon. c) Colorimetric determination of organic carbon for estimating both TOC and WEOC.

The total nitrogen (N_{tot}) determination was carried out by elemental analysis with a Leco TruSpec CN analyzer, using finely ground soil samples. The carbon/nitrogen ratio was obtained from this variable and organic carbon.

We also estimated principal nutrients in soil solution (nitrate, phosphate, sulphate, and chloride) using the liquid extraction method in a 1:5 soil/water solution (10 g soil: 50ml water). Once the soil solution was obtained, the anions were measured by liquid chromatography with a PHOTOSTORE chromatograph, Chromeleon model, using a standard curve with a mixture of anions at concentrations of 0, 5, 10, 15 and 30 ppm.

References

Anderson JPE, Domsch KH (1978) A physiological method for the quantitative measurement of microbial biomass in soils. *Soil Biol Biochem*, 10:215–221.

Brand WA, Geilmann H, Crosson ER, Rella CW (2009) Cavity ring-down spectroscopy versus high-temperature conversion isotope ratio mass spectrometry; a case study on δ^2H and δ^{18}O of pure water samples and alcohol/ water mixtures. *Rapid Commun Mass Spectrom*, 23: 1879–1884.

De Bello F, Lavorel S, Díaz S, et al (2010) Towards an assessment of multiple ecosystem processes and services via functional traits. *Biodivers Conserv*, 19:2873–2893.

Cornelissen JHC, Lavorel S, Garnier E, et al (2003) A handbook of protocols for standardised and easy measurement of plant functional traits worldwide. *Aust J Bot*, 51:335.

Delgado-Baquerizo M, Maestre FT, Gallardo A, et al (2013) Decoupling of soil nutrient cycles as a function of aridity in global drylands. *Nature*, 502:672–676.

Diaz S, Cabido M, Casanoves F (1998) Plant functional traits and environmental filters at a regional scale. *J Veg Sci*, 9:113–122.

Embacher A, Zsolnay A, Gattinger A, Munch JC (2007) The dynamics of water extractable organic matter (WEOM) in common arable topsoils: I. Quantity, quality and function over a three year period. *Geoderma*, 139, 11–22.

Fenner M (1998) The phenology of growth and reproduction in plants. *Perspect Plant Ecol Evol Syst*, 1:78–91.

García JPG, Caparrós ÁS, Pérez EC, et al (2004) Hidrogeoquimica de las aguas subterráneas en la zona de cabo de gata. 10

García C, Gil F, Hernandez T, Trasar C (2003) Técnicas de análisis de parámetros bioquímicos en suelos: medida de actividades enzimáticas y biomasa microbiana. Madrid-España. 371 p.

Gázquez F, Mather I, Rolfe K, et al (2015) Simultaneous analysis of ^{17}O/^{16}O, ^{18}O/^{16}O and ^{2}H/^{1}H of gypsum hydration water by cavity ringdown laser spectroscopy. *Rapid Commun Mass Spectrom*, 21: 1997–2006.

Gorai M, Maraghni M, Neffati M (2010) Relationship between phenological traits and water potential patterns of the wild jujube *Ziziphus lotus* (L.) Lam. In southern Tunisia. *Plant Ecol Divers*, 3:273–280.

Klein T (2014) The variability of stomatal sensitivity to leaf water potential across tree species indicates a continuum between isohydric and anisohydric behaviours. *Funct Ecol*, 28:1313–1320.

Lang L, Wang X, Hasi E, Hua T (2013) Nebkha (coppice dune) formation and significance to environmental change reconstructions in arid and semiarid areas. *J Geogr Sci,* 23:344–358.

Lavorel S, Garnier E (2002) Predicting changes in community composition and ecosystem functioning from plant traits: revisiting the Holy Grail: *Plant response and effect groups*. *Funct Ecol,* 16:545–556.

Luo W, Zhao W, Liu B, Zhou H (2020) Nebkhas play important roles in desertification control and biodiversity protection in arid and semi-arid regions of China. *Ecosyst Health Sustain,* 6:1844550.

Machado MJ, Benito G, Barriendos M, Rodrigo FS (2011) 500 Years of rainfall variability and extreme hydrological events in southeastern Spain drylands. *J Arid Environ,* 75: 1244–1253.

Martín-Gómez P, Barbeta A, Voltas J, et al (2015) Isotope-ratio infrared spectroscopy: a reliable tool for the investigation of plant-water sources? *New Phytol* 207:914–927.

Mingorance MD, Barahona E, Fernández-Gálvez J (2007) Guidelines for improving organic carbon recovery by the wet oxidation method. *Chemosphere,* 68 (3): 409–413.

Mota JF, Peñas, J, Castro, H, et al (1996) Agricultural development vs biodiversity conservation: the Mediterranean semiarid vegetation in El Ejido (Almería, southeastern Spain). *Biodivers Conserv,* 5, 1597–1617.

Mori A, Niinemets Ü (2010) Plant responses to heterogeneous environments: scaling from shoot modules and whole-plant functions to ecosystem processes. *Ecol Res,* 25:691–692.

Ochoa-Hueso R, Eldridge DJ, Delgado-Baquerizo M, et al (2018) Soil fungal abundance and plant functional traits drive fertile island formation in global drylands. *J Ecol,*106:242–253.

Oyonarte C, Rey A, Raimundo J, et al (2012) The use of soil respiration as an ecological indicator in arid ecosystems of the SE of Spain: Spatial variability and controlling factors. *Ecol Indic,* 14:40–49.

Pérez-Harguindeguy N, Díaz S, Garnier E, et al (2013) New handbook for standardised measurement of plant functional traits worldwide. *Aust J Bot,* 61:167.

Pérez-Priego O, Testi L, Orgaz F, Villalobos FJ (2010) A large closed canopy chamber for measuring CO2 and water vapour exchange of whole trees. *Environ Exp Bot,* 68(2):131–138.

Reynolds James F., Smith D. Mark Stafford, Lambin Eric F., et al (2007) Global Desertification: Building a Science for Dryland Development. *Science,* 316:847–851.

Rey PJ, Cancio I, Manzaneda AJ, et al (2018) Regeneration of a keystone semiarid shrub over its range in Spain: habitat degradation overrides the positive effects of plant–animal mutualisms. *Plant Biol,* 20:1083-1092.

Römermann C, Bucher SF, Hahn M, Bernhardt-Römermann M (2016) Plant functional traits – fixed facts or variable depending on the season? *Folia Geobot,* 51:143–159.

Sack L, Melcher PJ, Liu WH, et al (2006) How strong is intracanopy leaf plasticity in temperate deciduous trees? *Ame J Bot,* 93:829–839.

Salguero-Gómez R, Casper BB (2011) A hydraulic explanation for size-specific plant shrinkage: developmental hydraulic sectoriality. *New Phytol,* 189:229–240.

Sánchez-Gómez P, Carrión MA, Hernández A, Guerra J (2003) *Libro Rojo de la Flora Silvestre protegida de la región de Murcia*. Consejería de Agricultura, Agua y Medio Ambiente, Murcia.

Schlesinger WH, Andrews JA (2000) Soil respiration and the global carbon cycle. Biogeochemistry, 48, 7–20.

Tengberg A, Chen D (1998) A comparative analysis of nebkhas in central Tunisia and northern Burkina Faso. *Geomorphology,* 22:181–192.

Tirado R (2009) 5220 Matorrales arborescentes con Ziziphus (*). In VV.Aaaa., Bases ecológicas preliminares para la conservación de los tipos de hábitat de interés comunitario en España. Ministerio de Medio Ambiente, y Medio Rural y Marino. 68 p.

Tirado R, Pugnaire FI (2003) Shrub spatial aggregation and consequences for reproductive success. *Oecologia,* 136:296–301.

Tyree MT, Ewers FW (1991) The hydraulic architecture of trees and other woody plants. *New Phytol* 119:345–360.

Vallejos A, Sola F, Yechieli Y, Pulido-Bosch A (2018) Influence of the paleogeographic evolution on the groundwater salinity in a coastal aquifer. Cabo de Gata aquifer, SE Spain. *J Hydrol* 557:55–66.

Wang X, Ma Q, Jin H, et al (2019) Change in Characteristics of Soil Carbon and Nitrogen during the Succession of Nitraria Tangutorum in an Arid Desert Area. *Sustainability,* 11:1146.

Werner C, Schnyder H, Cuntz M, et al (2012) Progress and challenges in using stable isotopes to trace plant carbon and water relations across scales. *Biogeosciences,* 9:3083–3111.

West AW, Sparling GP (1986) Modifications to the substrate-induced respiration method to permit measurement of microbial biomass in soils of differing water contents. *J Microbiol Methods,* 5:177–189.

3.RESULTS

CHAPTER I: Modular growth and functional heterophylly of the phreatophyte *Ziziphus lotus*: A trait-based study

M. Trinidad Torres-García, María J. Salinas-Bonillo, Manuel Pacheco-Romero, Javier Cabello

Department of Biology and Geology, Andalusian Centre for the Monitoring and Assessment of Global Change (CAESCG), University of Almería, Spain

ABSTRACT

The variation of plant functional traits, from the cell to the whole-plant level, is a central question in trait-based ecology with regard to understanding ecological strategies and adaptations that result from environmental drivers. Here, we analyzed whole-plant and leaf traits of the phreatophyte *Ziziphus lotus* (L.) Lam., a long-lived shrub that dominates one of the few terrestrial groundwater-dependent ecosystems (GDEs) in Mediterranean Basin drylands. We (a) assessed architectural traits and growth patterns, (b) analyzed leaf morpho-functional traits (specific leaf area, SLA, and stomata pore index, SPI) and physiological traits (gas exchange rates), as well as their variations within individuals, and (c) evaluated temporal variations in modular growth (i.e., sequential iteration of structural units) between growing seasons and in leaf traits within seasons. *Z. lotus'* growth pattern was based on the repetition of modules composed of shoots (short and long) and branches (flowering and plagiotropic) that promoted a functional differentiation between vegetative and reproductive structures, respectively. We identified morpho-functionally distinct leaves (i.e., heterophylly) borne on different types of branches. Leaves on flowering branches had higher SLA and water use efficiency (WUEi), but lower SPI and transpiration rates than leaves on vegetative ones. We also observed trade-offs in the elongation of vegetative and flowering structures between growing seasons: the shorter the long shoots, the larger the flowering branches. The modular differentiation and heterophylly of *Z. lotus* might contribute to prioritizing the investment of resources of this phreatophyte, either for growth or reproduction, and could improve the efficiency in uptake and conservation of resources in drylands.

Keywords: functional traits, heteroblasty, modular unit, plant architecture, Rhamnaceae.

INTRODUCTION

Plant functional traits are any morphological, physiological, or phenological characteristic of the individuals that affect plant fitness (Pérez-Harguindeguy et al., 2013). The study of functional traits has enhanced our understanding about plant performance in a variety of contexts, from xeric (Carlson et al., 2016) to mesic environments (Peguero-Pina et al., 2012), and from grasslands (Herz et al., 2017) to forests (Yin et al., 2018). The intraspecific variability of such traits, which can occur among and within individuals, is shaped by genetic variation and phenotypic plasticity in response to the environment (Albert et al., 2010). Such responses at individual level determine those of populations and communities and hence, regulate the functioning of the ecosystem (Garnier et al., 2016). In terrestrial groundwater-dependent ecosystems (GDEs), dominated by phreatophytes, plants mostly respond to changes in the hydrologic regime (Eamus et al., 2006). However, how functional traits vary with environmental conditions, from the cell to the whole-plant level, is still a central question in trait-based ecology (Shipley et al., 2016), since it contributes to gaining insights about plant ecological strategies (Lavorel and Garnier, 2002).

Plant architecture is the result of the equilibrium between endogenous growth and environmental constraints and represents a critical whole-plant adaptation (Barthélémy and Caraglio, 2007). Plants are modular organisms that grow by the repetition of basic functional units (i.e., buds, shoots, branches) (Harper, 1997), whose shape, size, and number can show intraspecific variability in response to environmental factors (Barthélémy and Caraglio, 2007; Jarčuška and Milla, 2012; Mori and Niinemets, 2010). Notably, plants can respond to biotic and abiotic factors altering their morphology, growth, or reproductive pattern at the module level (Kawamura, 2010; She et al., 2017). In the arid and semiarid regions of the Mediterranean Basin, where plant species with different biogeographical origins converge, a great diversity of adaptations can be observed (Nardini et al., 2014). Branching architecture and spinescence, for example, are whole-plant traits related to defense against herbivores (Pérez-Harguindeguy et al., 2013). Modular architectures in resource-poor environments foster the concentration of water and nutrients in specific sections of the plant, limiting the transfer of such scarce resources to the whole canopy (Salguero-Gómez and Casper, 2011). Likewise, differences in light conditions, either xeric or mesic environments, can promote heterogeneity in bud size and number, or even in

leaves with different morphological and physiological properties (e.g., shade vs sun leaves) that contribute to light capture and the photosynthetic efficiency of the plants (de Kroon et al., 2005). Modularity emerges as a strategy to allocate resources to adapt to contrasting environments (Harper, 1997). To better understand how environmental factors affect the performance of woody plants with complex and large architecture such as trees and shrubs, trait-based studies at module level are recommended (de Kroon et al., 2005; Kawamura, 2010).

Leaves are the organs that most rapidly respond to environmental factors such as water stress (Hao et al., 2017). Differences in leaf shape, reduced leaf area, and low stomatal densities are mechanisms for dealing with drought conditions (Hao et al., 2017). A particularly adaptive mechanism that numerous plants display to optimize their response to environmental heterogeneity is heterophylly, i.e., exhibiting notable differences in leaf morphology within a single individual (Leigh et al., 2011; Nakayama et al., 2017). Examples of heterophylly are observed in aquatic plants with submerged and floating leaves (Nakayama et al., 2017), in terrestrial plants with sun/shade leaves (Sack et al., 2006), or in plants that develop different types of shoots (short vs long) (Leigh et al., 2011). Leaf morphology affects leaf functioning (i.e., photosynthetic rates, transpiration, energy balance) and plays an essential role in adapting plants to environmental conditions (Kusi and Karsai, 2020; Larcher, 2003; Mishio et al., 2007). Although several studies investigate intra-crown variability of leaf functional traits (Hao et al., 2017; Tanaka-Oda et al., 2010; Vlasveld et al., 2018), species are commonly described by mean trait values and intraspecific and/or intra-individual variability is often neglected (Albert et al., 2010). The context-dependence of functional traits encourages the accurate characterization of such traits within species (Funk et al., 2017) and at the module level, particularly in the current changing environment.

We focus on the long-lived and winter-deciduous phreatophyte *Ziziphus lotus* (L.) Lam. (Rhamnaceae), a native shrub from North Africa, Middle East, and South Europe (mainly Spain) (Sánchez-Gómez et al., 2003), where constitutes one of the few GDEs in European drylands (Guirado et al., 2018). This arborescent cushion-like shrub develops deep roots up to 60 meters (Le Houérou, 2006) to reach the water table, and has been recently identified as a facultative phreatophyte with anisohydric behavior (Torres-García et al.,

2021). Besides, *Z. lotus* is the engineer species of an ecosystem under particular conservation concern in Europe (92/43/EEC Habitats Directive). In this study, we aimed to assess whole-plant and leaf traits as well as their temporal variations to understand better the functioning of this species that dominates a GDEs in the Mediterranean basin drylands. We aimed for (1) identifying architectural and growth patterns, (2) assessing leaf morpho-functional and physiological traits as well as their variations within individuals, and (3) evaluating temporal variations in modular growth (i.e., sequential iteration of structural units) between growing seasons and in leaf traits within the season.

METHODOLOGY

Study site and methodological design

We conducted the study in the coastal plain of the Cabo de Gata-Nijar Natural Park (36°49′20″N, 2°16′50″W) in the southeast of Spain, where the most extensive and best-preserved population of *Z. lotus* in Europe is located (Cancio et al., 2017; Rey et al., 2018; Tirado, 2009). Climate is characterized by mild mean annual temperatures (18°C) and scarce precipitation (220 mm year^{-1}) with a typically Mediterranean interannual variation (i.e., precipitation is unevenly distributed within the year, mainly occurring during autumn and winter) (Machado et al., 2011). Previous studies confirm the facultative dependence on groundwater of *Z. lotus,* which can be uptaken up to 25 m deep in the study area (Torres-García et al., 2021). Here, we selected 24 individuals of *Z. lotus* for sampling and monitoring growth architecture, phenology, and morpho-functional and physiological traits during the species growing season (from April to October) (Table 1). We obtained meteorological data (monthly precipitation, mean temperature, and mean total evapotranspiration) during the three years of the research from a weather station 8 km from the study area, for results discussion.

Table 1. Summary of traits and variables assessed in this study.

Type of trait	Variable	Unit	Number[a], period
Whole-plant traits			
Size	Mean Range	cm	24 x 96 axes[b] (2017 – 2019)
Growth	Axes length at the end of the growing season (*one-year elongation*)	cm year^{-1}	24 x 24 axes[I] (2017-2018)
Phenological events	Leaf flushing Leaf abscission Flowering Fruiting		24 individuals (2017 – 2019)
Leaf traits			
Morpho-functional traits	Specific Leaf Area (SLA) Leaf area Leaf dry weight	cm^2 g^{-1} cm^2 mg	24 x 80 leaves[d] (2018)
	Stomatal Pore Index (SPI) Stomata density Stomata length	- no. Mm^{-2} µm	10 x 6 leaves (2018)
Physiological traits	Photosynthetic rate (A) Stomatal conductance (g_s) Transpiration rate I Intrinsic water use efficiency (WUEi)	µmol CO_2 m^{-2} s^{-1} mol H_2O m^{-2} s^{-1} mmol H_2O m^{-2} s^{-1} µmol CO_2/mol H_2O	24 x 8 leaves (May, July, Sep. 2018 – 2019)

(a) Number of samples per plant based on the 24 selected individuals (24 x) except for stomatal measurements with only 10 individuals.

(b) Axes refer to the four different types observed: short and long shoots and flowering and plagiotropic branches, 24 each.

(c) Axes refer to long shoots and flowering branches, 12 each.

(d) All sampled leaves include PB and FB leaves

Definition of *Ziziphus lotus* architecture and modular growth

The aboveground architecture consists of a set of thorny intricate shoots and branches which results from a repeated growth pattern of modular units each growing season. Such modular units are constituted by two types of shoots (short and long) that differed in their ability to elongate, and the branch types they developed (flowering and plagiotropic) (Fig. 1). Short shoots (SSs) have short internodes covered by non-photosynthetic leaves (cataphylls) that protect apical and lateral meristems. The lateral meristems of the SS develop one to six deciduous flowering branches (FBs) at the beginning of the growing season. The apical meristem becomes a long shoot (LS) that produce spiny lateral branches or plagiotropic branches (PBs). Each LS node carries one leaf with two curved stipular spines of equal size at both sides, and two basipetal meristems at the leaf axil. The proximal meristems can seldom produce late flowers although mostly develop SSs, which can potentially repeat the pattern and create new modular units the following growing season. The distal meristem becomes a PB, whose node also carries one leaf with two dimorphic stipular spines at the basis, although no axillary meristems or ramifications are detected. After the first growing season, neither the LSs nor the PBs produces new leaves at their nodes, remaining in the shrub as lignified non-leaved branches. This growth pattern and architecture is discernible along all the axes of the targeted individuals, regardless of their age.

Long shoots and the two types of branches (FBs and PBs) show a zig-zag pseudo-monopodial structure based on the linear succession of short monopodial axis with rhythmic and determined extension (Table 2), according to the concepts proposed by Barthélémy and Caraglio (2007) and to species phylogenetically close to *Z. lotus* (Tourn et al., 1992). However, the shoots grow orthotropically (vertical orientation), and the branches do plagiotropically (horizontal orientation). FBs markedly differ from the so-called PBs because of the complete abscission of the FBs at the end of the growing season. FBs also show bilateral symmetry in their growth with leaves arranged in only one plane.
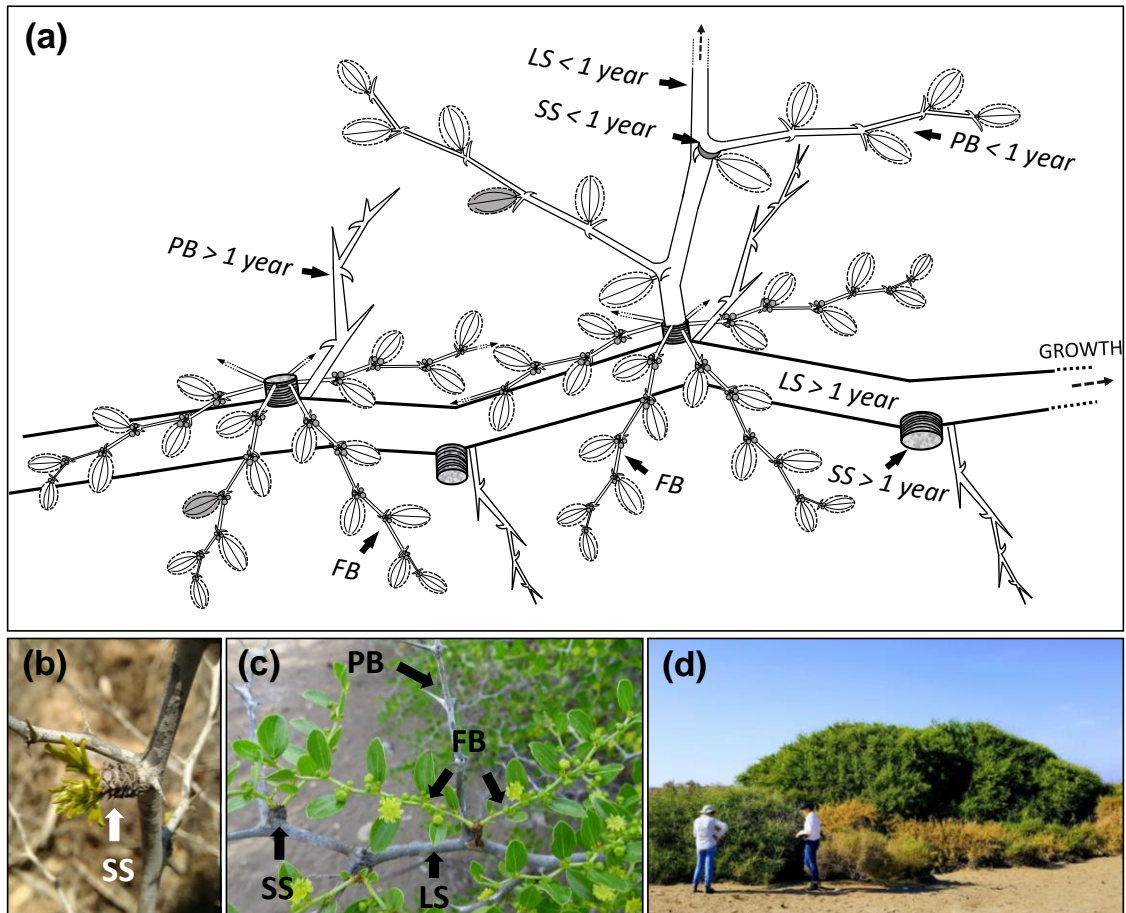
Figure 1. *Ziziphus lotus* architecture. (a) Scheme of a fragment of the long shoot (LS) older than one year that shows the components of the modular unit: short shoots (SSs), flowering branches (FBs), long shoots (LSs), and plagiotropic branches (PBs). The two types of morpho-functionally distinct leaves are shaded. (b) Detail of a short shoot with incipient flowering branches. (c) Detail of fully displayed FBs with buds and flowers, and disposition of the modular parts. (d) General aspect of *Z. lotus* plants in the study area: regular-size plant (front left) compared to the biggest individual in the area (back).

Whole-plant traits

We sampled 24 axes per plant (12 SSs and 12 LSs) distributed around the canopy at four points (north, east, south, and west orientations), to assess the species architecture (Table 1). We examined the whole axes pattern of each individual and tracked the selected shoots and branches throughout three growing seasons (2017, 2018, and 2019) to detect repetition of growth units and quantitatively evaluate the main structural axes (elongation of shoots and branches at the end of 2017 and 2018 growing season).

Table 2. Description of the axes of *Ziziphus lotus*.

	Shoots		Branches	
	Short (SS)	**Long (LS)**	**Plagiotropic (PB)**	**Flowering (FB)**
Growth Whether it is definite or indefinite[a†]	D	D	D	D
Extension Related to a endogenous cessation[b†]	Rh	Rh	Rh	Rh
Direction Related to growth orientation[c†]	O	O	Pla	Pla
Duration Related to the persistence of axes[d*]	P	P	P	De
Symmetry [e†] Related to the disposition of leaves and branches	Ra	Ra	Ra	B

(a) Determined or definite (D) vs. Indetermined or indefinite (I)

(b) Rhythmic (Rh, marked periodicity and cessation of extension) vs. Continuous (Co, no marked cessation)

(c) Plagiotropic (Pla) or horizontal vs. Orthotropic (O) or vertical

(d) Perennial (P) vs Deciduous (De)

(e) Radial (Ra), in all spatial directions vs. Bilateral (B), in one plane

† Concepts proposed by Barthélémy and Caraglio (2007)

* Description of Tourn et al. (1992) for Rhamanceae spp.

Leaf morpho-functional and physiological traits

To assess morpho-functional differences between leaves from different axes, we collected fully expanded sun-exposed leaves in June of 2018 and estimated the specific leaf area (SLA = fresh leaf area (cm^2) / dry mass (g), Pérez-Harguindeguy et al., 2013) and the stomatal pore index (SPI = stomatal density × guard cell length^2, Sack et al., 2003) (Table 1). For SLA, we harvested 80 leaves (10 leaves per branch type and orientation) from each of the 24 individuals around the plant canopy, to cover all intraindividual variability, although differentiating between leaves from flowering and plagiotropic branches. Fresh leaves were scanned using a leaf-area meter, and the area was estimated afterwards with the software Windias 3.2. Subsequently, leaves were oven-dried for 48 hours at 70ºC and weighed. For SPI, six fresh leaves per plant (three per branch type) were collected only from

10 out of 24 individuals because of the amount of time associated with processing and analysis, and we observed less inter- and intra-individual variability for this trait. Fresh leaves were fixed in FAA solution (40% formaldehyde: acetic acid: 50% ethanol; 2: 1: 10. v/v) and dehydrated through an alcohol series (50, 60, 70, 85, and 100%) before visualization. We took three images per leaf of its abaxial side in an area of 48.7 mm^2 with a Scanning Electron Microscope (SEM, Hitachi S-3500N) and measured the size of each stoma with Windias 3.2.

We also assessed gas exchange rates three times during the growing season (May, July, and September of 2018 and 2019) to evaluate physiological differences between leaves. Photosynthetic rate (A), stomatal conductance (g_s), and transpiration rate I were measured in eight leaves per plant (one leaf per branch type and orientation) with an open system infrared analyzer (IRGA) (Li6400XT; Li-Cor Inc., Lincoln, NE, USA) between 10:00 and 13:00 of sunny days. Conditions inside the chamber were maintained at ambient temperature (25 – 30ºC), flow rate of 400 µmol s^{-1}, CO_2 concentration of 400 µmol mol^{-1}, and light intensity of 1800 µmol m^{-2} s^{-1}. The intrinsic water use efficiency (WUEi) that represents the relation between A and g_s was derived afterwards.

Statistical analyses

To identify variations in the growth pattern of the two main types of branches (long shoots and flowering branches), we applied linear mixed effect models (LMM) with maximum elongation (length) of the axes during the growing season as response variable. Year was considered as fixed factors, and the individual plant, as a random effect. To test morpho-functional differences of the leaves that emerge from flowering and plagiotropic branches we applied one-way ANOVA. Finally, LMM was also used for analyzing leaf physiological traits (gas exchange variables) including branch type, month, and their interaction as fixed factors, and individual plant and year were considered as nested, random effects, respectively. Model selection was based on AIC index values (Akaike information criterion). Tukey's HSD test was used for multiple comparison. All variables were log-transformed to normalize model residuals, and analyses performed in Rstudio (Version 1.1.456).

RESULTS

***Ziziphus lotus* architecture and modular growth: whole-plant traits**

The size of short shoots (SSs) ranged between 0.11 and 2.09 cm (Table 3). They grow orthotropically by developing new cataphylls every growing season, and hence, the number of cataphylls and the size of the SSs depend on the age. Long shoots (LSs), with long internodes, elongated up to 129 cm year^{-1}, and produced plagiotropic branches (PBs) with a length of 9.40 cm on average. Likewise, flowering branches (FBs) emerged from the lateral meristems of the SSs and elongated up to 12.5 cm year^{-1}. FBs developed 1–7 flowers arranged in a dense dichasial cyme. Blooming occurs in such FBs in late spring (May-June) whereas fruiting happens at the beginning of the summer (June–July) (Fig. 2). On the contrary, the apical meristems of the SS eventually produce a long shoot (LS) at any time of the growing season, from the leaf flushing period (Fig. 2).

Table 3. Mean size (± standard error) and range (cm) of *Ziziphus lotus* shoots and branches

	Shoots		Branches	
	Short (SS)	**Long (LS)**	**Plagiotropic (PB)**	**Flowering (FB)**
Mean ± SE	0.71 ± 0.02	26.3 ± 0.67	9.40 ± 0.56	7.50 ± 0.08
Range	0.11 – 2.09	2.8 – 129	5.05 – 20.3	2.5 – 12.5

The elongation of the main types of branches (LSs and FBs) was significantly different between growing seasons ($P < 0.001$) (Fig. 3). The highest mean values of LSs were observed in 2017 (39.8 cm year^{-1}), whereas the lowest elongation occurred in 2018 (24.37 cm year^{-1}). Contrary, FBs showed higher mean elongation in 2018 compared to 2017 (7.00 and 5.59 cm year^{-1}, respectively).
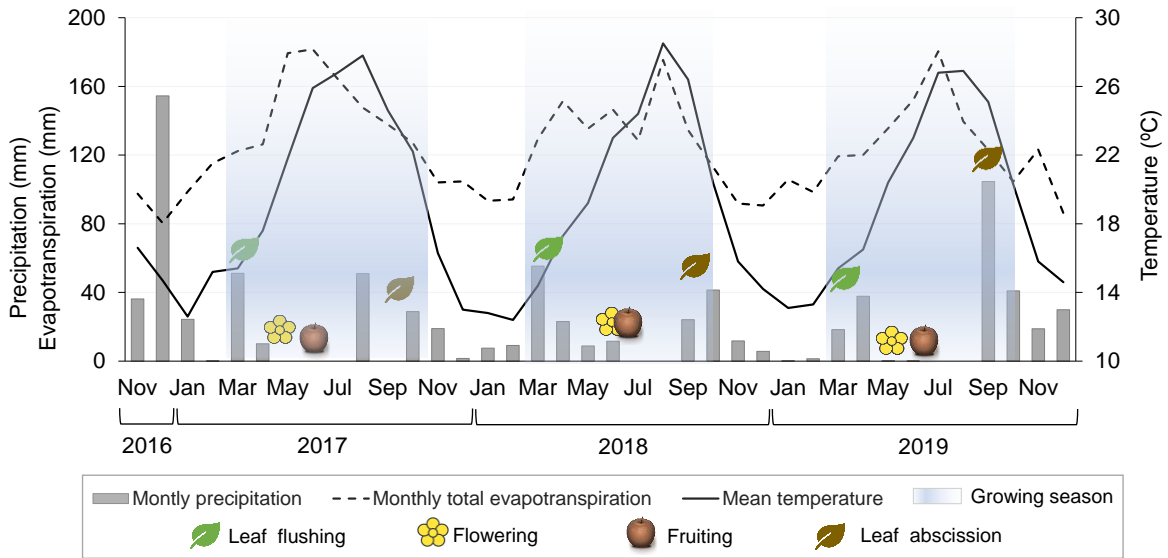
Figure 2. Meteorological data (bars and lines) and phenological events (icons) during the studied period (from November 2016 to December 2019).
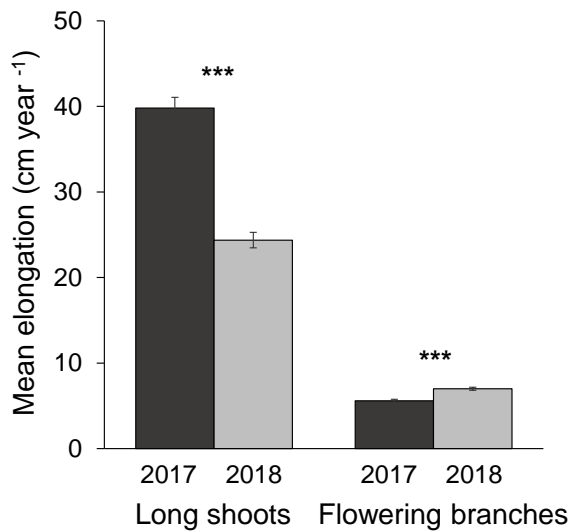
Figure 3. Mean elongation (cm year^{-1}) of long shoots and flowering branches of *Ziziphus lotus* at the end of two growing seasons (2017 and 2018). Significance: *** $P < 0.001$. Error bars represent standard error.

Leaf morpho-functional and physiological traits

Stomatal density was higher for leaves of vegetative shoots (i.e., PBs) compared to those of reproductive shoots (i.e., FBs) (Fig. 4, Fig. 5a). Likewise, SPI was higher in PB leaves, although stomatal length was not significantly different between leaf types. Leaves of PBs were larger and heavier, and therefore showed lower SLA than FB leaves (Fig. 5d, e and f). Regarding gas exchange rates, stomatal conductance (g_s) and transpiration rate I were higher, and water use efficiency (WUEi) lower in PB leaves (Fig. 5g, h, I and h). On the

contrary, photosynthetic rate (A) did not show significant differences between leaf types. When evaluating throughout the growing season, significant differences between leaves were observed (P < 0.001) (Fig. 6). PB and FB leaves had similar rates of g_s and E during most of the season. It was just in September when they differed, and higher values g_s and E were observed in PB leaves (Fig. 6b and c). Conversely, leaves showed significant differences in A at the end of summer (September), and also in Spring (May) when FB leaves had higher values (Fig. 6a). WUEi was higher just at the beginning of the growing season in FB leaves (Fig 6d). Independent of the type of leaves, higher values of A, g_s, and E were observed in *Z. lotus* plants in summer (July and September).
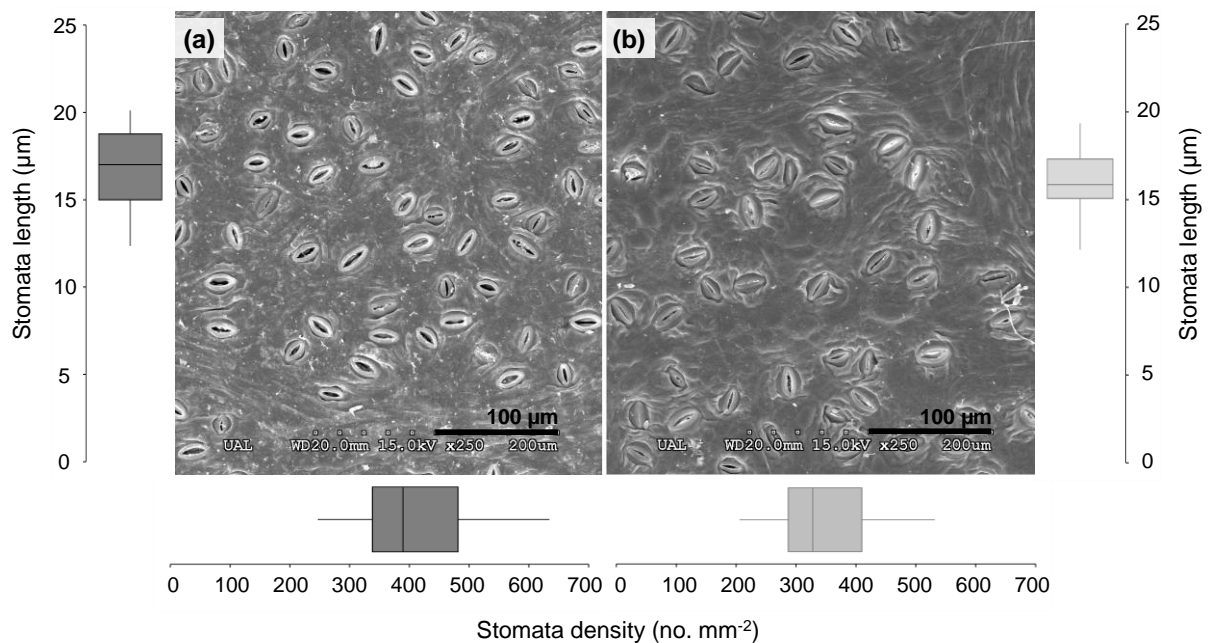
Figure 4. Scanning Electron Microscope (SEM) images of *Ziziphus lotus* stomata. (a) Section of a leaf from plagiotropic branches (PBs); (b) Section of a leaf from flowering branches (FBs). The distribution of stomata pore length (μm) and density (number of stomata per mm^2) are shown for each leaf type.
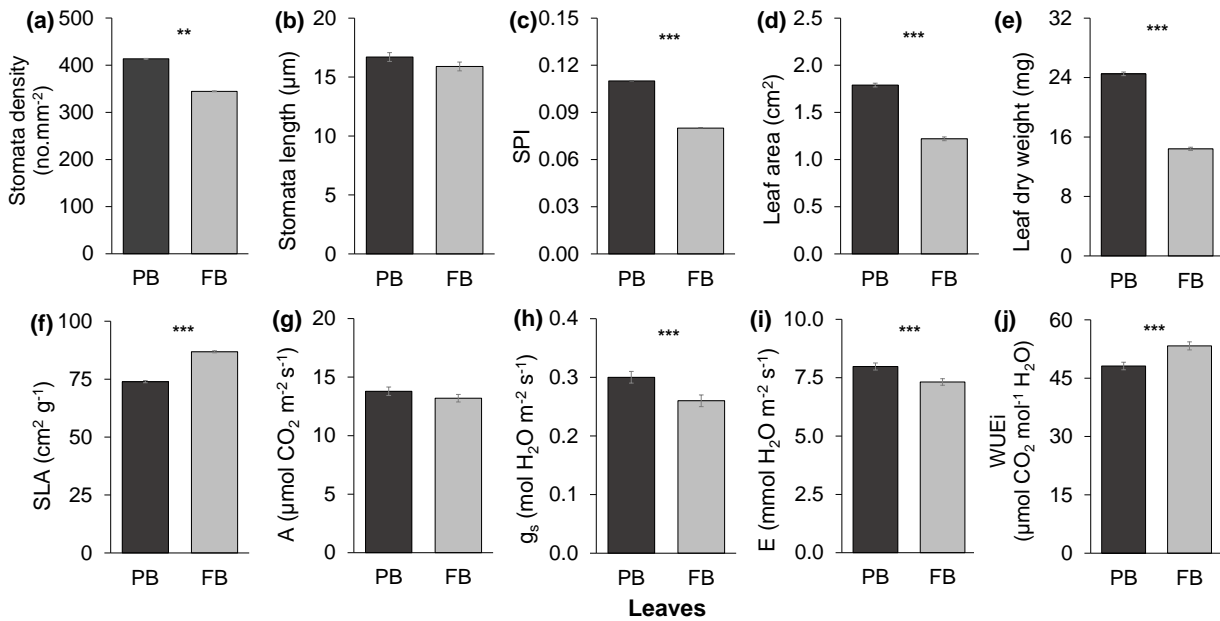
Figure 5. Differences in morpho-functional and physiological characteristics between leaves of plagiotropic (PB) and flowering branches (FB). Error bars represent standard error. Significance from one-factor ANOVA (in the case of morpho-functional traits) and LMM (in physiological traits) testing for effects of leaf type: ***$P < 0.001$; **$P < 0.01$; no data: no significant.

DISCUSSION

Modular growth and cage architecture of *Ziziphus lotus*

The growth pattern of the long-lived shrub *Z. lotus* is based on the seasonal repetition of modular units composed of shoots (short and long) and branches (flowering and plagiotropic), which have different states of differentiation and specialization frequently observed in structurally complex woody species (Barthélémy and Caraglio, 2007). We identified SSs as the basis of *Z. lotus* growth since they could develop orthotropic vegetative shoots (i.e., LSs) as well as plagiotropic reproductive branches (i.e., FBs). Both the bilateral symmetry observed in FBs and the great and nearly exclusive production of floral organs, associated these branches with reproductive and photosynthetic functions (Barthélémy and Caraglio, 2007). Leaves from FBs showed higher photosynthetic rates in May when flowering was at its peak. On the contrary, LSs and their PBs, with radial symmetry, coupled with vegetative growth and space colonization (Leigh et al., 2011). This suggests that LSs could mainly be involved in spatial exploitation, providing their leaves in PBs an extensive foliar surface for assimilation function during their first growing season (Barthélémy and Caraglio, 2007). In the following season, these PBs (and the oldest ones)

remain in the LSs constituting a system of non-leaf woody spiny branches. This type of growth produces a whole-plant intricate and dense structure, the so-called "cage" architecture (Charles-Dominique et al., 2017). Such architecture is frequently described in woody species that grow in environments with high herbivores pressure, being a response to such selective force (Charles-Dominique et al., 2016). This may be the case of *Ziziphus* species (approximately 140 taxon), as they are usually pantrotical distribution thorny shrubs which have evolved in habitats with intense herbivory (Islam and Simmons, 2006). These findings provide further insight into the functional differentiation of structural components of large shrubs with a complex growth like *Z. lotus*.
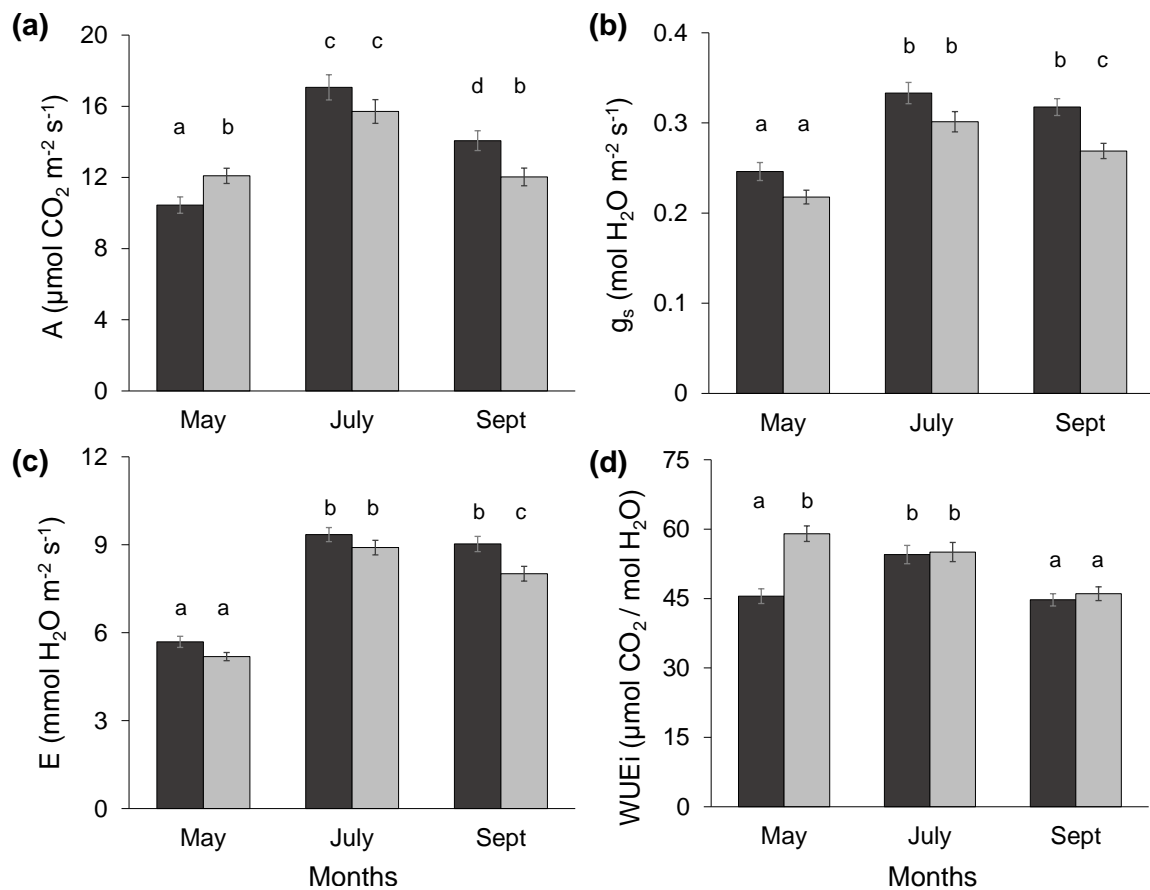
Figure 6. Foliar gas exchange rates for the two different leaves (Plagiotropic branch leaves: dark bars; Flowering branch leaves: light bars) of *Ziziphus lotus* in May, July, and September. (a) Photosynthetic rate, A, (b) stomatal conductance, g_s, (c) transpiration rate, E, and (d) intrinsic water use efficiency, WUEi. Error bars show the standard error and letters indicate significant differences between leaf types and month ($P < 0.001$) from the linear mixed effect model (LMM).

Differences in leaf traits revealed functional heterophylly

Morpho-functional differences found between the two types of leaves (from flowering and plagiotropic branches) proved *Z. lotus* heterophylly. The deciduous FBs developed leaves with reduced leaf area and high SLA, which is a trait negatively related to leaf sclerophylly, longevity, and gas exchange rates (Pérez-Harguindeguy et al., 2013). FBs require extra water and energy for reproductive functions (Fenner, 1998; Moore, 1992), and therefore more efficient leaves are needed. As smaller leaves have a greater capacity for maintaining leaf temperature closer to ambient levels (Jones 2001), the amount of water lost by transpiration is reduced in FB leaves, increasing their WUEi. Additionally, such leaves with lower stomatal density might reduce the investment in stomatal production and maintenance, while maintaining photosynthetic rate (Carlson et al., 2016). Stomata represent the gate that connects plants with the atmosphere, playing a pivotal role in the balance between CO_2 uptake for photosynthesis and water loss during transpiration (Bucher et al., 2016; Xu and Zhou, 2008). Likewise, the relation between stomata size and density, reflected in SPI, has an impact on gas exchange and determines the maximum stomatal conductance (Nobel, 1999). Thus, the smaller leaf size and lower stomatal density of FB leaves might be an adaptation related to higher water use efficiency and plant productivity in xeric environments (Peguero-Pina et al., 2020).

Plagiotropic branches, which are involved in branch extension, developed leaves related to vegetative growth with lower SLA and higher stomatal density and SPI. Furthermore, the plagiotropic position of these branches might increase light interception and leaf overheating, having a positive effect on transpiration rates (Peguero-Pina et al., 2020). However, we observed a vertical orientation of PB leaves (erectophily) widely described in drylands, which could reduce energy inputs while maintaining the cooling effect of transpiration (Leigh et al., 2017). Thus, higher stomatal density and SPI, coupled with larger leaves that require further transpirative efforts to dissipate heat in drylands, might explain the higher rates of water loss (i.e., higher transpiration rate, E) of PB leaves. Additionally, because of similar photosynthetic rates but higher stomatal conductance, PB leaves were less efficient in the use of water (i.e., lower WUEi) than FB leaves. Therefore, heterophylly supports the functional difference between leaves related to the reproductive branches and leaves in charge of capturing the resources for vegetative growth.

Variations in whole-plant and leaf traits

Disentangling the species' modular growth is essential for identifying modular response, which can be related to the variability of resource availability (Kawamura, 2010). Considering that Z. lotus is a facultative phreatophyte that constitutes GDEs in arid regions (Guirado et al., 2018; Tirado, 2009; Torres-García et al., 2021), water availability might not be a limiting factor for growing during the dry season. We observed that LSs can emerge at any time of the growing season, although preferably they do it at the beginning of spring, elongating up to late summer. Even though the mechanisms that promote the activation and further elongation of the apical meristem to develop LSs are not clear enough, evidence suggests that abiotic signals such as light, temperature, or resource availability would be involved (Leigh et al., 2011). In the case of this facultative phreatophyte, continuous groundwater availability throughout the season might assure the LS elongation. However, the greater elongation of such shoots was observed during the driest years with scarce spring precipitation (2017), in contrast to FBs that extended more during the wet spring of 2018 (Fig. 3). Although the growth of *Z. lotus* shoots and branches showed significant inter-annual differences, such variation cannot be fully attributed to meteorological conditions, and could be associated with a cyclic phenomenon of resource investment. In this sense, long-term monitoring would contribute to gain insights into the growth patterns of such facultative phreatophytes and their relationship with climate.

The functional heterophylly observed in *Z. lotus* differed throughout the growing season. Previous studies showed that groundwater availability and anisohydric characteristic of *Z. lotus* promote higher gas exchange levels during the Mediterranean summer (Torres-García et al., 2021). Here, we show how such increases depended on the leaf functional type. At the beginning of the season, higher carbon assimilation is needed in FB leaves to overcome the energy-investment in reproductive organs formation (Fenner, 1998). Conversely, at the end of the summer, leaves from FBs reduced their transpiration rates, whereas the PB leaves maintained it. After flowering and fruiting, and shortly before leaf abscission, reproductive leaves lose their functionality earlier than vegetative ones as a result of the easier decomposition nature of higher-SLA leaves (Pérez-Harguindeguy et al., 2013). The higher degree of sclerophylly (referred to low-SLA leaves) can be related to

enhanced wilting resistance of PB leaves, which would allow maintaining transpiration rates for longer under drought stress (Costa-Saura et al., 2016). Our findings are consistent with the hypothesis that heterophylly is an advantage to overcome temporal variability and to adapt to environmentally harsh conditions (i.e., water stress, Moore, 1992).

Developing functionally different modular units might allow *Z. lotus* to prioritize resource allocation either to grow or to reproduce depending on the environmental conditions and resource availability. Our findings suggest an investment trade-off between reproduction and growth widely observed in arid-adapted shrubs (She et al., 2017; Weiner et al., 2009). *Z. lotus* reproduction investment, that can be related to the length of FBs, might be more dependent on wet meteorological conditions at the beginning of the season, whereas vegetative elongation seems decoupled from precipitation. Thus, the greater the reproduction investment (higher elongation of FBs), the lower the growth (lower extension of LSs). These outcomes allow to better understanding the strategy of such long-lived phreatophyte to overcome the stressful conditions of drylands. However, climate change projections in the Mediterranean basin for the second half of the XXIst century predict precipitation reductions and temperature increases (Giorgi and Lionello, 2008), that could be to the detriment of *Z. lotus* reproduction. Additionally, the reduction of groundwater reservoirs, also as consequence of the rise in groundwater consumption by the human population (Eamus et al., 2015, 2016; Klove et al., 2014), might limit the growth of this phreatophytic species, jeopardizing its persistence.

CONCLUSIONS

This trait-based analysis allowed us to gain understanding on the functioning of the long-lived phreatophyte *Ziziphus lotus* and to uncover a modular growth pattern that showed temporal variations. Whereas long shoots and plagiotropic branches were focused on vegetative growth and space colonization, particularly during drier and warmer years, flowering branches were in charge of reproductive functions, more largely in wetter conditions. We detected functional differentiation of the modular units and their responses, which was supported by morpho-functional and physiological different leaves (heterophylly). Both modular differentiation and heterophylly might promote the investment of resources to particular functions throughout the growing season, either to

grow or to reproduce. We consider these mechanisms could contribute to regulate *Z. lotus* growth, protect itself against herbivory, and improve its efficiency in uptaking and preservation of resources. The deep root system and modular growth make this species drought-avoiding, whereas the anisohydric behavior and leaf phenology are more related to drought-tolerance strategies. Although groundwater and its continuous use by the plant ensured the development of this phreatophytic species in arid regions, upcoming climate change effects can challenge the persistence of *Z. lotus*. Reduced precipitations and increased atmospheric evaporative demand could lead to groundwater depletions, jeopardizing the survival of this species and the GDE it constitutes in the Mediterranean Basin. These findings will contribute to understanding the strategies and mechanisms that underlie the survival of long-lived woody plants with large architecture, and particularly of those that constitute complex systems such as GDEs in arid regions.

REFERENCES

Albert CH, Thuiller W, Yoccoz NG, et al (2010) Intraspecific functional variability: extent, structure and sources of variation. *J Ecol*, 98: 604-613.

Barthélémy D, Caraglio Y (2007) Plant Architecture: A Dynamic, Multilevel and Comprehensive Approach to Plant Form, Structure and Ontogeny. *Ann Bot* 99:375–407.

Bucher SF, Auerswald K, Tautenhahn S, et al (2016) Inter- and intraspecific variation in stomatal pore area index along elevational gradients and its relation to leaf functional traits. *Plant Ecol* 217:229–240.

Cancio I, González-Robles A, Bastida JM, et al (2017) Landscape degradation affects red fox (Vulpes vulpes) diet and its ecosystem services in the threatened *Ziziphus lotus* scrubland habitats of semiarid Spain. *J Arid Environ* 145:24–34.

Carlson JE, Adams CA, Holsinger KE (2016) Intraspecific variation in stomatal traits, leaf traits and physiology reflects adaptation along aridity gradients in a South African shrub. *Ann Bot*, 117:195–207.

Charles-Dominique T, Barczi JF, Le Roux E, Chamaille-Jammes S (2017) The architectural design of trees protects them against large herbivores. *Funct Ecol*, 13: 1710–1717.

Charles-Dominique T, Davies TJ, Hempson GP, et al (2016) Spiny plants, mammal browsers, and the origin of African savannas. *PNAS*, 113:E5572.

Costa-Saura JM, Martínez-Vilalta J, Trabucco A, et al (2016) Specific leaf area and hydraulic traits explain niche segregation along an aridity gradient in Mediterranean woody species. *Perspect Plant Ecol Evol Syst,* 21:23–30.

De Kroon H, Huber H, Stuefer JF, Van Groenendael JM (2005) A modular concept of phenotypic plasticity in plants: Research review. *New Phytol,,* 166(1), 73–82.

Eamus D, Froend R, Loomes R, et al (2006) A functional methodology for determining the groundwater regime needed to maintain the health of groundwater-dependent vegetation. *Aust J Bot* 54:97.

Eamus D, Fu B, Springer AE, Stevens LE (2016) Groundwater Dependent Ecosystems: Classification, Identification Techniques and Threats. In: Jakeman AJ, Barreteau O, Hunt RJ, et al. (eds) *Integrated Groundwater Management.* Springer International Publishing, Cham, pp 313–346

Eamus D, Zolfaghar S, Villalobos-Vega R, et al (2015) Groundwater-dependent ecosystems: recent insights, new techniques and an ecosystem-scale threshold response. *Hydrol Earth Syst Sci* 12:4677–4754.

Fenner M (1998) The phenology of growth and reproduction in plants. *Perspect Plant Ecol Evol Syst,* 1:78–91.

Funk JL, Larson JE, Ames GM, et al (2017) Revisiting the Holy Grail: using plant functional traits to understand ecological processes. *Biol Revi,* 92: 1156-1173.

Garnier E, Navas M, Grigulis K (2016) *Plant Functional Diversity: Organism traits, community structure, and ecosystem properties.* Oxford University Press.

Giorgi F, Lionello P (2008) Climate change projections for the Mediterranean region. *Glob Planet Change,* 63: 90–104.

Guirado E, Alcaraz-Segura D, Rigol-Sánchez JP, et al (2018) Remote-sensing-derived fractures and shrub patterns to identify groundwater dependence. *Ecohydrology,* 11:e1933.

Harper, J.L. (1977). *Population Biology of Plants.* London, Academic Press.

Hao J, Yue N, Zheng C (2017) Analysis of changes in anatomical characteristics and physiologic features of heteromorphic leaves in a desert tree, Populus euphratica. *Acta Physiol Plant,* 39:160.

Herz K, Dietz S, Haider S, et al (2017) Drivers of intraspecific trait variation of grass and forb species in German meadows and pastures. *J Veg Sci,* 28: 705-716.

Islam MB, Simmons MP (2006) A Thorny Dilemma: Testing Alternative Intrageneric Classifications within Ziziphus (Rhamnaceae). *Syst Bot,* 31:826–842

Jarčuška B, Milla R (2012) Shoot-level biomass allocation is affected by shoot type in Fagus sylvatica. *J Plant Ecol*, 5:422–428.

Jones, CS (2001) The functional correlates of heteroblastic variation in leaves: Changes in form and ecophysiology with whole plant ontogeny. *Bol Soc Argent Bot*, 36:171–184

Kawamura K (2010) A conceptual framework for the study of modular responses to local environmental heterogeneity within the plant crown and a review of related concepts. *Ecol Res*, 25:733–744.

Kusi J, Karsai I (2020) Plastic leaf morphology in three species of Quercus: The more exposed leaves are smaller, more lobated and denser. *Plant Species Biol*, 35: 24– 37.

Larcher W (2003) *Physiological Plant Ecology*. Fourth ed. Springer-Verlag, New York

Lavorel S, Garnier E (2002) Predicting changes in community composition and ecosystem functioning from plant traits: revisiting the Holy Grail: Plant response and effect groups. *Funct Ecol*, 16:545–556.

Le Houérou HN (2006) Agroforestry and silvopastoralism: The role of trees and shrubs (Trubs) in range rehabilitation and development. *Science et changements planétaires/Sécheresse* 17:343–348

Leigh A, Sevanto S, Close JD, Nicotra AB (2017) The influence of leaf size and shape on leaf thermal dynamics: does theory hold up under natural conditions? *Plant Cell Environ*, 40: 237– 248.

Leigh A, Zwieniecki MA, Rockwell FE, et al (2011) Structural and hydraulic correlates of heterophylly in Ginkgo biloba. *New Phytol*, 189:459–470.

Machado MJ, Benito G, Barriendos M, Rodrigo FS (2011) 500 Years of rainfall variability and extreme hydrological events in southeastern Spain drylands. *J Arid Environ*, 75: 1244– 1253.

Mishio M, Kawakubo N, Kachi N (2007) Intraspecific variation in leaf morphology and photosynthetic traits in Boninia grisea Planchon (Rutaceae) endemic to the Bonin Islands, Japan. *Plant Species Biol,* 22: 117-124.

Moore PD (1992) A leaf for all seasons. *Nature,* 360(6400), 110–111.

Mori A, Niinemets Ü (2010) Plant responses to heterogeneous environments: scaling from shoot modules and whole-plant functions to ecosystem processes. *Ecol Res* 25:691–692.

Nakayama H, Sinha NR, Kimura S (2017) How Do Plants and Phytohormones Accomplish Heterophylly, Leaf Phenotypic Plasticity, in Response to Environmental Cues. *Front Plant Sci*, 8:1717.

Nardini A, Lo Gullo MA, Trifilò P, Salleo S (2014) The challenge of the Mediterranean climate to plant hydraulics: Responses and adaptations. *Environ Expe Bot* 103:68–79.

Nobel PS (1999) *Physicochemical and environmental plant physiology*. Academic Press, San Diego, London.

Peguero-Pina JJ, Flexas J, Galmés J, et al (2012) Leaf anatomical properties in relation to differences in mesophyll conductance to CO2 and photosynthesis in two related Mediterranean Abies species. *Plant Cell Environ*, 35: 2121-2129.

Peguero-Pina JJ, Vilagrosa A, Alonso-Forn D, et al (2020) Living in Drylands: Functional Adaptations of Trees and Shrubs to Cope with High Temperatures and Water Scarcity. *Forests*, 11, 1028.

Pérez-Harguindeguy N, Díaz S, Garnier E, et al (2013) New handbook for standardised measurement of plant functional traits worldwide. *Aus J Bot*, 61:167.

Rey PJ, Cancio I, Manzaneda AJ, et al (2018) Regeneration of a keystone semiarid shrub over its range in Spain: habitat degradation overrides the positive effects of plant-animal mutualisms. *J Plant Biol*, 20:1083–1092.

Sack LP, Cowan D, Jaikumar N, Holbrook NM (2003) The 'hydrology' of leaves: co-ordination of structure and function in temperate woody species. *Plant Cell Environ*, 26: 1343–1356.

Sack L, Melcher PJ, Liu WH, et al (2006) How strong is intracanopy leaf plasticity in temperate deciduous trees? *Ame J Bot*, 93:829–839.

Salguero-Gómez R, Casper BB (2011) A hydraulic explanation for size-specific plant shrinkage: developmental hydraulic sectoriality. *New Phytol*, 189:229–240.

Sánchez-Gómez P, Carrión MA, Hernández A, Guerra J (2003) *Libro Rojo de la Flora Silvestre protegida de la región de Murcia*. Consejería de Agricultura, Agua y Medio Ambiente, Murcia.

She W, Bai Y, Zhang Y, et al (2017) Plasticity in Meristem Allocation as an Adaptive Strategy of a Desert Shrub under Contrasting Environments. *Front Plant Sci*, 8:1933.

Shipley B, De Bello F, Cornelissen JHC et al (2016) Reinforcing loose foundation stones in trait-based plant ecology. *Oecologia*, 180: 923–931.

Tanaka-Oda A, Kenzo T, Kashimura S, et al (2010) Physiological and morphological differences in the heterophylly of Sabina vulgaris Ant. In the semi-arid environment of Mu Us Desert, Inner Mongolia, China. *J Arid Environ*, 74:43–48.

Tirado R. (2009). 5220 Matorrales arborescentes con *Ziziphus* (*). In VV.Aaaa., *Bases ecológicas preliminares para la conservación de los tipos de hábitat de interés comunitario en España*. Ministerio de Medio Ambiente, y Medio Rural y Marino. 68 p.

Torres-García MT, Salinas-Bonillo MJ, Gázquez-Sánchez F, et al (2021) Squandering water in drylands: the water-use strategy of the phreatophyte *Ziziphus lotus* in a groundwater-dependent ecosystem. *Ame J Bot*, 108(2): 1–13.

Tourn GM, Tortosa RD, Medan D (1992) Rhamnaceae with multiple lateral buds: an architectural analysis. *Bot J Linn Soc*. 108:275–286.

Vlasveld C, O'Leary B, Udovicic F, Burd M (2018) Leaf heteroblasty in eucalypts: biogeographic evidence of ecological function. *Aus J Bot*, 66:191.

Weiner J, Campbell LG, Pino J, Echarte L (2009) The allometry of reproduction within plant populations. *J Ecol*, 97:1220–1233.

Xu Z, Zhou G (2008) Responses of leaf stomatal density to water status and its relationship with photosynthesis in a grass. *J Exp Bot*, 59:3317–3325.

Yin Q, Wang L, Lei M, et al (2018) The relationships between leaf economics and hydraulic traits of woody plants depend on water availability. *Sci Tot Environ*, 621, 245-252.

CHAPTER II: Squandering water in drylands: the water-use strategy of the phreatophyte *Ziziphus lotus* in a groundwater-dependent ecosystem

M. Trinidad Torres-García[1,2], María J. Salinas-Bonillo[1,2], Fernando Gázquez-Sánchez[1,2], Ángel Fernández-Cortés[1,2], José I. Querejeta[3] and Javier Cabello[1,2]

[1] Department of Biology and Geology, Universidad de Almería, Spain
[2] Andalusian Centre for the Monitoring and Assessment of Global Change (CAESCG), University of Almería, Spain
[3] Centro de Edafología y Biología Aplicada del Segura, Consejo Superior de Investigaciones Científicas (CEBAS-CSIC), Murcia, Spain

ABSTRACT

PREMISE: Water is the most limiting factor in dryland ecosystems, and plants are adapted to cope with this constraint. Particularly vulnerable are hreatophytic plants from groundwater-dependent ecosystems (GDEs) in regions that have to face water regime alterations due to the impacts of climate and land-use changes.

METHODS: We investigated two aspects related to the water-use strategy of a keystone species that dominates one of the few terrestrial GDEs in European drylands (*Ziziphus lotus*): where it obtains water and how it regulates its use. We (1) evaluated plants' water sources and use patterns using a multiple-isotope approach (δ^2H, δ^{18}O, and Δ^{13}C); (2) assessed the regulation of plant water potential by characterizing the species on an isohydric–anisohydric continuum; and (3) evaluated plants' response to increasing water stress along a depth-to-groundwater (DTGW) gradient by measuring foliar gas Exchange and nutrient concentrations.

RESULTS: *Ziziphus lotus* behaves as a facultative or partial phreatophyte with extreme anisohydric stomatal regulation. However, as DTGW increased, *Z. lotus* (1) reduced the use of groundwater, (2) reduced total water uptake, and (3) limited transpiration water loss while increasing water-use efficiency. We also found a physiological threshold at 14 m depth to groundwater, which could indicate maximum rooting length beyond which optimal plant function could not be sustained.

CONCLUSIONS: Species such as *Z. lotus* survive by squandering water in drylands because of a substantial groundwater uptake. However, the identification of DTGW thresholds indicates that drawdowns in groundwater level would jeopardize the functioning of the GDE.

Keywords: anisohydry, arid regions, deep-rooted shrub, foliar nutrient concentration, gas-exchange rates, Rhamnaceae, stable isotopes, water potential, water-use efficiency.

INTRODUCTION

Plant productivity in terrestrial ecosystems of arid regions, covering 41% of Earth's land surface (Reynolds et al., 2007), is limited by water availability (Newman et al., 2006; Nolan et al., 2018). These ecosystems suffer from prolonged drought periods since they are characterized by less annual precipitation than potential evapotranspiration (Newman et al., 2006). Several species can mitigate these constraints by accessing stable groundwater resources (O'Grady et al., 2006). The current and projected precipitation decrease and temperature increase in the Mediterranean Region (Giorgi and Lionello, 2008), along with the increasing demand of groundwater for human use (Eamus et al., 2016), pose a major risk for such species. This is the case of phreatophytes that support groundwater-dependent ecosystems (GDEs) (Kløve et al., 2014; Eamus et al., 2015, 2016), whose decoupled productivity from climate conditions represents a critical ecosystem function for drylands. Exploring the physiological response of such phreatophytes along groundwater depth gradients is key to understanding their response to reductions in water availability (Garrido et al., 2018), both as consequence of climate change and the increase in human demand for groundwater.

Plants have developed coherent physiological and morphological strategies to cope with water limitations (Lambers and Oliveira, 2019). Two main strategies related to the water movement in the soil–plant system have been identified in terrestrial plants that face such constraints: drought avoidance and drought tolerance (Nardini et al., 2014). Drought-avoiding species can minimize water loss (water savers) or maximize water uptake (water spenders), thereby maintaining high tissue water status, whereas drought-tolerant plants go through large fluctuations in water potential while maintaining their metabolic activity (Arndt et al., 2001; Reigosa et al., 2004; Nguyen et al., 2017). Within the drought-avoidance strategy, some plants from arid regions exert strict stomatal control (closing their stomata) to reduce stomatal conductance, thus limiting water loss to keep water potentials within adequate bounds (isohydric species) (Glenn et al., 2013; Martínez-Vilalta and García-Forner, 2016). Other plants reduce their leaf area through leaf shedding during drought to limit transpiration (Newman et al., 2006), or even display a genetically pre-programmed drought-deciduous leaf phenology to avoid water stress during summer when water is scarcer (Sperry and Hacke, 2002). In contrast, some species invest in deep roots to access

more stable water sources and maximize water uptake (Jackson et al., 2000). These species are called phreatophytes (well plants; Meinzer, 1927) and can freely access groundwater (Glenn et al., 2013), although some of them have a limited capacity to maintain stable water potentials (anisohydric species). Anisohydric behavior is not restricted to phreatophytes and is observed in desert shrubs like *Juniperus monosperma* (Engelm.) Sarg. And the shallow-rooted *Larrea tridentata* DC., which also shows plasticity in its hydraulic behavior related to environmental conditions (Guo et al., 2020).

Groundwater-dependent ecosystems are often characterized by the presence of phreatophytes that can vary in their degree of dependence on groundwater (Hultine et al., 2020). A dual-isotope approach offers the potential to gain insight into temporal and spatial variability of plant water sources and the interrelation of carbon and water fluxes (Werner et al., 2012; Eamus et al., 2016). Indeed, stable hydrogen (δ^2H) and oxygen ($\delta^{18}O$) isotopes are used to find out which is the dominant water source for plants, assuming differences in isotopic composition between water sources (Lin and Sternberg, 1993; Dawson et al., 2002). This approach compares the stable isotope composition in xylem water to that in precipitation, soil water, intermediate water of the vadose zone, or groundwater (Moreno-Gutiérrez et al., 2012; Eamus et al., 2015; Rumman et al., 2018; Nolan et al., 2018). Although this approach is based on the assumption that isotopic fractionation does not occur during root water uptake in terrestrial plants (Dawson and Ehleringer, 1991; Dawson et al., 2002), several studies have reported fractionated isotopic signatures in xylem water of xerophytic and halophytic species (Lin and Sternberg, 1993, Ellsworth and Williams, 2007). Particularly, hydrogen isotope fractionation may occur during water uptake in suberized and lignified roots with less-porous membranes, which are associated with salt exclusion functions (Lin and Sternberg 1993). Compared to oxygen, discrimination against deuterium is more common in this type of membranes (Ellsworth and Williams, 2007). Additionally, the carbon stable isotope composition of plant tissues ($\delta^{13}C$) is a widely used ecological indicator of plants function (Dawson et al., 2002). Particularly, leaf carbon isotope discrimination ($\Delta^{13}C$) has been used as a time-integrated measure of intrinsic water-use efficiency (WUEi) that depends on the ratio between intercellular and ambient CO_2 concentration (ci/ca) (Flanagan et al., 1992; Moreno-Gutiérrez et al., 2012; Prieto et al., 2018). Recent studies have shown that leaf (or sapwood) $\Delta^{13}C$ can respond to changes in

rooting depth and groundwater use in phreatophytes; thus, carbon isotopes in leaves can serve as a reliable indicator of depth-to-groundwater (DTGW) in dryland ecosystems (Zolfaghar et al., 2014; Garrido et al., 2016; Rumman et al., 2018).

Depth-to-groundwater is a key variable that defines groundwater availability for phreatophytes (Eamus et al., 2016; Nolan et al., 2017). Differences in rooting patterns among coexisting species promote water-source partitioning and enable them to exploit different ecohydrological niches, which is key for the persistence of functional diverse plant communities in drylands (Zencich et al., 2002; Querejeta et al., 2007; Skelton et al., 2015; Nolan et al., 2017, Guo et al., 2018). Regions with a long dry season, such as Mediterranean climate regions, host species with the deepest root systems (Jackson et al., 1996), but also small shrubs and herbs with other strategies to survive such as sclerophylly or drought-deciduousness (Reigosa et al., 2004). In phreatophytes, hydraulic redistribution is a widely reported strategy that also benefits understory species (Scott et al., 2008). Consisting in lifting water from deeper moist soil layers to shallower dry ones, it contributes to enhance nutrient availability and to maintain the water and carbon balance of the ecosystem at multiple temporal scales (Cardon et al., 2013; Hultine et al., 2020). Likewise, plants nutrients uptake and their accumulation in leaves are mainly driven by water availability (Salazar-Tortosa et al., 2018). Thus, phreatophytes' ability to access permanent water from depth enables plants not only to survive for prolonged rainless periods while keeping stomata open (Zencich et al., 2002), but may also enhance nutrient acquisition and ensure growth (Cardon et al., 2013).

Anisohydric plants show no discernible water potential thresholds for stomatal closure and can maintain high gas exchange rates during the dry season, although they run the risk of xylem cavitation and hydraulic failure (McDowell et al., 2008; Glenn et al., 2013; Nardini et al., 2014; Roman et al., 2015). Thus, anisohydric species generally show higher water usage and primary productivity in drylands than isohydric species, which reduce their stomatal conductance (g_s) under drought stress imposed by conditions such as high atmospheric demand and low soil water availability (McDowell et al., 2008). However, several studies have challenged the concept of fixed hydraulic behavior by showing that individual plants can vary along the isohydry–anisohydry continuum, according to differences in spatiotemporal environmental conditions (Feng et al., 2019; Guo et al., 2020). Whether

phreatophytes are more or less iso- or anisohydric has important implications for the productivity of arid regions (Nolan et al., 2017) and for the ecohydrology of the GDEs (van der Molen et al., 2011; Roman et al., 2015).

Understanding water sources and transport regulation in phreatophytes is key for disentangling GDE functioning and forecasting response patterns to hydrological and climatic changes. Here we incorporate both questions simultaneously into the study of the deep-rooted shrub *Ziziphus lotus* (L.) Lam (Rhamnaceae), an example of keystone species in a GDE of Mediterranean arid region (Le Houérou, 2006). In contrast to drought-deciduous plants that avoid water loss, *Z. lotus* is a winter deciduous species that is photosynthetically active during the dry Mediterranean summer. Previous studies have established the tight spatial relationship between *Z. lotus* distribution and groundwater availability through satellite images (Guirado et al., 2018) although to date no field analyses have proved this dependence conclusively. The main aims of this study were to reveal the degree of dependency and use of groundwater by *Z. lotus* and the mechanism that regulates water transport through the plant along a DTGW gradient. We hypothesized that (1) *Z. lotus* depends on groundwater to sustain its high physiological activity during the dry summer and, consequently, to support the ecosystem functioning. If so, we predicted that (2) greater DTGW will foster more negative plant water potentials and lower stomatal conductance and transpiration (i.e., tighter stomatal regulation and more isohydric behavior), and (3) higher water-use efficiency because of lower groundwater availability and use.

MATERIALS AND METHODS

Study site

The study was conducted on the coastal plain of Cabo de Gata-Níjar Natural Park, southeastern Spain (36°49′20″N, 2°16′50″W) during 2018 and 2019. Climate is typical semiarid Mediterranean characterized by hot and dry summers and mild winters. The mean annual temperature is 18ºC, and mean precipitation is 220 mm/year, which mainly occurs in autumn and winter (Machado et al., 2011). The plain is located over a small and shallow aquifer that belongs to the western part of the larger aquifer Hornillo-Cabo de Gata. Its geological structure corresponds to the foothills of the sedimentary basin of Sierra

Alhamilla mountains (1000 m.a.s.l), ~20 km to the north, and to superimposed Quaternary marine deposits (Vallejos et al., 2018).

The arborescent shrub *Ziziphus lotus* (L.) Lam (Rhamnaceae) is the dominant species in the study area (Tirado 2009). Due to its large size and hemispherical canopy, *Z. lotus* accumulates substantial amounts of organic matter underneath and fosters favorable microclimatic conditions for plants to thrive in drylands (Tirado and Pugnaire, 2003). Thus, this phreatophyte behaves as the key engineer species of the GDE that it constitutes (Guirado et al., 2018). *Z. lotus* is mainly distributed along the Middle East area and the southern Mediterranean coast, being also sparsely present in the southeastern Iberian Peninsula and Sicily (Sánchez-Gómez et al., 2003). In our study area, other Mediterranean shrubs can be found such as the summer deciduous *Lycium intricatum* Boiss., *Withania frutescens* (L.) Pauquy, and the evergreen *Thymelaea irsuta* (L.) Endl. (Tirado and Pugnaire, 2003; Tirado, 2009). For the study, we selected 16 individuals of *Z. lotus* located along a DTGW gradient from 2 to 25 m depth, and associated with a network of boreholes used for long-term monitoring of the aquifer (two plants located less than 50 m far from each borehole) (Appendix 1, see Supplementary Material of this chapter). The electrical conductivity of the groundwater at each borehole also varies widely (from 3500 to 11000 µS/cm). We used these 16 individuals for stable isotope and nutrient composition analyses to explore the strategies of *Z. lotus* in water acquisition and use. We also selected eight additional plants, randomly distributed along the coastal plain, to increase samples number (24 in total) for a general characterization of the species along the isohydric–anishohydric spectrum. Water potential and leaf gas-exchange were measured several times during the growing season in May (late spring), July (mid-summer), and September (late summer) of 2018 and 2019, whereas plants for stable isotope analyses were sampled in May of 2019 when their physiological activity is highest (Guirado et al., 2018).

Xylem water extraction and hydrogen and oxygen stable isotopes analysis

We analyzed the isotopic composition (δ^2H and $\delta^{18}O$) of plant stem water, precipitation, and groundwater, aiming to assess the water acquisition strategies of *Z. lotus*. For the stems, we cut and debarked three suberized branch sections from the 16 plants associated to the boreholes. Single stem samples were stored at -20ºC in glass vials tightly sealed by

lids and wrapped with Parafilm (Fisher Scientific, Waltham, MA, USA) to minimize potential evaporation before xylem water extraction in the laboratory. The same glass vials were introduced in the cryogenic vacuum distillation system, which achieves yields higher than 99% and low organic contamination (Millar et al., 2018). Defrosted samples (1.8 ± 0.5 g) were heated in vacuo (10–3 mBar) to a final temperature of 100°C for approximately 2 h, and the extracted water was cryogenically trapped using liquid nitrogen. Once the process was completed, extracted water vapor was defrosted at room temperature in sealed conditions and transferred to capped glass vials for isotopic analysis. Additionally, we collected groundwater samples from the boreholes (n = 24), 4 m below the water table, in May, July, and September 2019. However, because we observed signs of evaporated water in some samples, we finally showed 18 of the 24 samples. We also collected rainwater samples on a rain-event basis (n = 20) from March 2019 to February 2020 from a pluviometer at a weather station 8 km far from the study area.

The δ^2H and $\delta^{18}O$ in xylem water, groundwater, and precipitation were measured simultaneously by cavity ringdown spectroscopy (CRDS). This technique is increasingly used for isotopic analyses since it allows the simultaneous measurement of oxygen and hydrogen isotopes with high accuracy (Martín-Gómez et al., 2015). A L2140-I Picarro water isotope analyzer was used (Steig et al., 2014), interfaced with an A0211 high-precision vaporizer (Picarro, Santa Clara, CA, US). Contamination of plant-extracted water by organic compounds can produce spectroscopic interferences in the measurements, affecting the accuracy and precision of the isotopic data (Martín-Gómez et al., 2015; Millar et al., 2018; Barbeta et al., 2020). To avoid such potential organic contamination, we removed combustible organic compounds from water samples using a Picarro micro-combustion module (MCM) (Band et al., 2009; Gázquez et al., 2015). The MCM comprises an 8-cm long cylindrical cartridge filled with a pyrolytic catalyst heated at 400°C, which was placed in-line between the vaporizer and the water isotope analyzer. The instrument used dry air (containing 21% O_2) as the carrier gas. Previous studies suggested that the efficiency of this approach for the removal of organics from the water steam can be limited if the concentrations of alcohols and other volatiles are high (Martín-Gomez et al., 2015; Millar et al., 2018; Barbeta et al., 2020); thus, additional data post-processing may be needed to obtain accurate isotopic results. To check whether the pyrolytic catalyst was efficient in

removal of organics, we used the ChemCorrect software (Picarro). This piece of software uses a suit of spectral indicators, including the spectral baseline and the residual noise, amongst others, to flag the presence of organic compounds in the water steam (Picarro, 2010). ChemCorrect did not find spectroscopic issues in any of the samples analyzed in this study, so additional data processing was not applied.

Each sample (three per plant) was injected 10 times into the vaporizer, which was heated to 110°C. Memory effects from previous samples were avoided by rejecting the first three analyses. The results were normalized against V-SMOW by analyzing internal standards before and after each set of 20 samples. Values for the final seven injections were averaged with a typical in-sample precision (±1 SD) of ±0.04‰ for $\delta^{18}O$ and ±0.18‰ for δ^2H.

Water potential and leaf gas exchange rates

We measured stem water potential in four branches of the 24 selected plants using a Scholander pressure chamber (SKPM1405, Skye Instruments, Powys, UK). Predawn water potential (Ψ_{pd}) was measured between 05:30 and 06:30 hours (1 h before sunrise) and midday water potential (Ψ_{md}), between 13:30 and 14:30 hours in four stems per individual plant. On the same days, we measured leaf gas exchange rates in eight leaves per individual between 10:00 and 13:00 hours with a portable infrared gas analyzer (Li-6400XT; LI-COR Inc., Lincoln, NE, USA). Chamber conditions during measurements were ambient temperature at 25 – 30ºC, flow rate of 400 µmol s^{-1}, CO_2 concentration of 400 µmol mol^{-1}, and light intensity of 1800 µmol m^{-2} s^{-1}. We measured vapor pressure deficit (VPD) and leaf transpiration rate I to detect the response of E to the diel increment of VPD. We also obtained the photosynthetic rate (A) and the stomatal conductance (g$_s$). All measures were repeated in the three sampling periods of 2018 and 2019 (late spring, mid-summer, and late summer).

Isohydric–anisohydric continuum metrics

Several metrics have been proposed to quantify drought response strategies and to place species along the isohydric–anisohydric continuum (Klein, 2014; Li et al., 2019; Martínez-Vilalta et al., 2014). Here we developed two main metrics that fall into two different categories related to stomatal regulation (Li et al., 2019). First, we performed a linear regression analysis to obtain the slope (σ) of the regression between midday (Ψ_{md}) and

predawn water potential (Ψ_{pd}). According to Martínez-Vilalta et al. (2014), the slope of this regression (σ) indicates the degree of isohydric–anisohydry; σ = 0 refers to extreme isohydric plants, σ > 1 refers to extreme anisohydric, and 0 < σ < 1 are intermediate between the two extremes. This analysis highlights the stomatal control to avoid/allow water loss (Li et al., 2019). For this, we used average values of individuals during the whole growing season, but also compartmentalized the analysis monthly, differentiating between periods during the growing season (late spring, mid-summer, and late summer), and sites related to DTGW. Second, we estimated the maximum range of daily leaf water potential variation (hereafter maximum daily range, $\Delta\Psi_{max}$), which is obtained from the maximum daily difference between Ψ_{md} and Ψ_{pd} (Klein, 2014; Li et al., 2019). This metric, related to the stringency of stomatal regulation within safety margins to prevent hydraulic failure (Skelton et al., 2015; Li et al., 2019), was analyzed based on DTGW and period during the growing season. Additionally, to complete the characterization of the *Z. lotus* along the isohydric–anisohydric spectrum, we used gas exchange data (A, g_s, and E) and assessed the relationship between VPD and E (Urban et al., 2017; Drake et al., 2018).

Leaf nutrients and carbon stable isotopes composition

To explore the variability in plant resource-use and establish the link between leaf carbon isotope composition and rooting depth in response of the DGTW gradient (Prieto et al., 2018; Rumman et al., 2018), we also analyzed foliar nutrient concentrations and carbon isotope discrimination in the *Z. lotus* population. We collected 30 leaves per individual from the same 16 plants associated to the boreholes, stored them in paper bags, and ultimately oven-dried them at 60ºC for 48 h to finely ground to powder. A subsample of foliar material was used for stable carbon isotopes analysis and another subsample for nutrients analysis. Leaf Na, P, K, Ca, Mg, S, Fe, Cu and Zn concentrations were measured by inductively coupled plasma optical emission spectrometry (ICP-OES, Thermo Elemental Iris Intrepid II XDL, Franklin, MA, US) after a microwave-assisted digestion with HNO_2–H_2O_2 (4:1, v:v). Foliar N concentration was also analyzed by a CHNOS Elemental Analyzer (vario ISOTOPE cube, Elementar, Hanau, Germany) interfaced to an IsoPrime100 mass spectrometer (Isoprime, Cheadle, UK) in the CSIB at the University of California, Berkeley.

For $\delta^{13}C$ analyses, we used a combustion module (CM) coupled to a CRDS System (G2201-I Analyzer, Picarro). Powdered samples of leaves in tin capsules (~1.25 mg) were loaded into the CM by an autosampler (Costech Analytical Technologies, Valencia, CA, US), achieving complete combustion at 1200°C. The released CO_2 passed through a water filter and a GC-column and was transferred to a Picarro Liaiso A0301 interface and finally inputted into CRDS for analysis. The system assembly uses ultra-high purity (UHP) N_2 as the carrier gas and pure O_2 for combustion. Four replicates per sample were analyzed, and $\delta^{13}C$-isotope values were referenced to the Vienna PeeDee Belemnite (V-PDB) scale. = L-Glutamic acid standards USGS40 ($\delta^{13}C$ VPDB = -26.4‰) and USGS41a ($\delta^{13}C$ VPDB = +37.6‰), supplied by USGS/Reston Stable Isotope Laboratory, were used to calibrate the CM-CRDS system. Sugarcane ($\delta^{13}C$ VPDB = -11.7‰), urea ($\delta^{13}C$ VPDB = -49.2‰) and $NaHCO_3$ ($\delta^{13}C$ VPDB = -10.9‰) were used as working reference standards for consecutive rounds of $\delta^{13}C$ analyses. We also analyzed four replicates for each standard. Based on these internal (secondary) standards, the precision ranged between 0.06 – 0.35‰ (1 SD, n = 16) and the accuracy from -0.25 to 0.28‰. We calculated foliar carbon isotope discrimination ($\Delta^{13}C$) from $\delta^{13}C$, using the following equation (Werner et al., 2012):

$$\Delta^{13}C = (\delta^{13}Ca - \delta^{13}Cp) / (1 + \delta^{13}Cp)$$

where $\delta^{13}Ca$ and $\delta^{13}Cp$ were the $\delta^{13}C$ values of the CO_2 in air and the plant, respectively. The value used for $\delta^{13}Ca$ was -9.7‰, on average, which was obtained from air samples collected in the study area during the field surveys and through using a portable diaphragm pump and 1-L Ritter bags for air sample storage. We immediately measured $\delta^{13}C$ of ambient CO_2 in the laboratory by using the same CRDS analyzer (Picarro G2201-i).

Data analyses

The relationship between δ^2H and $\delta^{18}O$ in xylem water, precipitation, and groundwater, was examined through regression analyses. To identify groundwater use patterns, we assessed the response of each stable isotope (δ^2H and $\delta^{18}O$ in xylem water and groundwater, and $\Delta^{13}C$ in leaves) to a DTGW gradient. In the case of hydrogen isotopes, further analysis was developed to establish the relationship of δ^2H with the electrical conductivity of groundwater (i.e., groundwater salinity). Regarding stem water potential, we performed a general linear regression between Ψ_{md} and Ψ_{pd} with monthly average

values to obtain the slope of the regression line (σ). We also assessed this relationship by differentiating between sites with different water table depths. Additionally, we evaluated the response of Ψ_{pd} to the DTGW gradient, differentiating between periods. Temporal and spatial differences in $\Delta\Psi_{max}$ were also tested using a two-way analysis of variance (ANOVA) with a Tukey's honestly significant difference (HSD) post-hoc test. As regards leaf gas exchange rates, the general relationship between E and VPD during the whole growing season was assessed through a regression analysis, as well as the relationship between DTGW with mean leaf gas exchange fluxes (A, g_s, and E). Finally, leaf nutrients concentrations (Na, P, K, Ca, Mg, S, Fe, Cu and Zn) were also regressed against DTGW. To determine thresholds related to groundwater availability and access by roots, we looked for breakpoints in functions with DTGW by applying segmented regression analyses (Toms and Lesperance, 2003). The best-fitting function was selected by maximizing the statistical coefficient of explanation. The least squares method was applied to the resulting regression lines while minimizing the sum of squares of the differences between observed and calculated values of the dependent variables. When no significant breakpoint was found, we selected simple linear regression to explain the responses to DTGW. All analyses were undertaken in R 3.5.2 (R Core Team, 2018) with the packages stats and segmented.

RESULTS

Water isotope composition

The stable isotope analyses of groundwater revealed δ^2H values that ranged from -38.2 to -44.9‰, with an average of -41.3 ± 0.4‰, and $\delta^{18}O$ values from -5.47 to -6.52‰, with an average of -6.10 ± 0.06‰ (Fig. 1). Groundwater $\delta^{18}O$ showed rather homogeneous values along the DTGW gradient (light blue circles) (Fig. 2). Compared with groundwater, xylem water showed lower δ^2H values and higher $\delta^{18}O$ ones (-45.4 ± 0.4‰ and -4.71 ± 0.09‰ on average, respectively), although a significant linear regression between them was found (R^2 = 0.54, P = 0.001) (Fig. 1). Thus, we observed a mean isotopic offset between groundwater and xylem water of -4.1‰ for δ^2H and 1.4‰ for $\delta^{18}O$. Regarding oxygen isotopes, we found a significant increase in xylem water $\delta^{18}O$ values (green triangles) with increasing DTGW up to 14 m (R^2 = 0.71, P < 0.001) (Fig. 2). Beyond this threshold, the segmented regression analysis showed that $\delta^{18}O$ became independent of DTGW (slope =

-0.012). We also observed a significant increase in xylem water δ^2H values with both DTGW ($R^2 = 0.26$, P = 0.016) and electrical conductivity ($R^2 = 0.41$, P = 0.007) although xylem water δ^2H values were consistently lower than those of groundwater (Appendix 2). Differences between groundwater and xylem water δ^2H values decreased with DTGW and conductivity, thus larger offsets of δ^2H occurred at sites with the shallowest and less salty groundwater.
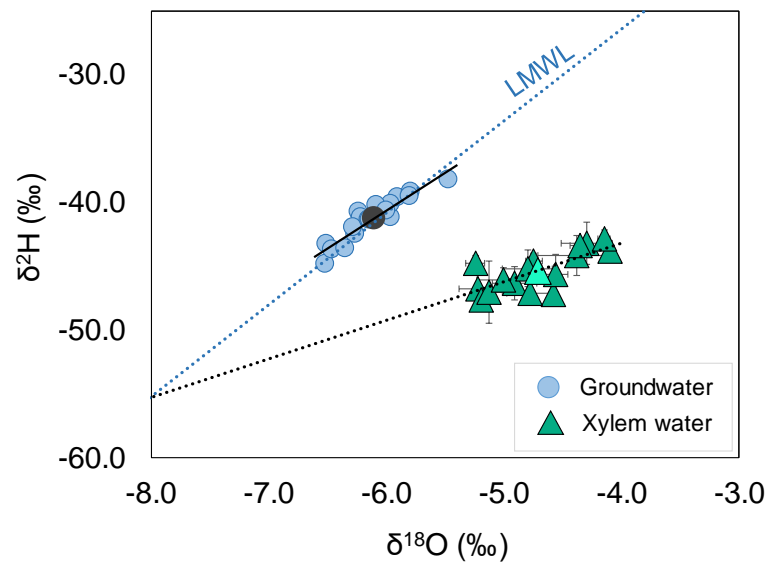
Figure 1. Relationship between mean δ^2H and $\delta^{18}O$ values in groundwater (light-blue circles) and xylem water in *Ziziphus lotus* (green triangles). Means are displayed for each water source (black circle and light-green triangle, respectively). The local meteoric water line (LMWL, blue dotted line, y = 7.2x + 2.36, $F_{1, 18} = 452.4$, $R^2 = 0.96$, P < 0.001), the groundwater line (black solid line, y = 5.97x - 4.81, $F_{1, 17} = 118.2$, $R^2 = 0.87$, P < 0.001), and the xylem water line (black dotted line, y = 3.1x - 31.14, $F_{1, 14} = 16.6$, $R^2 = 0.54$, P = 0.001) are also shown. Error bars represent ± SE.
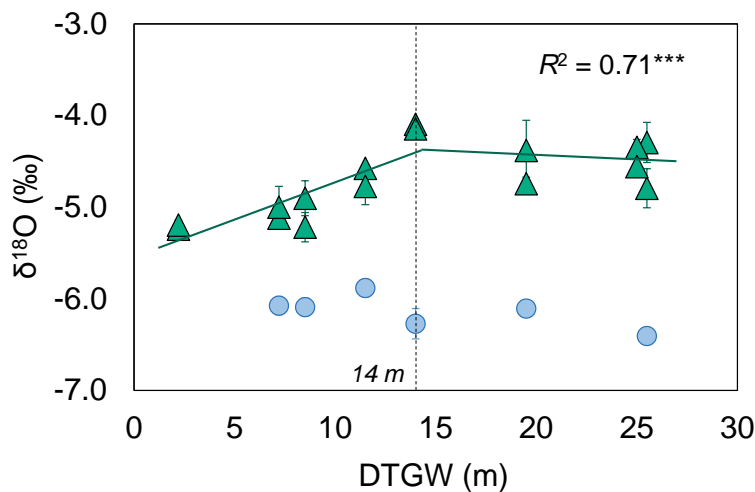
Figure 2. Relationship between xylem water $\delta^{18}O$ values found in *Ziziphus lotus* shrubs and depth-to-groundwater (DTGW). Light-blue circles represent groundwater and green triangles, xylem water. Dashed line indicates the breakpoint of the segmented regression (14 m). Significance: ***P < 0.001; $F_{1, 14} = 11.07$. Error bars represent ± SE.

Leaf water potential and gas exchange rates

Average predawn water potential (Ψ_{pd}) ranged between -0.3 and -1.4 MPa across time (Fig. 3), being generally lower (more negative) at the end of the dry season (September, red squares). As Ψ_{pd} declined, midday water potential (Ψ_{md}) also decreased linearly with a slope of 1.43 MPa MPa-1 ($F_{1, 72}$ = 76.52, R^2 = 0.51, P < 0.001), far from the 1:1 line. In May and July, Ψ_{md} was lower than Ψ_{pd} (Appendix 3) as the linear regression fell significantly below the 1:1 line by 0.92 and 1.62 MPa respectively (P < 0.001), with a slope that also differed from 1 ($F_{1, 24}$ = 13.06, P = 0.001 and $F_{1, 22}$= 12.5, P = 0.002, respectively). In September, a negative tendency similar to July could be observed, although it was not significant. Therefore, the slopes of the Ψ_{md} to Ψ_{pd} regressions (σ) revealed the extreme anisohydric behavior of the species (σ = 1.43), which was more pronounced in spring (σ = 1.37) than in summer (σ = 0.85).

Figure 3. Relationship between predawn (Ψ_{pd}) and midday (Ψ_{md}) plant water potentials during the 2018 and 2019 growing seasons. Green triangles refer to May (late spring), yellow circles to July (mid-summer), and red squares to September (late summer). The solid line shows the significant Ψ_{pd}–Ψ_{md} regression line, whereas the dashed one indicates the 1:1 line. Significance: ***P < 0.001. Error bars represents ± SE.
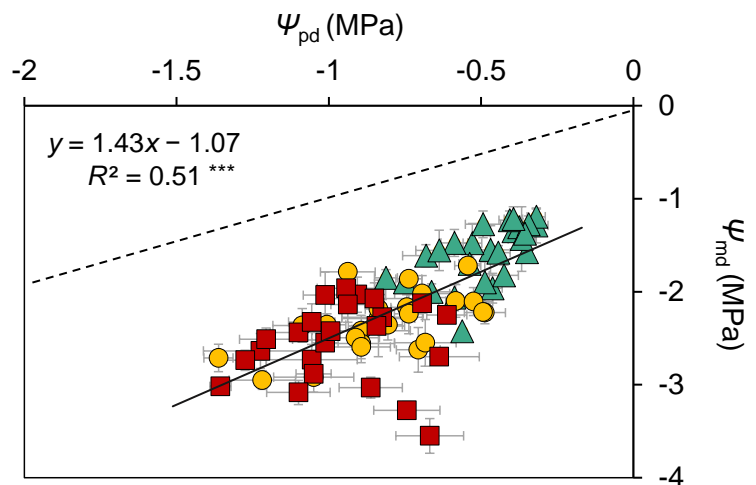
When comparing between sites, plants with the shallowest water tables (Fig. 4A–D) consistently had Ψ_{pd} values higher (less negative) than -1.1 MPa, whereas the plant with the deepest DTGW (25.5 m at site B9) had Ψ_{pd} values lower than -1.5 MPa (Fig. 4I). Indeed, the significant relationships between Ψ_{pd} and DTGW in summer confirmed lower Ψ_{pd} values at sites with the deepest water tables, both in July and September (Fig. 5B and C). In all cases, the regression analysis between Ψ_{pd} and Ψ_{md} revealed significant relationships with slopes higher than 1 MPa MPa^{-1}. Site B2 is noteworthy for its steep slope (3.19 MPa MPa^{-1}) (Fig. 4B). Additionally, plants from sites B1 and B2, with the lowest DTGW (2 m and 7 m, respectively), showed higher values of maximum daily range in water potentials ($\Delta\Psi_{max}$ values of 1.6 and 1.7 MPa, respectively, Fig. 6). The two-way ANOVA revealed that plants

at site B2 had significantly higher $\Delta\Psi_{max}$ values than the rest of the plants ($F_8 = 10.88$, P < 0.001). During the growing season, $\Delta\Psi_{max}$ varied ($F_2 = 148.66$, P < 0.001), being much lower in spring (May) than in summer (July and September) (inset in Fig. 6). This temporal trend is also observed in the regression of VPD against transpiration rate (E), where E significantly increased with VPD ($F_{1, 70} = 24.95$, $R^2 = 0.26$, P < 0.001) from spring to summer (Fig. 7). Thus, the response of E did not reveal stomatal limitation with increasing VPD, at least up to 4.5 kPa. However, we observed a significant reduction of both mean E and g_s with increasing DTGW up to 14 m (Fig. 8).
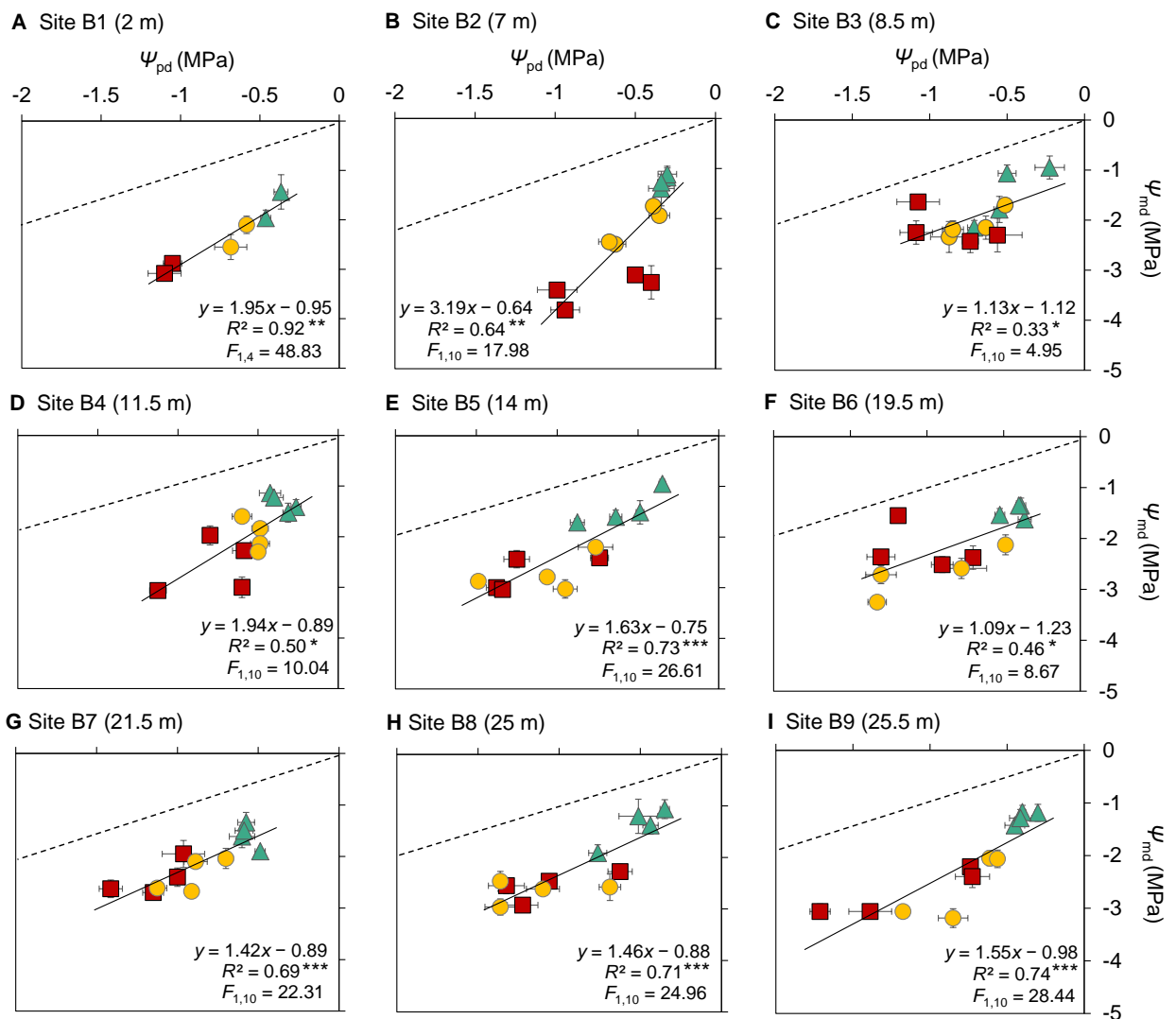
Figure 4. Relationship between predawn (Ψ_{pd}) and midday (Ψ_{md}) plant water potentials at different sites, ranging from shallow water tables (A) to deeper ones (I). Groundwater depth at each site is indicated in brackets. Green triangles represent data from May, yellow circles from July, and red squares from September. Solid lines show the Ψ_{pd}–Ψ_{md} regression line, whereas dashed lines represent the 1:1 line. Significance: ***P < 0.001, **P < 0.01, *P < 0.05. Error bars represents ± SE.
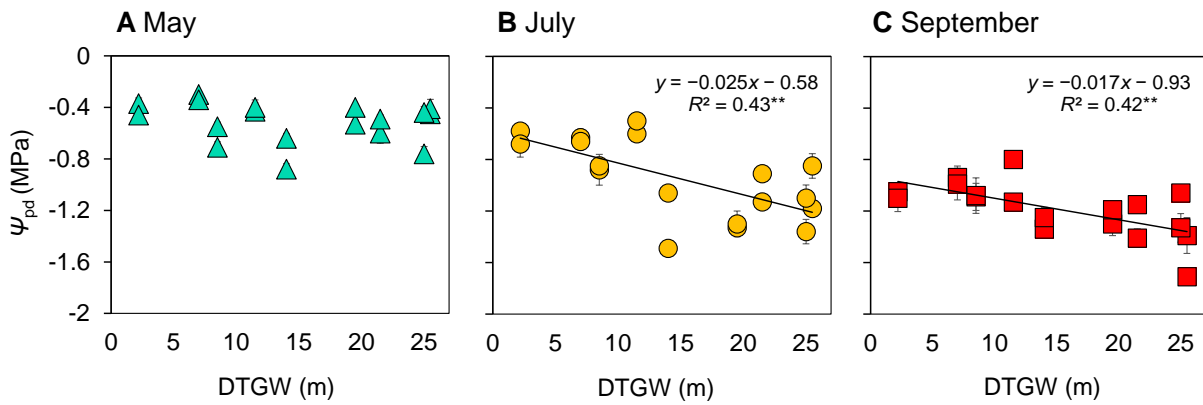
Figure 5. Relationship between predawn water potentials (Ψ_{pd}) in *Ziziphus lotus* shrubs and depth-to-groundwater (DTGW) in May (A), July (B), and September (C) of 2019. Lines show significant linear regressions. The equation of the regression and the goodness of the fit (R^2) are shown for significant analyses (July: $F_{1, 16}$ =11.88, September: $F_{1, 16}$ = 11.53). Significance: **$P < 0.01$. Error bars represents ± SE.
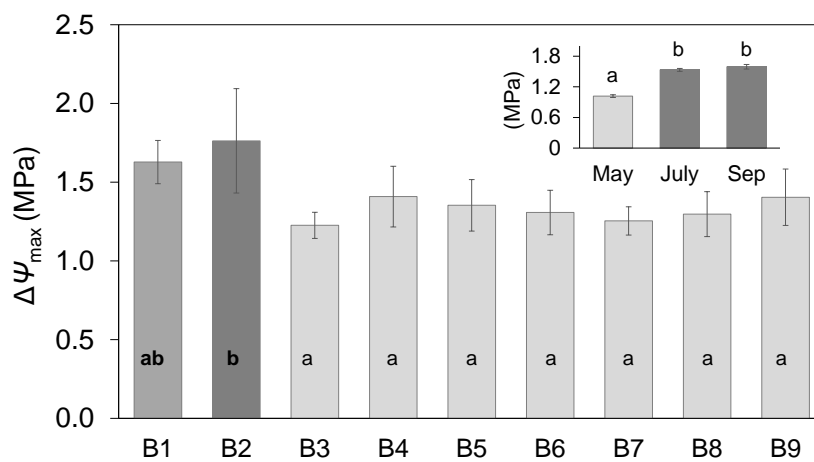
Figure 6. Mean and ± SE of plant water potential maximum daily range ($\Delta\Psi_{max}$) by sites and months (inset) in *Ziziphus lotus* shrubs. Letters represent significant differences between groups ($P < 0.05$).
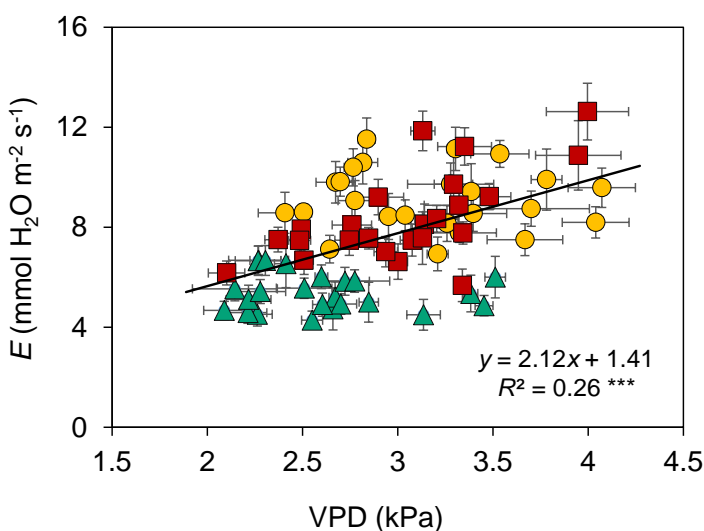
Figure 7. Relationship between vapor pressure deficit (VPD) and transpiration rate (E) in *Ziziphus lotus*. Data from 2018 and 2019 is shown. Green triangles represent data from May, yellow circles from July, and red squares from September. Solid line shows the significant regression. Significance: ***P < 0.001. The equation of the regression and the goodness of the fit (R^2) and SEs (error bars) are also shown.
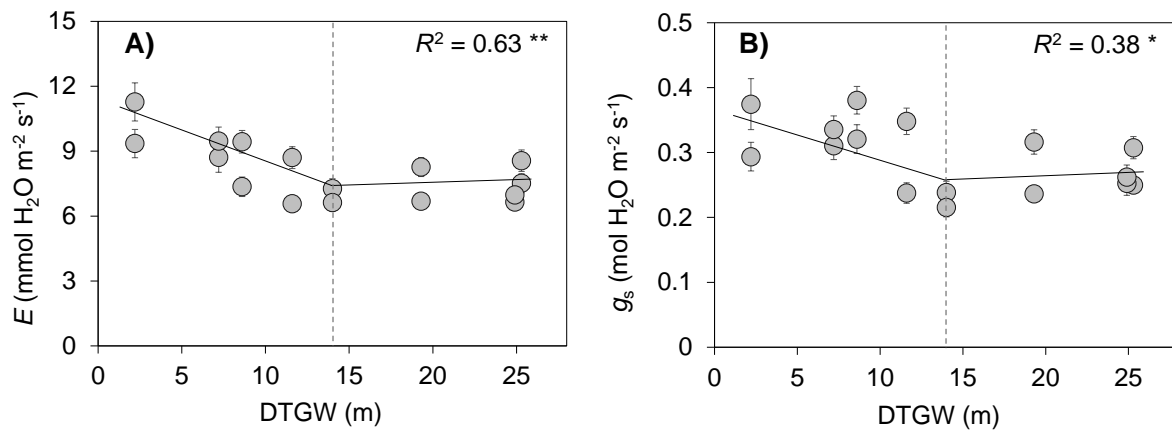
Figure 8. Relationship between depth-to-groundwater (DTGW) and transpiration rate, E (A) and stomatal conductance, g_s (B) in *Ziziphus lotus* shrubs. Data represent means for the 2018 and 2019 growing seasons. Solid lines show the significant segmented regressions and R^2, the goodness of the fit. Dashed lines indicate the breakpoint at 14 m (E: $F_{1, 14}$ = 8.74; g_s: $F_{1, 14}$ = 5.09). Significance: **P < 0.01, *P < 0.05. Error bars represent ± SE.
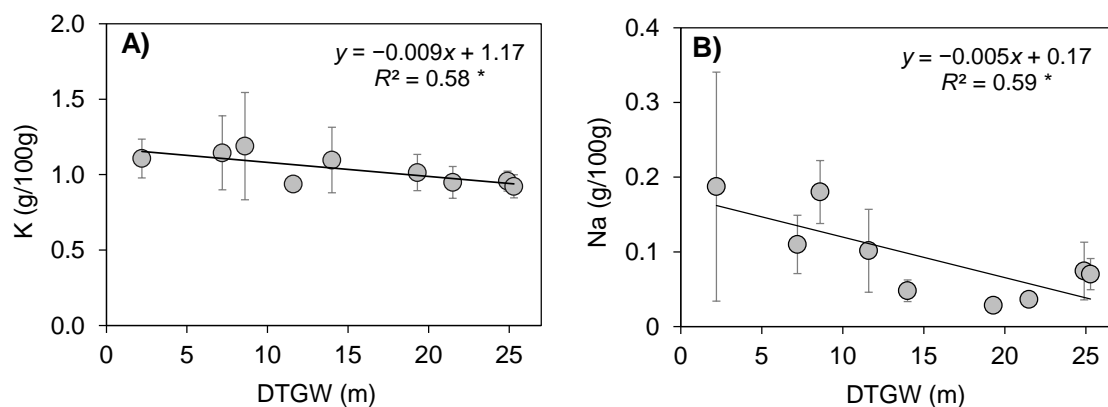
Figure 9. Relationship between depth-to-groundwater (DTGW) and foliar concentrations of potassium, K (A) and sodium, Na (B) in *Ziziphus lotus* shrubs. The equation of the regression and the goodness of the fit (R^2) are shown. Significance: *P < 0.05. Error bars represent ± SE.

Leaf nutrients and carbon isotope composition

Leaf nutrient analysis revealed that DTGW did not significantly influence the foliar concentrations of most essential plant macro- and micronutrients (i.e., N, P, Ca, Mg, S, Fe, Cu, and Zn; Appendix 4). However, a significant relationship was found for K and Na ($F_{1, 7}$ = 9.91, R^2 = 0.58, P < 0.05; and $F_{1, 7}$ = 10.07, R^2 = 0.59, P < 0.05, respectively), as higher foliar concentrations of these nutrients were found at sites where DTGW was relatively shallow (Fig. 9). Furthermore, foliar carbon isotope discrimination ($\Delta^{13}C$) was significantly correlated with DTGW (Fig. 10). The segmented regression (R^2 = 0.59, P = 0.036) showed a pronounced decline of $\Delta^{13}C$ with increasing DTWG at the sites where DTGW was relatively

shallow (DTGW < 13.3 m, slope = - 0.15). From that point, the relationship became more stable (slope = - 0.013, P < 0. 036).
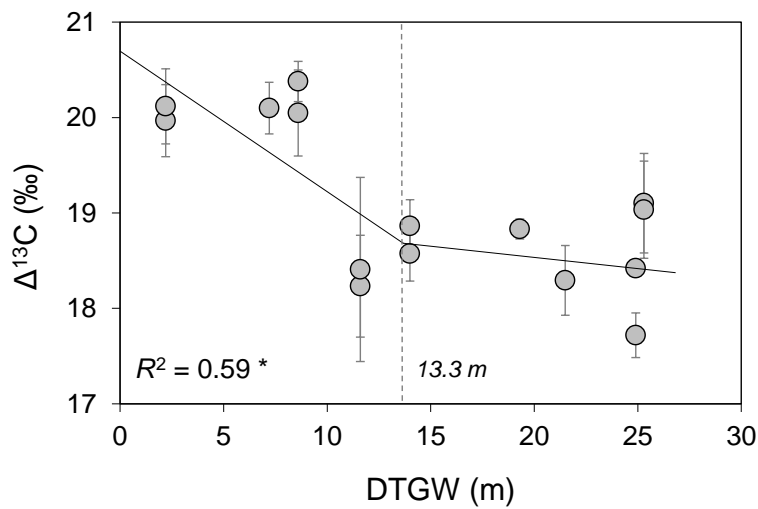
Figure 10. Relationship between carbon isotope discrimination ($\Delta^{13}C$) values in leaves and depth-to-groundwater (DTGW) in *Ziziphus lotus* shrubs. Lines represent significant segmented regression ($F_{1, 14}$ = 11.82, R^2 = 0.59, *P = 0.036). Dashed line indicates the breakpoint of the regression (13.3 m). Error bars represent ± SE.

DISCUSSION

This study assessed two main aspects related to the water-use strategy of a deep-rooted shrub of drylands, *Ziziphus lotus*: the water source and transport regulation. Our findings support partial dependence of this species on groundwater, which points to the partial decoupling of its productivity from current precipitation. Such dependency might be facultative and compatible with the simultaneous utilization of other sources of water (e.g., soil water or intermediate water of the vadose zone) because there was not a perfect match between the stable isotope values of xylem water and groundwater at any site. However, we found a shift in the stable isotope composition of the source of water used along a DTGW gradient, even though there are still some uncertainties about the precise identity of the water sources used during the growing season. Nonetheless, the dependency of predawn water potential, stomatal conductance, transpiration rate, leaf $\Delta^{13}C$, and xylem water $\delta^{18}O$ values on DTGW suggest that groundwater is an important source of water for *Z. lotus*, particularly at sites with shallow water tables and during the harsh dry summer. For mobilizing abundant groundwater, the species showed an extreme anisohydric stomatal regulation characterized by the absence of any discernible water potential

thresholds for stomatal closure and by strong increases in transpiration flux during the warmest and driest period when soil water availability is lowest and VPD is highest (mid and late summer). Nevertheless, we also observed spatiotemporal variability in the stomatal regulation in response to groundwater depth, which suggests this can be a response mechanism of the species to contrasting environmental conditions. Overall, these attributes support the general hypothesis that *Z. lotus* squanders water, a profligate resource use strategy that becomes more pronounced as DTGW decreases and groundwater becomes more easily accessible to roots.

Groundwater dependency

Our findings suggest a facultative groundwater dependency in *Z. lotus* that indicates that the productivity of the ecosystem is partially decoupled from current precipitation (Appendix 5) (Hultine et al., 2020). Neither $\delta^{18}O$ nor $\delta^{2}H$ values in xylem water completely match those of the groundwater isotopic signature, which indicates that such dependence is not exclusive. The $\delta^{18}O$ offset of 1.4‰ on average between xylem water and groundwater might indicate that *Z. lotus* is a partial or facultative phreatophyte that also obtains some water from an additional unknown source (e.g., the soil or the intermediate vadose zone) aside from groundwater.

Fractionation of hydrogen (but not oxygen) isotopes can occur during root water uptake (Dawson et al., 2002; Ellsworth and Williams, 2007; Barbeta et al., 2020). Hydrogen fractionation may occur in most xerophytic and halophytic plants, which possess suberized roots that promote the symplastic pathway of water uptake at the expense of the apoplastic pathway (Ellsworth and Williams, 2007). This mechanism avoids root water leakage to surrounding dry or saline soils (Reinoso et al., 2004) and has been measured to be up to 9‰ discrimination against deuterium for the phreatophyte Prosopis velutina (Ellsworth and Williams, 2007). More recently, isotopic offsets of -11‰ and -15‰ between soil and stem water have been found in the temperate species *Fagus sylvatica* L. (Barbeta et al., 2020) and the xerophytic species *Acacia caven* Mol. (Poca et al., 2019) respectively. Here, our results showed a $\delta^{2}H$ mean offset of -4.1‰ between groundwater and xylem water, reaching -7.5‰ at 11.5 m depth, that cannot be attributed to methodological issues or organic contamination. Firstly, the micro-combustion module (MCM) successfully

eliminated the organic compounds that could have been co-extracted during cryogenic vacuum distillation of xylem water, which is reported to be one of the techniques that extracts less amount of organic compounds (Millar et al., 2018). Secondly, we found no evidence of potentially contaminated samples with organics (e.g., alcohols), as confirmed by the ChemCorrect software. Finally, considering that organic compounds concentration is sample dependent and that it affects more one isotope than the other (Martín-Gómez et al., 2015), we would expect no correlation between δ^2H and $\delta^{18}O$ values if organics are present. Nonetheless, we show a significant relationship between them (R^2 = 0.54, P = 0.001), which cannot be explained by a systematic bias. The isotopic offset between xylem water and groundwater is more pronounced when groundwater availability and transpiration are greater, which might be due to hydrogen fractionation during water uptake and other plant and soil processes discussed in Barbeta et al. (2020). Larger amounts of water entering the roots through the symplastic pathway at sites with shallow and less saline groundwater tables might lead to greater deuterium depletion of xylem water compared with groundwater. However, more specific studies should be conducted to provide further insights into hydrogen isotope fractionation in *Z. lotus* roots.

Groundwater appears to be the key water source for *Z. lotus*, particularly at sites with shallow water tables where its availability and accessibility to roots would be greater. The increase in xylem water $\delta^{18}O$ values with increasing DTGW suggests a change in the pattern of water use, which might indicate a progressive reduction in groundwater uptake up to a DTGW threshold of 14 m. Roots might find difficulties to obtain groundwater beyond this depth, switching to greater utilization of soil water or intermediate water of the vadose zone to compensate for this difficulty. Such pattern is supported by more negative values of predawn water potential in summer as DTGW increases. Because of free access to groundwater, deep-rooted species can maintain more stable predawn water potentials (Jackson et al., 2000; Martínez-Vilalta and García-Forner, 2016). However, since *Z. lotus* might behave as a facultative or partial phreatophyte, it is reasonable to expect a negative trend in predawn water potential with DTGW. Besides rooting depth, predawn water potential is largely affected by soil water availability (West et al., 2012; Martínez-Vilalta and García-Forner, 2016; Nardini et al., 2016), which is reduced throughout the dry Mediterranean summer. The sampling of stems for stable isotope analyses of xylem water

was conducted in spring during a period of moderate water stress (May), as supported by relatively high predawn water potential values. Therefore, groundwater use might be lower at this point of the growing season, which would explain the lack of perfect overlap between xylem and groundwater isotopic values. Nonetheless, the species might increase the uptake of groundwater during the drier later part of the growing season as consequence of the progressive reduction in soil water availability. Likewise, when DTGW is beyond 14 m, *Z. lotus* plants might become more dependent on water from the unsaturated vadose zone, which will increase drought vulnerability (Zencich et al., 2002). In any case, *Z. lotus* not only shows spatial variations in groundwater uptake, but also a seasonal groundwater disconnection because of leaf deciduousness during winter, which additionally define it as a facultative phreatophyte in this dryland ecosystem (Hultine et al., 2020).

We acknowledge that characterizing the variability of soil water isotopic composition with depth along the edaphic profile would have contributed to identify the additional water sources and to quantify their proportional contribution to total plant water uptake. Moreover, extending the sampling period to the summer would clarify the main water source of the species throughout its growing season. Unfortunately, neither the temporal variability of the isotopic composition of xylem water, nor the spatial one of soil water along the edaphic profile have been investigated yet. Our findings indicate that *Z. lotus* does not behave like a strict phreatophyte, but rather like a facultative or partial phreatophyte that primarily takes up groundwater for the most part but also uses water from another unknown sources.

Anisohydric behavior

The isohydric–anisohydric classification is strongly related to the plant water and carbon economy, since stomatal closure is the main mechanism to limit both water loss and carbon exchange at short time scales (Martínez-Vilalta and García-Forner, 2016). The slope of the linear regression between predawn and midday water potential reveals that *Z. lotus* plants show declining daytime water potentials (Ψ_{md}) in response to reductions in water availability (Ψ_{pd}). Plants undergo large fluctuations of their water potentials on a daily basis due to a loose stomatal control, as revealed by the large diel variation of water potentials

($\Delta\Psi_{max}$; Klein, 2014; Nardini et al., 2014). Our results suggest that *Z. lotus* plants do not constrain water loss strongly, indicating little stomatal limitation on photosynthesis and carbon assimilation; quite the contrary, this winter deciduous species shows maximum transpiration rates during the dry summer when VPD is higher. Together with high productivity, anisohydry also promotes leaf evaporative cooling to cope with high thermal stress, particularly in arid regions (Hultine et al., 2020). Both plant water potentials and leaf gas exchange rates confirm the extreme anisohydric strategy of *Z. lotus*, which is supported by groundwater access by roots and high atmospheric water demand. Nonetheless, hydraulic behavior of a plant results from the interplay between the plant's physiology and environmental conditions, which impede an exclusive and stable interpretation of such results (Feng et al., 2019).

The observed temporal variations in predawn and midday water potentials may respond to both the species water use strategy and the environmental condition. Our results showed a decrease in Ψmd from May to September as well as a transition from extreme anisohydric (σ = 1.37) to partial isohydric behavior (σ = 0.85). This response agrees with the increase in VPD, but also with a reduction in water availability (lower Ψ_{pd}) during summer. Several studies have already shown temporal variations in the hydraulic strategy of desert shrubs across seasons (Feng et al., 2019, Guo et al., 2020). Guo et al. (2020) attributed such dynamic behavior in Larrea tridentata to temporal variations in air temperature, VPD, soil water availability, and their interactions. Here, *Z. lotus* showed extreme anisohydry during the wet and productive spring, whereas partial isohydry was most common during the dry and hot summer. Therefore, although *Z. lotus* exhibits a dominant anisohydric behavior, variable environmental conditions may lead to plasticity in water potential regulation. Such plasticity might be critical to the success of this species in seasonally dry areas (Guo et al., 2020).

Our findings also point to high spatial variability in stomatal regulation among *Z. lotus* individuals that might result from differences in water availability and rooting depth (Hultine et al., 2020). Feng et al. (2019) reported spatial variations in the hydraulic response of *Quercus douglasii* to drought across different conditions of soil moisture availability. Here, differences among individuals related to spatial differences in DTGW can induce

different hydraulic responses. Plants at sites with a shallower groundwater table (lower DTGW) showed an extreme anisohydric behavior. Consistent with our hypothesis, these results point to high transpiration rates and physiological activity because of higher water availability to roots at these depths (Gries et al., 2003). On the contrary, plants at sites with the greatest DTGW showed the lowest Ψ_{pd} values, what suggests some degree of water stress due to increased hydraulic limitation or physiological restriction (groundwater availability and/or rooting depth) (West et al., 2012; Nardini et al., 2016). In fact, other authors (Rais et al., 2017) have recorded leaf accumulation of osmotically active compounds (proline, water soluble carbohydrates, and soluble N compounds) in water stressed individuals of *Z. lotus*. Conversely, the nonsignificant relationship between photosynthetic rate (A) and DTGW (Appendix 6) highlights that *Z. lotus* plants keep assimilating carbon despite increasing stomatal limitation (low g_s and E) even at sites with deep water tables. Although sparse measurement of leaf gas exchange rates were obtained, these results further confirm the anisohydric behavior of the species and suggest a great physiological plasticity to adapt to different water table depths. This plasticity in terms of rooting depth and stomatal regulation may partially buffer phreatophytes from climate change effects (Hultine et al., 2020).

Besides spatiotemporal hydraulic regulation shifts and winter deciduousness, *Z. lotus* coexist with both perennial and summer deciduous species at the ecosystem level (Tirado and Pugnaire, 2003). Such contrasting phenologies would promote hydrological niche separation and a dynamic carbon balance in this dryland ecosystem (Dawson et al., 2002; Werner et al., 2012). Dryland productivity significantly enhances the terrestrial carbon sink, particularly during wet periods (Poulter et al., 2014). However, under water limitation, photosynthetic activity and plant productivity in these ecosystems are severely restricted (Nolan et al., 2018). This restriction is also applicable to ecosystems relying on groundwater to function (i.e., GDEs) and to the species that have the ability of making use of it to survive (i.e., phreatophytes). Shallow water tables and access to plentiful water in GDEs dominated by anisohydric strategies likely promote vegetation productivity and carbon sequestration in drylands, which may have a significant impact on the global terrestrial carbon sink. However, maintaining relatively high leaf gas exchange rates in *Z. lotus* is a risky strategy that would jeopardize the GDE if the predicted aquifer overexploitation, groundwater level

drawdown, and climate change trends for the Mediterranean Region occur (Giorgi and Lionello, 2008). These findings are thus highly relevant to the ecohydrology of the GDEs (van der Molen et al., 2011; Roman et al., 2015) and to the primary productivity and carbon balance of drylands over time (Nolan et al., 2017).

Nutrient acquisition and depth threshold for groundwater use

Nutrient cycling and acquisition by plants are strongly driven by water availability (Salazar-Tortosa et al., 2018). Our results showed lower concentration of K and Na in *Z. lotus* leaves when water availability to roots was reduced (at higher DTGW). This poorer nutritional status likely has negative implications for plant osmoregulation and osmoprotection during water stress periods (Sardans and Peñuelas, 2015). Particularly important is K, given that reduced concentrations in leaves may constrain leaf osmoregulation and stomatal regulation and opening (Arquero et al., 2006). The lower concentration of K agrees with lower g_s and E with greater DTGW. However, the decoupling of most leaf nutrients (e.g., N, P, Cu, Fe) from DTGW indicates a remarkable capacity to take up nutrients even under water stress. We suggest that *Z. lotus* could be carrying out hydraulic redistribution by its deep roots to facilitate nutrient uptake from dry upper soil layers (Caldwell et al., 1998; Cardon et al., 2013). The highest concentrations of soil organic matter and nutrients are present in the dry upper soil layers, which under drought conditions will reduce their microbial activity. Hydraulic redistribution is a key process in drylands that provides moisture to such generally dry soil, thereby facilitating nutrient acquisition by plants (Cardon et al., 2013). Widely reported in facultative phreatophytes (Scott et al., 2008; Hultine et al., 2020), this process might explain the few significant relationships between leaf nutrients concentrations in *Z. lotus* and water availability along a DTGW gradient.

Finally, the negative relationship between groundwater use and DTGW is also supported by leaf carbon stable isotopes. The response of leaf $\Delta^{13}C$ to increasing DTGW in *Z. lotus* follows the same pattern observed for predawn water potentials and leaf water fluxes (E and g_s), i.e., a decrease up to 13 − 14 m. Above this DTGW threshold, *Z. lotus* plants are less efficient in their water use (higher $\Delta^{13}C$) and show less water stress and more anisohydric behavior because they have greater groundwater availability and thus, they use more water (higher g_s and E). Conversely, below that DTGW threshold, they show

markedly increased stomatal regulation and water-use efficiency, and decreased transpiration in response to lower groundwater availability or accessibility by roots. A similar DTGW threshold for groundwater use was also reported for the deep-rooted phreatophyte Corymbia opaca in arid regions of Australia (Rumman et al., 2018). The consistency of our results with those of previous studies supports the use of leaf Δ^{13}C as potentially indicative of rooting depth and groundwater access in *Z. lotus* and other species of GDEs in arid regions (Zolfaghar et al., 2014; Garrido et al., 2018; Rumman et al., 2018). Furthermore, these findings allow for establishing a threshold use of groundwater that could reflect the maximum rooting depth of the species for optimal functioning in dryland GDEs. Despite the ability of these phreatophytes to develop deep root systems, the resilience of the GDEs will depend on the capacity to overcome drawdowns in water table levels and rises in atmospheric water demand linked to ongoing climate warming and drying.

CONCLUSIONS

We used stable isotopes (δ^2H, δ^{18}O, and Δ^{13}C), plant water potentials (Ψ_{pd}, Ψ_{md}, $\Delta\Psi_{max}$), leaf gas exchange measurements (A, g_s, and E), and leaf nutrient concentrations to reveal how the winter deciduous *Z. lotus* thrives in drylands. We uncovered the ability of the species to obtain groundwater through deep roots and its extreme anisohydric behavior, which becomes more pronounced with higher water availability (in spring and at sites with shallower groundwater tables). However, we found that most measured plant traits were strongly affected by DTGW. With this multi-pronged approach, we established a DTGW threshold at 13 – 14 m, which differentiates plants according to their water relations (i.e., the source of water and the regulation of its use). As DTGW increases, *Z. lotus* (1) decreases its dependence on groundwater, (2) reduces transpiration water loss while increasing water-use efficiency, and (3) fractionates less hydrogen through roots, possibly due to reduced water uptake and transpiration rates. Therefore, this groundwater-use threshold may reveal the maximum rooting depth of this phreatophyte for optimal functioning and suggests the existence of breakpoints in phreatophytes of arid regions that affect plant ecophysiological functioning. Our findings provide insight into the response of GDEs to the expected water table drawdowns as a consequence of both progressive climate

aridification that would reduce aquifer recharge and water content in the vadose zone and of the increased overexploitation of groundwater by humans. Therefore, we suggest that anisohydric species like *Z. lotus* with facultative dependence on groundwater in drylands, despite having mechanisms to cope with water stress, would be threatened if global change predictions are fulfilled.

REFERENCES

Arndt SK, Clifford SC, Wanek W, et al (2001) Physiological and morphological adaptations of the fruit tree Ziziphus rotundifolia in response to progressive drought stress. *Tree Physiol,* 21:705–715.

Arquero O, Barranco D, Benlloch M (2006) Potassium Starvation Increases Stomatal Conductance in Olive Trees. *HortScience,* 41:433–436.

Barbeta A, Gimeno TE, Clavé L, et al (2020) An explanation for the isotopic offset between soil and stem water in a temperate tree species. *New Phytol,* 227:766–779.

Brand WA, Geilmann H, Crosson ER, Rella CW (2009) Cavity ring-down spectroscopy versus high-temperature conversion isotope ratio mass spectrometry; a case study on δ^2H and $\delta^{18}O$ of pure water samples and alcohol/ water mixtures. *Rapid Commun Mass Spectrom*, 23: 1879–1884.

Caldwell MM, Dawson TE, Richards JH (1998) Hydraulic lift: consequences of water efflux from the roots of plants. *Oecologia,* 113:151–161.

Cardon ZG, Stark JM, Herron PM, Rasmussen JA (2013) Sagebrush carrying out hydraulic lift enhances surface soil nitrogen cycling and nitrogen uptake into inflorescences. *PNAS,* 110:18988–18993.

Dawson TE, Ehleringer JR (1991) Streamside trees that do not use stream water. *Nature,* 350:335–337.

Dawson TE, Mambelli S, Plamboeck AH, et al (2002) Stable Isotopes in Plant Ecology. *Ann Rev Ecol Evol Syst,* 33:507–559.

Drake JE, Tjoelker MG, Vårhammar A, et al (2018) Trees tolerate an extreme heatwave via sustained transpirational cooling and increased leaf thermal tolerance. *Global Change Biol,* 24:2390–2402.

Eamus D, Fu B, Springer AE, Stevens LE (2016) Groundwater Dependent Ecosystems: Classification, Identification Techniques and Threats. In: Jakeman AJ, Barreteau O, Hunt

RJ, et al. (eds) *Integrated Groundwater Management*. Springer International Publishing, Cham, pp 313–346

Eamus D, Zolfaghar S, Villalobos-Vega R, et al (2015) Groundwater-dependent ecosystems: recent insights, new techniques and an ecosystem-scale threshold response. *Hydrol Earth Syst Sci,* 12:4677–4754.

Ellsworth PZ, Williams DG (2007) Hydrogen isotope fractionation during water uptake by woody xerophytes. *Plant Soil,* 291:93–107.

Feng X, Ackerly DD, Dawson TE, et al (2019) Beyond isohydricity: The role of environmental variability in determining plant drought responses. *Plant Cell Environ,* 42:1104–1111.

Flanagan LB, Ehleringer JR, Marshall JD (1992) Differential uptake of summer precipitation among co-occurring trees and shrubs in a pinyon–juniper woodland, *Plant Cell Environ,* 15: 831–836.

Garrido M, Silva H, Franck N, et al (2018) Evaluation of Morpho-Physiological Traits Adjustment of Prosopis tamarugo Under Long-Term Groundwater Depletion in the Hyper-Arid Atacama Desert. *Front Plant Sci,* 9:453.

Garrido M, Silva P, Acevedo E (2016) Water Relations and Foliar Isotopic Composition of Prosopis tamarugo Phil., an Endemic Tree of the Atacama Desert Growing at Three Levels of Water Table Depth. *Front Plant Sci,* 7

Gázquez F, Mather I, Rolfe K, et al (2015) Simultaneous analysis of $^{17}O/^{16}O$, $^{18}O/^{16}O$ and $^2H/^1H$ of gypsum hydration water by cavity ringdown laser spectroscopy. *Rapid Commun Mass Spectrom,* 21: 1997–2006.

Giorgi F, Lionello P (2008) Climate change projections for the Mediterranean region. *Glob Planet Change* 63: 90–104.

Glenn EP, Nagler PL, Morino K, Hultine KR (2013) Phreatophytes under stress: transpiration and stomatal conductance of saltcedar (Tamarix spp.) in a high-salinity environment. *Plant Soil,* 371:655–673

Gries D, Zeng F, Foetzki A, et al (2003) Growth and water relations of Tamarix ramosissima and Populus euphratica on Taklamakan desert dunes in relation to depth to a permanent water table. *Plant Cell Envir,* 26:725–736.

Guirado E, Alcaraz-Segura D, Rigol-Sánchez JP, et al (2018) Remote-sensing-derived fractures and shrub patterns to identify groundwater dependence. *Ecohydrology,* 11:e1933.

Guo JS, Hultine KR, Koch GW, et al (2020) Temporal shifts in iso/anisohydry revealed from daily observations of plant water potential in a dominant desert shrub. *New Phytol,* 225:713–726.

Guo JS, Hungate BA, Kolb TE, Koch GW (2018) Water source niche overlap increases with site moisture availability in woody perennials. *Plant Ecol,* 219:719–735.

Hultine KR, Froend R, Blasini D, et al (2020) Hydraulic traits that buffer deep-rooted plants from changes in hydrology and climate. *Hydrol Proc,* 34:209–222.

Jackson RB, Canadell J, Ehleringer JR, et al (1996) A global analysis of root distributions for terrestrial biomes. *Oecologia,* 108:389–411.

Jackson RB, Sperry JS, Dawson TE (2000) Root water uptake and transport: using physiological processes in global predictions. *Trends Plant Sci,* 5:482–488.

Klein T (2014) The variability of stomatal sensitivity to leaf water potential across tree species indicates a continuum between isohydric and anisohydric behaviours. *Funct Ecol,* 28:1313–1320.

Kløve B, Ala-Aho P, Bertrand G, et al (2014) Climate change impacts on groundwater and dependent ecosystems. *J Hydrol,* 518:250–266.

Lambers H, Oliveira RS (2019) Plant Water Relations. In: Lambers H, Oliveira RS (eds) *Plant Physiological Ecology*. Springer International Publishing, Cham, pp 187–263

Le Houérou HN (2006) Agroforestry and silvopastoralism: The role of trees and shrubs (Trubs) in range rehabilitation and development. *Science et changements planétaires/Sécheresse* 17:343–348

Li X, Blackman CJ, Peters JMR, et al (2019) More than iso/anisohydry: Hydroscapes integrate plant water use and drought tolerance traits in 10 eucalypt species from contrasting climates. *Functi Ecol,* 33:1035–1049.

Lin G, da S. L. Sternberg L (1993) Hydrogen Isotopic Fractionation by Plant Roots during Water Uptake in Coastal Wetland Plants. In: *Stable Isotopes and Plant Carbon-water Relations*. Elsevier, pp 497–510

Machado MJ, Benito G, Barriendos M, Rodrigo FS (2011) 500 Years of rainfall variability and extreme hydrological events in southeastern Spain drylands. *J Arid Environ*, 75: 1244–1253.

Martínez-Vilalta J, Garcia-Forner N (2017) Water potential regulation, stomatal behaviour and hydraulic transport under drought: deconstructing the iso/anisohydric concept: Deconstructing the iso/anisohydric concept. *Plant Cell Environ,* 40:962–976.

Martínez-Vilalta J, Poyatos R, Aguadé D, et al (2014) A new look at water transport regulation in plants. *New Phytol,* 204:105–115.

Martín-Gómez P, Barbeta A, Voltas J, et al (2015) Isotope-ratio infrared spectroscopy: a reliable tool for the investigation of plant-water sources? *New Phytol,* 207:914–927.

McDowell N, Pockman WT, Allen CD, et al (2008) Mechanisms of plant survival and mortality during drought: why do some plants survive while others succumb to drought? *New Phytol,* 178:719–739.

Meinzer OE (1927) Plants as indicators of groundwater. U. S. Geological Survey, Water-Supply Paper 577. U. S. Government Printing Office, Washington, D.C., USA.

Millar C, Pratt D, Schneider DJ, McDonnell JJ (2018) A comparison of extraction systems for plant water stable isotope analysis. *Rapid Commun Mass Spectrom* 32(13): 1031-1044

van der Molen MK, Dolman AJ, Ciais P, et al (2011) Drought and ecosystem carbon cycling. *Agric For Meteorol,* 151: 765–773.

Moreno-Gutiérrez C, Dawson TE, Nicolás E, Querejeta JI (2012) Isotopes reveal contrasting water use strategies among coexisting plant species in a Mediterranean ecosystem. *New Phytol,* 196:489–496.

Nardini A, Casolo V, Dal Borgo A, et al (2016) Rooting depth, water relations and non-structural carbohydrate dynamics in three woody angiosperms differentially affected by an extreme summer drought: Rooting depth and plant hydraulics. *Plant Cell Environ,* 39:618–627.

Nardini A, Lo Gullo MA, Trifilò P, Salleo S (2014) The challenge of the Mediterranean climate to plant hydraulics: Responses and adaptations. *Environ Exp Bot,* 103:68–79.

Newman BD, Wilcox BP, Archer SR, et al (2006) Ecohydrology of water-limited environments: A scientific vision: OPINION. *Water Resour Res,* 42.

Nguyen QN, Polle A, Pena R (2017) Intraspecific variations in drought response and fitness traits of beech (Fagus sylvatica L.) seedlings from three provenances differing in annual precipitation. *Trees* 31:1215–1225

Nolan RH, Fairweather KA, Tarin T, et al (2017) Divergence in plant water-use strategies in semiarid woody species. *Funct Plant Biol,* 44:1134.

Nolan RH, Tarin T, Rumman R, et al (2018) Contrasting ecophysiology of two widespread arid zone tree species with differing access to water resources. *J Arid Environ,* 153:1–10.

O'Grady AP, Eamus D, Cook PG, Lamontagne S (2006) Groundwater use by riparian vegetation in the wet - dry tropics of northern Australia. *Aus J Bot,* 54:145.

Poca M, Coomans O, Urcelay C, et al (2019) Isotope fractionation during root water uptake by Acacia caven is enhanced by arbuscular mycorrhizas. *Plant Soil* 441: 485–497.

Poulter B, Frank D, Ciais P, et al (2014) Contribution of semi-arid ecosystems to interannual variability of the global carbon cycle. *Nature* 509:600–603.

Prieto I, Querejeta JI, Segrestin J, et al (2018) Leaf carbon and oxygen isotopes are coordinated with the leaf economics spectrum in Mediterranean rangeland species. *Funct Ecol,* 32:612–625.

Querejeta JI, Estrada-Medina H, Allen MF, Jimenez-Osornio JJ (2007) Water source partitioning among trees growing on shallow karst soils in a seasonally dry tropical climate. *Oecologia* 152: 26– 36.

R Core Team. 2018. R: A Language and Environment for Statistical Computing (Version 3.5.2). R Foundation for Statistical Computing, Vienna, Austria.

Rais C, Lazraq A, Nechad I, et al (2017) The biochemical and metabolic profiles of the leaves in *Ziziphus lotus* L. as a potential adaptive criterion to the environmental conditions. *J Mat Environ Sci,* 8: 1626-1633.

Reigosa MJ, Pedrol N, Sanchez A (2004) *La ecofisiología vegetal: una ciencia de síntesis*. Paraninfo, Madrid, Spain.

Reinoso H, Sosa L, Ramírez L, Luna V (2004) Salt-induced changes in the vegetative anatomy of Prosopis strombulifera (Leguminosae). *Can J Bot,* 82:618–628.

Reynolds JF, Smith DMS, Lambin EF, et al (2007) Global desertification: building a science for dryland development. *Science,* 316: 847–851.

Roman DT, Novick KA, Brzostek ER, et al (2015) The role of isohydric and anisohydric species in determining ecosystem-scale response to severe drought. *Oecologia,* 179:641–654.

Rumman R, Cleverly J, Nolan RH, et al (2018) Speculations on the application of foliar 13 C discrimination to reveal groundwater dependency of vegetation and provide estimates of root depth and rates of groundwater use. *Hydrol Earth Syst Sci,* 22:4875–4889.

Salazar-Tortosa D, Castro J, Villar-Salvador P, et al (2018) The "isohydric trap": A proposed feedback between water shortage, stomatal regulation, and nutrient acquisition drives differential growth and survival of European pines under climatic dryness. *Glob Change Biol,* 24, 4069– 4083.

Sánchez-Gómez P, Carrión MA, Hernández A, Guerra J (2003) *Libro Rojo de la Flora Silvestre protegida de la región de Murcia*. Consejería de Agricultura, Agua y Medio Ambiente, Murcia.

Sardans J, Peñuelas J (2015) Potassium stoichiometry and global change. *Glob Ecol Biogeo* 24: 261-275.

Scott RL, Cable WL, Hultine KR (2008) The ecohydrologic significance of hydraulic redistribution in a semiarid savanna: Hydraulic redistribution in a semiarid savanna. *Water Resour Res,* 44.

Skelton RP, West AG, Dawson TE (2015) Predicting plant vulnerability to drought in biodiverse regions using functional traits. *PNAS,* 112:5744–5749.

Sperry JC, Hacke UG (2002) Desert shrub water relations with respect to sol characteristics and plant functional type. *Funct Ecol,* 16: 367–378.

Steig EJ, Gkinis V, Schauer AJ, et al (2014) Calibrated high-precision 17O-excess measurements using laser-current tuned cavity ring-down spectroscopy. *Atmos Meas Tech,* 7: 2421.

Tirado R. (2009). 5220 Matorrales arborescentes con Ziziphus (*). In VV.AAaa., *Bases ecológicas preliminares para la conservación de los tipos de hábitat de interés comunitario en España*. Ministerio de Medio Ambiente, y Medio Rural y Marino. 68 p.

Tirado R, Pugnaire FI (2003) Shrub spatial aggregation and consequences for reproductive success. *Oecologia,* 136:296–301.

Toms J, Lesperance M (2003) Piecewise regression: a tool for identifying ecological thresholds. *Ecology,* 84: 2034-2041.

Urban J, Ingwers MW, McGuire MA, Teskey RO (2017) Increase in leaf temperature opens stomata and decouples net photosynthesis from stomatal conductance in Pinus taeda and Populus deltoides x nigra. *J Exp Bot,* 68:1757–1767.

Vallejos A, Sola F, Yechieli Y, Pulido-Bosch A (2018) Influence of the paleogeographic evolution on the groundwater salinity in a coastal aquifer. Cabo de Gata aquifer, SE Spain. *J Hydrol,* 557:55–66.

Werner C, Schnyder H, Cuntz M, et al (2012) Progress and challenges in using stable isotopes to trace plant carbon and water relations across scales. *Biogeosciences,* 9:3083–3111.

West AG, Dawson TE, February EC, et al (2012) Diverse functional responses to drought in a Mediterranean-type shrubland in South Africa. *New Phytol,* 195: 396–407.

Zencich SJ, Froend RH, Turner JV, Gailitis V (2002) Influence of groundwater depth on the seasonal sources of water accessed by Banksia tree species on a shallow, sandy coastal aquifer. *Oecologia,* 131:8–19.

Zolfaghar S, Villalobos-Vega R, Cleverly J, et al (2014) The influence of depth-to-groundwater on structure and productivity of Eucalyptus woodlands. *Aus J Bot,* 62:428.

SUPLEMENTARY MATERIAL

Appendix 1. Location of study area and distribution of plants of *Ziziphus lotus* and boreholes. Large triangles: location of the 16 individual plants analyzed for stable isotope and nutrient composition; small triangles, location of eight additional plants used for water potential and gas-exchange measurements. Numbers indicate depth-to-groundwater (meters) at each borehole. Note that at 21.5 m to the water table, we do not have isotopic data neither from groundwater nor from xylem water.
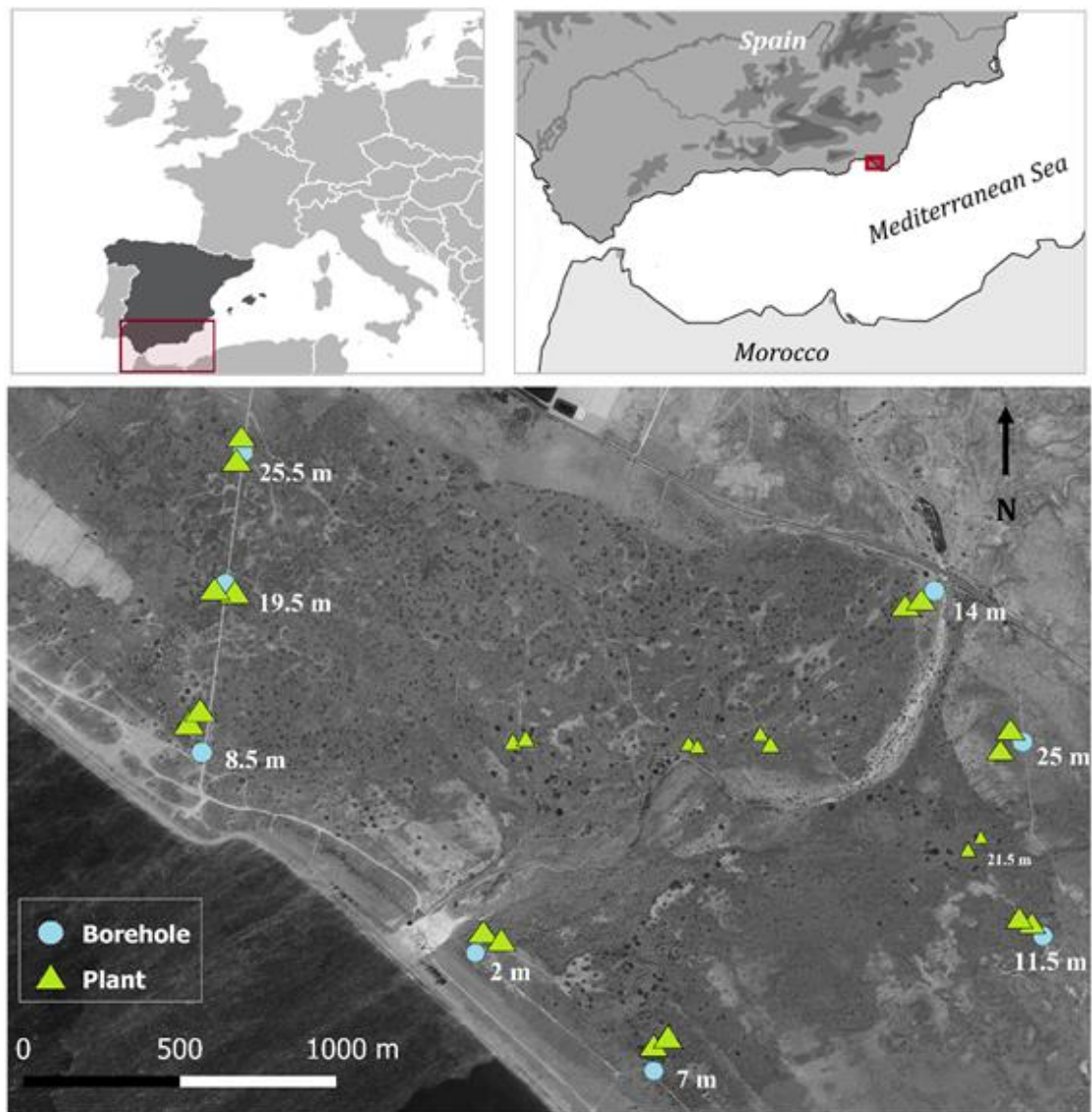
Appendix 2. Relationship between xylem water δ^2H values in *Ziziphus lotus* shrubs and depth-to-groundwater (DTGW) (A) and groundwater electrical conductivity (B). Light-blue circles represent groundwater and green triangles, xylem water. The goodness of the fit (R^2), F-statistics, and degrees of freedom are shown for the regression analysis. Significance values of the xylem: **$P < 0.01$, *$P < 0.05$; Error bars represent $\pm$ SE.
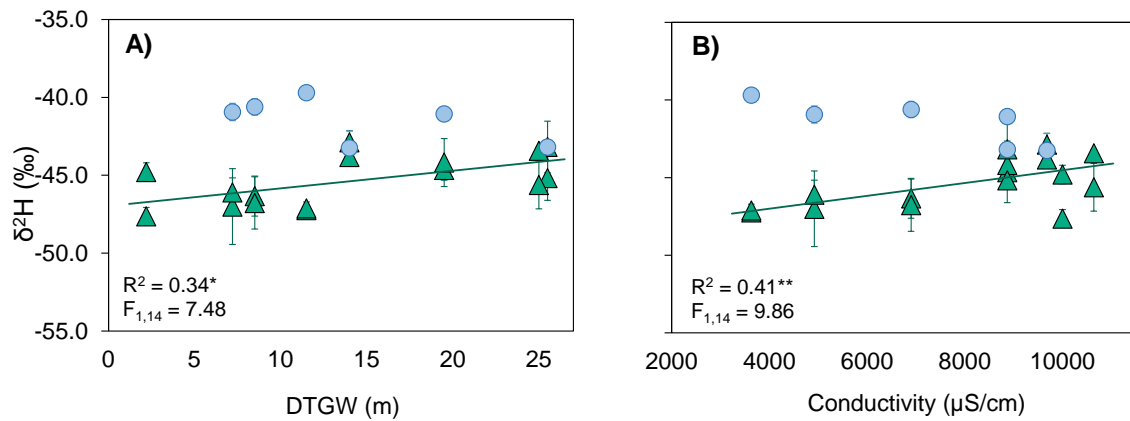
Appendix 3. Relationship between predawn (Ψ_{pd}) and midday (Ψ_{md}) water potentials in *Ziziphus lotus* shrubs during the growing season, disaggregated in May (A, green triangles), July (B, yellow circles), and September (C, red squares). Data from 2018 and 2019 pooled together are shown. The solid lines show the significant Ψ_{pd} to Ψ_{md} regressions whereas the dashed ones represent the 1:1 line. The equation of the regressions and the goodness of the fit (R^2) are also shown. Significance: **P < 0.01, no data: no significance. Error bars represent ± SE.
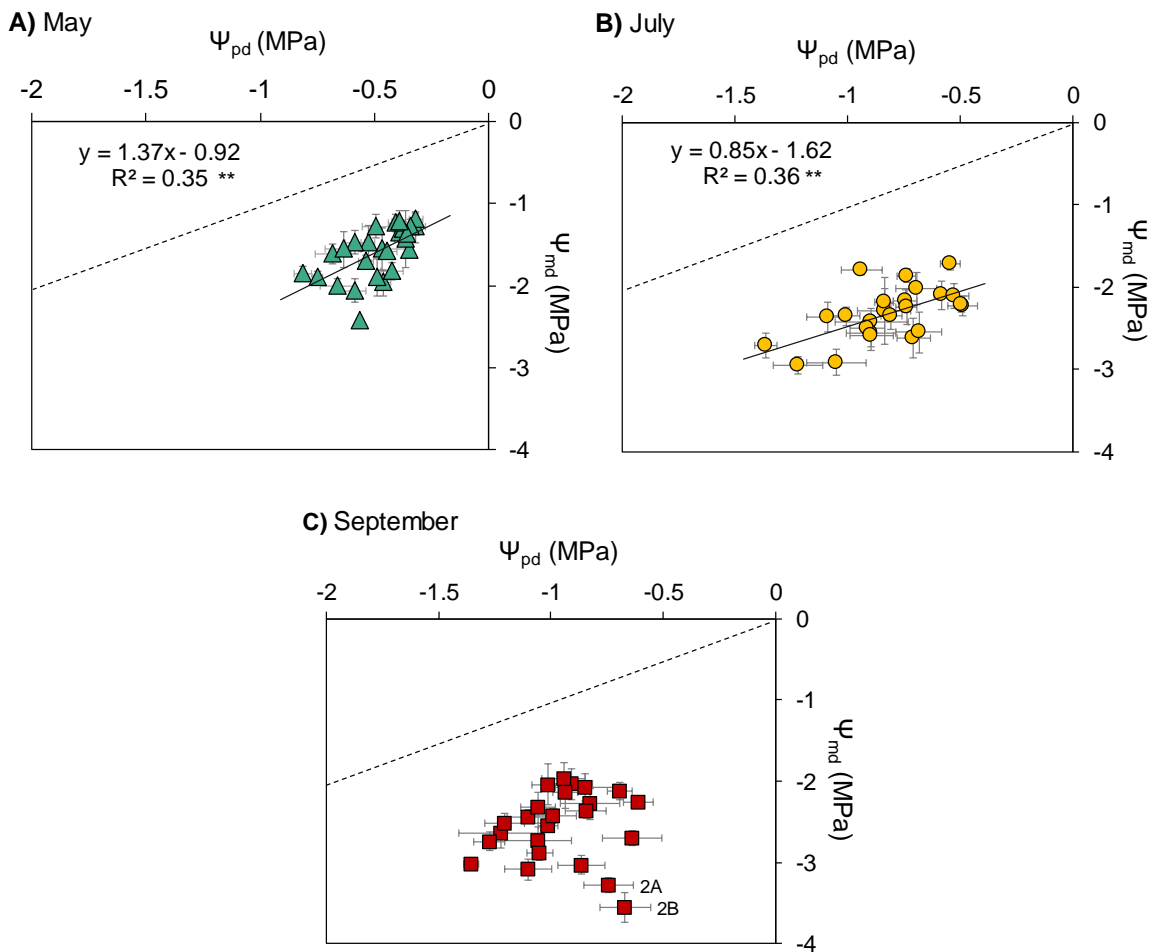
Appendix 4. Relationship between depth-to-groundwater (DTGW) and concentration of macro- and micronutrients in leaves.
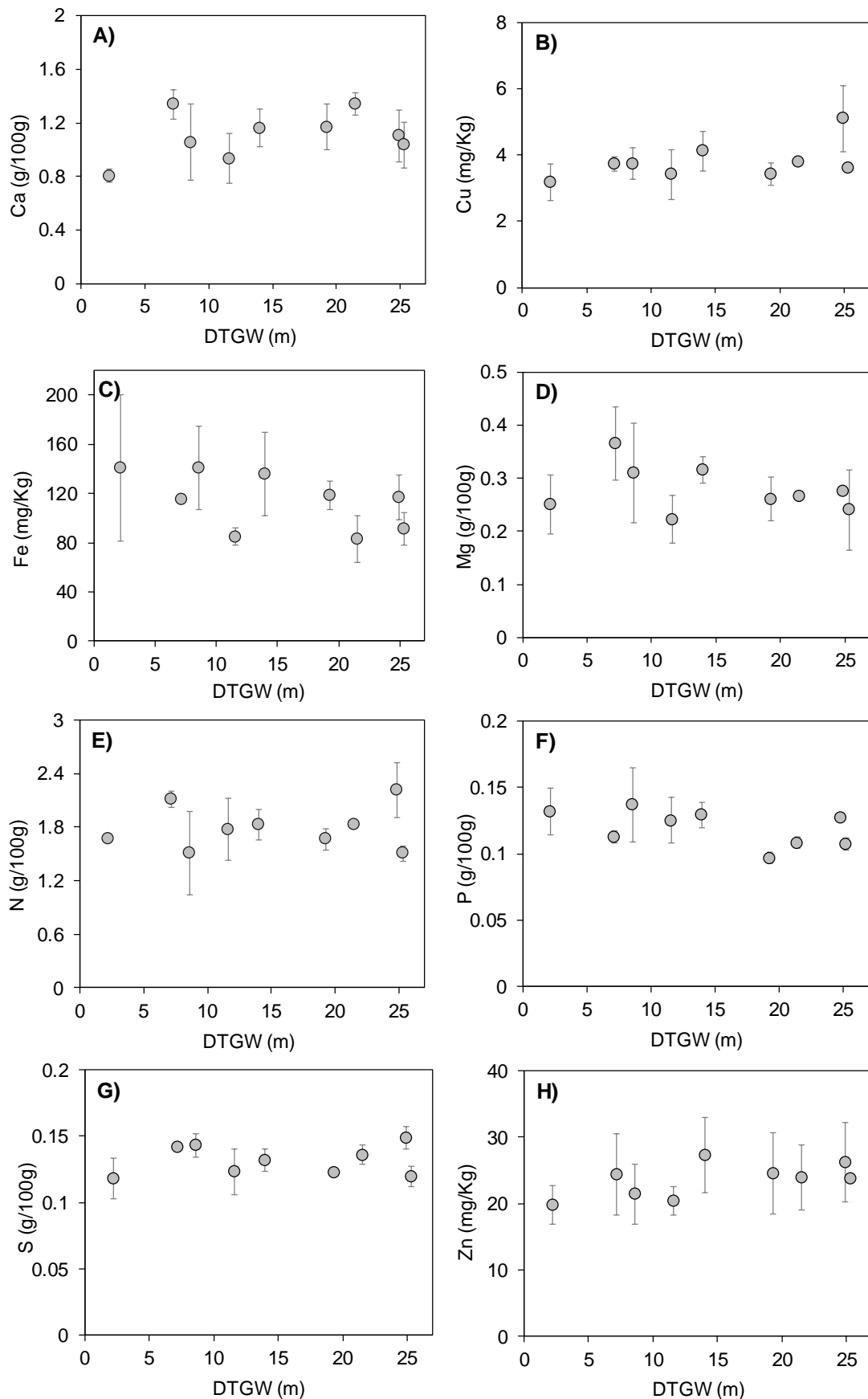
Appendix 5. Monthly precipitation during the studied period (A) and its mean stable isotope composition from March 2019 to January 2020 (B). Black circles in panel B represent $\delta^{18}O$ values whereas gray circles show δ^2H ones. Dashed line at 0‰ differentiates between positive and negative isotopic values.
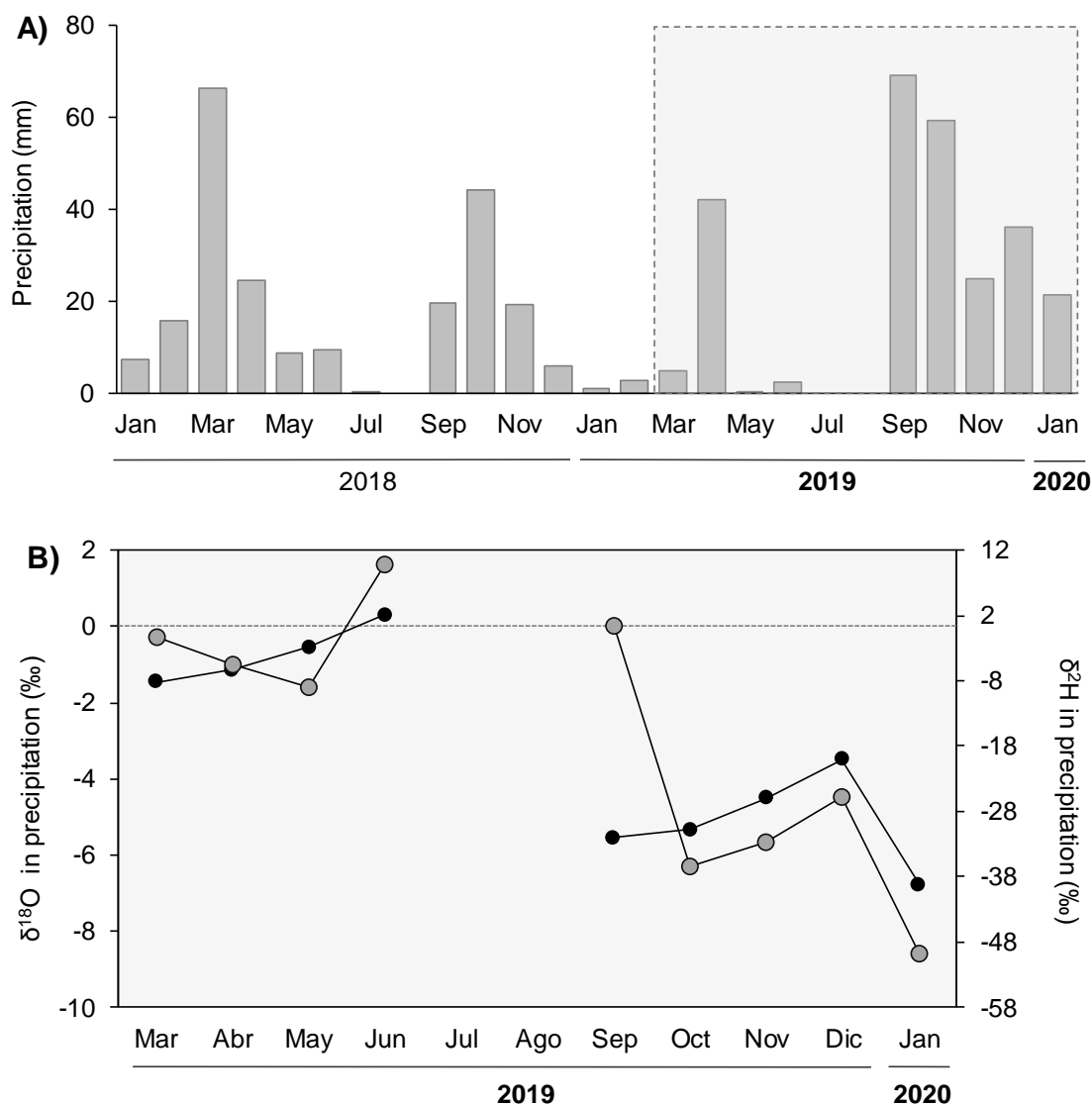
Appendix 6. Relationship (nonsignificant) between depth-to-groundwater (DTGW) and photosynthetic rate, A. Mean values of the 2018 and 2019 growing seasons are shown. Error bars represent ± SE.
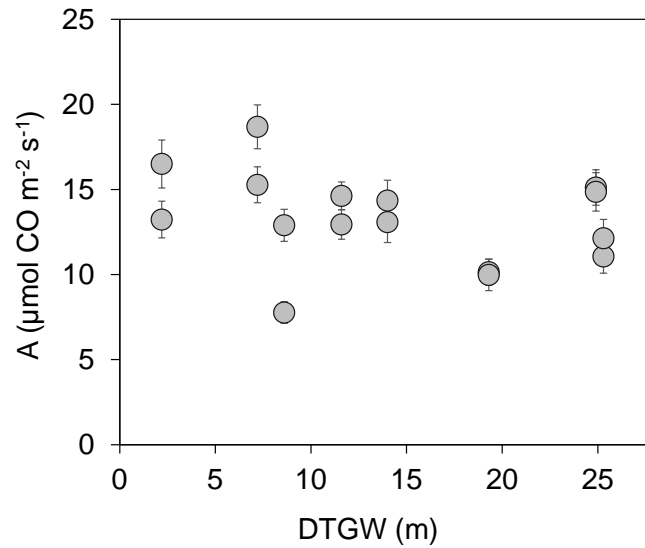
CHAPTER III: A multiple-trait analysis of ecohydrological acclimatisation in a dryland phreatophytic shrub

M. Trinidad Torres-García[1,2], María J. Salinas-Bonillo[1,2], Jamie R. Cleverly[3], Juan Gisbert[1], Manuel Pacheco-Romero[1,2] and Javier Cabello[1,2]

[1] Department of Biology and Geology, Universidad de Almería, Spain
[2] Andalusian Centre for the Monitoring and Assessment of Global Change (CAESCG), University of Almería, Spain
[3] School of Life Sciences, Faculty of Science, University of Technology Sydney, Australia

ABSTRACT

Water is the main limiting factor for groundwater-dependent ecosystems (GDEs) in drylands. Predicted climate change (precipitation reductions and temperature increases) and anthropogenic activities such as groundwater drawdown jeopardise the functioning of these ecosystems, presenting new challenges for their management. We developed a trait-based analysis to examine the spatiotemporal variability in the ecophysiology of *Ziziphus lotus*, a long-lived phreatophyte that dominates one of the few terrestrial GDEs of semiarid regions in Europe. We assessed morpho-functional traits and stem water potential along a naturally occurring gradient of depth-to-groundwater (DTGW, 2–25 m) in a coastal aquifer, and throughout the species-growing season. Increasing DTGW and salinity negatively affected photosynthetic and transpiration rates, increasing plant water stress (lower predawn and midday water potential), and positively affected Huber value (sapwood cross-sectional area per leaf area), reducing leaf area and likely, plant hydraulic demand. However, the species showed greater salt-tolerance at shallow depths. Despite groundwater characteristics, higher atmospheric evaporative demand in the study area, which occurred in summer, fostered higher transpiration rates and water stress, and promoted carbon assimilation and water loss more intensively at shallow water tables. This multiple-trait analysis allowed us to identify plant ecophysiological thresholds related to the increase in salinity, but mostly in DTGW (13 m), and in the evaporative demand during the growing season. These findings highlight the existence of tipping points in the functioning of a long-lived phreatophyte in drylands and can contribute to the sustainable management of GDEs in southern Europe, paving the way for further studies on phreatophytic species.

Keywords: depth-to-groundwater gradient, ecophysiological threshold, groundwater salinity, plant functional traits, Rhamnaceae, *Ziziphus lotus.*

INTRODUCTION

Water is an essential global resource for humans and ecosystems, particularly in arid regions where it is the most limiting factor (Newman et al., 2006). Arid and semiarid regions are characterized by low and shifting water availability across space and time (Eamus et al., 2013), thus vegetation has to live with water limitation or explore new water sources below ground (Arndt et al., 2001; Nardini et al., 2014). In this sense, groundwater reservoirs are crucial for the functioning of vegetation (O'Grady et al., 2006) in the ecosystems that have access to this hidden water source, the so-called groundwater-dependent ecosystems (GDEs) (Eamus et al., 2006). GDEs of arid regions are highly vulnerable to alterations in the hydrological regime because their structure and functioning depend on it (Eamus et al., 2006). Groundwater condition, i.e., water quality and quantity, affects GDEs, and groundwater exploitation or pollution jeopardizes their structure and function as well as the species that constitute them (Zolfaghar et al. 2014; Eamus et al. 2015). How the function of GDEs in drylands is affected by groundwater variations is a primary concern for scientists, managers, and policymakers who have to design sustainable plans to manage groundwater resources in the face of climate change (Kløve et al., 2014).

Fluctuations in groundwater depth can be detrimental to the functioning of GDEs and the deep-rooted phreatophytic vegetation that tap groundwater (Naumburg et al., 2005). Groundwater drawdown can salinize both soils and water in arid regions due to the exclusion of salts by plants during water uptake or to the exposure of deeper and saltier groundwater (Jobbágy and Jackson, 2007; Runyan and D'Odorico, 2010). Seawater intrusion, as an indirect effect of water table decline near the coast, is one of the main drivers of coastal aquifer salinization. Likewise, groundwater availability for plants can depend on salinity, which has shown substantial consequences in phreatophytic productivity, even inducing diebacks (Jolly et al., 1993; Doody and Overton, 2009; Runyan and D'Odorico, 2010). Even though salinity is a significant abiotic stress that intensifies drought impacts and water unavailability, there is little research on plant response to both groundwater salinity and depth (Kath et al., 2015; Hussain and Al-Dakheel, 2018).

Groundwater-dependent ecosystems are among the terrestrial ecosystems most vulnerable to climate change effects, and their ability to persist will depend on the

resilience of phreatophytic vegetation to groundwater decline (Hultine et al., 2020). It is widely recognized that anthropogenic activities alter the groundwater regime, either directly through groundwater exploitation or indirectly through land-use change (Eamus et al., 2015, 2016), which in turn can promote soil and groundwater salinization (Jobbágy and Jackson, 2007; Nosetto et al., 2008). Additionally, future climate change, expressed in the Mediterranean basin by a reduction in precipitation and an increase in temperature (Giorgi and Lionello 2008), will reduce groundwater recharge and raise evapotranspiration rates. Modelling carbon-water relationships will help us predict how hydrological changes can affect GDEs in terms of survival and productivity, thus addressing human impacts (Naumburg et al., 2005; Newman et al., 2006). To test vegetation response to altered water regimes, scientists usually resort to spatial gradients of aridity, altitude, water availability, and soil nutrients, among others (Lavorel and Garnier, 2002; Wright et al., 2004; Mitchell and O'Grady, 2015). Topography, for instance, can promote gradients in water availability, which cause critical variations in plant structure and function (Williams et al., 1996). The study of a species response to reduced water availability along environmental gradients will provide insight for identifying ecophysiological thresholds in phreatophytic vegetation (Eamus et al., 2006). Such thresholds might be related to the limits for maintaining high ecophysiological functioning in a "safe operating space" rather than the physical disconnection between vegetation and groundwater. Despite the definition of these tipping points is still scarce, particularly in European GDEs (Froend and Drake, 2006, González et al., 2012; Garrido et al., 2016), its knowledge is essential for a sustainable management in drylands.

Plant functional traits that refer to morphological, physiological, and phenological characteristics of the vegetation (Perez-Harguindeguy et al., 2013) provide insight about plant ecological strategies, contributing to understanding how vegetation responds to abiotic factors (Lavorel and Garnier, 2002). This "bottom-up" approach that relates plant traits to environmental gradients is a way forward for facing important ecological questions (Cornelissen et al., 2003). In GDEs, plant functional traits are the vehicle to assess different aspects of ecosystem functioning as they respond to changes in the hydrologic regime (Eamus et al., 2006). In this sense, an understanding of the connection between morpho-

functional and hydraulic traits with groundwater characteristics (i.e., groundwater depth, salinity, and temperature) will be crucial for predicting climate change effects upon GDEs.

Numerous morpho-functional traits such as Huber value (Hv), wood density, specific leaf area (SLA), and gas-exchange rates show variation across depth-to-groundwater (DTGW) gradients in arid and semiarid environments (Stromberg et al., 1996; Gazal et al., 2006; Butler et al., 2007; Carter and White, 2009; Zolfaghar et al., 2014; Osuna et al., 2015; Sommer et al., 2016; Nolan et al., 2017a). Hydraulic traits such as water potential are strongly correlated with DTGW gradients, as shown in phreatophytic oaks, eucalyptus, and acacias from California and Western and Central Australia (Carter and White, 2009; Osuna et al., 2015; Nolan et al., 2017a). Here, we explore a GDE dominated by the winter-deciduous phreatophyte *Ziziphus lotus* (L.) Lam. (Rhamnaceae) in a small coastal plain in the southeast of Spain where spatiotemporal variations in groundwater salinity and temperature were also assessed. We evaluated the relationships among a broad suite of traits including stem water potential, gas-exchange rate, intrinsic water-use efficiency (WUEi), Huber value (Hv), wood density, and specific leaf area (SLA), across a naturally occurring DTGW gradient related to distance from the coastline. We also assumed that seawater intrusion could more adversely affect plants near the coast. Thus, we hypothesized that spatiotemporal fluctuations of both groundwater availability and quality would drive differences in the ecophysiological functioning of *Z. lotus.* These differences could help us to identify ecophysiological thresholds, which will provide valuable insight to face upcoming management challenges in GDEs. To test these hypotheses, we address the following specific questions: Are there spatiotemporal variations in plant functional traits? Do these variations respond to groundwater conditions? Is there any discernible threshold in the ecophysiological functioning of *Z. lotus*? What factors drive the threshold?

METHODOLOGY

Site description

The study was conducted on a coastal plain at the western part of the Cabo de Gata-Níjar Natural Park, southeastern Spain (Fig. 1). The climate is characterized as Mediterranean and semiarid, with hot and dry summers and mild, wet winters. Mean annual temperature is 18ºC, and mean annual precipitation is 220 mm (Machado et al. 2011), which is unevenly

distributed during spring and autumn in scarce, short, and infrequent rainfall events (Appendix 1). The coastal plain is underlain by a shallow aquifer, comprised of Plio-Pleistocene conglomerates, with aeolian sands beneath it and Pliocene marine marls at the base. The geology originated from the sedimentary fill of the Bay of Almería with materials from the Sierra Alhamilla mountains (1000 m.a.s.l) and from coastal marine deposits from the Quaternary period (Vallejos et al. 2018). Eight boreholes located along the study area form a net for groundwater observation that discerns between 3 sites (east plain, west plain, and the seasonal stream that crosses it) and shows a natural occurring DTGW gradient based on coastline distance and topography.
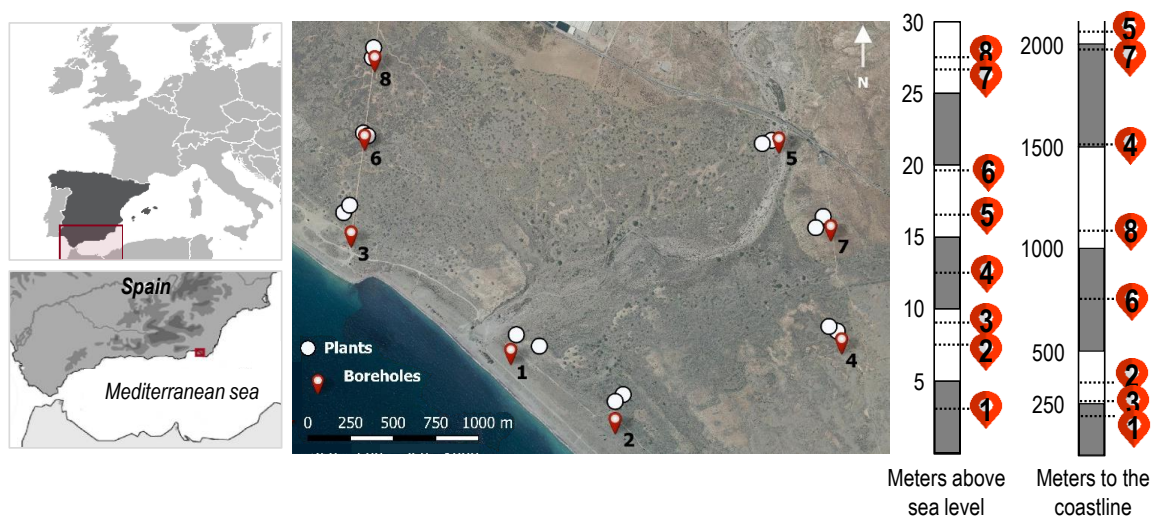
Figure 1. Location of the study area in the coastal plain of Cabo de Gata-Níjar Natural Park, southeastern Spain. Distribution of the boreholes (1 to 8) and the related plants of *Ziziphus lotus* (circles, n = 16) are shown. Bars indicate distance to the coastline (m) and meters above sea level (m.a.s.l) at each site.

The winter-deciduous phreatophyte *Z. lotus* is the dominant species of this coastal plain ecosystem, which is comprised of *Z. lotus* and other shallow-rooted Mediterranean shrubs such as Lycium intricatum, Salsola oppositifolia, and Withania frutescens (Tirado 2009). *Z. lotus* distributes along the Mediterranean basin, being native from North Africa, the Middle East, and southern Europe, mainly Spain, where it constitutes one of the few terrestrial GDEs in European drylands (Guirado et al. 2018; Torres-García et al. 2021). It is a slow-growing, long-lived shrub that has not substantially changed in size or shape in the past 70 years in the study area. The vegetation on this coastal plain shows a patchy, dispersed pattern typical of arid and semi-arid Mediterranean regions, where *Z. lotus* is associated

with biodiversity islands (Tirado 2009). *Z. lotus* is responsible for most of the photosynthetic activity during summer, whereas the rest of the vegetation constituting the island grows in winter, entailing a replacement in the drivers of the primary productivity of the ecosystem (Guirado et al. 2018). *Z. lotus* partially depends on groundwater to survive (Torres-García et al. 2021) by developing a dual root system that can reach up to 60 m deep (Le Houérou 2006) whilst also maintaining active roots near the surface. Vegetation sampling was made on a total of 16 adult individuals of *Z. lotus* (1 – 3 m tall and 50–200 m^2 area) selected next to each bore (two per bore at a maximum distance of 130 m) (Fig. 1) in three specific periods of 2019 growing season: late-spring (May), mid-summer (July), and late-summer (September).

Hydrologic and climatic measurements

Each bore contained two sensors (Hobo U20 Water level logger and Hobo U24 conductivity logger, Onset Comp. Coorp., Bourne, MA, USA) to obtain DTGW, electrical conductivity (i.e., salinity), and groundwater temperature (T_{GW}) every 15 minutes since May 2019. For regression analysis, we obtained mean values from each of the sampling periods. In the same way, we collected daily climatic data from Almería airport meteorological station (Spanish meteorological agency) located 8 km from the study area. Monthly precipitation (P) and mean monthly temperature (T_{air}) were used (measured with a Thies Precipitation Transmitter, Göttingen, Germany; and a Vaisala HUMICAP HMP155, Helsinki, Finland, respectively).

Plant traits

We analysed three traits related to the plant water potential, four physiological traits from leaf gas-exchange rates, and three morphological traits We measured water potential during the growing season at predawn (Ψ_{pd}) and midday (Ψ_{md}) in four stems on each of the 16 individuals using a Scholander pressure chamber (SKPM1405, Skye Instruments, Powys, UK). Measurements were taken before sunrise for Ψ_{pd} (from 06:00 to 07:00 hours in May and July and from 06:30 to 07:30 hours in September) and during the peak insolation for Ψ_{md} (between 13:00 and 14:00 hours). Mean values for each plant and period were calculated, and the maximum daily range ($\Delta\Psi_{max}$) was derived afterward as the difference between Ψ_{pd} and Ψ_{md}. We measured leaf gas exchange in 8 sun-exposed leaves per plant

around four different points of the outer part of the canopy (north, east, south, and west) between 10:00 and 13:00 hours on the same days as water potential was measured. A portable infrared gas analyser (Li-6400XT; LI-COR Inc., Lincoln, NE, USA) was used with the following conditions in the chamber to standardise all measures: flow rate, 400 µmol s^{-1}; CO_2 concentration, 400 µmol mol^{-1}; and light intensity, 1800 µmol m^{-2} s^{-1}. Ambient temperature was kept, which varied between 25 – 30 °C. We obtained photosynthetic rate (A), stomatal conductance (g_s), transpiration rate (E), vapour pressure deficit (VPD), and WUEi was calculated from the ratio between A and g_s.

Finally, to gather morphological traits, we cut three branches of similar size per plant in July from which all leaves were removed. We measured sapwood cross-sectional area with a digital calliper in the base of each branch. Sapwood was distinguished from heartwood by the colour difference. We also estimated wood density as the volume of a piece of branch (π x radius^2 x length) divided by its dry weight (after 48 h at 60°C). We scanned all the leaves with a digital leaf-area meter (WinDIAS, Cambridge, UK) to calculate total leaf area per branch and used ten of the leaves to estimate the SLA of the plants, which represents the relationship between the leaf area and its dry weight (after 48 h at 60°C). We calculated the Hv per plant from the ratio between the mean sapwood cross-sectional area to the mean total leaf area.

Data analysis

We applied a two-way ANOVA for each groundwater characteristic and functional trait to assess intraspecific variability, both temporal (between sampling periods) and spatial (between sampling sites). Because SLA, Hv, and wood density were only measured once, we performed a one-way ANOVA for these traits. All traits were log-transformed except for water potentials due to the negative nature of their values. We undertook Tukey's HSD post-hoc test after significant differences were found. To further examine the effects of the main stressors (salinity and DTGW) on plant response, differences in gas exchange and water potential traits between pairs of bores were tested by a Student's t test. We also performed multiple bivariate linear regressions to test whether a single regression could describe individual functioning. Some regressions were made with mean values, as variability over time was not observed, whereas others were made with monthly data to

detect seasonal patterns. Finally, we analysed multiple trait relationships across all variables with a principal component analysis (PCA). Traits were scaled prior to the analysis to obtain a unit variance. Spearman correlation analysis was applied, and the contribution of each trait in the PCA was assessed to select those variables that provide the best representation and improve the analysis. Because of that, SLA, WUEi, and wood density were not included in the final analysis. We performed all analyses in R 3.5.2 (R Core Team 2018).

RESULTS

Spatiotemporal variations in groundwater

We observed significant differences in DTGW, salinity, and T_{GW} between sites, across the growing season, and for their interaction (P < 0.001; df = 7, 4). These variables increased during the growing season, although with different patterns. First, DTGW that ranged from 2.1 m (bore 1) to 25.4 m (bore 8) (Fig. 2a) increased across the growing season, although not substantially (Appendix 2). It was just at the inner-plain sites where an average increase of 18 cm was observed at the end of the season (bore 8). Near the coast, we observed more noticeable temporal fluctuations although these did not entail overall DTGW increments (Fig. 2c, d, e, and Appendix 2). Second, T_{GW} gradually increased during summer (Appendix 3), despite its narrow range in average monthly values (from 21.78 to 23.98°C, Appendix 2). These rises mainly affected bores with the shallowest water tables such as bore 1, that showed wider fluctuations, and bore 2, that had the steepest increase. Finally, groundwater salinity, which ranged from 3360 µS/cm (bore 4) to 11000 µS/cm (bore 7), increased in bores 1, 3 and 7, but particularly in bore 7 where a rise in almost 1000 µS/cm was observed (Appendix 2 and Appendix 3). For these three groundwater properties, fluctuations were larger near the coast where water tables were shallower (bores 1 to 3) than in the other bores.
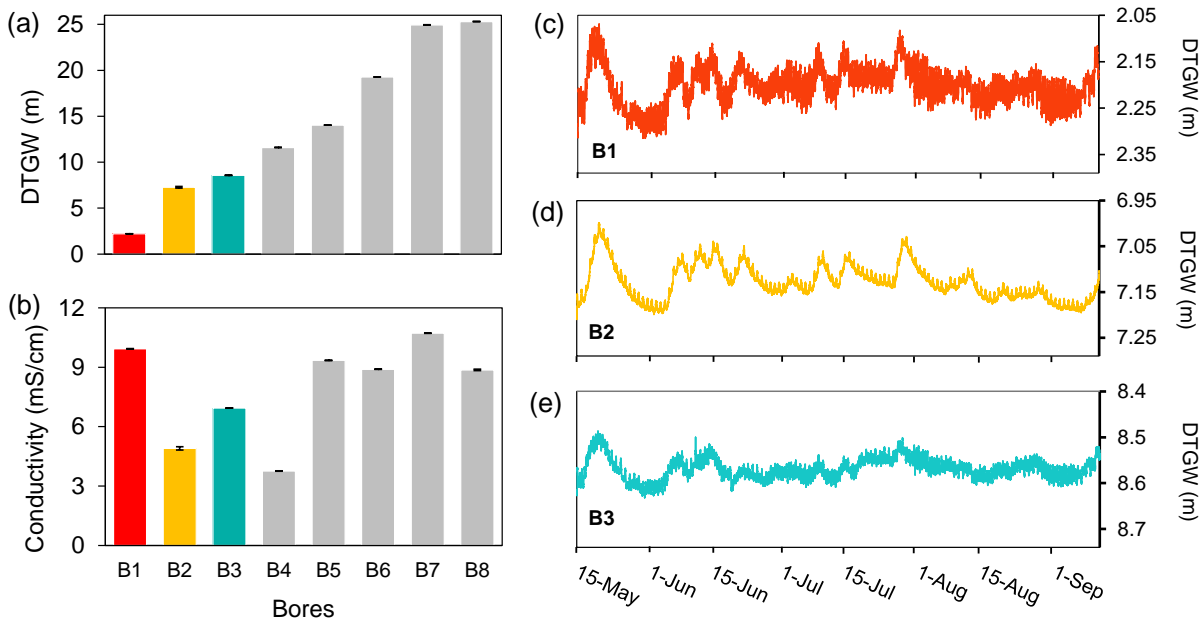
Figure 2. Mean a) depth-to-groundwater (DTGW, m) and b) groundwater salinity (electrical conductivity, mS/cm) at different sites (bores) ± SE. Temporal fluctuations of DTGW in the shallowest and closest to the coast bores are also shown (c, d, and e).

Spatiotemporal variations in plant traits and their relationship with groundwater

Plant traits also showed significant differences between sampling periods, sites, and the interaction between them (Table 1 and Appendix 4). Overall, gas exchange (A and E) in *Z. lotus* leaves was higher in summer (July and September) and at those sites with the shallowest water tables. Regarding water loss, plants from bores 1 to 4 (DTWG < 11.6 m) showed the highest g_s, especially during July and September when it reached 0.42 ± 0.03 mol H_2O m^{-2} s^{-1}, whereas bores 5 to 8 (DTGW > 14.0 m), had the lowest values. It is also noticeable that high rates of E for plants from bores 1, 2, and 3 occurred in July and September, but also from bore 8 (25.3 m). Nevertheless, A showed significant differences in summer just at some locations (interaction term, P < 0.001, df = 14), although general differences between months were not observed (individual term, P = 0.1, df = 2, Appendix 4). Individuals next to bores 2 and 5 (with a DTGW of 7.3 and 14.0 m respectively) had higher photosynthetic rates in July, whereas plants near bores 6 and 8 (with 19.3 and 25.3 m respectively) showed lower values at the end of summer (Table 1). In general, individuals next to bores 1 and 2 had the highest rates of A, whereas bore 8 showed the lowest ones. Contrary to A, WUEi was low at not only the shallowest water tables, but also at the deepest

and saltiest ones. Regarding water potential, more negative values of both Ψ_{pd} and Ψ_{md} were observed in July and September at sites with the highest DTGW (bores 5 to 8). Ψ_{pd} ranged between -0.32 ± 0.02 MPa in May to -1.55 ± 0.09 MPa in September (at bore 2 and bore 8, respectively), whereas Ψ_{md} showed values between -1.18 ± 0.04 MPa in May to -3.13 ± 0.10 MPa in July (bore 4 and bore 8, respectively).

Table 1. Summary of mean values of traits (± standard error) from plants next to each bore in the three sampling periods: May, July, and September. Depth-to-groundwater (DTGW) of each site is showed as well as the significant differences (P < 0.05) between months in each site (different letters). Photosynthetic rate (A), stomatal conductance (g_s), transpiration rate (E), intrinsic water-use efficiency (WUEi), predawn (Ψ_{pd}) and midday (Ψ_{md}) water potential, and vapour pressure deficit (VPD).

Bore DTWG (m)	Month	A (μmol CO_2 m^{-2} s^{-1})	g_s (mol H_2O m^{-2} s^{-1})	E (mmol H_2O m^{-2} s^{-1})	WUEi (μmol CO_2 / mol H_2O)	Ψ_{pd} (MPa)	Ψ_{md} (MPa)	VPD (kPa)
Bore 1 2.2 m	May	15.32 ± 1.69 a	0.33 ± 0.05 a	7.84 ± 0.81 a	50.53 ± 3.88 a	-0.42 ± 0.03 a	-1.74 ± 0.19 a	2.82 ± 0.04 a
	July	13.77 ± 1.87 a	0.35 ± 0.04 a	10.94 ± 1.08 b	37.92 ± 2.54 a	-0.63 ± 0.05 a	-2.33 ± 0.17 b	3.39 ± 0.06 b
	Sep	15.51 ± 1.12 a	0.32 ± 0.02 a	12.16 ± 0.67 b	48.11 ± 1.95 a	-1.08 ± 0.05 b	-2.98 ± 0.08 c	3.91 ± 0.03 b
Bore 2 7.3 m	May	16.17 ± 1.77 a	0.23 ± 0.02 a	5.81 ± 0.48 a	73.84 ± 5.30 a	-0.32 ± 0.02 a	-1.23 ± 0.09 a	2.63 ± 0.04 a
	July	24.88 ± 2.36 b	0.40 ± 0.05 b	10.60 ± 1.05 b	73.52 ± 8.85 a	-0.64 ± 0.04 b	-2.49 ± 0.04 b	2.96 ± 0.06 a
	Sep	15.83 ± 1.47 a	0.32 ± 0.04 ab	14.10 ± 1.42 b	53.39 ± 3.42 b	-0.96 ± 0.07 c	-3.63 ± 0.10 c	4.78 ± 0.07 b
Bore 3 8.6 m	May	11.13 ± 1.58 a	0.22 ± 0.03 a	6.41 ± 0.61 a	48.55 ± 4.31 a	-0.63 ± 0.04 a	-1.97 ± 0.15 a	2.93 ± 0.05 a
	July	9.48 ± 0.95 a	0.41 ± 0.03 b	10.95 ± 0.74 b	23.96 ± 2.34 b	-0.86 ± 0.06 b	-2.26 ± 0.17 a	2.87 ± 0.08 a
	Sep	11.08 ± 1.52 a	0.42 ± 0.03 b	11.89 ± 0.68 b	25.96 ± 2.94 b	-1.08 ± 0.08 c	-1.94 ± 0.17 a	3.09 ± 0.06 a
Bore 4 11.6 m	May	14.34 ± 1.40 a	0.25 ± 0.03 a	6.74 ± 0.61 a	61.69 ± 5.37 a	-0.41 ± 0.04 a	-1.18 ± 0.04 a	2.82 ± 0.07 a
	July	13.68 ±1.57 a	0.38 ± 0.04 b	10.99 ± 0.85 b	35.62 ± 1.98 b	-0.55 ± 0.03 a	-1.95 ± 0.15 b	3.09 ± 0.09 a
	Sep	10.57 ± 1.26 a	0.22 ± 0.03 a	5.73 ± 0.59 a	52.29 ± 4.37 ab	-0.96 ± 0.07 b	-2.52 ± 0.23 c	2.91 ± 0.13 a
Bore 5 14.0 m	May	6.84 ± 0.98 a	0.14 ± 0.01 a	3.67 ± 0.36 a	49.67 ± 4.01 a	-0.76 ± 0.05 a	-1.66 ± 0.07 a	2.71 ± 0.03 a
	July	13.26 ± 1.09 b	0.16 ± 0.01 a	7.45 ± 0.54 b	87.32 ± 8.69 b	-1.28 ± 0.09 b	-2.83 ± 0.08 b	4.68 ± 0.04 b
	Sep	10.12 ± 1.75 ab	0.24 ± 0.02 b	7.14 ± 0.42 b	40.64 ± 4.87 a	-1.29 ± 0.04 b	-2.74 ± 0.14 b	3.08 ± 0.05 a
Bore 6 19.3 m	May	15.07 ± 1.56 a	0.25 ± 0.03 a	6.28 ± 0.73 a	67.19 ± 6.30 a	-0.46 ± 0.03 a	-1.44 ± 0.08 a	2.61 ± 0.04 a
	July	8.35 ± 1.50 b	0.22 ± 0.03 a	8.26 ± 0.92 a	37.20 ± 2.29 b	-1.31 ± 0.05 b	-2.98 ± 0.14 b	4.09 ± 0.06 b
	Sep	9.67 ± 1.64 b	0.24 ± 0.02 a	8.11 ± 0.53 a	39.70 ± 5.70 b	-1.24 ± 0.05 b	-1.96 ± 0.16 c	3.50 ± 0.05 b
Bore 7 25.0 m	May	12.13 ± 1.42 a	0.16 ± 0.02 a	4.43 ± 0.41 a	75.87 ± 4.01 a	-0.60 ± 0.07 a	-1.64 ± 0.15 a	2.88 ± 0.04 a
	July	12.33 ± 1.20 a	0.17 ± 0.01 a	7.25 ± 0.53 b	72.17 ± 2.42 a	-1.23 ± 0.08 b	-2.79 ± 0.11 b	4.23 ± 0.07 b
	Sep	13.27 ± 1.41 a	0.32 ± 0.03 b	6.91 ± 0.43 b	41.47 ± 2.24 b	-1.19 ± 0.07 b	-2.51 ± 0.08 b	2.23 ± 0.03 a
Bore 8 25.3 m	May	10.74 ± 1.26 a	0.22 ± 0.03 a	5.47 ± 0.53 a	51.91 ± 5.19 a	-0.43 ± 0.05 a	-1.36 ± 0.08 a	2.56 ± 0.05 a
	July	11.52 ± 1.52 a	0.26 ± 0.03 a	10.71 ± 0.68 b	44.52 ± 4.93 a	-1.01 ± 0.08 b	-3.13 ± 0.10 b	4.44 ± 0.14 b
	Sep	7.16 ± 1.33 b	0.29 ± 0.02 b	10.38 ± 0.54 b	23.77 ± 4.09 b	-1.55 ± 0.09 c	-3.06 ± 0.08 b	3.63 ± 0.09 c

Hv also showed significant differences across sites (P = 0.027) (Appendix 5). The Hv of the plants at bore 1 with shallow groundwater (3.58 ± 0.08) was significantly lower than that of plants at bores 7 and 8 with deep groundwater (11.40 ± 0.22 and 9.34 ± 0.84 respectively). Neither SLA nor wood density showed significant spatial variability.

Most of the traits significantly responded to spatial (A, g_s, and Hv), temporal (Ψ_{md}), or spatiotemporal variations (E and Ψ_{pd}). First, bivariate linear regressions revealed a weak negative relationship with DTGW for most gas-exchange traits during the growing season (Fig. 3), except for WUEi. By contrast, no relationship was observed between these traits and groundwater salinity (Appendix 6). However, comparing by pairs, we revealed significant differences between plants at sites with different conditions (e.g., similar DTGW and different salinity). When comparing plants at bore 4 (intermediate DTGW and low salinity) and bore 1 (low DTGW and high salinity), they only differed in E and Ψ_{md}, showing
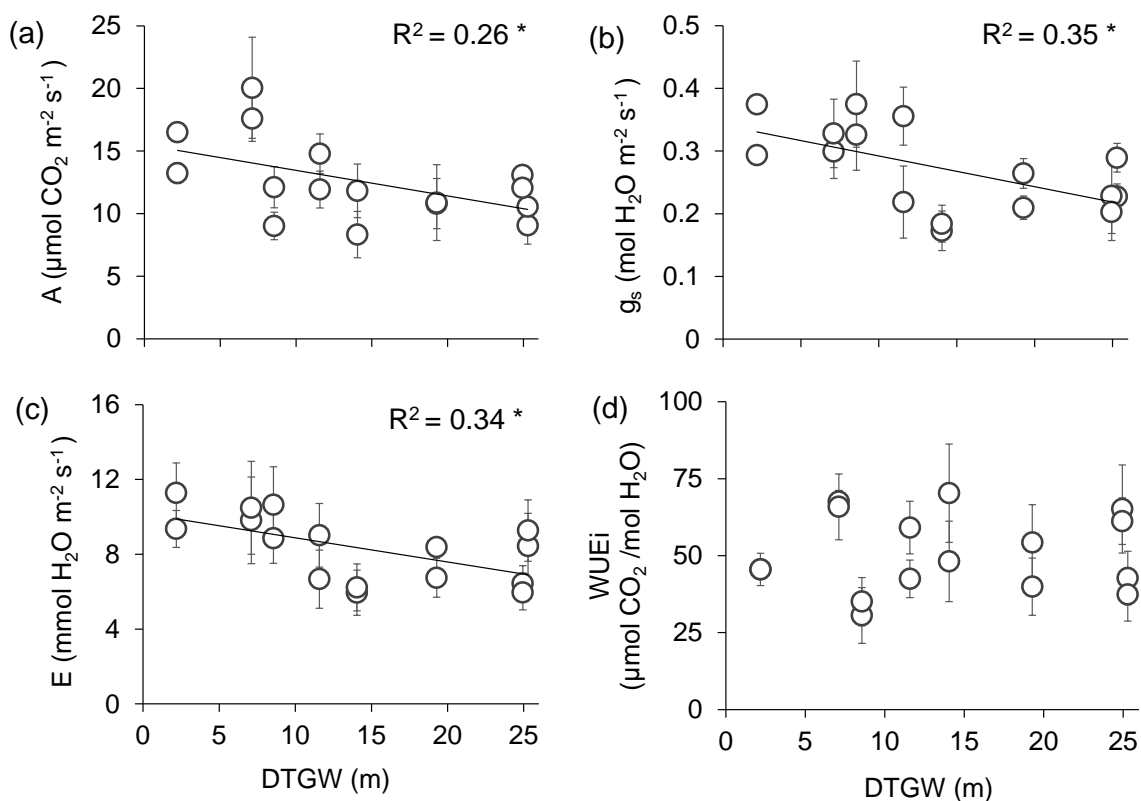
Figure 3. Bivariate linear regression between depth-to-groundwater (DTGW) and *Ziziphus lotus* gas exchange rates: a) photosynthetic rate (A), b) stomatal conductance (g_s), c) transpiration rate (E), and d) intrinsic water-use efficiency (WUEi). Mean values per plant are displayed ± SE. Lines represent significant linear regressions and R^2, the goodness of the fit. Significance of the regression: *P < 0.05.

higher water loss and also stress at bore 1 (Appendix 7). When comparing plants from bore 4 and bore 5 (both intermediate DTGW but low and high salinity respectively), we observed higher E, g_s, and A values when salinity is lower. Regarding water potential, Ψ_{pd} was the only variable that showed a significant linear relationship to both DTGW and salinity, in which Ψ_{pd}, but neither Ψ_{md} nor $\Delta\Psi_{max}$, was significantly lower when DTGW and salinity were large (Fig. 4 and Appendix 8). Nonetheless, salinity seemed to be related to more negative values of Ψ_{pd} (bore 3 and bore 5 vs. bore 4) but also Ψ_{md} (bore 5 vs. bore 4). Our results also showed that at large DTGW, plants exhibited higher Hv values than when DTGW was small (Fig. 5), even though wood density and SLA did not respond to groundwater spatial gradients (Appendix 9). Therefore, DTGW was the main variable related to spatial variation in most single traits.
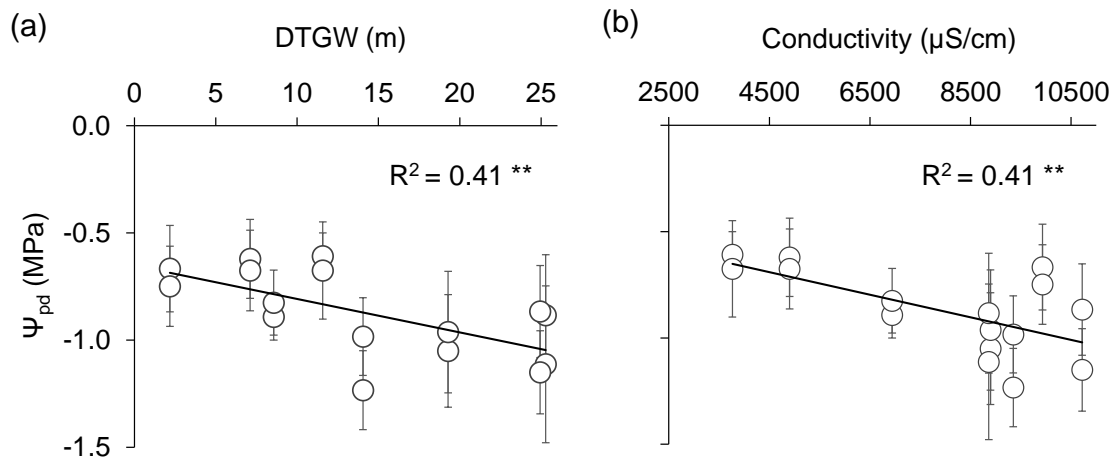
Figure 4. Bivariate linear regression between water potential at predawn (Ψ_{pd}) of *Ziziphus lotus* and a) depth-to-groundwater (DTGW) and b) groundwater electrical conductivity. Mean values per plant are displayed ± SE. Lines represent significant linear regressions and R^2, the goodness of the fit. Significance of the regression: **P < 0.01.
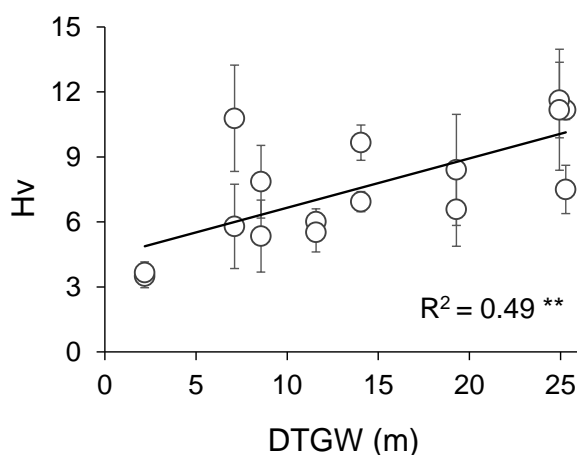
Figure 5. Bivariate linear regression between depth-to-groundwater (DTGW) and Huber value (Hv) of Ziziphus lotus. Mean values per plant are displayed ± SE. The line represents the significant linear regression and R^2, the goodness of the fit. Significance of the regression: **P < 0.01.

The transpiration rate was positively correlated with VPD (Fig. 6a), which represents temporal variations in climatic conditions. In May, both E and VPD showed lower values, with little variability across bores, whereas in summer (July and September), the increase in VPD was parallel to the rise in E. The general increase in VPD during the season enhanced transpiration rates more over the shallowest water tables than at the deepest ones (Fig. 6b). However, VPD did not show any significant relationship with other traits related to gas exchange (Appendix 10). The overall increment of VPD from spring to summer was related to more negative Ψ_{pd} and Ψ_{md} values, as shown in the regression analysis (Fig. 7a and b).

Temporal analysis of the relationships between traits also revealed that A, E, and g_s were positively related to each other, despite salinity, and particularly during spring. Nonetheless, WUEi (= A / g_s) was positively related to A and negatively related to g_s in summer exclusively (Appendix 11). Our results also showed a negative relationship of Ψ_{pd} with these gas-exchange traits both in spring (A: R^2 = 0.40, P = 0.008; g_s: R^2 = 0.37, P = 0.012; E: R^2 = 0.30, P = 0.015) and summer (A: R^2 = 0.25, P = 0.003; g_s: R^2 = 0.28, P = 0.002; E: R^2 = 0.14, P = 0.037). As water availability decreased (lower Ψ_{pd}), A, g_s, and E were reduced, but no response was observed with an increase of plant stress (lower Ψ_{md}) at any time (Appendix 11).
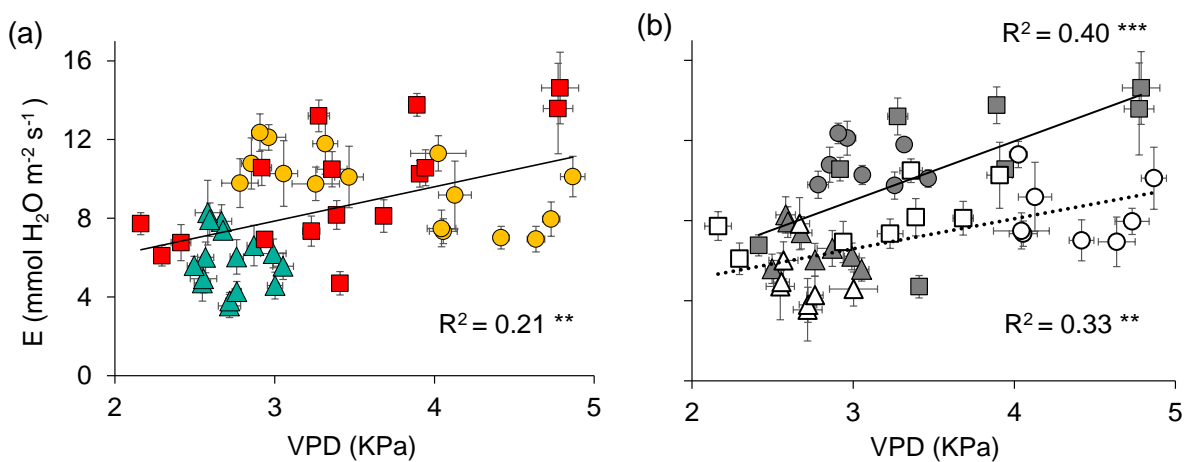
Figure 6. Bivariate linear regression between vapour pressure deficit (VPD) and transpiration rate (E) during the growing season of *Ziziphus lotus*. Mean values per plant are displayed ± SE, differenciating between a) the three sampling periods (May: green triangles, July: yellow circles, and September: red squares), and b) the three periods and shallow sites (DTGW < 12 m: grey symbols), and deep sites (DTGW > 12 m: open symbols). Significance of the regression: ***P < 0.001, **P < 0.01.

(a)

(b)
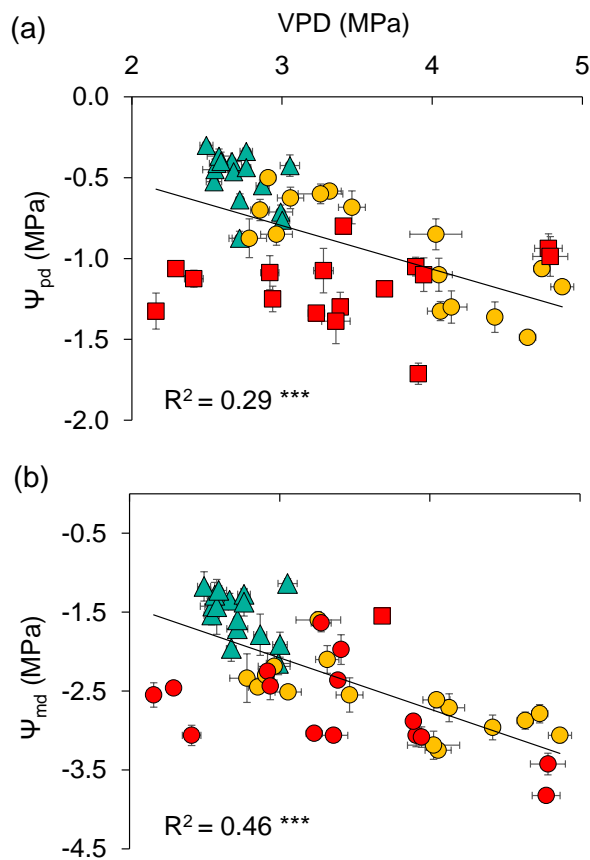
Figure 7. Bivariate linear regression between vapour pressure deficit (VPD) and a) predawn, and b) midday water potential (Ψ_{pd} and Ψ_{md}, respectively). Monthly values per plant are displayed ± SE. Colours and shapes represent sampling periods: May (Green triangles), July (Yellow circles), and September (Red squares). R^2 represents the goodness of the fit. Significance of the regression: ***P < 0.001.

Multiple trait relationship for identifying ecophysiological thresholds

PCA revealed multiple trait relationships that were not identified with simple regression analysis. The two first components of the PCA explained 63.5% of the variation across plants (Fig. 8a). The first component (PC1), accounting for 37.6% of the total variation, showed strong loadings for climatic variables (i.e., T_{air}, precipitation) as well as stem water potential (i.e., Ψ_{pd} and Ψ_{md}) and E. The second component (PC2) explained 25.9 % of the variance and showed strong loadings for groundwater traits (particularly DTGW but also T_{GW}), A and g_s. Groundwater salinity and Hv also contributed to PC2, although to a lesser extent. As a result, axis 1 showed a temporal gradient from the warmest and driest months that overlap to each other (July and September) with higher E and VPD, to the mild and humid spring (May), when water availability was higher (high Ψ_{pd}) and plant stress lower (high Ψ_{md}) (Fig. 8b). By contrast, axis 2 showed a DTGW gradient (Fig. 8c and d) where plants closer to the water table exhibited higher A and g_s but lower Hv. The PCA revealed two distinct clusters based on groundwater characteristics (DTGW, salinity) and their associated gas-exchange traits (A, g_s): one for plants at sites with shallow DTGW (< 12m, Fig. 8c), and the other for plants at sites with salty and deep DTGW (> 8800 μS/cm and 14 m, Fig. 8d).
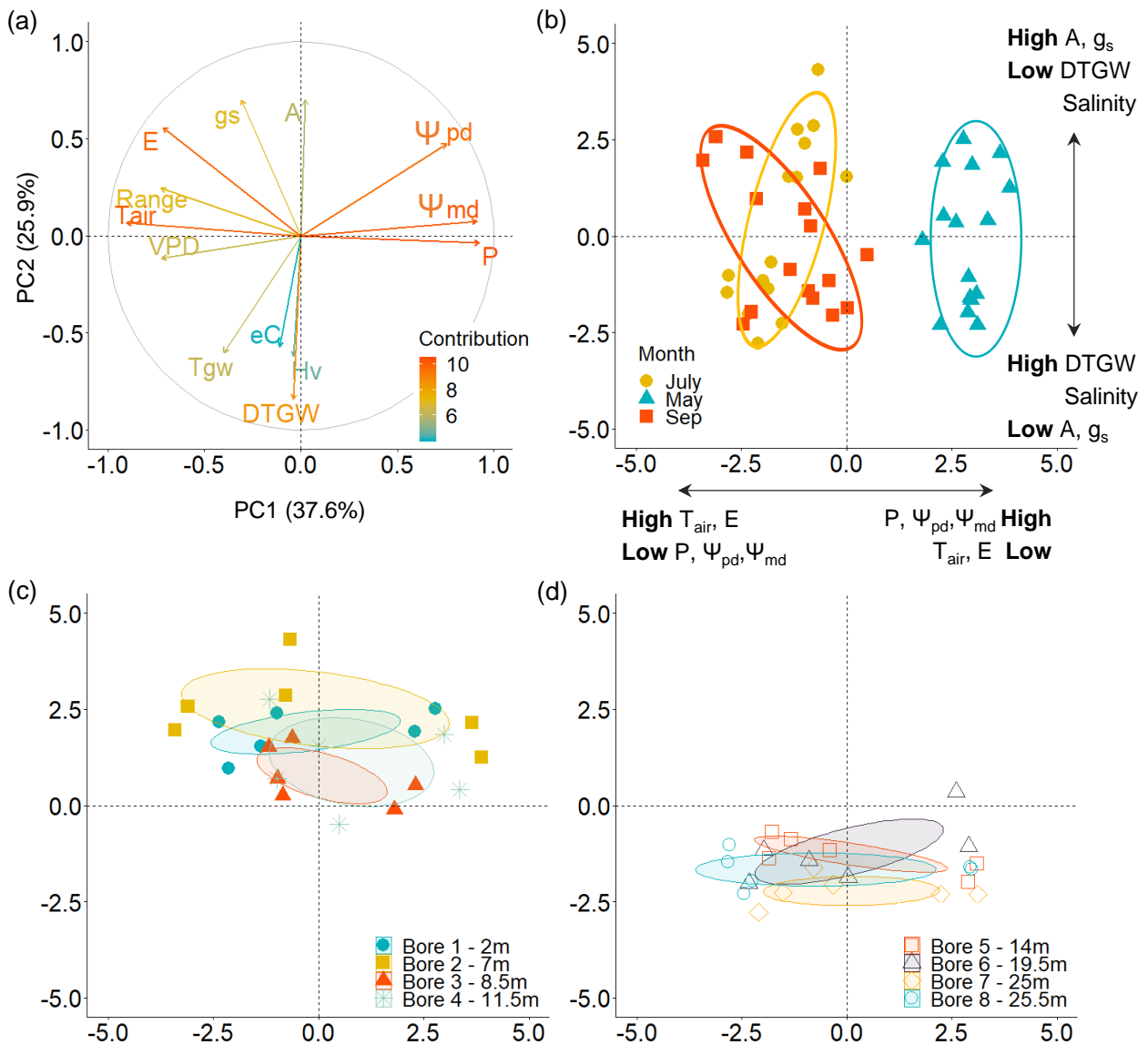
Figure 8. Principal component analysis (PCA). a) Contribution of the variables from high (redish arrows) to low contribution (bluish arrows). b) Representation of each individual of *Ziziphus lotus* in the PCA space by month; and representation by site, differentiating between c) sites with DTGW lower than 12 m, and d) higher than 14 m. Horizontal and vertical arrows in panel (b) show the main variables contributing to each axis (PC1 and PC2, respectively): photosynthetic rate (A), stomatal conductance (g_s), transpiration rate (E), predawn and midday water potential (Ψ_{pd} and Ψ_{md}), maximum daily range (range), Huber value (Hv), depth-to-groundwater (DTGW), electrical conductivity (salinity, eC), vapour pressure deficit (VPD), precipitation (P), and air temperature (T_{air}).

DISCUSSION

In this study, we examined the ecophysiological response of the long-lived phreatophyte *Ziziphus lotus* to a DTGW gradient, in a coastal GDE of the Mediterranean basin. We found that DTGW and salinity had a significant, additive effect on the ecophysiological function of this phreatophyte, as hypothesised. We further found that some traits were more strongly correlated to fluctuations in DTGW and salinity (e.g., A and g_s), whereas others were more strongly related to seasonal fluctuations in atmospheric conditions (e.g., E, Ψ_{pd}, Ψ_{md}). By applying a multiple-trait approach, we were able to identify plant ecophysiological thresholds related to the groundwater characteristics and seasonality throughout the growing season.

Spatiotemporal variations in *Z. lotus'* traits and their relationship with groundwater

Our findings revealed spatiotemporal variations in *Z. lotus* traits, which were related to both groundwater and seasonal climatic conditions. The spatial variability in DTGW might explain the response patterns of gas exchange throughout the growing season. Increasing DTGW negatively affected carbon assimilation and water loss, as previously observed in GDEs of Australia and the United States (Butler et al. 2007; Carter and White 2009; Osuna et al. 2015; Sommer et al. 2016). Thus, deep-rooted species, particularly from arid and semiarid regions, can face physiological constraints fostered by deep water sources (Nardini et al. 2014). Here, A, g_s, and E might decrease with the increase in DTGW as consequence of such constraints. In summer, the importance of groundwater availability increased, as shown by the rise in these gas-exchange rates as consequence of higher net radiation and temperature (O'Grady et al. 1999; Sommer et al. 2016), and this rise in gas-exchange rates was more pronounced in plants at shallower DTGW. On the contrary, plants at deep water tables did not experience such noticeable increase in ecophysiological activity, which could be also determined by high groundwater salinity. Even though the effects of groundwater availability and salinity cannot be uncoupled straightforwardly because of the nature of the study area, paired comparison of the sites suggested the negative effect of salinity in carbon assimilation (Appendix 7). Nevertheless, we observed that neither carbon assimilation nor water loss was completely compromised at any point of the growing season and at any DTGW, since the lowest mean rates of A and g_s were

observed in May, reaching 6.84 µmol CO_2 $m^{-2}s^{-1}$ and 0.14 mol H_2O $m^{-2}s^{-1}$ respectively at bore 5 (Table 1). This result can be explained by *Z. lotus* accessing and using groundwater continuously during its growing season to avoid stomatal closure, even in summer (Torres-García et al. 2021). In this sense, the low values of WUEi we observed in summer and the lack of relationship with DTGW agree with having access to a water source, likely groundwater, since large WUEi is widely associated with groundwater usage where precipitation in scarce (Eamus et al. 2013; Cleverly et al. 2016; Rumman et al. 2018). A similar behaviour is observed in phreatophytic vegetation with access to groundwater (Nolan et al. 2017b, 2018; Rumman et al. 2018). Additionally, *Z. lotus* transpiration rate did not decline in summer; in fact, it increased with VPD, more significantly at shallow water tables, suggesting that summer conditions could induce higher rates when sufficient groundwater is available (Nolan et al. 2018; Eamus and Prior, 2001), and that groundwater availability to the plant depends on climatic conditions. Despite the risk of hydraulic failure due to this anisohydric behaviour (Torres-García et al. 2021) and the physiological limitations of tapping water from deep sources, *Z. lotus* plants can maintain high gas exchange under current conditions.

The naturally occurring gradient also explained the spatial variability in Ψ_{pd} and responses to differences in water availability. Ψ_{pd} largely reflects the water potential of the rooting area (Hinckley et al. 1978) and indicates groundwater access by plants when values are barely negative (Carter and White 2009). *Although Z. lotus* plants showed values that did not fall below -1.55 MPa, which is high given the solute potential, we found a negative trend of Ψ_{pd} not only with increasing DTGW but also with salinity. Groundwater salinity increased with DTGW away from the coast, which could be due to a marine incursion during the Holocene that penetrated the inner parts of the plain, constituting a lagoon which dried up over time and increased the salinity of the area (Vallejos et al. 2018). Therefore, it is not a recent process of seawater intrusion that induced differences in *Z. lotus* population, but a past event that fostered different salinity conditions across the landscape. This result is contrary to our assumption that seawater intrusion could affect salinity near the coast. Instead, we found that the combination of deep groundwater and high salinity away from the coast might promote water stress in the root zone as well as a drought-like condition in the plant (Kath et al. 2015). Although *Z. lotus* showed little

evidence of water deficit (slightly negative water potentials even in summer) and have continuous access to groundwater during its growing season (Torres-García et al. 2021), Ψ_{pd} and Ψ_{md} correlated with DTGW and salinity. Particularly, salinity might have induced lower water potential at the root surface, reducing water uptake and photosynthetic rate in *Z. lotus*, as in other species from GDEs (Kath et al. 2015). These constraints seem to affect plants with access to intermediate and deep groundwater. In fact, a previous isotopic analysis in the area showed that *Z. lotus* plants might be reducing water uptake and triggering some stomatal regulation because of higher groundwater depth and salinity (Torres-García et al. 2021). Other authors demonstrated the accumulation of osmotically active compounds such as proline and water-soluble carbohydrates in *Z. lotus* leaves in response to salt and/or drought stress (Rais et al. 2017). Therefore, groundwater salinity might induce different adaptation mechanisms in *Z. lotus* to cope with this stress. Our results also bear consistent evidence of the salt-tolerance of *Z. lotus*, at least up to a groundwater electrical conductivity of 11000 µS/cm, and particularly at shallow groundwater tables.

Coupled with DTGW and salinity gradients, temporal groundwater depletion might induce water-deficit stress, particularly in the late summer (Naumburg et al. 2005; Sommer et al. 2016). Our results revealed a significant decrease in both Ψ_{pd} and Ψ_{md} from spring to summer, although DTGW did not substantially decline during the growing season. We consider that the temporal fluctuations observed in groundwater level are insufficient to induce such a response, as maximum differences reported during the growing season reached just 18 cm in bore 8. Even daily fluctuations observed at the shallowest and closer-to-the-coast sites, which can reflect groundwater use due to transpiration (Dahm et al. 2002; Thibault et al. 2017) or the effect of tides on the coastal aquifer (Vallejos et al. 2015; Levanon et al. 2017), had little effect on groundwater salinity. Additionally, the slight differences observed in groundwater temperature are insufficient to substantive affect viscosity related to DTGW or xylem water assent and thus, to infer large physiology effect on vegetation (Jensen and Taylor, 1961). Thus, the significant decrease in the water potential during the growing season was due to other factors such as atmospheric evaporative demand. The negative response of both Ψ_{pd} and Ψ_{md} to increased VPD throughout the growing season shows the decisive effect of the high summer temperature

on plant regulation, highlighting the importance of VPD in promoting transpiration when water availability is not limiting (Sulman et al. 2016; Amitrano et al. 2019). However, in these GDEs where daily and seasonal groundwater fluctuations are minor, phreatophytes run the risk of maximizing productivity over safety (Hultine et al. 2020), which can also be fostered by the anisohydric behaviour of the species (Torres-García et al. 2021). Being an anisohydric phreatophyte in arid and semiarid regions seems to be a risky option, which can only be overcome in some species by plasticity in individuals for responding to upcoming environmental conditions through shifts in hydraulic traits such us higher root area to leaf area ratios or higher resistance to xylem cavitation (Hultine et al. 2020).

Different responses observed in *Z. lotus* transpiration rates could also be generated by differences in xylem traits such as sapwood area (Attia et al. 2015), or in leaf area. Our results revealed that Hv (the ratio of sapwood area to leaf area) was higher at deeper groundwater sites, as already reported for other phreatophytes of mesic (Zolfaghar et al. 2014) and xeric environments (Carter and White 2009). Larger Hv is observed in drought tolerant plants (Canham et al. 2009) because of higher sapwood area to support leaf area and/or less leaf area supported by such sapwood (Carter and White 2009). Higher sapwood area observed in plants at deep sites (Appendix 12) could enhance *Z. lotus* capacity for water supply (Butterfield et al. 2021), and compensate the evaporative demand, particularly in summer. On the one hand, *Z. lotus* plants with less reliable groundwater supply (deep DTGW) seem to make smaller investments in leaf area than plants at shallow sites (Appendix 12). This mechanism might allow *Z. lotus* to cope with reduced water availability by decreasing their hydraulic demand and, therefore, their transpiration rates at a canopy level (Gazal et al. 2006; Carter and White 2009; Zolfaghar et al. 2014). Indeed, reductions of aboveground biomass are acknowledged to be a common adaptation when plants cannot overcome the anatomical and functional adaptation cost of water scarcity (Naumburg et al. 2005).

In contrast to Hv, wood density was largely independent of groundwater because it depends on development of modified cell types (e.g., xylem vessels, fibres) (Lachenbruch and McCulloh 2014). Likewise, our results showed that SLA was independent of DTGW, as has been reflected in some studies along water availability gradients (Nolan et al. 2017a). In this case, as SLA refers to the ratio of leaf area to leaf dry mass, or the inverse of leaf

thickness (Pérez-Harguindeguy et al. 2013), SLA would be conserved as an adaptation to light levels and aridity. By contrast, leaf area reductions are medium-to-long-term adaptations to limit water loss (Zolfaghar et al. 2014) that *Z. lotus* might have developed to address DTGW coupled to weak stomatal control (i.e., anisohydry). Despite being able to explain the variability of plant traits, the weak but significant relationships obtained revealed how difficult it is to define the functioning of a complex ecosystem like a GDE by a single regression for a given pair of traits.

Ecophysiological thresholds and future considerations

Assessing the expression of multiple traits provides tools to predict patterns of change in GDEs in response to variability in groundwater and across seasons (Hultine et al. 2020). A multiple-trait analysis revealed that the variability observed in the functioning of *Z. lotus* could be explained by the combination of both temporal variations in climatic conditions during the growing season of the species and the spatial differences in groundwater characteristics of the study area. Temporal differences from spring to summer showed a decrease in water potential with increased transpiration rates, promoted by environmental conditions (lower humidity, higher temperatures, and evaporative demand). This response could have fostered evaporative cooling, regulating leaf temperature for maintaining the plant carbon balance (Drake et al. 2018) and suggesting the decline in water potential was insufficient to indicate water stress. Thus, *Z. lotus* plants could avoid extreme thermal stress that can damage the photosynthetic machinery whilst preventing a steep decline in photosynthetic rate. However, sufficient water availability is required to maintain evaporative cooling, which is essential under ongoing increases of both mean air temperatures and the severity of heat waves (Urban et al. 2017).

By contrast to temporal fluctuations, the ecophysiological functioning of *Z. lotus* across space was explained by the combination of groundwater availability (mainly determined by DTGW) and salinity (expressed by electrical conductivity). Salinity is commonly present in arid ecosystems with phreatophytic vegetation because of reduced precipitation, which prevents leaching of salts, and evaporation, which leaves salts behind (Glenn et al. 2013). We found that the DTGW gradient coincided with a salinity gradient such that the deepest groundwater was also saltiest. Without the ability to discriminate between these

characteristics at high depths, we observed that higher groundwater salinity combined with larger DTGW affected the ecophysiology of *Z. lotus* and promoted remarkable differences along the naturally occurring gradient. Notwithstanding, at shallow sites, the effect of salinity is blurred by greater water availability, suggesting that DTGW is a more determinant factor for *Z. lotus* ecophysiological functioning. Thus, we identified a response threshold at 12-14 m, mainly promoted by differences in gas-exchange rates, which is consistent with previous studies about the species (Torres-García et al. 2021). Saltier and deeper groundwater have a substantial effect on plants, reducing water uptake, and diminishing gas exchange (Kath et al. 2015). Such threshold might point to the DTGW limits for maintaining high ecophysiological functioning and could be used as a baseline for managing this GDE.

Under predicted climate change for semiarid regions of the Mediterranean basin, anisohydric phreatophytes like *Z. lotus* would increase their transpiration rates as well as the risk of hydraulic failure despite their relative drought tolerance (McDowell et al. 2008). For the related GDE, this means that an increase in groundwater discharge and associated increases in DTGW could also promote salinization (Jobbágy and Jackson 2007; Runyan and D'Odorico 2010). The expected decrease in precipitation will not support recharge or salt leaching, and salinization can continue until it reaches the tolerance threshold of the species. Once salinity intolerance is reached, further groundwater uptake might be compromised, along with plant survival (Nosetto et al. 2008). Furthermore, processes of seawater intrusion can occur in coastal aquifers because of the reduction in groundwater, what would result in ecosystem-scale changes in hydraulic and functional traits (Runyan and D'Odorico 2010, Hultine et al. 2020). The concern is also whether a depletion in groundwater level would exceed the root growth rate (Orellana et al. 2012), or even if temporal fluctuations would have a long-term impact on plant ecophysiology. In the case of the long-lived phreatophyte *Z. lotus*, our results suggest that its salt-tolerance confers to the plants the ability to escape from the effect of the stress when groundwater availability is greater. However, phreatophytes that obtain groundwater from deep water tables and that already experience some physiological constraints (e.g., over 14 m in the case of *Z. lotus*), could be intensively jeopardized by groundwater variations in the future.

CONCLUSIONS

In this research, we assessed spatiotemporal variations both in groundwater properties of a GDE in a semiarid region and in the morpho-functional traits of the phreatophyte that dominates this ecosystem: *Ziziphus lotus*. The naturally occurring DTGW gradient and associated monitoring field station have provided an interesting scenario to assess ecophysiological differences related to water availability for phreatophytic vegetation. Here, we show that both groundwater depth and salinity are highly connected to the ecophysiological functioning of phreatophytic vegetation in drylands. Nevertheless, no evidence of seawater intrusion seemed to affect *Z. lotus* plants so far, and groundwater salinity could be related to past events of seawater rise. Differences in climatic conditions throughout the growing season drove temporal variability in *Z. lotus* response, with summer conditions promoting carbon assimilation and water loss in this winter deciduous phreatophyte, more intensively at shallow water tables. The multiple-trait analysis led to identifying spatial and temporal ecophysiological thresholds that depend on groundwater availability and salinity, as well as atmospheric evaporative demand. Under the expected reductions in groundwater reservoirs as consequence of both climate aridification and the increase in groundwater consumption and drawdown by human overexploitation, understanding the functioning of GDEs of arid and semiarid regions and defining ecophysiological thresholds of their phreatophytic vegetation will provide valuable insight to face upcoming management challenges.

REFERENCES

Amitrano C, Arena C, Rouphael Y, et al (2019) Vapour pressure deficit: The hidden driver behind plant morphofunctional traits in controlled environments. *Ann App Biol,* 175:313–325

Arndt SK, Clifford SC, Wanek W, et al (2001) Physiological and morphological adaptations of the fruit tree Ziziphus rotundifolia in response to progressive drought stress. *Tree Physiol,* 21:705–715

Attia Z, Domec J-C, Oren R, et al (2015) Growth and physiological responses of isohydric and anisohydric poplars to drought. *Exp Bot,* 66:4373–4381

Butler JJ, Kluitenberg GJ, Whittemore DO, et al (2007) A field investigation of phreatophyte-induced fluctuations in the water table: Phreatophyte-induced fluctuations. *Water Resourc Res,* 43

Butterfield BJ, Palmquist EC, Hultine KR (2021) Regional coordination between riparian dependence and atmospheric demand in willows (Salix L.) of western North America. *Divers Distrib,* 27: 377– 388

Canham CA, Froend RH, Stock WD (2009) Water stress vulnerability of four Banksia species in contrasting ecohydrological habitats on the Gnangara Mound, Western Australia. *Plant Cell Environ,* 32: 64-72

Carter JL, White DA (2009) Plasticity in the Huber value contributes to homeostasis in leaf water relations of a mallee Eucalypt with variation to groundwater depth. *Tree Physiol,* 29:1407–1418

Cleverly J, Eamus D, Van Gorsel E, et al (2016) Productivity and evapotranspiration of two contrasting semiarid ecosystems following the 2011 global carbon land sink anomaly. *Agric For Meteorol,* 220:151-159

Cornelissen JHC, Lavorel S, Garnier E, et al (2003) A handbook of protocols for standardised and easy measurement of plant functional traits worldwide. *Aus J Bot,* 51:335.

Dahm CN, Cleverly JR, Coonrod JEA, et al (2002) Evapotranspiration at the land/water interface in a semi-arid drainage basin. *Freshw Biol,* 47:831-843

Doody TM, Overton IC (2009) Riparian vegetation changes from hydrological alteration on the River Murray, Australia - Modelling the surface water-groundwater dependent ecosystem. In: Taniguchi M. Burnett WC, Fukishima Y, et al (eds) *From Headwaters to the Ocean - Hydrological Changes and Watershed Management*. Taylor and Frances Group, London pp 395–400.

Drake JE, Tjoelker MG, Vårhammar A, et al (2018) Trees tolerate an extreme heatwave via sustained transpirational cooling and increased leaf thermal tolerance. *Glob Change Biol,* 24:2390–2402

Eamus D, Cleverly J, Boulain N, et al (2013) Carbon and water fluxes in an arid-zone Acacia savanna woodland: An analyses of seasonal patterns and responses to rainfall events. *Agric For Meteorol,* 182–183:225–238

Eamus D, Froend R, Loomes R, et al (2006) A functional methodology for determining the groundwater regime needed to maintain the health of groundwater-dependent vegetation. *Aus J Bot,* 54:97

Eamus D, Fu B, Springer AE, Stevens LE (2016) Groundwater Dependent Ecosystems: Classification, Identification Techniques and Threats. In: Jakeman AJ, Barreteau O, Hunt

RJ, et al. (eds) *Integrated Groundwater Management*. Springer International Publishing, Cham, pp 313–346

Eamus D, Prior L (2001) Ecophysiology of trees of seasonally dry tropics: Comparisons among phenologies. In: *Advances in Ecological Research*. Elsevier, pp 113–197

Eamus D, Zolfaghar S, Villalobos-Vega R, et al (2015) Groundwater-dependent ecosystems: recent insights, new techniques and an ecosystem-scale threshold response. *Hydrol Earth Sys Sci Discuss,* 12:4677–4754

Froend RH, Drake PL (2006) Defining phreatophyte response to reduced water availability: preliminary investigations on the use of xylem cavitation vulnerability in Banksia woodland species. *Aus J Bot,* 54:173

Garrido M, Silva P, Acevedo E (2016) Water Relations and Foliar Isotopic Composition of Prosopis tamarugo Phil., an Endemic Tree of the Atacama Desert Growing at Three Levels of Water Table Depth. *Front Plant Sci,* 7

Gazal RM, Scott RL, Goodrich DC, Williams DG (2006) Controls on transpiration in a semiarid riparian cottonwood forest. *Agric For Meteorol,* 137:56–67

Giorgi F, Lionello P (2008) Climate change projections for the Mediterranean region. *Glob Planet Change,* 63: 90–104

Glenn EP, Nagler PL, Morino K, Hultine KR (2013) Phreatophytes under stress: transpiration and stomatal conductance of saltcedar (Tamarix spp.) in a high-salinity environment. *Plant Soil,* 371:655–673

González E, González-Sanchis M, Comín, FA, Muller E (2012) Hydrologic thresholds for riparian forest conservation in a regulated large Mediterranean river. *River Res Appl,* 28: 71-80

Guirado E, Alcaraz-Segura D, Rigol-Sánchez JP, et al (2018) Remote-sensing-derived fractures and shrub patterns to identify groundwater dependence. *Ecohydrology,* 11:e1933

Hinckley TM, Lassoie JP, Running SW (1978) Temporal and spatial variations in water status of forest trees. *For Sci,* 24, a0001–z0001

Hultine KR, Froend R, Blasini D, et al (2020) Hydraulic traits that buffer deep-rooted plants from changes in hydrology and climate. *Hydrol Process,* 34:209–222

Hussain MI, Al-Dakheel AJ (2018) Effect of salinity stress on phenotypic plasticity, yield stability, and signature of stable isotopes of carbon and nitrogen in safflower. *Environ Sci Pollut Res,* 25:23685–23694

Jensen RD, Taylor SA (1961) Effect of temperature on water transport through plants. *Plant Physiol,* 36(5):639-642

Jobbágy EG, Jackson RB (2007) Groundwater and soil chemical changes under phreatophytic tree plantations. *J Geophys Res,* 112:G02013

Jolly ID, Walker GR, Thorburn PJ (1993) Salt accumulation in semi-arid floodplain soils with implications for forest health. *J Hydrol,* 150:589–614

Kath J, Powell S, Reardon-Smith K, et al (2015) Groundwater salinization intensifies drought impacts in forests and reduces refuge capacity. *J App Ecol* 52:1116–1125

Kløve B, Ala-Aho P, Bertrand G, et al (2014) Climate change impacts on groundwater and dependent ecosystems. *J Hydrol,* 518:250–266

Lachenbruch B, McCulloh KA (2014) Traits, properties, and performance: how woody plants combine hydraulic and mechanical functions in a cell, tissue, or whole plant. *New Phytol,* 204:747–764

Lavorel S, Garnier E (2002) Predicting changes in community composition and ecosystem functioning from plant traits: revisiting the Holy Grail. *Funct Ecol,* 16:545–556

Le Houérou HN (2006). Agroforestry and silvopastoralism: The role of trees and shrubs (Trubs) in range rehabilitation and development. *Sécheresse*, 17(1), 343–348.

Levanon E, Yechieli Y, Gvirtzman H, Shalev E (2017) Tide-induced fluctuations of salinity and groundwater level in unconfined aquifers – Field measurements and numerical model. *J Hydrol,* 551:665–675

Machado MJ, Benito G, Barriendos M, Rodrigo FS (2011) 500 Years of rainfall variability and extreme hydrological events in southeastern Spain drylands. *J Arid Environ,* 75: 1244–1253

McDowell N, Pockman WT, Allen CD, et al (2008) Mechanisms of plant survival and mortality during drought: why do some plants survive while others succumb to drought? *New Phytol,* 178:719–739

Mitchell P, O'Grady A (2015) Adaptation of Leaf Water Relations to Climatic and Habitat Water Availability. *Forests,* 6:2281–2295

Nardini A, Lo Gullo MA, Trifilò P, Salleo S (2014) The challenge of the Mediterranean climate to plant hydraulics: Responses and adaptations. *Environ Exp Bot,* 103:68–79

Naumburg E, Mata-gonzalez R, Hunter RG, et al (2005) Phreatophytic Vegetation and Groundwater Fluctuations: A Review of Current Research and Application of Ecosystem Response Modeling with an Emphasis on Great Basin Vegetation. *Environ Manage,* 35:726–740

Newman BD, Wilcox BP, Archer SR, et al (2006) Ecohydrology of water-limited environments: A scientific vision: OPINION. *Water Resour Res,* 42:W06302

Nolan RH, Fairweather KA, Tarin T, et al (2017a) Divergence in plant water-use strategies in semiarid woody species. *Funct Plant Biol,* 44:1134

Nolan RH, Tarin T, Fairweather KA, et al (2017b) Variation in photosynthetic traits related to access to water in semiarid Australian woody species. *Funct Plant Biol,* 44:1087

Nolan RH, Tarin T, Rumman R, et al (2018) Contrasting ecophysiology of two widespread arid zone tree species with differing access to water resources. *J Arid Environ,* 153:1–10

Nosetto MD, Jobbágy EG, Tóth T, Jackson RB (2008) Regional patterns and controls of ecosystem salinization with grassland afforestation along a rainfall gradient: Patterns and controls of salinization. *Glob Biogeochem Cycles,* 22, GB2015

O'Grady AP, Eamus D, Cook PG, Lamontagne S (2006) Groundwater use by riparian vegetation in the wet - dry tropics of northern Australia. *Aus J Bot,* 54:145

O'Grady AP, Eamus D, Hutley LB (1999) Transpiration increases during the dry season: patterns of tree water use in eucalypt open-forests of northern Australia. *Tree Physiol,* 19:591–597

Orellana F, Verma P, Loheide SP, Daly E (2012) Monitoring and modeling water-vegetation interactions in groundwater-dependent ecosystems: Groundwater-dependent ecosystems. *Rev Geophys,* 50: RG3003

Osuna JL, Baldocchi DD, Kobayashi H, Dawson TE (2015) Seasonal trends in photosynthesis and electron transport during the Mediterranean summer drought in leaves of deciduous oaks. *Tree Physiol,* 35:485–500

Pérez-Harguindeguy N, Díaz S, Garnier E, et al (2013) New handbook for standardised measurement of plant functional traits worldwide. *Aus J Bot,* 61:167

Rais C, Lazraq A, Nechad I, et al (2017) The biochemical and metabolic profiles of the leaves in *Ziziphus lotus* L. as a potential adaptive criterion to the environmental conditions. *J Mat Environ Sci,* 8:1626-1633

Rumman R, Cleverly J, Nolan RH, Tarin T, Eamus D (2018). Speculations on the application of foliar 13C discrimination to reveal groundwater dependency of vegetation and provide estimates of root depth and rates of groundwater use. *Hydrol Earth Syst Sci,* 22: 4875–4889

Runyan CW, D'Odorico P (2010) Ecohydrological feedbacks between salt accumulation and vegetation dynamics: Role of vegetation-groundwater interactions: Salt accumulation and vegetation dynamics. *Water Resourc Res,* 46: W11561

Sommer B, Boggs DA, Boggs GS, et al (2016) Spatiotemporal patterns of evapotranspiration from groundwater-dependent vegetation: Spatiotemporal Patterns of Evapotranspiration from Phreatophytes. *Ecohydrology,* 9:1620–1629

Stromberg JC, Tiller R, Richter B (1996) Effects of Groundwater Decline on Riparian Vegetation of Semiarid Regions: The San Pedro, Arizona. *Ecol Appl,* 6:113–131 https://doi.org/10.2307/2269558

Sulman BN, Roman DT, Yi K, et al (2016) High atmospheric demand for water can limit forest carbon uptake and transpiration as severely as dry soil: VPD control of gpp and transpiration. *Geophys Res Lett,* 43:9686–9695

Thibault JR, Cleverly JR, Dahm CN (2017) Long-term water table monitoring of Rio Grande riparian ecosystems for restoration potential amid hydroclimatic challenges. *Environ Manage,* 60:1101-1115

Tirado R (2009) 5220 Matorrales arborescentes con Ziziphus (*). In VV.AAaa., Bases ecológicas preliminares para la conservación de los tipos de hábitat de interés comunitario en España. Ministerio de Medio Ambiente, y Medio Rural y Marino. 68 p

Torres-García MT, Salinas-Bonillo MJ, Gázquez-Sánchez F, et al (2021) Squandering water in drylands: The water-use strategy of the phreatophyte *Ziziphus lotus* in a groundwater-dependent ecosystem. *Ame J Bot,* 108(2):236-248

Urban J, Ingwers MW, McGuire MA, Teskey RO (2017) Increase in leaf temperature opens stomata and decouples net photosynthesis from stomatal conductance in Pinus taeda and Populus deltoides x nigra. *J Exp Bot,* 68:1757–1767

Vallejos A, Sola F, Pulido-Bosch A (2015) Processes Influencing Groundwater Level and the Freshwater-Saltwater Interface in a Coastal Aquifer. *Water Resourc Manage,* 29:679–697

Vallejos A, Sola F, Yechieli Y, Pulido-Bosch A (2018) Influence of the paleogeographic evolution on the groundwater salinity in a coastal aquifer. Cabo de Gata aquifer, SE Spain. *J Hydrol,* 557:55–66

Wright IJ, Reich PB, Westoby M, et al (2004) The worldwide leaf economics spectrum. *Nature,* 428:821–827

Zolfaghar S, Villalobos-Vega R, Cleverly J, et al (2014) The influence of depth-to-groundwater on structure and productivity of Eucalyptus woodlands. *Aus J Bot,* 62:428

SUPLEMENTARY MATERIAL

Appendix 1. Meteorological data from Almería airport meteorological station (Spanish meteorological agency) located 8 km from the study area. Monthly precipitation (P) and mean monthly temperature (Tair) from 2019 are shown as well as mean precipitation and temperature from the period comprised between 2000 and 2020.
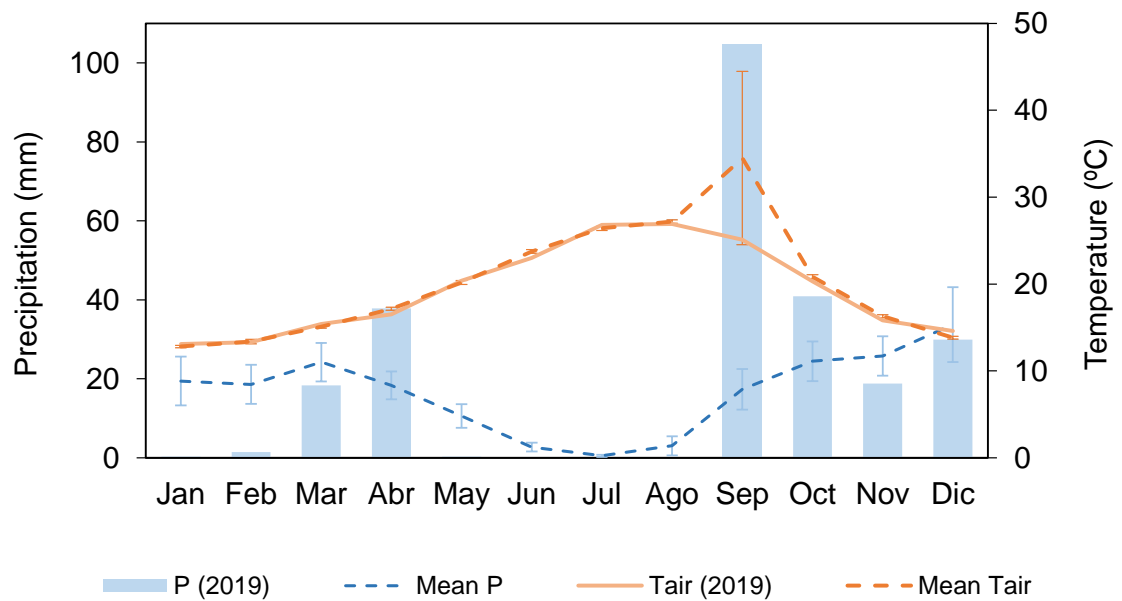
Appendix 2. Monthly mean depth-to-groundwater (DTGW), electrical conductivity, and groundwater temperature (T_{GW}) ± standard deviation of the study area. Letters show significant differences between months in each bore ($P < 0.05$) from the one-way ANOVAs of the log-transformed data.

Site	Month	DTGW (m)		Conductivity (µS/cm)		T_{GW} (°C)	
Bore 1	May	2.216 ± 0.062	a	9886.94 ± 232.68	a	22.34 ± 0.16	a
	June	2.204 ± 0.039	b	9724.87 ± 356.32	b	22.76 ± 0.14	b
	July	2.180 ± 0.031	c	9931.36 ± 144.60	c	23.24 ± 0.40	c
	August	2.211 ± 0.027	d	10238.92 ± 172.30	d	23.48 ± 0.44	d
	September	2.219 ± 0.036	e	10558.87 ± 79.92	e	23.44 ± 0.36	e
Bore 2	May	7.540 ± 0.107	a	4999.83 ± 136.73	a	21.78 ± 0.09	a
	June	7.393 ± 0.220	b	4923.47 ± 116.03	b	21.87 ± 0.07	b
	July	7.111 ± 0.028	c	4901.45 ± 98.18	c	22.05 ± 0.08	c
	August	7.144 ± 0.018	d	4887.18 ± 56.33	d	22.36 ± 0.11	d
	September	7.175 ± 0.015	e	4915.15 ± 37.81	c	22.60 ± 0.03	e
Bore 3	May	8.568 ± 0.038	ab	6727.07 ± 236.24	a	23.20 ± 0.02	a
	June	8.575 ± 0.022	c	6882.98 ± 162.60	b	23.33 ± 0.05	b
	July	8.562 ± 0.021	a	6941.25 ± 158.59	c	23.45 ± 0.04	c
	August	8.569 ± 0.015	b	6947.63 ± 227.98	c	23.50 ± 0.04	d
	September	8.574 ± 0.020	bc	7067.78 ± 218.15	d	23.54 ± 0.03	e
Bore 4	May	11.570 ± 0.012	a	3505.97 ± 91.94	a	23.08 ± 0.03	a
	June	11.578 ± 0.010	ab	3594.25 ± 137.55	b	23.24 ± 0.07	b
	July	11.579 ± 0.007	b	3763.78 ± 118.79	c	23.41 ± 0.04	c
	August	11.603 ± 0.015	c	3638.82 ± 110.58	d	23.49 ± 0.01	d
	September	11.632 ± 0.007	d	3489.15 ± 24.97	e	23.53 ± 0.02	e
Bore 5	May	14.029 ± 0.011	a	10066.35 ± 79.38	a	22.79 ± 0.03	a
	June	14.038 ± 0.010	ab	9924.46 ± 253.57	b	22.93 ± 0.05	b
	July	14.050 ± 0.008	c	9348.57 ± 138.00	c	23.05 ± 0.03	c
	August	14.040 ± 0.008	b	9576.74 ± 51.84	d	23.12 ± 0.01	d
	September	14.016 ± 0.007	d	9604.76 ± 5.43	e	23.14 ± 0.01	e
Bore 6	May	19.249 ± 0.012	a	8850.21 ± 9.61	ab	23.38 ± 0.02	a
	June	19.274 ± 0.023	b	8848.58 ± 27.72	a	23.51 ± 0.05	b
	July	19.284 ± 0.010	b	8896.21 ± 86.76	c	23.65 ± 0.04	c
	August	19.282 ± 0.009	b	8865.31 ± 6.29	b	23.74 ± 0.03	d
	September	19.291 ± 0.007	b	8885.51 ± 11.90	c	23.81 ± 0.02	e
Bore 7	May	24.905 ± 0.036	a	10178.71 ± 530.56	a	23.30 ± 0.03	a
	June	24.929 ± 0.025	b	10363.50 ± 192.98	b	23.45 ± 0.05	b
	July	24.942 ± 0.014	b	10718.59 ± 72.17	c	23.57 ± 0.03	c
	August	24.966 ± 0.017	c	10931.73 ± 46.89	d	23.65 ± 0.03	d
	September	24.976 ± 0.016	c	11026.51 ± 11.72	e	23.72 ± 0.01	e
Bore 8	May	25.231 ± 0.009	a	8944.37 ± 3.98	a	23.51 ± 0.03	a
	June	25.238 ± 0.023	a	8906.29 ± 20.50	b	23.66 ± 0.06	b
	July	25.286 ± 0.021	b	8862.76 ± 21.27	c	23.81 ± 0.04	c
	August	25.364 ± 0.023	c	8822.75 ± 9.59	d	23.91 ± 0.03	d
	September	25.408 ± 0.008	d	8796.77 ± 7.24	e	23.98 ± 0.02	e

Appendix 3. Spatiotemporal variations in groundwater temperature, T_{GW} (a) and groundwater electrical conductivity (b) for the study period (15 May 2019 - 11 September 2019).
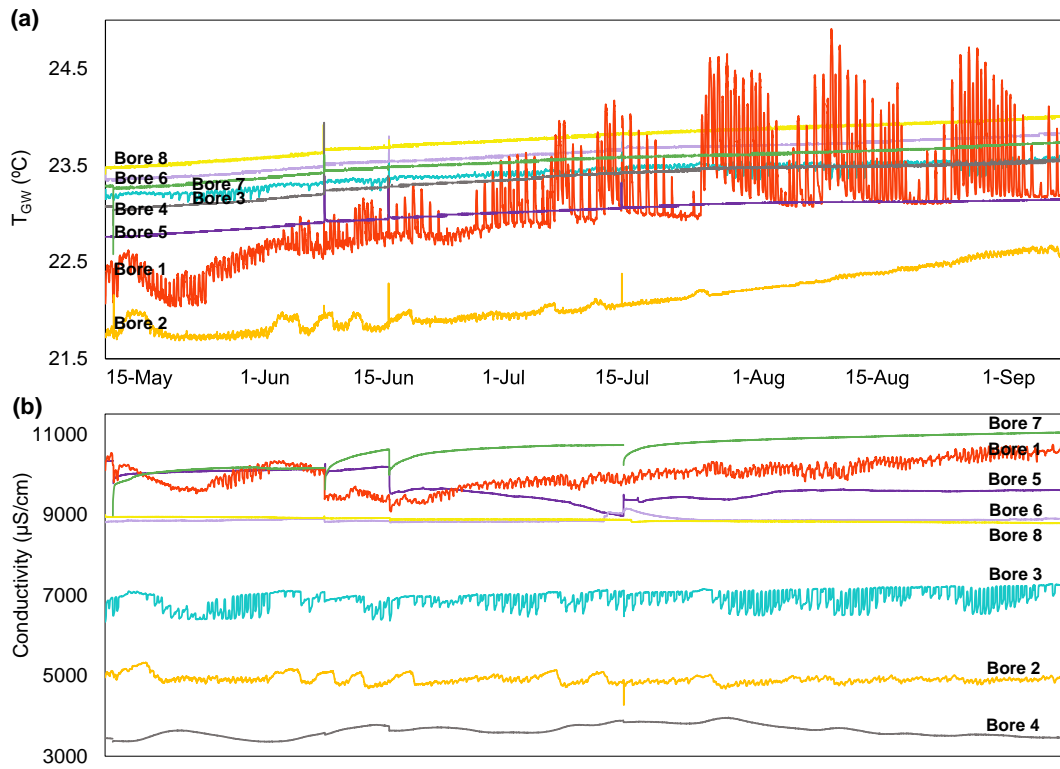
Appendix 4. Results of the two-way ANOVA applied to the morpho-functional and hydraulic variables of *Ziziphus lotus*: photosynthetic rate (A), stomatal conductance (g_s), transpriation rate (E), intrinsic water-use efficiency (WUEi), predawn (Ψ_{pd}) and midday (Ψ_{md}) water potential, and vapour pressure defficit (VPD). Significance and degree of freedom of the sum of squares of each trait are shown. Significance: ***$P < 0.001$, **$P < 0.01$, n.s: no significance.

		A	g_s	E	WUEi	Ψ_{pd}	Ψ_{md}	VPD
Bore	df = 7	***	***	***	***	***	***	**
Month	df = 2	n.s	***	***	***	***	***	***
Interaction	df = 14	***	***	***	***	***	***	***

Appendix 5. Mean Huber value (Hv), Specific Leaf Area (SLA), and wood density (± standard error) of *Ziziphus lotus* at each site. Letters show significant difference between sites ($p < 0.05$) from one-way ANOVA.

Bores	Hv	SLA (cm^2/g)	Wood density (g/cm^3)
Bore 1 (2.2 m)	3.58 ± 0.08 a	86.33 ± 7.01 a	0.82 ± 0.02 a
Bore 2 (7.3 m)	8.29 ± 2.49 ab	99.04 ± 9.15 a	0.79 ± 0.02 a
Bore 3 (8.6 m)	6.60 ± 1.26 ab	70.37 ± 3.71 a	0.78 ± 0.01 a
Bore 4 (11.6 m)	5.77 ± 0.25 ab	79.73 ± 6.15 a	0.74 ± 0.08 a
Bore 5 (14.0 m)	8.30 ± 1.36 ab	78.58 ± 4.98 a	0.79 ± 0.07 a
Bore 6 (19.3 m)	7.50 ± 0.91 ab	87.16 ± 8.17 a	0.80 ± 0.02 a
Bore 7 (25.0 m)	11.40 ± 0.22 b	82.83 ± 5.31 a	0.76 ± 0.03 a
Bore 8 (25.3 m)	9.34 ± 0.84 b	85.75 ± 7.51 a	0.85 ± 0.05 a

Appendix 6. Bivariate linear regression between gas-exchange traits of *Ziziphus lotus* (photosynthetic rate, A; stomatal conductance, g_s; transpriation rate, E; and intrinsic water use efficiency, WUEi) and groundwater conductivity (a, c, e, g) and groundwater temperature (b, d, f, h). Mean values per plant are displayed ± standard error. Lines represent the linear regression, R^2, the goodness of the fit, and P, the significance of each analysis (no data: no significance).
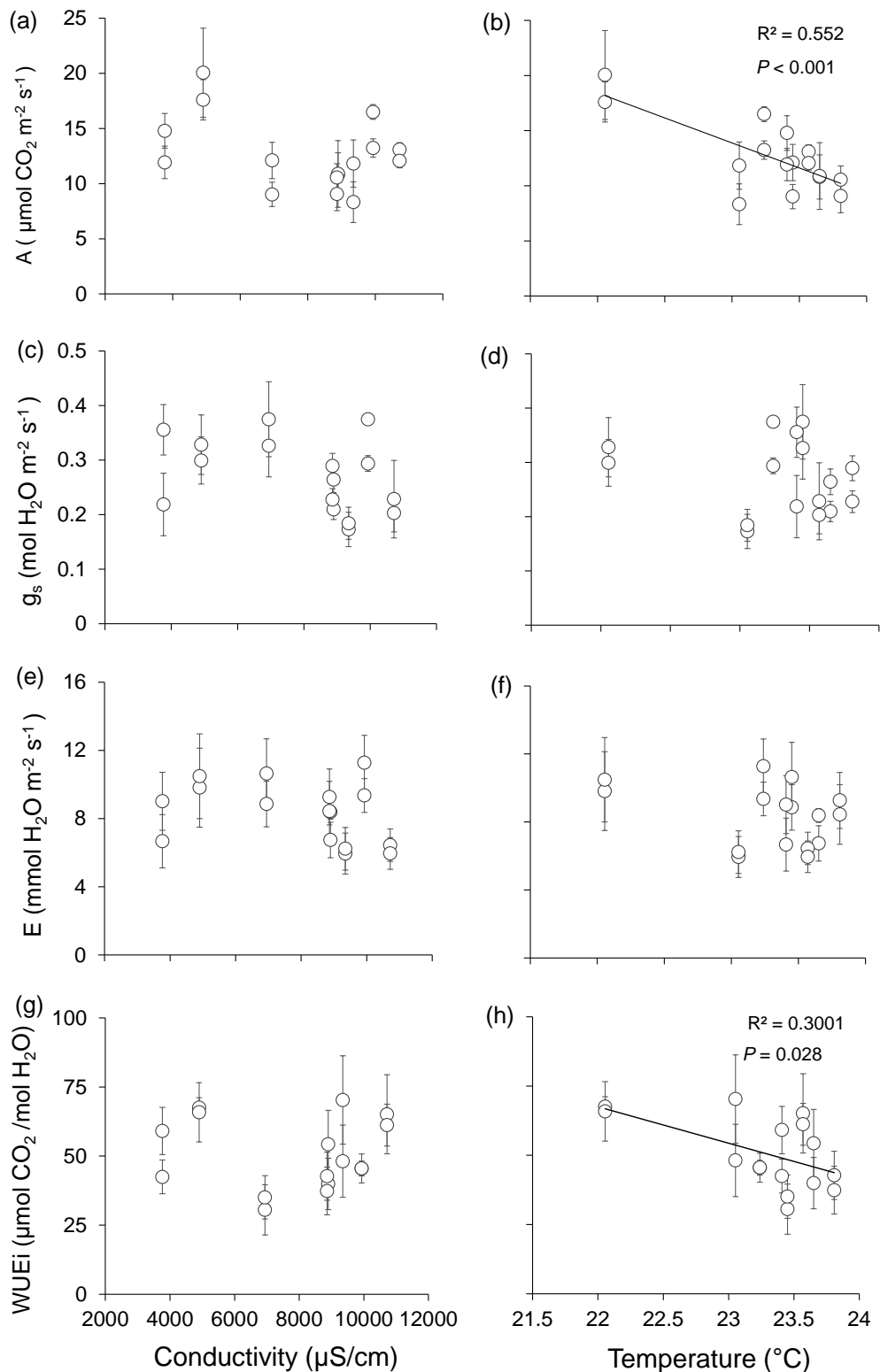
Appendix 7. Paired comparison of leaf gas exchange traits and water potential of *Ziziphus lotus* plants at sites with different groundwater characteristics. The number of wavy lines bellow each number (bore number) represents depht-to-groundwater, from shallow (4 lines) to deep groundwater (1 line); colors indicate levels of salinity: hight (red), intermediate (yellow), low (blue). Mean values per site are indicated ± standard error. E: transpriation rate; gs: stomatal conductance; A: photosynthetic rate; Ψ_{md}: midday water potential; Ψ_{pd}: predawn water potential. Note that only significant differences between these bores from each variable are included (t-test, $P < 0.05$).
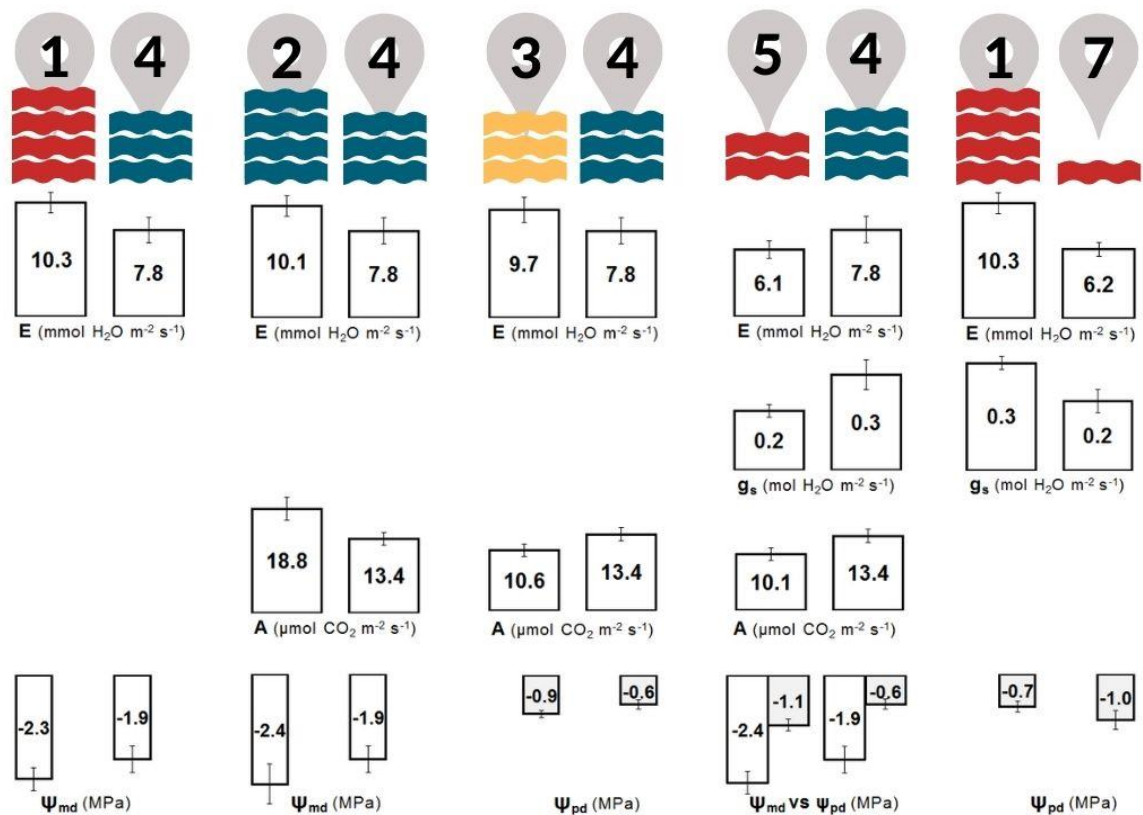
Appendix 8. Bivariate linear regression between groundwater characteristics (depth-to-groundwater, electrical conductivity, temperature) and hydraulic traits (Ψ_{pd}: predawn water potential, Ψ_{md}: midday water potential, $\Delta\Psi_{max}$: maximum daily range). Mean values per plant are displayed ± standard error. Lines represent the linear regression, R^2, the goodness of the fit, and P, the significance of each analysis (no data: no significance).
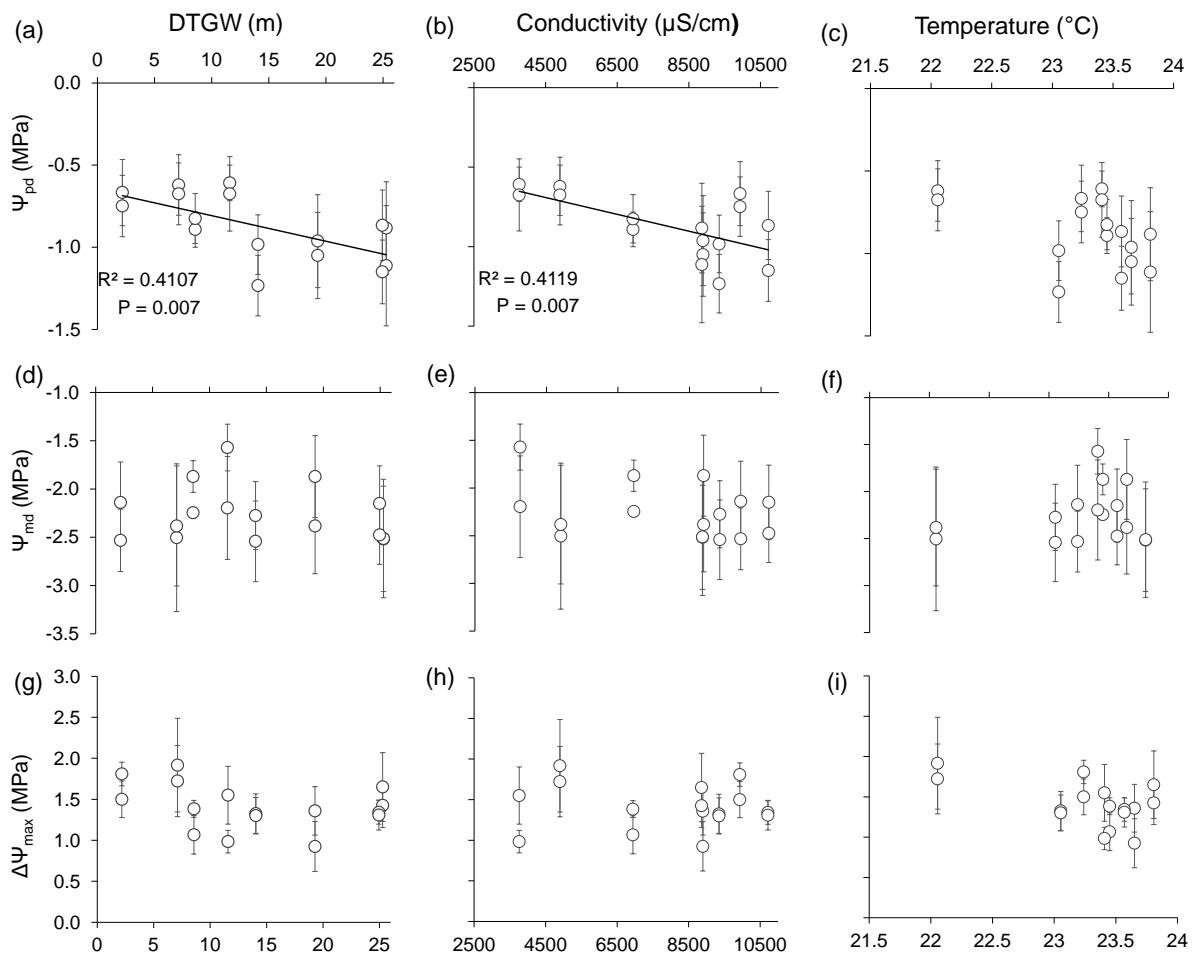
Appendix 9. Bivariate linear regression between groundwater characteristics and morphological traits: Huber value (Hv), Wood density, and Specific leaf area (SLA). Mean values per plant are displayed ± standard error. Lines represent the linear regression, R^2, the goodness of the fit, and P, the significance of each analysis (no data: no significance).
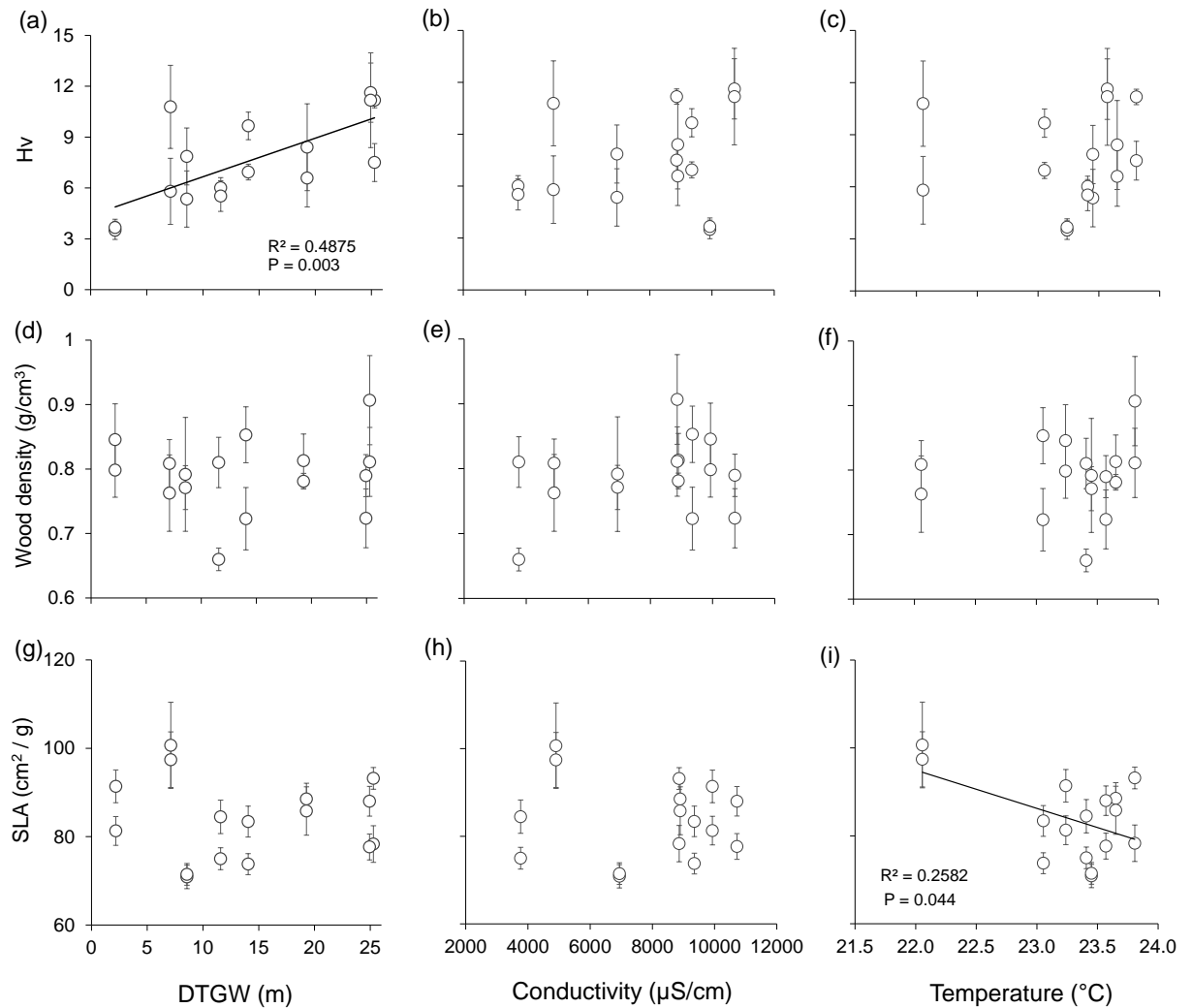
Appendix 10. Relationship between vapour pressure deficit (VPD) and gas-exchange traits: photosynthetic rate (A), stomatal conductance (g_s), and intrinsic water-use efficiency (WUEi) (nonsignificant). Monthly values per plant are displayed ± standard error. Different colours represent sampling periods (May: green, July: yellow, and September: red).
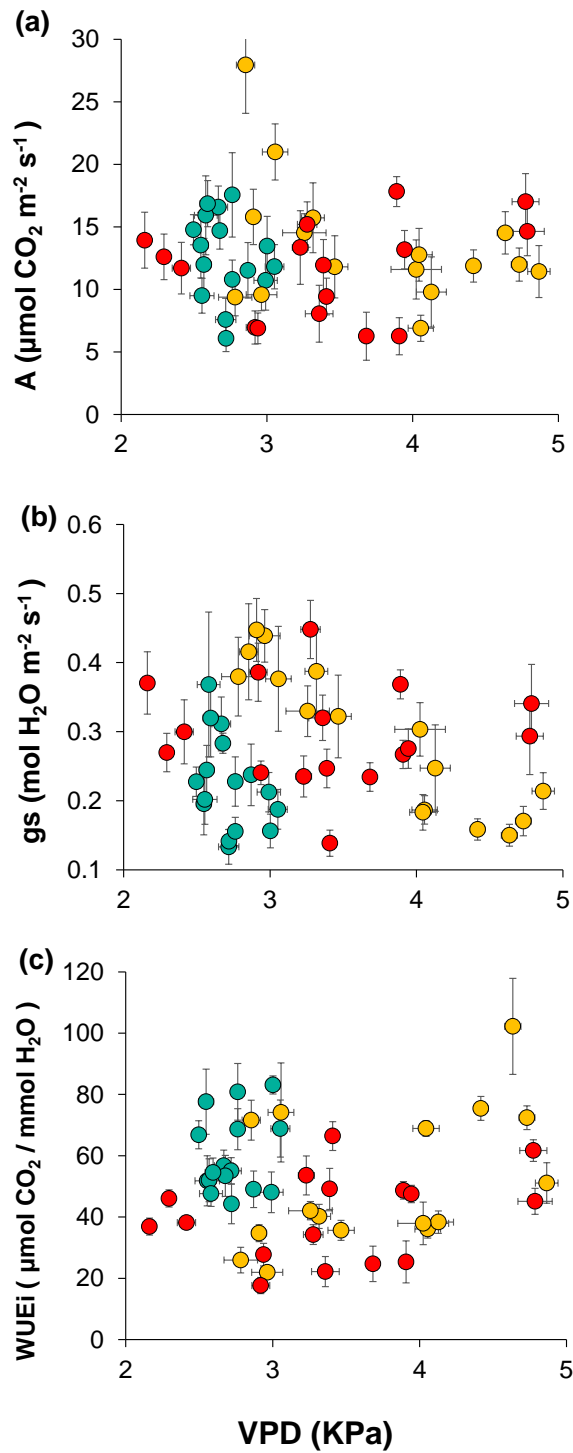
Appendix 11. Bivariate linear regression between gas-exchange and hydraulic traits of *Ziziphus lotus*: photosynthetic rate (A), stomatal conductance (g_s), transpriation rate (E), intrinsic water-use efficiency (WUEi), and predawn (Ψ_{pd}) and midday (Ψ_{md}) water potential. Montly values per plant are displayed ± standard error. Colours and shapes represent sampling periods (May: green triangles, July: yellow circles, and September: red squares). Lines represent significant linear regression: dotted lines and boxes show spring regression analysis (May) and solid lines and boxes represent summer regression (July + September). The goodness of the fit (R^2) and the significance of each analysis (*P*) are showed in the respective boxes.
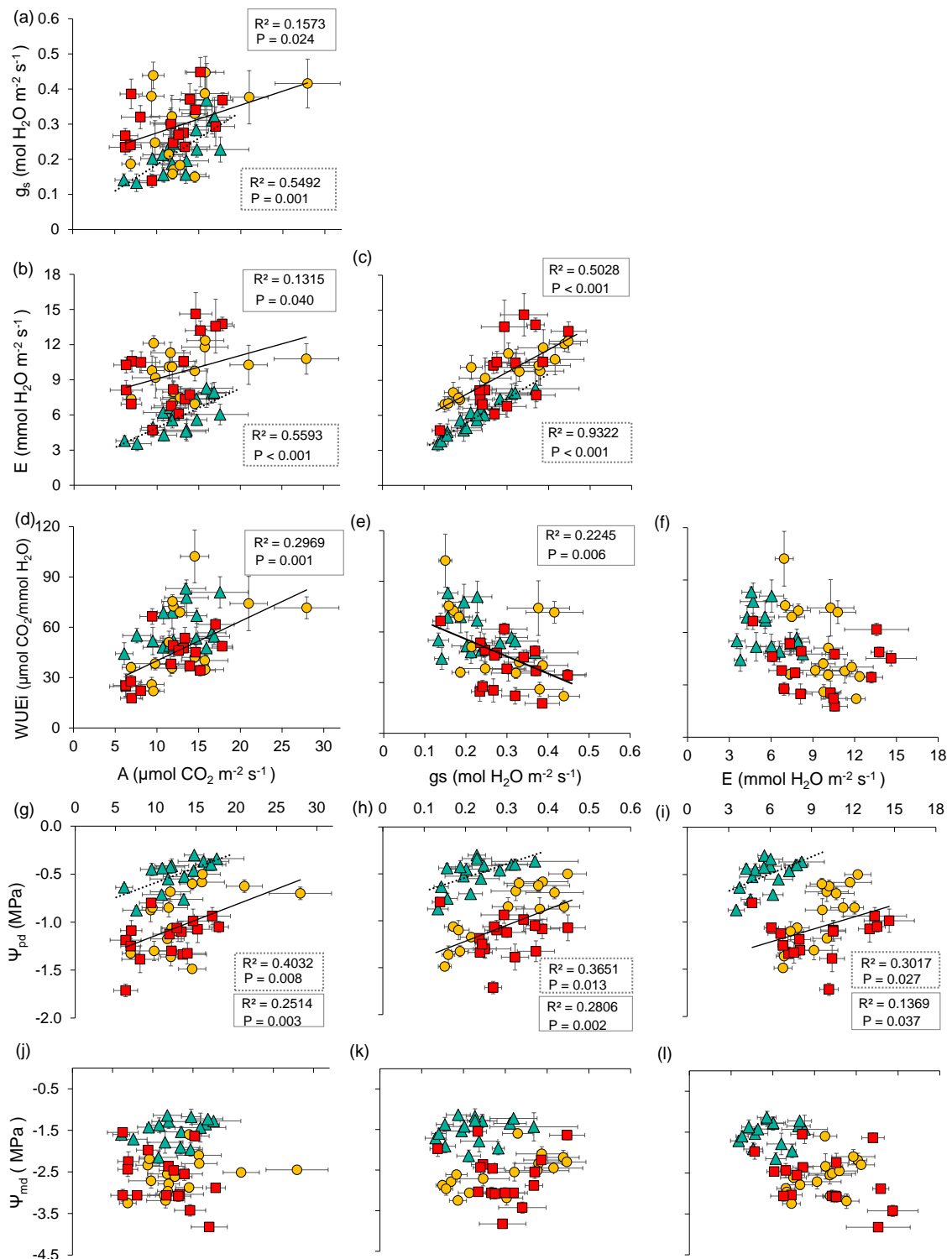
Appendix 12. Bivariate linear regression between the terms of Huber value (leaf area and sapwood cross-sectional area) and depth-to-groundwater (DTGW). Mean values per plant are displayed ± standard error. Lines represent the linear regression, R^2, the goodness of the fit, and P, the significance of each analysis.
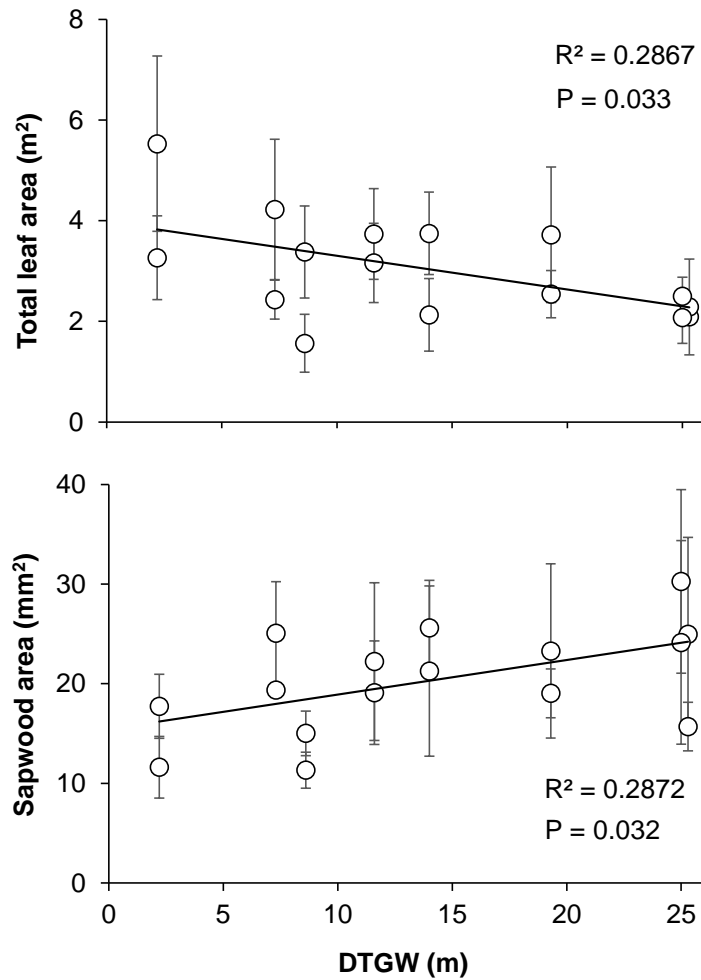
CHAPTER IV: Decoupled soil biological activity and vegetation dynamics in a groundwater-dependent ecosystem in drylands

M. Trinidad Torres-García[1,2], Cecilio Oyonarte[2,3], Javier Cabello[1,2], Emilio Guirado[2,4], Borja Rodríguez-Lozano[3] and María J. Salinas-Bonillo[1,2]

[1] Department of Biology and Geology, Universidad de Almería, Spain
[2] Andalusian Centre for the Monitoring and Assessment of Global Change (CAESCG), University of Almería, Spain
[3] Department of Agronomy, University of Almería, Spain
[4] Instituto Multidisciplinar para el Estudio del Medio "Ramón Margalef", University of Alicante, Spain

ABSTRACT

Water availability controls the functioning of dryland ecosystems, driving a patchy vegetation distribution, unequal nutrient availability, soil respiration in pulses, and limited productivity. Groundwater-dependent ecosystems (GDEs) are acknowledged to be decoupled from precipitation, since their vegetation relies on groundwater sources. Despite their relevance to enhanced productivity in drylands, our understanding of how different components of GDEs interconnect (i.e., soil, vegetation, water) remains limited. We studied the GDE dominated by the deep-rooted phreatophyte *Ziziphus lotus*, a winter-deciduous shrub adapted to arid conditions along the Mediterranean basin. We aimed to disentangle whether vegetation and soil activity are decoupled in the dryland GDE, and whether fertile islands contribute to modulate soil response to rainfall. We assessed (1) soil and vegetation dynamics over time (soil CO_2 efflux and plant activity), (2) the effect of the patchy distribution on soil quality (properties and nutrient availability), and soil biological activity (microbial biomass and mineralization rates) as essential elements of biogeochemical cycles, and (3) the implications for preserving GDEs and their biogeochemical processes under climate change effects. We found that soil respiration and mineralization promptly responded to precipitation pulses, whereas the functioning of the phreatophytic and even non-phreatophytic vegetation was decoupled from rainfall. Soil quality was higher under-canopy, hence the intense soil biological activity we observed (microbial biomass and mineralization rates). Our findings highlight the decoupling between soil and vegetation activity in dryland ecosystems, more intensely with phreatophytic vegetation. Phreatophytes promote fertile islands, enhancing soil quality and decomposition processes. However, these processes are jeopardized by climate change effects and land degradation in GDEs due to the dependence of soil activity on: (1) precipitation for activation, and (2) phreatophytic vegetation for litter input and soil quality. Therefore, desertification might modify biogeochemical cycles by disrupting key ecosystem processes such as soil microbial activity, organic matter mineralization, and plant productivity.

Keywords: fertility island, normalized difference vegetation index (NDVI), soil microbial biomass, semi-arid region, soil quality, *Ziziphus lotus*.

INTRODUCTION

Arid and semiarid regions, covering 41% of Earth's land surface (Reynolds et al. 2007), are characterized by less annual precipitation than potential evapotranspiration, leading to prolonged dry periods (Newman et al., 2006). Since water shortage limits biological activity, their ecosystems are considered to be of low productivity (Noy-Meir, 1973; Tucker and Reed, 2016), because their primary production is partially controlled by precipitation events (Austin et al., 2004). Global-scale studies have shown the increasing importance of dryland ecosystems and their carbon stocks in the global carbon cycle (Poulter et al., 2014). However, our understanding of the spatiotemporal coupling of the different ecosystem components remains limited.

Climate controls on biogeochemical cycles are critical in arid and semiarid regions where biological activity mainly depends on water availability (Delgado-Baquerizo et al., 2013). The presence of water after long dry periods usually triggers a cascade of physical, chemical, and biological processes (Potts et al., 2008) that depend on the magnitude and frequency of the precipitation event (Austin et al., 2004). Overall, precipitation events occurring in the dry season increase aboveground net primary productivity because of the alleviation of drought stress (Thomey et al., 2011). Higher water availability after a drought period also promotes the immediate net carbon release by enhancing soil respiration (Rs) (Birch effect; Birch, 1959) that encompasses both the autotrophic respiration of plant roots and rhizosphere activity, and the heterotrophic respiration of microbial communities (Oyonarte et al., 2012; Schlesinger and Andrews, 2000). The effect of precipitation on Rs and soil carbon stocks will depend on the distribution of available resources and soil microorganisms (Austin et al., 2004).

The study of carbon fluxes in dryland ecosystems is particularly challenging due to the marked seasonality of precipitation and high spatial heterogeneity of vegetation, nutrients, and resources. The spatial distribution of the vegetation in patches (Aguiar and Sala, 1999) leads to unequal distribution of nutrients and water and thus, to the development of "islands of resources" or "fertile islands" surrounded by relatively infertile soils (Reynolds et al., 1999). Shrub-dominated vegetation promotes sediment and nutrient accumulation under the canopy (Wang et al., 2019; Zhang et al., 2011). These accumulations can form

structures called nebkhas, which are mainly observed in desert or coastal areas with patchy vegetation and high wind activity (Lang et al., 2013; Zhang et al., 2011).The heterogeneity of these ecosystems contributes to the spatial variability of carbon and nitrogen pools (Austin et al., 2004).

The abundance, diversity, and composition of soil microbial communities regulate key ecosystem processes in drylands, such as litter decomposition and organic matter mineralization (Delgado-Baquerizo et al., 2016; Ochoa-Hueso et al., 2018). Microbial activity releases C and nutrients from soil organic matter (SOM), which are essential for plant nutrient availability (Lambers and Oliveira, 2019). Larger amounts of litter and organic matter accumulated under the plant canopy promotes higher decomposition rates by microbial activity (Gallardo and Schlesinger, 1992). In contrast, bare soils accumulate less SOM, and its mineralization is mainly driven by abiotic factors such as solar radiation (i.e., photodegradation), particularly in drylands during summer (Rey et al., 2011). Thus, dryland ecosystems can also show significant heterogeneity in the degradation and mineralization processes driven by the spatial distribution of the vegetation in fertile islands and the climatic conditions.

Terrestrial groundwater-dependent ecosystems (GDEs) are constituted by phreatophytic vegetation that access to the groundwater via the capillary fringe (i.e., the unsaturated zone above the water table) and the development of deep root systems (Eamus et al. 2006; Glen et al. 2013). GDEs represent a distinctive type of ecosystem in drylands where water limitation is mitigated. The functioning of the entire ecosystem is often inferred from phreatophytes and therefore, the ecosystem productivity is considered to be decoupled from precipitation (Eamus et al., 2006; Sommer and Froend, 2011). GDEs maintain critical functions in drylands since phreatophytes have more available water to sustain photosynthesis, and therefore to grow for longer periods than other dryland ecosystems.

The groundwater reliance of GDEs means that variations in groundwater availability would significantly alter the structure and function of the ecosystem, and even degrade it irreversibly (Colvin et al., 2003; Eamus et al., 2006). Climate change effects in drylands, which include decreases in water availability, more irregular and intense rainfall events, and prolonged droughts (Guiot and Cramer, 2016), are likely to reduce groundwater recharge

(Eamus et al., 2006) and alter water and biogeochemical cycles. Consequently, it will affect essential ecosystem functions such as primary production and microbial mineralization (Delgado-Baquerizo et al., 2013; Querejeta et al., 2021).

Recent studies have focused on defining the relationship of phreatophytes with groundwater (Antunes et al., 2018; Torres-García et al., 2021b; Zolfaghar et al., 2014), or with nutrient acquisition (Querejeta et al., 2021), whereas the interconnection with essential processes occurring in the soil, such as soil respiration or mineralization, are less studied in GDEs. Moreover, the potential for groundwater connection to enhance soil fertility and soil quality in drylands is overlooked. Here, we focus on the GDE dominated by the long-lived, winter-deciduous phreatophyte *Ziziphus lotus* (L.) Lam. (Rhamnaceae) in a semiarid region in the south-western continental Europe. As *Z. lotus* is a facultative phreatophyte and the keystone species that dominates the GDE, the ecosystem functioning is partially decoupled from precipitation (Torres-García et al., 2021b). Nevertheless, the marked seasonality and scarcity of precipitation, and the high spatial heterogeneity of vegetation in arid and semiarid ecosystems can promote differences in soil and vegetation activity responses, hence in the coupling-decoupling of the components of the GDE.

Despite soil biological activity in drylands is strongly tied to precipitation events (Austin et al., 2004; Rey et al., 2011; Vargas et al., 2018; Rey et al., 2021), we hypothesize that both vegetation and soil activity will be decoupled to precipitation in arid GDEs. Besides, the fertile island dominated by phreatophytic species could be an essential element for modulating respiration pulses linked to precipitation events. Therefore, we aimed to assess (1) the dynamics of soil respiration (Rs) and vegetation over the seasons, (2) the effect of the fertile islands on soil biological activity and quality (soil properties and nutrient availability), and (3) the implications for preserving arid GDEs and their biogeochemical processes under climate change effects.

MATERIALS AND METHODS

Site description

The study was conducted in a semiarid shrubland in Cabo de Gata-Níjar Natural Park, Southeast of Spain (36.830606, -2.293612), where the phreatophyte *Ziziphus lotus* is the

keystone species of the protected European Habitat 'arborescent matorral with Ziziphus' (Habitat 5220*, 92/43/CEE) (Fig. 1). The climate is characterized as Mediterranean and semiarid, with hot, dry summers, mild winters and mean annual temperature of 18ºC (Machado et al., 2011). During summer (mostly July and August) scarcely any precipitation event occurs in the area (Appendix 1, see Suplementary Material of this Chapter). The mean annual precipitation of 220 mm is unevenly distributed during spring and autumn, although with intense and short recurrent events (i.e., precipitation pulses) in the late summer.

Z. lotus is a winter-deciduous shrub very well adapted to semiarid and arid conditions due to its deep root system and dependence on groundwater (Guirado et al., 2018), which confer the ability to thrive during summer (Torres-García et al., 2021b). *Z. lotus* can be found in vast territories in North Africa and the Middle East, and it is sparsely present in south Europe, particularly in southeast Spain, Sicily, and Cyprus (Sánchez-Gómez et al., 2003; Guirado et al., 2017). Its individuals (up to 4 m tall and 200 m2 area; Guirado et al., 2019) constitute vegetation patches with less sizable Mediterranean shrubs such as *Salsola oppositifolia* Desf., *Lycium intricatum* Boiss., *Withania frutescens* (L.) Pauquy, and *Asparagus albus* L. The vegetation shows a dispersed pattern with a patchy distribution typical of arid and semiarid regions (Tirado, 2009). *Z. lotus* is responsible for most of the photosynthetic activity during summer, whereas the rest of the vegetation grows in winter. Litter is accumulated beneath the *Z. lotus* canopy whereas the rest of the soil surface is mostly bare or with sparse, tiny, annual plants.

Beneath the canopy the soil is deeper (albic Arenosols, more than 50 cm) with different horizonts (Ah, Bw, C), whereas the space between plants shows shallow soils (calcaric Leptosols, c.a. 20 cm) without soil horizonation (Ah, Cmk). Both typologies show a sandy texture (> 90% of sand), low water retention capacity, and alkaline pH.

Experimental design and sampling

Four patches dominated by *Z. lotus* were selected in the coastal plain at the southeast of Spain in April 2018. For each patch we selected three sites under the canopy (hereafter: under-canopy) and three surrounding sites with bare soil (inter-canopy), 2 to 4 m apart from vegetation (Fig. 1). At each site we placed polyvinyl chloride (PVC) collars to monitor

Rs dynamics and collected three soil subsamples from the first 10 cm of the topsoil around each collar to obtain a composite sample. Sampling was conducted in August 2019 just before the late-summer rainfall. Composite samples were air-dried at 25ºC approximately, sieved to 2 mm (fine-earth fraction) to remove litter and coarse gravels, and then divided and stored at 4ºC in two subsets, one for mineralization experiments and other for soil property analysis.
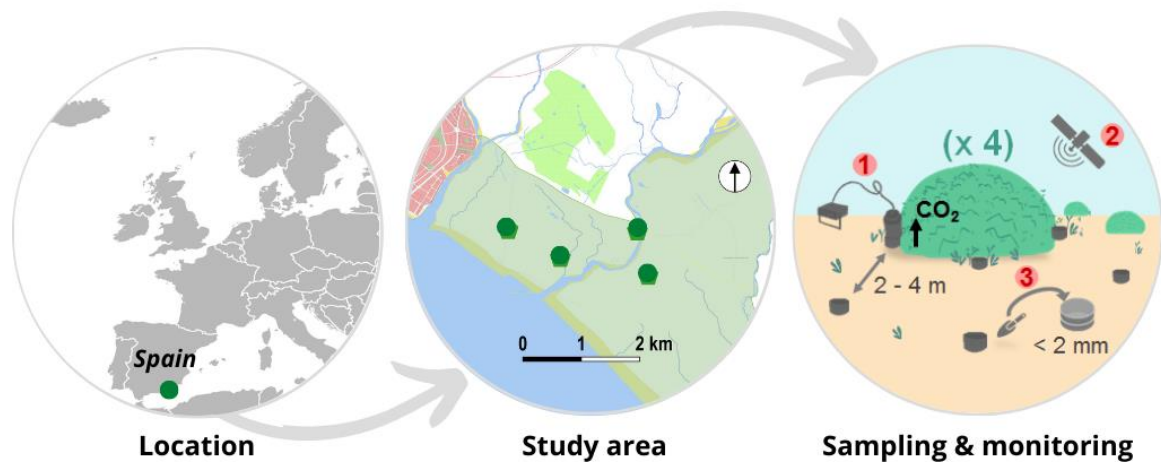
Figure 1. Location, study area, and experimental design in patches of *Ziziphus lotus*. Right circle summarizes the methodological sections of sampling and monitoring: (1) in situ soil respiration monitoring, (2) remote sensing monitoring, and (3) soil sampling for mineralization and soil properties analyses.

In situ soil respiration measurements

To obtain monthly discrete measurement of CO_2 effluxes from April of 2018 to April 2019, we used a manual and portable opaque soil chamber system (EGM-4, PP-systems, Hitchin, UK). The chamber was located over the PVC collars (15 cm in diameter and 7 cm in height) that were inserted 3.5 cm into the soil and placed around the four selected patches to obtain soil respiration measurements, both under-canopy and inter-canopy (Fig. 1). The 24 collars remained undisturbed until the end of the experiment. Small grasses, litter, and insects were carefully removed from each collar before measuring. Because of the low CO_2 efflux rates, each collar was monitored for 120 s and measurements were recorded every 4 seconds to ensure reliable data. CO_2 efflux was estimated from the slopes of the CO_2 molar fractions of the confined air versus time (Pérez-Priego et al. 2010). Soil temperature was measured at 5 cm depth with a digital thermometer and soil volumetric water content (SWC) was recorded with a portable theta probe (ML2x, Devices Ltd., Cambridge, UK) next

to each collar and at the time of Rs measurement. All measurements were completed between 11:00 and 13:00 to avoid strong diurnal fluctuations, and in random order each time to avoid biased estimates.

Vegetation functioning from remote sensing monitoring

To assess one-year vegetation and soil activity dynamics in the GDE, we compared the seasonal dynamics of normalized difference vegetation index (NDVI; Smith et al., 2019) obtained from equation 1 in the patches dominated by *Z. lotus*.

$$NDVI = \frac{R_{NIR} - R_{RED}}{R_{NIR} + R_{RED}} \tag{1}$$

where R_{NIR} is the reflectance of the near infrared band and R_{RED} is the reflectance of the red band.

The NDVI derived from satellite images (e.g., Landsat, MODIS/Terra), is widely used as a surrogate of net primary productivity (Paruelo et al., 1997; Tian et al., 2017). We used the reflectance in images provided by Cubesats (3m/pixel and 4 bands [red, green, blue, NIR]) from Planet (https://www.planet.com/) adjusting the monthly NDVI (eq. 1) calculation to canopy (e.g., from 4 to 16 cloud-free pixels per sample inside the patch) and inter-canopy influence on bare soil (4 pixels per sample) in the study period (April 2018 - April 2019).

Soil mineralization experiments

We developed two mineralization experiments in the laboratory to assess microbial biomass and mineralization dynamics. First, we used the soil-induced respiration method (SIR) to assess microbial biomass carbon (C_{mic}) in real time, as described in Anderson and Domsch (1978). Briefly, under-canopy and inter-canopy soil samples (12 samples each x 3 replicates) were pre-incubated for 24 h in glass jars at 25°C, after adding water (Appendix 2). Subsequently, a glucose solution was added to stimulate respiration and remove substrate limitation. The glass jars that contained the soil samples were immediately sealed with plastic gas-tight lids that had septum ports with rubber septa. Samples were incubated for 6 h with control conditions of humidity (60% of soil water holding capacity) and temperature (25°C). A 0.5 ml volume of air was captured from the sealed jars to assess CO_2 concentration using an infrared CO_2 Analyser (Q-box SR1LP Soil respiration package,

Qubit Systems, Canada). C_{mic} was then estimated according to the recalibration of West and Sparling (1986) at 25°C (eq. 2) from the original equation of Anderson and Domsch (1978):

$$C_{mic} = 32.8 * [CO_2] + 3.7 \qquad (2)$$

where C_{mic} is expressed in µg g^{-1}soil, and $[CO_2]$ refers to the concentration of CO_2 (µl CO_2 g^{-1}soil h^{-1}).

The second experiment consisted of the evaluation of soil mineralization dynamics. In this case, the dry soil samples were pre-incubated for 24 h at 25°C. Water was then added, the samples were sealed, and the first measurement was obtained one hour afterwards to capture the initial pulse of CO_2. The same conditions of humidity (65% of soil water holding capacity) and temperature (25°C) were maintained throughout the experiment. A volume of 0.5 ml of air was obtained from the sealed jars and CO_2 concentration was immediately measured with the infrared CO_2 analyser. After each measurement, the jars with the samples were opened to refresh the headspace with the room air and immediately sealed until the next day. We continued measuring CO_2 concentration every 24h for 23 days, when measures stabilized.

Soil properties analyses

Two carbon fractions were analysed: (1) total organic carbon content (TOC) and (2) water extractable organic carbon (WEOC). TOC was determined by the Walkley-Black dichromate oxidation procedure modified by Mingorance et al. (2007) using a UV-spectrophotometer. WEOC was extracted following the procedure described in Embarcher et al. (2007). Briefly, 25 g of soil sample was shaken for 30 min with 10 mM CaCl2 with a soil:solvent ratio of 1:2 (w/w). The solution was centrifuged for 15 min at 6000 rpm to accelerate the subsequent filtration. The solution was then desiccated, and the carbon content estimated from the residue using the same method as for TOC (Mingorance et al., 2007).

Total nitrogen (N_{tot}) was determined by elemental analysis with a Leco TruSpec CN analyzer, using fine soil samples. The carbon/nitrogen ratio was obtained from this variable and TOC.

The main components in the soil solution (nitrite, nitrate, phosphate, and sulphate) were also estimated using the liquid extraction method in a 1:5 soil/water solution (10 g soil: 50 ml water). Once the soil solution was obtained, anions were measured by liquid chromatography with a PHOTOSTORE chromatograph, Chromeleon model, using a standard curve with a mixture of anions at concentrations of 0, 5, 10, 15 and 30 ppm.

Statistical analysis

A linear mixed-effects model was used to analyse the spatial (cover: under-canopy vs. inter-canopy) and temporal (time: month) effects, as well as the interaction of both factors, on soil respiration (Rs), soil water content (SWC), and soil temperature separately. Canopy, time, and their interaction were established as fixed effects of the model, whereas individual plants and collars nested to the canopy conditions were random effects. The best fitting model was selected based on restricted maximum likelihood (REML) values. To detect temporal variations in the dynamic of vegetation (NDVI), a two-way analysis of variance (ANOVA) was applied.

To identify spatial differences in C_{mic}, mineralization rate and soil properties (soil-nutrient availability and carbon fractions) we used a one-way ANOVA. We also used an analysis of covariance (ANCOVA) to compare the relationship between mineralization rates and soil carbon under- and inter-canopy. All analyses were performed in R with the functions lmer from the 'lme4' package, and lm and aov from the 'stats' package (version 3.5.2, R Core Team 2018).

RESULTS

Soil and vegetation dynamics

Our results revealed significant spatio-temporal differences in soil temperature, soil water content, CO_2 effluxes, and vegetation activity (Table 1 and Fig. 2). Mean soil temperature was significantly higher inter-canopy than under-canopy, ranging from 14°C to 37°C (Fig. 2a). In spring and particularly in summer, we observed higher temperatures but also wider differences between canopies, whereas such differences and general mean soil temperature decreased in autumn and winter, reaching a minimum in December (14.2 ± 0.5°C and 15.7 ± 0.7°C under- and inter-canopy respectively). Likewise, mean soil water

content (SWC) was significantly higher inter-canopy (Table 1), although no seasonal dynamic was noticed (Fig. 2b). It was just in the single measurements of October and April when maximum values were recorded. Precipitation events were also more intense and frequent during these periods (early autumn and spring, Appendix 1).

Table 1. Mean values (± SE) of soil environmental conditions (temperature and water content, SWC), CO_2 efflux, and normalized difference vegetation index (NDVI) for the period 2018/2019, differentiating between under- and inter-canopy. F-statistic and significance of the analysis are shown (***P < 0.001).

	Under-canopy	Inter-canopy	*F*	Significance
Soil Temp. (ºC)	22.62 ± 0.65	26.49 ± 0.73	13.71	***
SWC (%)	3.63 ± 0.19	4.88 ± 0.19	77.68	***
CO_2 efflux (μmol CO_2 m^{-2} s^{-1})	1.02 ± 0.10	0.58 ± 0.02	48.27	***
NDVI[a]	0.23 ± 0.01	0.08 ± 0.01	168.8	***

(a) Differences between canopy and inter-canopy

Conversely, mean CO_2 efflux was 1.8 times greater under-canopy than inter-canopy (Table 1). Maximums mean rates occurred under-canopy in October 2018 (2.44 ± 0.13 μmol CO_2 m^{-2} s^{-1}) and April 2019 (3.62 ± 0.43 μmol CO_2 m^{-2} s^{-1}), whereas minimum one was measured in March inter-canopy (0.31 ± 0.04 μmol CO_2 m^{-2} s^{-1}) (Fig. 2c). The linear mixed effect model revealed that both soil temperature and water content affected CO_2 efflux (F = 22.49, P < 0.001, R^2 = 0.22), although with greater influence of the latter (P < 0.001) than the former (P = 0.002).

When analysing vegetation activity (measured as NDVI), we observed significant differences between canopy and inter-canopy (Table 1). Maximum rates of NDVI for the vegetated areas were found in June and December and minimum ones were observed in September and March (Fig. 2d). Whereas the vegetation activity increased in spring with the rise of soil temperature, the inter-canopy signal showed a decrease from May to August. Later in autumn, both NDVI curves increased.
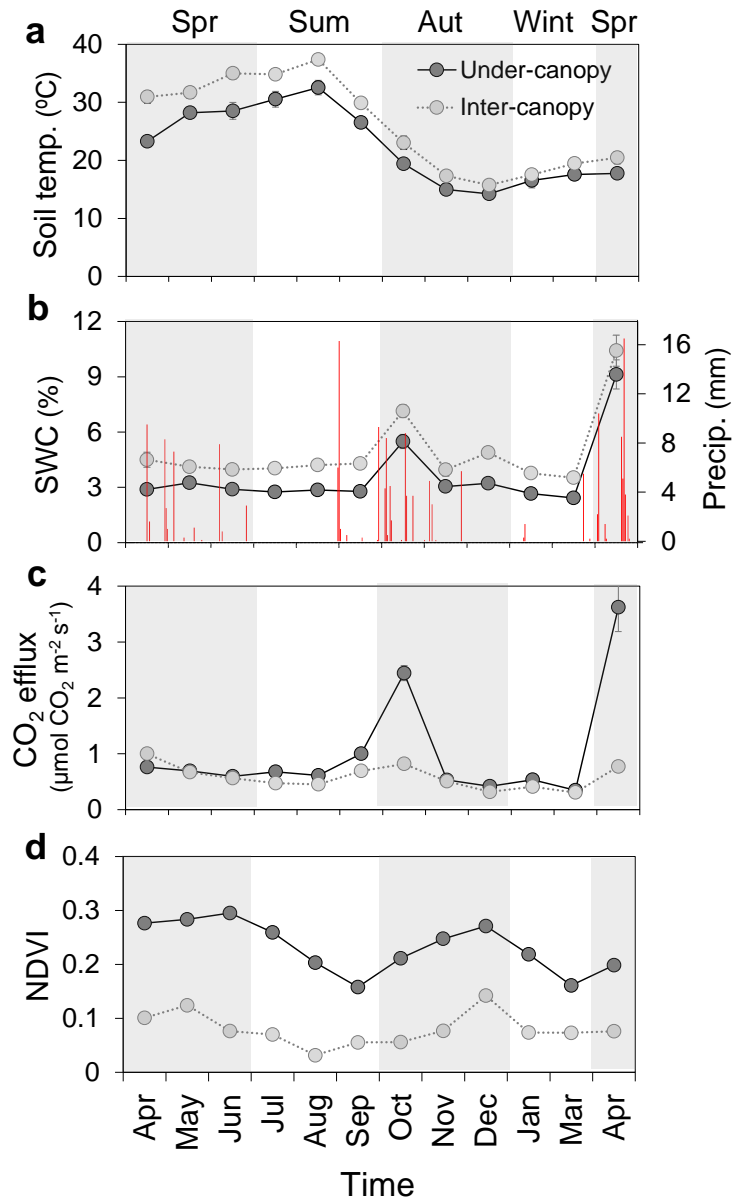
Figure 2. Dynamics of variables related to soil and vegetation functioning from April 2018 to April 2019. Mean values (± SE) under-canopy (dark circles) and inter-canopy (light ones) of (a) soil temperature, (b) soil water content (SWC) and daily precipitation in the study area (red bars; data from the Spanish Meteorological Agency), and (c) CO_2 efflux. d) Monthly mean normalized difference vegetation index (NDVI) of the canopy (dark circles) and inter-canopy (light ones). Note that no measurements were obtained in February 2019.

Soil microbial biomass and mineralization rates

The incubation experiments revealed higher levels of soil microbial biomass (C_{mic}) and mineralization rates under-canopy than inter-canopy (Table 2). C_{mic} was twice as high under-canopy (7.51 ± 0.13 mg kg^{-1}soil) as inter-canopy (3.90 ± 0.02 mg kg^{-1}soil), whereas the magnitude of soil mineralization rate was approximately 16 times higher under-canopy (Table 2). Soil mineralization experienced a rapid decrease during the first 24 hours of incubation, both under- and inter-canopy (from Day 1 to Day 2; Fig. 3). We observed clear differences between mineralization curves with higher rates and more complex dynamics under-canopy, and lower and constant rates inter-canopy. The steep decline continued up

to Day 10 under-canopy, although with higher CO_2 concentrations on Day 6 and Day 8. We also recorded a peak on Day 6 inter-canopy. From Day 10, minor fluctuations were observed at both sites. The differences between the mineralization under- and inter-canopy increased with time, reaching maximums on Day 8 and 17 (rates of 36- and 29-times higher under-canopy, respectively).

Table 2. Mean soil carbon biomass and soil mineralization rate, after 23 days of incubation (± SE), differentiating between under- and inter-canopy. F-statistic and significance of the ANOVA are shown (***P < 0.001).

	Under-canopy	Inter-canopy	*F*	Significance
C_{mic} (mg kg^{-1}soil)	7.51 ± 0.13	3.90 ± 0.02	729.6	***
Mineralization rate[a] (μgCO$_2$ g^{-1} soil h^{-1})	114.81 ± 7.79	7.15 ±1.03	459.6	***

(a) after incubating for 23 days
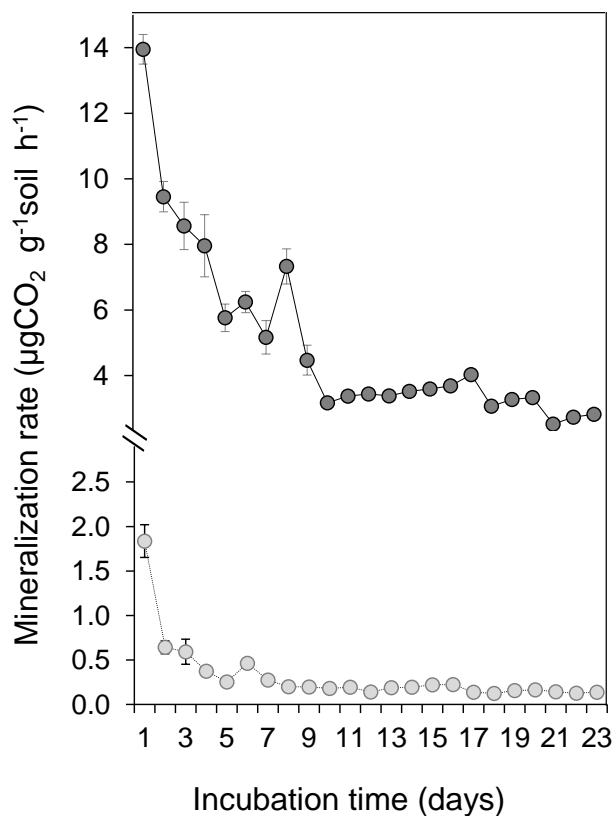
Figure 3. Dynamic of soil mineralization rate (μgCO$_2$ g^{-1} soil h^{-1}) during 23-day incubation experiment. Mean values (±SE) under-canopy (dark circles) and inter-canopy (light ones) are shown.

Soil properties and fertility

In general, we observed higher concentrations of carbon and nutrients under-canopy than inter-canopy (Table 3). Both total organic carbon (TOC) and the extractable fraction (WEOC) were significantly higher under-canopy ($P < 0.001$). Regarding nitrogen, higher concentrations were also found under-canopy as total nitrogen (N_{tot}), whereas the ratio C:N was not significantly different between sites ($P = 0.07$).

Between the soil solution components, the difference between canopy conditions was variable. Regarding nitrates (NO_3^-), under-canopy soils showed higher concentrations, whereas nitrites (NO_2^-) nor sulfate (SO_4^{2-}) concentrations did show spatial differences either. In the case of phosphate (PO_4^{3-}), we did not observe signals of this element inter-canopy whereas the mean value obtained under-canopy came from 2 of the 4 monitored patches.

Table 3. Mean values of the soil organics fractions (total organic carbon, TOC; water extractable organic carbon, WEOC; total nitrogen, N_{tot}; ratio carbon:nitrogen, C:N) and main components in soil solution (nitrate, NO_3^-; nitrite, NO_2^-; sulphate, SO_4^{2-}; phosphate, PO_4^{3-}) (± SE), differentiating between under- and inter-canopy. F- statistic and significance of the ANOVA are shown (***$P < 0.001$, ns: non-significant, na: non-assessed).

	Under-canopy	Inter-canopy	*F*	Significance
Soil organic fraction				
TOC (g kg^{-1} soil)	8.00 ± 0.88	1.27 ± 0.15	57.26	***
WEOC (g kg^{-1} soil)	0.14 ± 0.01	0.05 ± 0.01	32.27	***
N_{tot} (g kg^{-1} soil)	0.73 ± 0.09	0.13 ± 0.01	35.79	***
C:N	11.37 ± 0.65	9.45 ± 0.74	3.76	ns
Soil solution components				
NO_3^- (mg kg^{-1} soil)	9.20 ± 1.24	0.62 ± 0.04	81.11	***
NO_2^- (mg kg^{-1} soil)	0.21 ± 0.03	0.57 ± 0.32	3.34	ns
SO_4^{2-} (mg kg^{-1} soil)	112.9 ± 18.9	95.4 ± 12.8	0.51	ns
PO_4^{3-} (mg kg^{-1} soil)	3.04 ± 0.22	-	-	na

We found positive regressions between soil carbon and mineralization rates (Fig. 4). Generally, higher concentrations of WEOC and TOC were related to higher initial pulse of CO_2 (mineralization rate in 1 hour) ($R^2 = 0.71$, $P < 0.001$, $df = 22$; $R^2 = 0.65$, $P < 0.001$, $df = 22$, respectively) (Fig. 4a, b). However, these relationships varied between covers, since the initial pulse of CO_2 was only related to WEOC under-canopy ($R^2 = 0.64$, $P = 0.002$, $df = 1,10$; Fig. 4a), and to TOC inter-canopy ($R^2 = 0.65$, $P = 0.001$, $df = 1,10$; Fig. 4b). Similarly, the total mineralization rate after 23 days was significantly related with WEOC ($R^2 = 0.56$, $P < 0.001$, $df = 22$) and TOC ($R^2 = 0.65$, $P < 0.001$, $df = 22$) (Fig. 4c, d), although in this case the particular significant regressión occurred just with TOC inter-canopy ($R^2 = 0.63$, $P = 0.002$, $df = 1,10$) (Fig. 4d).
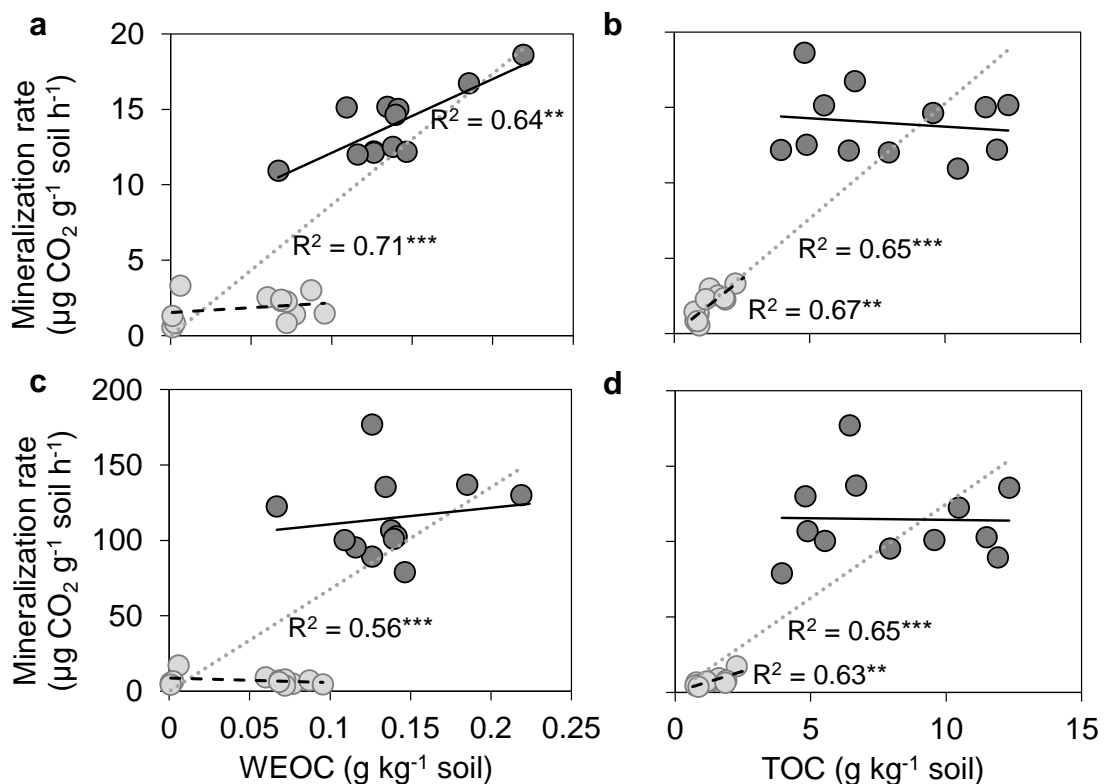
Figure 4. Relationships between soil organics fractions and soil mineralization rates at the beginning of the experiment (1 hour) (a - b) and after 23 days (c - d). Panels a and c refer to water extractable organic carbon (WEOC) and b and d to total organic carbon (TOC). Dark circles represent under-canopy values and light ones, inter-canopy. Grey dotted lines show general regressions, whereas solid black line refers to under-canopy regressions and dashed black lines to inter-canopy ones. The goodness of the fit (R^2) and P-value are shown next to its regression line when significant. Significance: ***P < 0.001, **P < 0.01.

DISCUSSION

Soil and vegetation dynamics in a groundwater-dependent ecosystem in drylands

Our study showed a decoupling of soil biological activity and vegetation dynamics of a GDE in drylands and a partial decoupling from precipitation. In arid ecosystems, differences in soil respiration (Rs) throughout the year can largely be explained by variations in soil water content, and its temporal variability was coupled to precipitation pulses (Vargas et al. 2018). Rainfall and soil moisture are one of the main drivers of Rs in most arid and semiarid ecosystems (Austin et al., 2004; Morillas et al., 2017; Noy-Meir, 1973; Rey et al., 2011; Rey et al., 2021) due to the effect of rewetting associated with precipitation events (Birch effect; Birch, 1959).

Soil moisture increases can rapidly stimulate Rs, and particularly its heterotrophic component, by increasing decomposition processes of readily available carbon products that accumulate in the soil during previous dry periods (Austin et al., 2004; Sponseller, 2007). We detected two major soil CO_2 effluxes in autumn and spring when some precipitation events increased SWC. This effect has already been recorded in this semiarid region for grasslands and shrubs (Rey et al., 2011; Rey et al., 2021). In October, we might expect that the accumulation of labile carbon and microbial biomass during summer, due to reduced soil moisture and the interruption of biological decomposition, would foster greater Rs when SWC increases (Austin et al., 2004). However, the precipitation event that occurred at the beginning of September (16.3 mm) could have driven the consumption of such accumulated carbon and a lower response if compared with the one in April. The timing between the rainfall of September and the measurement can explain such difference (Appendix 3). The effect of rewetting could have been underrepresented because soil CO_2 effluxes in arid and semiarid ecosystems can swiftly return to pre-rain values within a few days (Sponseller, 2007). In April, after a long period with low SWC, a high precipitation pulse was recorded (10.4 mm) and the timing between it and the measurement was shorter (Appendix 3), which could have promoted the record of such an intense response. Therefore, the magnitude of the precipitation events, and mostly the interval between them determines CO_2 efflux in drylands (Sponseller, 2007), which showed a lack of seasonality derived from the precipitation pulses (Vargas et al., 2018).

The autotrophic component of Rs can also respond to soil moisture as plants rapidly activate the photosynthetic mechanisms after rewetting (López-Ballesteros et al., 2016). However, vegetation showed a seasonal bimodal dynamic decoupled to the carbon pulse dynamic and from SWC. Whereas vegetation activity derived from the NDVI showed maximums in June and December, corresponding to the activity of winter-deciduous and summer-deciduous species respectively, SWC had maximums in October and April. This mismatch reveals the low response of the vegetation to SWC, particularly of *Z. lotus* that relies on groundwater (Torres-García et al., 2021b). The phenology of the non-phreatophytic vegetation showed a slow response to Autumn precipitation, increasing from September to December. The vegetation dynamics entails a decoupling between Rs and *Z. lotus* activity because it occurs during the driest and warmest period and suggests that the major component of Rs in this dryland GDE is derived from heterotrophic respiration (Tang and Baldocchi, 2005).

This decoupling between soil biological activity, measured in terms of Rs, and vegetation has also been described in other arid ecosystems without phreatophytic vegetation. Lopez-Ballesteros et al. (2015) found in a field experiment an immediate response of Rs to precipitation, whereas the vegetation needed 6 to 7 days to activate its assimilation mechanisms. Vargas et al. (2018) found in an 18-month monitoring of continuous measurements that most of the precipitation events failed to activate assimilation processes in vegetation whereas a respiration response occurred in all cases.

Soil temperature also affected Rs, although to a lesser extent, as reported by other studies in the area (Oyonarte et al., 2012; Rey et al., 2011). Soil temperature can directly increase Rs, although several studies have reported that temperature sensitivity of Rs can decrease when some thresholds are surpassed (15°C, Conant et al., 2004; 20°C, Rey et al., 2011, Oyonarte et al., 2012). Additionally, temperature might be only relevant when there is sufficient soil moisture for microbial activity (Almagro et al., 2009). Thus, it is likely that in our study, the high soil temperature (above 20°C during most of the year) and the generally low SWC would have reduced the effect of temperature on Rs.

Fertile island effect on soil biological activity and soil quality

Soil CO_2 effluxes and environmental conditions differed spatially because of vegetation and soil heterogeneity that characterize these dryland ecosystems (Austin et al., 2004). As expected, higher CO_2 effluxes were observed under-canopy, and the differences with inter-canopy rates increased during wet periods (October and April). Such spatial differences can be explained by higher root density, but also organic carbon and nutrients that largely accumulate under-canopy as a result of litter deposition, soil biota mineralization, and decomposition (Sponseller, 2007; Tucker and Reed, 2016). However, these effects are difficult to separate in the field, and particularly when SWC is limiting.

Inter-canopy soils showed higher SWC than under-canopy ones, contrary to expectations. Phreatophytes in arid and semiarid environments can contribute to enhancing SWC under-canopy because large canopies shade direct sun radiation, prevent high soil temperatures, and increase soil moisture content (Cao et al., 2016). Nonetheless, the great vegetation density in the patches, and the high transpiration rate of species such as *Z. lotus* (Torres-García et al., 2021b) will deplete soil water faster under-canopy (Martınez-Vilalta and Garcia-Forner, 2017). Contrary, bare soils, which are highly exposed to the evaporative component, can maintain wetter conditions on the near surface since the loss of water by capillarity can be interrupted because of the absence of the transpirative component. In any case, CO_2 effluxes were higher under-canopy, since the amount of available material to be decomposed, which barely accumulates inter-canopy, limits soil biological activity and carbon pulses (Gallardo and Schlesinger, 1992; Rey et al., 2017).

When removing the autotrophic component and water limitation by bringing the soils into the laboratory, the carbon fluxes might be attributed to the carbon substrate, microbial biomass, and mineralization rates (Butterly et al., 2009; Gallardo and Schlesinger, 1992). The higher organic carbon (both TOC and WEOC) under-canopy is related to vegetation cover and its litter inputs, whereas the low and scarcely mineralizable organic carbon observed inter-canopy supports the hypothesis that nutrients and organic matter availability is limited outside the canopy. Additionally, both carbon fractions were positively related to mineralization rates, since TOC and WEOC inform about the degree of organic matter decomposition (Embarcher et al., 2007). Thus, the labile carbon fraction was related

to the first stage of mineralization rate (the first hour of incubation) under-canopy because of higher microbial biomass that easily decomposes such fraction. Contrary, TOC was related to the mineralization rate inter-canopy, both at the beginning of the mineralization and after the 23-day accumulation process. Therefore, not only the amount of soil carbon determines the carbon fluxes, but also the way that carbon is available for microbial decomposition (Rey et al., 2017).

The larger amount of litter that accumulates under-canopy promotes a spatial heterogeneity in the microbial biomass and their decomposition rates (Gallardo and Schlesinger, 1992). The fast mineralization rates observed under-canopy when soil moisture is maintained (from 13.95 to 3.17 μgCO_2 g^{-1} soil h^{-1} in 9 days) evidence a pattern similar to those occurring in tropical forests when organic carbon is swiftly decomposed (e.g., Whitaker et al., 2014). Moreover, the reduction in the mineralization rates and the oscillating pattern observed might reflect shifts in the microbial community composition (Butterly et al., 2009) combined with the consumption of labile first, and more recalcitrant carbon sources later. In fact, soil microbial communities are commonly more functionally diverse under-canopy than in bare soils (García et al., 2018). Overall, both the quantity and quality of litter inputs determine the diversity in soil microbial communities (Ochoa-Hueso et al., 2018) and the rates of carbon and nitrogen cycling (Chen and Stark, 2000). Soil microbial diversity and the nutrient cycling might be enhanced here by combining the morpho-functional distinct leaves of *Z. lotus* (leaves with high and low specific leaf areas and decomposition rates, Pérez-Harguindeguy et al., 2013) and the litter of associated summer-deciduous species (Torres-García et al., 2021c). The mineralization of carbon and nitrogen is a fundamental biogeochemical process that maintains the fertility of the soil under the plants, and which products are essential for increasing biomass production and decreasing the risk, extent, and severity of desertification (Lal, 2003).

Soil quality (i.e., physical-chemical properties strongly related to soil organic carbon pool and desertification process, Lal, 2001) can also determine differences in CO_2 effluxes (Oyonarte et al., 2012). Coarser soil texture, lower organic carbon content, and hence lower biological activity can contribute to CO_2 diffusion within the soil and to increase carbon fluxes to the atmosphere during dry periods (Oyonarte et al. 2012). Overall, desert soils in arid and semiarid regions typically have low organic carbon and total nitrogen

concentrations as a consequence of low contents of silt and clay (Wang et al. 2019). Additionally, the reduced vegetation cover and productivity derived from aridity, promote the heterogeneity of carbon inputs to the soil (Ruiz-Sinoga et al., 2012). The higher content of sand found inter-canopy and the higher erosion susceptibility of these areas might have reduced the retention capacity of nutrients (Lal, 2001; Campos et al., 2020). Contrary, the formation of *nebkhas* (i.e., coppice dunes) promote the accumulation of sediments, organic carbon, and nutrients under-canopy (Wang et al. 2019), as reflected in our results (higher WEOC, TOC, NO_3^-, and N_{tot}). Indeed, the concentration of NO_3^- and PO_4^{3-} under-canopy were much larger than the mean values of other Mediterranean shrublands (Morillas et al., 2017). Therefore, our outcomes are consistent with the well-known "fertile islands" definition (Maestre et al., 2001; Ochoa-Hueso et al., 2018), and with the possibility that the phreatophyte *Z. lotus* enhances soil quality in drylands.

Implications for conservation under climate change

Terrestrial ecosystems of arid and semiarid regions are highly vulnerable to soil degradation and desertification (Rey et al., 2011, Martínez-Valderrama et al., 2020), despite the beneficial effect of fertile islands (Lal, 2001). Global warming will alter global air circulation patterns, which will affect precipitation regimes across scales, reducing rainfall amounts in the Mediterranean basin and prolonging drought periods (Guiot and Cramer, 2016). Such effects will limit soil moisture and groundwater recharge (Eamus et al., 2006). When soil moisture and/or groundwater sources are reduced, vegetation growth in GDEs is limited, hence the supply of organic matter into the soil, which drives lower nutrients, structural stability, and water holding capacity (Ruiz-Sinoga et al., 2012). In drylands, precipitation frequency will particularly alter soil respiration (Vargas et al., 2018) as well as soil microbial activity and organic matter decomposition (Prieto et al., 2019), also in GDEs (Fig. 5).

Higher temperatures would increase atmospheric evaporative demand, and hence, plant photosynthetic activity and growth (Torres-García et al., 2021a; Wu et al., 2011). In the case of the phreatophyte *Z. lotus*, higher atmospheric evaporative demand would increase photosynthetic and transpiration rates, but also groundwater uptake when it is easily available (groundwater depth < 13 m in the study area) (Torres-García et al., 2021a, 2021b).

Atmospheric CO_2 increases can also stimulate plant growth, root respiration, and organic matter mineralization, contributing to soil carbon losses (Bardgett et al., 2013). However, reduced precipitation, soil moisture, and groundwater availability (groundwater discharge due to phreatophytic transpiration and groundwater exploitation), might compromise both soil-nutrient availability and plant productivity (Querejeta et al., 2021).
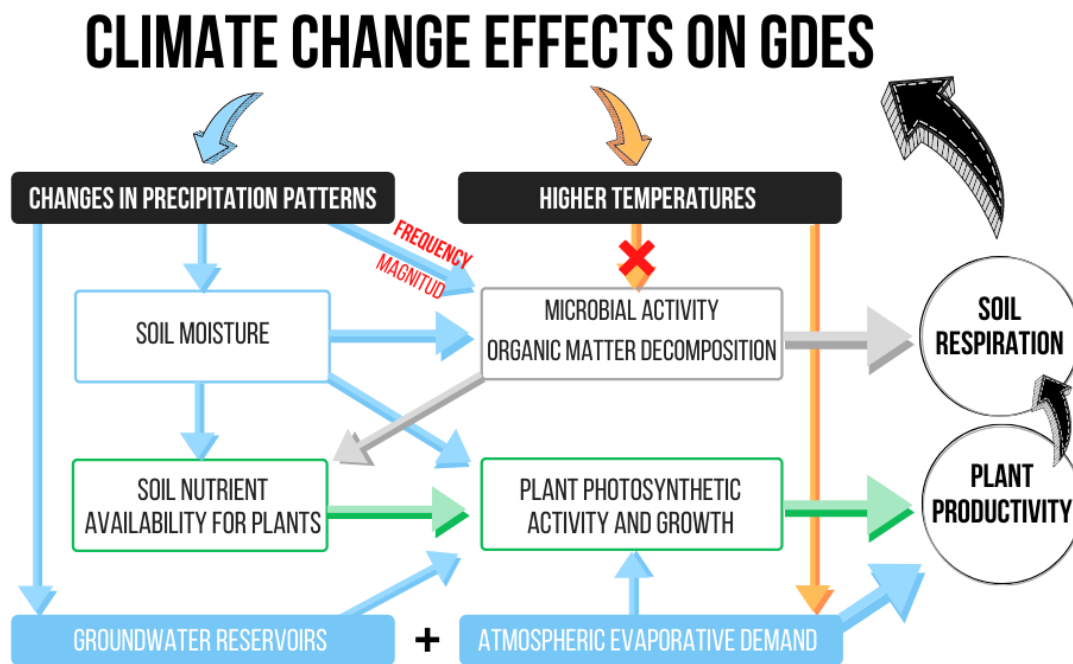
Figure 5. Conceptual diagram of climate change effects over groundwater-dependent ecosystems (GDEs) from the literature (Bardgett et al. 2013; Querejeta et al. 2021) and the results obtained from this study (red marks). Bluish sections refer to water components, whereas greenish and greyish ones represent plant and soil components respectively.

Prolonged droughts during summer can diminish nutrient uptake for species with dimorphic root systems (Querejeta et al., 2021) such as *Z. lotus,* since plant nutrient uptake and accumulation in leaves depend on water availability (Salazar-Tortosa et al., 2018). Because of its winter-deciduousness, *Z. lotus* has reduced wet periods when obtaining water and nutrients from the topsoil (Torres-García et al., 2021b). Reduced nutrient acquisition can drive lower accumulation of nutrients on leaves, which could also contribute to reducing litter quality. Changes in plant traits can alter the functional composition of the associated soil microbial community, thus driving changes in decomposition and mineralization processes (De Bello et al., 2010). In a final stage, the loss

of *Z. lotus* plants might promote low-quality, heterogeneous soils like inter-canopy ones, which would increase the effect of desertification. This cascade of disturbances might severely affect soil respiration patterns in drylands, particularly in those ecosystems that rely on groundwater, altering carbon cycles globally (Bardgett et al., 2013), hence fostering climate change effects.

CONCLUSIONS

In this study we show how the soil and vegetation components of a groundwater-dependent ecosystem (GDE) in semiarid regions are decoupled between them and partially decoupled to precipitation. Whereas the activity of the phreatophytic vegetation was not dependent on rainfall, non-phreatophytic vegetation showed a delayed response. Particularly, soil respiration and mineralization processes were coupled to precipitation pulses typical of drylands. The greater effect of soil moisture on soil biological activity suggests the importance of water resources to promote the functioning of the soil component of GDEs. Soil activity as well as carbon fractions and nutrients were higher in the patches of vegetation (under-canopy) than in bare soils (inter-canopy), highlighting the "fertile island" effect promoted by the phreatophytic vegetation. Overall, phreatophytic vegetation in the GDEs enhances soil quality and microbial composition in drylands under a continuous organic matter input (under-canopy). However, our findings expose the vulnerability of arid GDEs to climate change effects and land degradation, due to the dependence of soil biological processes on precipitation for activation, and on phreatophytic vegetation for litter input and soil quality. The loss of one fertile island in drylands could be detrimental to the functional diversity of these ecosystems, since it might drive irreversible changes in processes such as soil microbial activity, organic matter mineralization, and productivity.

REFERENCES

Aguiar MR, Sala OE (1999) Patch structure, dynamics and implications for the functioning of arid ecosystems. *Trends Ecol Evol*, 14 (7): 273-277.

Almagro M, Lopez J, Querejeta JI, Martinez-Mena M (2009) Temperature dependence of soil CO_2 efflux is strongly modulated by seasonal patterns of moisture availability in a mediterranean ecosystem. *Soil Biol Biochem*, 41, 594–605.

Anderson JPE, Domsch KH (1978) A physiological method for the quantitative measurement of microbial biomass in soils. *Soil Biol Biochem*, 10, 215–221.

Antunes C, Chozas S, West J, et al (2018) Groundwater drawdown drives ecophysiological adjustments of woody vegetation in a semi-arid coastal ecosystem. *Glob Change Biol*, 24, 4894–4908.

Austin AT, Yahdjian L, Stark JM, et al (2004) Water pulses and biogeochemical cycles in arid and semiarid ecosystems. *Oecologia*, 141, 221–235.

Bardgett RD, Manning P, Morriën E, De Vries FT (2013) Hierarchical responses of plant-soil interactions to climate change: consequences for the global carbon cycle. *J Ecol*, 101, 334–343.

de Bello F, Lavorel S, Díaz S, et al (2010) Towards an assessment of multiple ecosystem processes and services via functional traits. *Biodivers Conserv*, 19, 2873–2893.

Birch H (1959) The effect of soil drying on humus decomposition and nitrogen availability. *Plant Soil*, 12, 9–31.

Butterly CR, Bünemann EK, McNeill AM, et al (2009) Carbon pulses but not phosphorus pulses are related to decreases in microbial biomass during repeated drying and rewetting of soils. *Soil Biol Biochem*, 41, 1406–1416.

Campos A, Suárez G, Laborde J (2020) Analyzing vegetation cover-induced organic matter mineralization dynamics in sandy soils from tropical dry coastal ecosystems. *Catena*, 185, 104264.

Cao C, Abulajiang Y, Zhang Y (2016) Assessment of the effects of phytogenic nebkhas on soil nutrient accumulation and soil microbiological property improvement in semi-arid sandy land. *Ecol Eng*, 91, 582–589.

Chen J, Stark JM (2000) Plant species effects and carbon and nitrogen cycling in a sagebrush-crested wheatgrass soil. *Soil Biol Biochem*, 32:47–57.

Cleveland CC, Reed SC, Keller AB (2014) Litter quality versus soil microbial community controls over decomposition: a quantitative analysis. *Oecologia*, 174, 283–294.

Colvin C, Le Maitre D, Hughes S (2003) Assessing Terrestrial Groundwater Dependent Ecosystems in South Africa. Water Research Commission, WRC Report No. 1090-2/03.

Conant RT, Dalla-Bettab P, Klopatekc CC, Klopatekd JM (2004) Controls on soil respiration in semiarid soils. *Soil Biol Biochem*, 35, 945–951.

Delgado-Baquerizo M, Maestre FT, Gallardo A, et al (2013) Decoupling of soil nutrient cycles as a function of aridity in global drylands. *Nature*, 502, 672–676.

Delgado-Baquerizo M, Maestre FT, Reich PB, et al (2016) Microbial diversity drives multifunctionality in terrestrial ecosystems. *Nat Commun*, 7, 10541.

Eamus D, Froend R, Loomes R, et al (2006) A functional methodology for determining the groundwater regime needed to maintain the health of groundwater-dependent vegetation. *Aust J Bot*, 54, 97.

Eamus D, Zolfaghar S, Villalobos-Vega R, et al (2015) Groundwater-dependent ecosystems: recent insights, new techniques and an ecosystem-scale threshold response. *Hydrol Earth Syst Sci Discuss*, 12, 4677–4754.

Embacher A, Zsolnay A, Gattinger A, Munch JC (2007) The dynamics of water extractable organic matter (WEOM) in common arable topsoils: I. Quantity, quality and function over a three year period. *Geoderma*, 139, 11–22.

Gallardo A, Schlesinger WH (1992) Carbon and nitrogen limitations of soil microbial biomass in desert ecosystems. *Biogeochemistry*, 18, 1–17.

Garcia DE, Lopez BR, de-Bashan LE, et al (2018) Functional metabolic diversity of the bacterial community in undisturbed resource island soils in the southern Sonoran Desert. *Land Degrad Dev*, 29: 1467–1477.

Glenn EP, Nagler PL, Morino K, Hultine KR (2013) Phreatophytes under stress: transpiration and stomatal conductance of saltcedar (Tamarix spp.) in a high-salinity environment. *Plant Soil*, 371:655–673

Guirado E, Alcaraz-Segura D, Rigol-Sánchez JP, et al (2018) Remote-sensing-derived fractures and shrub patterns to identify groundwater dependence. *Ecohydrology*, 11, e1933.

Guirado E, Blanco-Sacristán J, Rigol-Sánchez JP, et al (2019) A Multi-Temporal Object-Based Image Analysis to Detect Long-Lived Shrub Cover Changes in Drylands. *Remote Sensing*, 11(22):2649.

Guirado E, Tabik S, Alcaraz-Segura D, et al (2017) Deep-learning Versus OBIA for Scattered Shrub Detection with Google Earth Imagery: *Ziziphus lotus* as Case Study. *Remote Sensing*, 9(12):1220.

Guiot J, Cramer W (2016) Climate change: The 2015 Paris Agreement thresholds and Mediterranean basin ecosystems. *Science*, 354: 4528–4532.

Lal R (2001) Potential of Desertification Control to Sequester Carbon and Mitigate the Greenhouse Effect. In: Rosenberg NJ, Izaurralde RC (Eds.), *Storing Carbon in Agricultural Soils: A Multi-Purpose Environmental Strategy*. Springer Netherlands, Dordrecht, pp. 35–72.

Lal R (2003) Global potential of soil carbon sequestration to mitigate the greenhouse effect. *Crit Rev Plant Sci*, 22, 151–184.

Lambers H, Oliveira RS (2019) *Plant Physiological Ecology*. Springer International Publishing, Cham.

Lang L, Wang X, Hasi E, Hua T (2013) Nebkha (coppice dune) formation and significance to environmental change reconstructions in arid and semiarid areas. *J Geogr Sci*, 23, 344–358.

López-Ballesteros A, Serrano-Ortiz P, Sánchez-Cañete EP, et al (2016) Enhancement of the net CO_2 release of a semiarid grassland in SE Spain by rain pulses: Rain Pulses Enhance Net CO_2 Release. *J Geophys Res Biogeosci*, 121, 52–66.

Machado MJ, Benito G, Barriendos M, Rodrigo FS (2011) 500 Years of rainfall variability and extreme hydrological events in southeastern Spain drylands. *J Arid Environ*, 75: 1244–1253.

Maestre FT, Bautista S, Cortina J, Bellot J (2001) Potential for using facilitation by grasses to establish shrubs on a semiarid degraded steppe. *Ecol Appl*, 11, 1641–1655.

Martínez-Valderrama J, Guirado E, Maestre FT (2020) Desertifying deserts. *Nat Sustain*, 3, 572–575.

Martínez-Vilalta J, Garcia-Forner N (2017) Water potential regulation, stomatal behaviour and hydraulic transport under drought: deconstructing the iso/anisohydric concept: Deconstructing the iso/anisohydric concept. *Plant Cell Environ*, 40:962–976.

Mingorance MD, Barahona E, Fernández-Gálvez J (2007) Guidelines for improving organic carbon recovery by the wet oxidation method. *Chemosphere*, 68 (3): 409–413.

Morillas L, Roales J, Portillo-Estrada M, Gallardo A (2017) Wetting-drying cycles influence on soil respiration in two Mediterranean ecosystems. *Eur J Soil Biol*, 82, 10–16.

Newman BD, Wilcox BP, Archer S., et al (2006) Ecohydrology of water-limited environments: A scientific vision. *Water Resour Res*, 42, W06302.

Noy-Meir I (1973) Desert ecosystems: environment and producers. *Ann Rev Ecol Syst*, 4:25–51.

Ochoa-Hueso R, Eldridge DJ, Delgado-Baquerizo M, et al (2018) Soil fungal abundance and plant functional traits drive fertile island formation in global drylands. *J Ecol*, 106, 242–253.

Oyonarte C, Rey A, Raimundo J, et al (2012) The use of soil respiration as an ecological indicator in arid ecosystems of the SE of Spain: Spatial variability and controlling factors. *Ecol Indic*, 14, 40–49.

Paruelo JM, Epstein HE, Lauenroth WK, Burke IC (1997) ANPP estimates from NDVI for the central grassland region of the United States. *Ecology*, 78: 953–958.

Pérez-Harguindeguy N, Díaz S, Garnier E, et al (2013) New handbook for standardised measurement of plant functional traits worldwide. *Aust J Bot*, 61, 167.

Pérez-Priego O, Testi L, Orgaz F, Villalobos FJ (2010) A large closed canopy chamber for measuring CO2 and water vapour exchange of whole trees. *Environ Exp Bot*, 68(2):131–138.

Potts DL, Scott RL, Cable JM, et al (2008) Sensitivity of mesquite shrubland CO_2 exchange to precipitation in contrasting landscape settings. *Ecology*, 89, 2900–2910.

Poulter B, Frank D, Ciais P, et al (2014) Contribution of semi-arid ecosystems to interannual variability of the global carbon cycle. *Nature*, 509, 600–603.

Prieto I, Almagro M, Bastida F, Querejeta JI (2019) Altered leaf litter quality exacerbates the negative impact of climate change on decomposition. *J Ecol*, 107: 2364– 2382.

Querejeta JI, Ren W, Prieto I (2021) Vertical decoupling of soil nutrients and water under climate warming reduces plant cumulative nutrient uptake, water-use efficiency and productivity. *New Phytol.,* 230, 1378–1393.

R Core Team (2018) R: a language and environment for statistical computing (version 3.5.2). R Foundation for Statistical Computing, Vienna, Austria. Website: http://www.r-project.org

Rey A, Carrascal LM, Báez CG, et al (2021) Impact of climate and land degradation on soil carbon fluxes in dry semiarid grasslands in SE Spain. *Plant Soil*, 461, 323–339.

Rey A, Oyonarte C, Morán-López T, et al (2017) Changes in soil moisture predict soil carbon losses upon rewetting in a perennial semiarid steppe in SE Spain. *Geoderma*, 287, 135–146.

Rey A, Pegoraro E, Oyonarte C, et al (2011) Impact of land degradation on soil respiration in a steppe (*Stipa tenacissima* L.) semi-arid ecosystem in the SE of Spain. *Soil Biol Biochem*, 43, 393–403.

Reynolds JF, Smith DMS, Lambin EF, et al (2007) Global Desertification: Building a Science for Dryland Development. *Science*, 316, 847–851.

Reynolds JF, Virginia RA, Kemp PR, et al (1999) Impact of drought on desert shrubs: effects of seasonality and degree of resource island development. *Ecol Monogr*, 69, 69–106.

Ruiz Sinoga JD, Pariente S, Diaz AR, Martinez Murillo JF (2012) Variability of relationships between soil organic carbon and some soil properties in Mediterranean rangelands under different climatic conditions (South of Spain). *Catena*, 94, 17–25.

Salazar-Tortosa D, Castro J, Villar-Salvador P, et al (2018) The "isohydric trap": A proposed feedback between water shortage, stomatal regulation, and nutrient acquisition drives differential growth and survival of European pines under climatic dryness. *Glob Chang Biol*, 24, 4069–4083.

Salguero-Gómez R, Casper BB (2011) A hydraulic explanation for size-specific plant shrinkage: developmental hydraulic sectoriality. *New Phytol*, 189, 229–240.

Sánchez-Gómez P, Carrión MA, Hernández A, Guerra J (2003). Libro Rojo de la Flora Silvestre protegida de la región de Murcia. Consejería de Agricultura, Agua y Medio Ambiente, Murcia, Spain.

Schlesinger WH, Andrews JA (2000) Soil respiration and the global carbon cycle. *Biogeochemistry*, 48, 7–20.

Smith WK, Dannenberg MP, Yan D, et al (2019) Remote sensing of dryland ecosystem structure and function: Progress, challenges, and opportunities. *Remote Sens Environ*, 233, 111401.

Sommer B, Froend R (2011) Resilience of phreatophytic vegetation to groundwater drawdown: Is recovery possible under a drying climate? *Ecohydrology*, 4, 67–82.

Sponseller RA (2007) Precipitation pulses and soil CO_2 flux in a Sonoran Desert ecosystem. *Glob Change Biol*, 13, 426–436.

Tang J, Baldocchi DD (2005) Spatial–temporal variation in soil respiration in an oak–grass savanna ecosystem in California and its partitioning into autotrophic and heterotrophic components. *Biogeochemistry*, 73, 183–207.

Thomey ML, Collins SL, Vargas R, et al (2011) Effect of precipitation variability on net primary production and soil respiration in a Chihuahuan Desert grassland: PRECIPITATION VARIABILITY IN DESERT GRASSLAND. *Glob Change Biol*, 17, 1505–1515.

Tian F, Brandt M, Liu YY, et al (2017) Mapping gains and losses in woody vegetation across global tropical drylands. *Glob Change Biol,* 23: 1748–1760.

Tirado R, Pugnaire FI (2003) Shrub spatial aggregation and consequences for reproductive success. *Oecologia*, 136, 296–301.

Torres-García MT, Salinas-Bonillo MJ, Cleverly JR, et al (2021a) A multiple-trait analysis of ecohydrological acclimatisation in a dryland phreatophytic shrub. *Oecologia*, 196, 1179–1193.

Torres-García MT, Salinas-Bonillo MJ, Gázquez-Sánchez F, et al (2021b) Squandering water in drylands: the water-use strategy of the phreatophyte *Ziziphus lotus* in a groundwater-dependent ecosystem. *Am J Bot*, 108, 236–248.

Torres-García MT, Salinas-Bonillo MJ, Pacheco-Romero M, Cabello J (2021c) Modular growth and functional heterophylly of the phreatophyte *Ziziphus lotus*: A trait-based study. *Plant Species Biol*, 1442-1984.12343.

Tucker CL, Reed SC (2016) Low soil moisture during hot periods drives apparent negative temperature sensitivity of soil respiration in a dryland ecosystem: a multi-model comparison. *Biogeochemistry*, 128, 155–169.

Vargas R, Sánchez-Cañete PE, Serrano-Ortiz P, et al (2018) Hot-Moments of Soil CO2 Efflux in a Water-Limited Grassland. *Soil Syst.*, 2, 47.

Wang X, Ma Q, Jin H, et al (2019) Change in Characteristics of Soil Carbon and Nitrogen during the Succession of *Nitraria Tangutorum* in an Arid Desert Area. *Sustainability*, 11, 1146.

West AW, Sparling GP (1986) Modifications to the substrate-induced respiration method to permit measurement of microbial biomass in soils of differing water contents. *J Microbiol Methods,* 5, 177–189.

Whitaker J, Ostle N, McNamara NP, et al (2014) Microbial carbon mineralization in tropical lowland and montane forest soils of Peru. *Front Microbiol*, 5.

Wu Z, Dijkstra P, Koch GW, et al (2011) Responses of terrestrial ecosystems to temperature and precipitation change: a meta-analysis of experimental manipulation: meta-analysis of experimental manipulation. *Glob Change Biol*, 17, 927–942.

Zhang P, Yang J, Zhao L, et al (2011) Effect of Caragana tibetica nebkhas on sand entrapment and fertile islands in steppe–desert ecotones on the Inner Mongolia Plateau, China. *Plant Soil*, 347, 79–90.

Zolfaghar S, Villalobos-Vega R, Cleverly J, et al (2014) The influence of depth-to-groundwater on structure and productivity of Eucalyptus woodlands. *Aust J Bot*, 62, 428.

SUPLEMENTARY MATERIAL

Appendix 1. Monthly precipitation and mean temperature during the study period (bars: April 2018 - April 2019) and mean values of the last 20 years (dashed lines) in the area. Error bars represent monthly SE for the 20-year period. Data from a meteorological station located 8 km from the study area (Almeria Airport Station - Spanish Meteorological Agency).
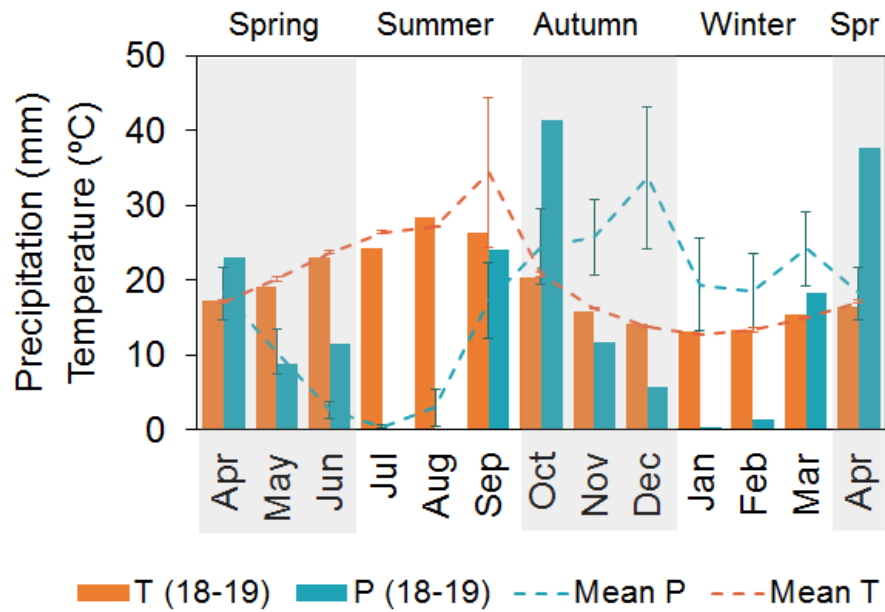
Appendix 2 Timeline of soil incubation experiments: 1) soil-induced respiration (SIR), and 2) soil mineralization dynamics. Blue arrows indicate water addition and orange one, glucose incorporation to the SIR experiment. Black dotted arrows represent CO_2 measurements.
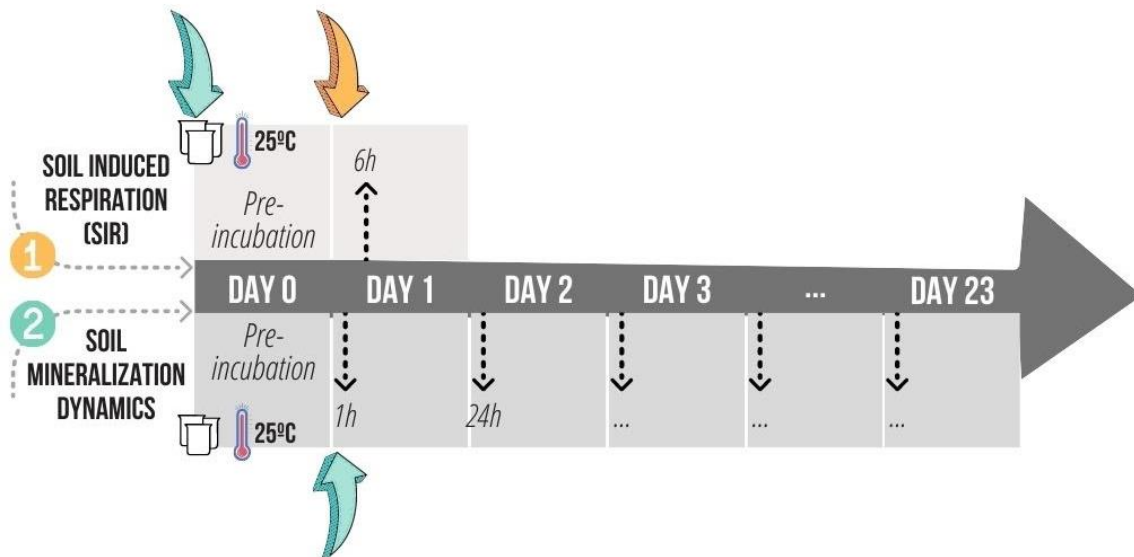
Appendix 3 Detailed information of sampling dates and rainfall prior to each soil respiration measurement.

Month	Sampling date	Days between sampling and last rainfall	Amount last rainfall before measurement (mm)	Total rainfall (mm)
		Sampling since last rainfall event [1]		Between measurements
April	20/04/2018	8	1.6	11.1
May	24/05/2018	7	1.1	20.4
Jun	29/06/2018	2	2.9	10.8
July	25/07/2018	28	2.9	0
August	13/08/2018	47	2.9	0
September	27/09/2018	18	1	23.3
October	17/10/2018	2	**8.4**	22
November	30/11/2018	10	3	30.3
December	27/12/2018	14	5.7	5.7
January	25/01/2019	43	5.7	0
March[2]	07/03/2019	34	1.4	1.4
April	01/04/2019	1	**10.4**	18.1

(1) Rainfall events and amounts were obtained from Almeria Airport meteorological station (AEMET), 8 km far from the study area. Bold numbers indicate precipitation amounts higher than 6 mm.

(2) Note that no measurements were obtained in February.

4. GENERAL DISCUSSION

Drylands cover more than 40% of Earth's land surface (Reynolds et al., 2007) and substantially contribute to the inter-annual variability of the global carbon sink (Poulter et al., 2014). Some plants adopt a drought avoidance strategy in these regions and develop extensive and deep root systems to maximize water uptake and meet evaporative demands (Jackson et al., 2000; Peguero-Pina et al., 2020). These plants, the so-called phreatophytes, drive ecosystems that rely on groundwater (GDEs) to maintain their functions and services, (Eamus et al., 2006, 2016). However, climate change effects (temperature increases and precipitation reductions with more frequent extreme events, Giorgi and Lionello, 2008; Guiot and Cramer, 2016), groundwater drawdown and pollution, and land-use changes might reduce water availability for phreatophytes, jeopardizing the structure and functions of terrestrial GDEs (Eamus et al., 2006). In this sense, understanding the ecological processes underlying plant water use, carbon and nutrient uptake, and soil-plant interactions in these ecosystems is critical for sustainable groundwater management, biodiversity conservation and climate change mitigation in drylands.

This PhD thesis provides knowledge of water, carbon, and nutrient cycles in a remarkable terrestrial GDE of Mediterranean Basin drylands. The natural depth-to-groundwater (DTGW) gradient of the study area and the groundwater-monitoring field station have provided an exceptional scenario for assessing the effects of expected water table decline on the functioning of this phreatophyte and the GDE it drives. Additionally, the seasonal climatic variability along the growing season (from wet and mild springs to hot and dry summers) contributed to understanding plant responses to climate change. Specifically, the results presented here contribute to: (1) knowing how water is used by the plants (anisohydric behavior) and from which source (partial use of groundwater); (2) understanding the processes of carbon assimilation, the growth patterns, and the strategies that underlie the persistence of this long-lived species in drylands (e.g., heterophylly); (3) disentangling soil-plant interactions and their relationships with water availability in this GDE; and (4) identifying plant ecophysiological thresholds related to atmospheric evaporative demand and depth to groundwater. Overall, it provides scientific evidence to managers and policymakers who must deal with the sustainable management of groundwater and ensure GDEs contributions to people in the face of global change.

4.1. *Ziziphus lotus'* water-use patterns

Disentangling plant water-use patterns deepens our understanding of ecosystem functions and hydrological processes in drylands (Zeppel and Eamus, 2008). One of the primary outcomes of this work has been the confirmation of *Z. lotus* reliance on groundwater. To date, evidence about this essential characteristic was reduced to the rooting depth – Le Houérou (2006) found roots of *Z. lotus* up to 60 m depth – and the spatial distribution of individuals across fractures of the territory – Guirado et al. (2018) revealed this spatial pattern that facilitates groundwater access. Adding new evidence, I demonstrated through stable isotope, gas exchange rates, and stem water potential (Chapter II) that *Z. lotus* is a facultative phreatophyte showing different spatiotemporal patterns in water use along the DTGW gradient.

Morpho-functional and physiological traits such as rooting depth, hydraulic architecture, and leaf area can explain spatial and temporal variations in plant water-use patterns (Zeppel and Eamus, 2008; Zofalghar et al., 2017). In the mid-term, plants might have increased resource allocation to the root system to improve water uptake (Markesteijn and Poorter, 2009; Nippert and Holdo, 2015), or reduced leaf area to limit water loss (Zolfaghar et al., 2014). Along the DGTW spatial gradient, we observed that plants with roots at shallow water tables generally obtained more water than those with deeper access to groundwater. Obtaining abundant groundwater might have contributed to higher leaf area and transpiration rates. Contrary, plants found more difficulties obtaining water at greater depths. In this way, they diminished aboveground biomass investment, reducing the hydraulic demand, and increased sapwood area, enhancing the capacity to supply water (Carter and White, 2009; Zolfaghar et al., 2014; Butterfield et al., 2021). This strategy was reflected in higher Huber values (Hv) at deeper sites (Chapter III), since Hv refers to the ratio of sapwood area to leaf area. Ultimately, lower water uptake could have caused lower transpiration, and higher water-use efficiency (WUE), expressed by low $\Delta^{13}C$ that provides a time-integrated estimate from the leaf was formed (Dawson et al., 2002; Moreno-Gutiérrez et al., 2012; Prieto et al., 2018).

Temporal variations in environmental conditions (e.g., solar radiation, atmospheric evaporative demand, soil moisture) can also influence plant water use (O'Grady et al., 1999;

Zeppel et al., 2004). I observed that variations in water availability due to climate seasonality induced a change in the source of water used by *Z. lotus*. Dryland plants have evolved to promptly utilize soil moisture available in shallow depths to maximize nutrient acquisition and growth (Ryel et al., 2010), shifting to deeper layers when the soil dries to sustain transpiration (Querejeta et al., 2007). As revealed by stable isotopes (Chapter II), when soil water availability was still high (May), plants preferentially used this water pool rather than groundwater. Therefore, the continuous reduction of soil moisture during the growing season, supported by the reduction of predawn water potential (Table 1, Chapter III), might increase plants reliance on groundwater despite the depth, as observed in other dryland phreatophytes with dimorphic root systems (Querejeta et al., 2007; Voltas et al., 2015).

The architecture and growth pattern of *Z. lotus*, based on the repetition of modules composed of short and long shoots and flowering and plagiotropic branches, promoted a functional differentiation in water use between vegetative and reproductive structures. Related to heterophylly, leaves from flowering branches (FB) require more resources for reproductive processes (Fenner, 1998; Moore, 1992). We observed that in May, when plants can obtain water and nutrients from the topsoil layer, flowering was at its maximum, and FB leaves showed a high photosynthetic rate. In contrast, in summer, FB leaves lost their functionality earlier than PB leaves, which maintained transpiration rates for longer. In contrast, PB leaves related to vegetative growth, showed lower specific leaf area (SLA), higher stomatal density, and lower WUE. Heterophylly confers heteroblastic species (i.e., with different types of shoots) an advantage to overcome harsh environmental conditions and temporal variability (Moore, 1992; Leigh et al., 2011).

At shorter-time scales, stomata play a more important role in regulating water and carbon fluxes between vegetation and the atmosphere than leaf area (Maseda and Fernández, 2006). In Chapter II, I found distinct patterns of stomatal regulation among *Z. lotus* individuals that might result from differences in environmental conditions varying over space and time (Feng et al., 2019; Hultine et al., 2020). Under differences in water availability, *Z. lotus* individuals experienced a wide range of midday water potential through the growing season, from -1.2 to -3.8 MPa, without stomatal limitations, which suggests different regulation strategies (Feng et al., 2019; Guo et al., 2020). Though

generally anisohydric, *Z. lotus* exhibited spatial variations in stomata sensitivity, showing those plants with better access to groundwater (i.e., lower DTGW) an extreme anisohydric behavior (i.e., lower stomatal control). Besides, higher vapor pressure deficit (VPD) during summer fostered higher anisohydric behavior than in spring and, thus temporal differences in plant water regulation. Less extreme anisohydric regulation might reduce the risk of hydraulic failure (Guo et al., 2020) in plants at sites with deep water tables. The high dependence on deep groundwater sources and the anisohydric regulation contributed to maintaining transpiration rates during drought, although it might diminish soil moisture and nutrient uptake, leading to reductions in plant photosynthesis and WUE (Fig. 1) (Querejeta et al., 2021).
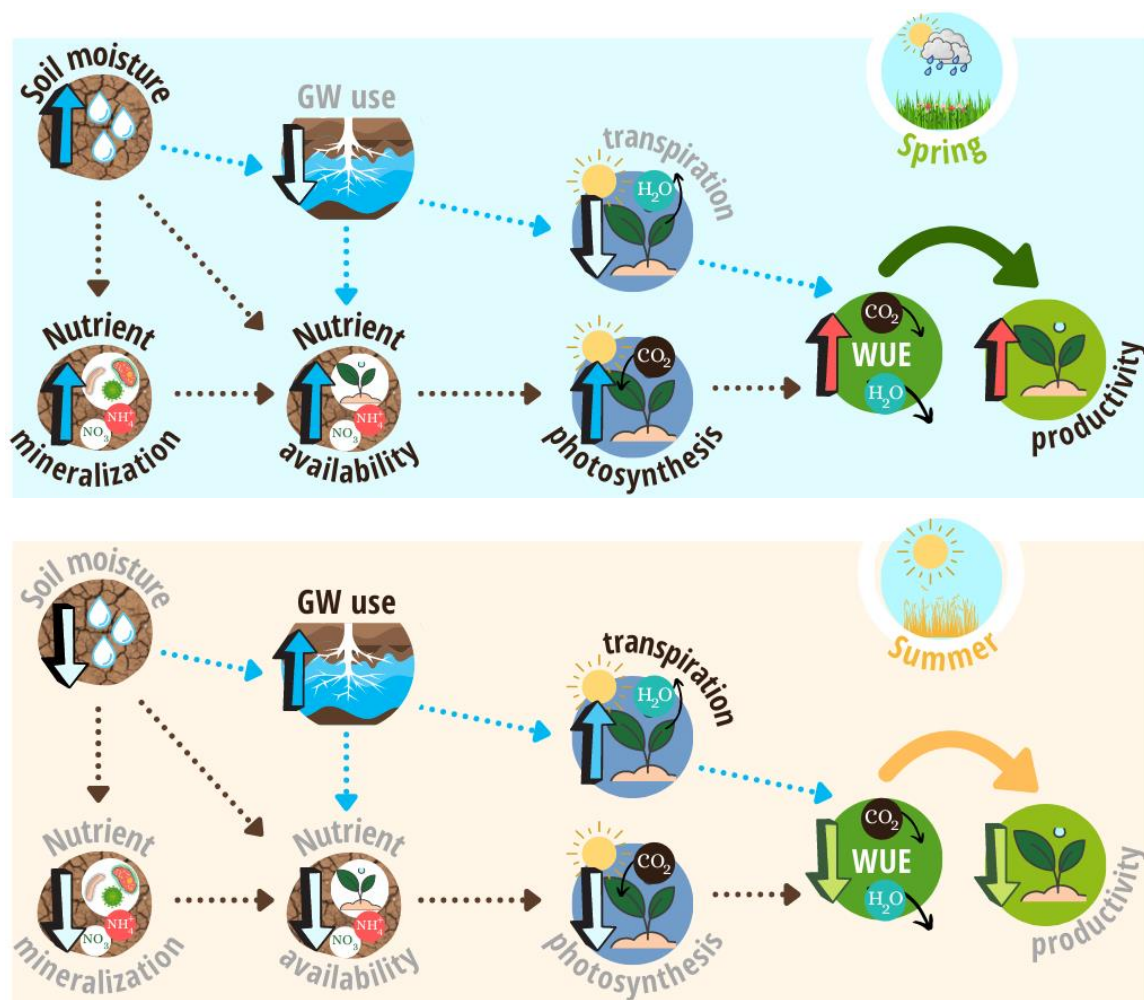
**Figure 1.** Temporal patterns of water use. Higher soil moisture in spring (top panel) can increase nutrient uptake and photosynthesis, thus increasing water-use efficiency and, likely, plant productivity. In the Mediterranean summer, or under reduced soil moisture conditions (lower panel), higher groundwater use fosters transpiration although limits nutrient uptake and photosynthesis, which is a detriment to WUE and productivity.

Variations in resource availability can also cause spatiotemporal differences in plant water and carbon fluxes (Liu et al., 2017; Querejeta et al., 2021). In Chapter II, I assessed leaf nutrient content to identify the nutritional (non-stomatal) limitation of photosynthesis because of the greater use of groundwater. Nutrients are essential for plant productivity and particularly for carbon and water balance (Fisher et al., 2012). Whereas phosphorus (P) is an essential component of ATP, nitrogen (N) is a component of enzymes that mediates the biochemical reactions in which carbon is reduced (e.g., photosynthesis) (Schlesinger and Bernhardt, 2020). Additionally, potassium (K) has a particular role in mitigating drought stress through mechanisms for controlling water conductance, stomata, and transpiration (Arquero et al., 2006; Sardans and Peñuelas, 2015). The non-significant results we obtained revealed the decoupling of most leaf nutrients from DTGW when groundwater use was low and soil water availability high (May), evidencing nutrient uptake independently of the spatial DTGW gradient. In contrast, we have found in additional analyses (not included in this thesis) a general decrease of leaf nutrient content during summer, when the reliance on groundwater sources increased (Fig. 2). This poor nutritional status might have contributed to the increase of transpiration in summer (Sardans and Peñuelas, 2015) with high VPD, and the reduction of photosynthetic rates (Querejeta et al., 2021), particularly in plants that obtain deeper groundwater (Table 1, Chapter III). Combining a lower photosynthetic rate with higher transpiration will reduce WUE, fostering the depletion of soil moisture and nutrient uptake (Querejeta et al., 2021). These results highlight the impact of global warming on vegetation growth in drylands, since climate change projections estimate that soil moisture decreases worldwide by the end of the 21st century 5-15% (Dai, 2013) might reduce soil nutrient availability for plants (Peñuelas et al., 2018).

4.2. The implications of *Z. lotus* fertile islands in the carbon balance of Mediterranean drylands

Dryland ecosystems are characterized by patchy distribution of vegetation, which contribute to the formation of fertile islands (Rynolds et al., 1999). Fertile island development depends on environmental factors (e.g., climate, edaphic characteristics), plant traits and structure (e.g., specific leaf area [SLA], plant height), and soil microbial communities (e.g., diversity and abundance) (Ochoa-Hueso et al., 2018). In Chapter IV, I

demonstrated that *Z. lotus* contributes to the formation of fertile islands, enhancing microbial activity, decomposition, soil quality, and likely, carbon sequestration in drylands.
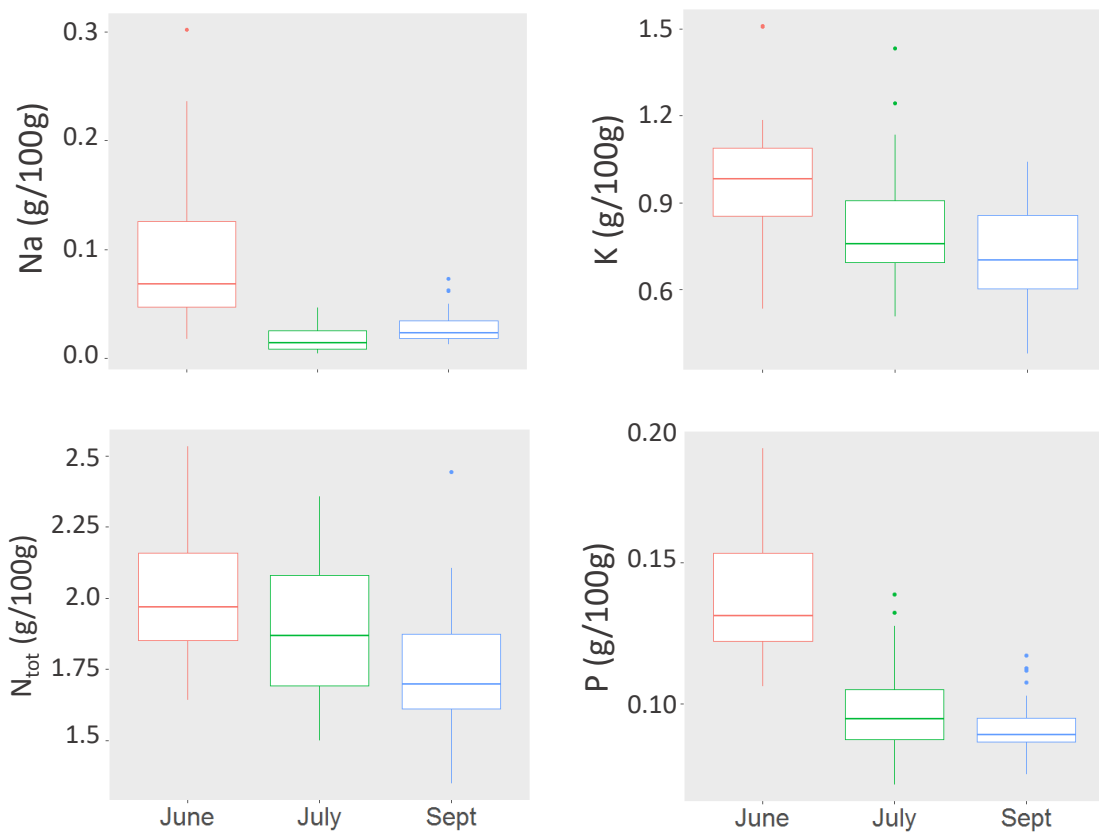
Figuer 2. Monthly significant differences of leaf nutrient content during summer (p-value < 0.001). Na: sodium, K: potassium, N_{tot}: total nitrogen, P: phosphorous.

According to the mass ratio hypothesis, the rate of an ecosystem function is primarily determined by the traits of the dominant species (Grime, 1998). *Z. lotus*, as dominant species, provides the vastest amount of litterfall in the vegetation patches due to its size and winter-deciduousness and hence, largely determines carbon balance. Its litterfall is composed of morphologically distinct leaves (high-SLA leaves [90 cm^2 g^{-1}] and low-SLA ones [75 cm^2 g^{-1}]) and the small and thin flowering branches (FBs) that fall at the end of its growing season (Chapter I). In addition, other summer-deciduous plants that live in *Z. lotus* patches, such as *Lycium intricatum* that develops high-SLA leaves (110-140 cm^2 g^{-1}, Hortal et al., 2017), contribute to the amount and diversity of litterfall under-canopy throughout the driest period. Because vegetation patches are composed of a mixture of seasonally deciduous, drought-deciduous, and evergreen shrubs, there is a continuous litter input (Whitford and Duval, 2002) that accumulates throughout the year under *Z. lotus* canopy.

Leaves with different SLA and nutrient content lead to stronger differences in heterotrophic respiration and decomposition rates (Pérez-Harguindeguy et al., 2013), being high-SLA leaves the drivers of stable carbon, and low-SLA ones of organic matter pools (Cleveland et al., 2014). Another plant trait that influences decomposition processes and promotes soil carbon sequestration is the content of recalcitrant carbon forms such as lignin, polyphenols, and tannins (De Deyn et al., 2008). Species with conservative leaves are characterized by greater allocation of mechanical tissues and low SLA and nutrient concentrations, which might have promoted more recalcitrant structural compounds and, thus, slower decomposition rates than acquisitive leaves (Cortez et al., 2007; de la Riva et al., 2019). Therefore, species such as *Z. lotus*, with relatively low SLA values and leaf nutrient content, can enhance the fertile island effect and contribute C sequestration in drylands (Valencia et al., 2015; Ochoa-Hueso et al., 2018). Additionally, whole-plant traits and the partitioning of carbon and nutrients between plant organs can also influence soil carbon sequestration (De Deyn et al., 2008). For instance, deep rooting contributes to the vertical allocation of C in the soil through the interaction between root rhizodeposits and turnover with soil minerals to form aggregates (Jobbagy and Jackson, 2000; Lorenz and Lal, 2005). In this sense, tall phreatophytes with intricate and dense canopies like *Z. lotus* can maintain high primary productivity rates in drylands due to groundwater use and anisohydric behavior (Chapter II).

Soil environmental conditions are also key controls of carbon balance. Soil moisture is essential in mineralization processes, diffusing nutrients through the soil (Sardans et al., 2008), and enhancing microbial biomass (Delgado-Baquerizo et al., 2013). We showed that soil activity (i.e., CO_2 effluxes) in *Z. lotus* GDE was coupled to precipitation, as widely occurs in dryland ecosystems (Austin et al., 2004; Sponseller, 2007; Morillas et al., 2017; Vargas et al., 2018; Rey et al., 2021). Soil moisture can promptly stimulate heterotrophic respiration (i.e., microbial activity) by increasing decomposition of available carbon that accumulates during dry periods (Austin et al., 2004; Sponseller, 2007). It can also stimulate autotrophic respiration (i.e., plant roots and rhizosphere activity) since plants can rapidly activate their photosynthetic mechanisms (López-Ballesteros et al., 2016). However, we observed a temporal decoupling between soil biological activity and the functioning of *Z. lotus* (measured through the NDVI vegetation index), due to its groundwater reliance.

The amount and quality (i.e., chemical and physical properties) of plant litter inputs will determine soil properties (Cleveland et al., 2014), the diversity of soil microbial communities (Ochoa-Hueso et al., 2018), the decomposition rates (Chen and Stark, 2000), carbon loss through soil respiration and leaching, and the carbon immobilization (De Deyn et al., 2008). Overall, to enhance soil C sequestration in the long-term, sustained primary productivity is required, as well as efficient feedback between plants and soil biota for carbon and nutrient cycling (Fontaine and Barot, 2005). According to the mass ratio hypothesis (Grime, 1998), and processes described above, *Z. lotus* largely contribute to carbon and nutrient cycling due to their substantial biomass, litter quality, and deep root system. Groundwater depletions will limit *Z. lotus* primary productivity to some extent, and hence, the ecosystem´s capacity for carbon sequestration. A tipping point that assures the maintenance of the ecophysiological functioning and the ecological processes could define that extent.

4.3. Ecophysiological thresholds in GDEs: robust evidence for managers and decision-makers in the face of climate change

The management of terrestrial GDEs requires a profound understanding of the functioning of phreatophytic species and the processes they lead, as well as the effect of the interactions between different drivers of global environmental change, such as climate change, habitat loss, fragmentation, and degradation (Eamus et al., 2006; Rey et al., 2018). Additionally, it requires deep knowledge about the regeneration perspectives and limits of acceptable change that ensure ecosystem health and its contributions to people. In this sense, managers and policymakers commonly want to know about the amount of water taken from the aquifers without risking GDEs (Eamus and Froed, 2006) and the prospective consequences of climate change effects on these ecosystems. In Chapters II and III, I defined ecophysiological thresholds related to the functioning of *Z. lotus* and the GDE it dominates in southeast Spain. Although phreatophytes may respond differently to groundwater depletion and depths according to the environmental conditions (e.g., atmospheric evaporative demand, salinity, water table decline rate) (González et al., 2012), identifying site-specific ecohydrological thresholds can be used as straightforward management evidence for poorly studied sites, while acquiring more generalizable scientific knowledge.

The decrease of soil water availability fosters higher xylem tension for plant water uptake, thus more negative water potentials (Tyree and Ewers, 1991). In xeric environments, plants are exposed to higher atmospheric evaporative demands than in mesic sites and hence must experience even lower water potentials. This fact means that some species must shift the stomatal sensitivity threshold towards more negative values to maintain leaf gas-exchange rates in drylands (Klein et al., 2014). Because of that, some dryland shrubs such as *Larrea tridentata* can tolerate water potentials of -9.5 MPa before xylem cavitation (Guo et al., 2020). Resistance to xylem cavitation confers drought tolerance to the plants, ensuring efficient water supply to leaves. The greater the cavitation resistance, the higher the gas-exchange rate and the potential for extracting water from dry soils (Linton et al., 1998).

Some phreatophytic shrubs can also tolerate negative and fluctuating water potentials (Naumburg et al., 2005). Chapter II showed the generally extreme anisohydric stomatal regulation of *Z. lotus*, although with a spatiotemporal variation in hydraulic response to water availability. *Z. lotus* exhibited extreme anisohydry during the wet spring and partial isohydry during the dry and hot summer, indicating some stomatal regulation under water stress. Nevertheless, we could not define a threshold in plant water potential that drives either xylem cavitation or stomatal closure under the current conditions of DTGW and VPD. Indeed, the response of *Z. lotus* transpiration rates did not reveal stomatal limitation with increasing VPD, at least up to 4.5 kPa. *Z. lotus* plants might have adapted the mechanisms to control water balance through the stomatal aperture and leaf area development on the one hand and water transport capacity in the xylem (including roots development) on the other. This behavior could allow plants to use water more effectively, mainly when the vapor pressure deficit is high, operating at high transpiration rates (Manzoni et al., 2013). However, projections of climate change impacts exacerbate the decrease of soil water and groundwater availability and the increase in VPD (Dai, 2013), which might overpass the tolerance limits of the species that were not found in the study area.

Regarding water table declines, there have not been previous in situ drought experiments to measure *Z. lotus* response, only laboratory analyses to evaluate growth and water relations of seedlings under water deficit stress (Maraghni et al., 2011; Maraghni et al., 2014; Maraghni et al., 2019). In the study area, temporal fluctuations in water table levels

did not entail significant responses, probably due to the narrow temporal scale of research. Therefore, a surrogate for manipulative in situ whole-plant experimentation is the assessment of phreatophyte ecophysiological curves over a range of groundwater depths (Froend and Drake, 2006). Both Chapters II and III showed the negative response of *Z. lotus* morpho-functional and physiological traits to the increase in DTGW. Results from stable isotopes analysis ($\delta^{18}O$ and $\Delta^{13}C$) and gas-exchange rates (E and g_s) pointed to a DTGW threshold at 12 – 14 m in this region, beyond which groundwater use was a constraint, and variations in *Z. lotus* response to increasing DTGW were minimal. This response was combined with higher salinity levels at deep water tables, fostering drought-like stress (Kath et al., 2015) with physiological constraints to obtain deep groundwater. By this mechanism, plants can escape from the effect of the stress when groundwater is more readily available (DTGW < 14 m). However, abrupt groundwater declines could diminish the ecophysiological functioning of phreatophytes like *Z. lotus* and cause extensive mortality when the root growth rate is exceeded (Orellana et al., 2012), even if the proposed threshold is not overtaken (Gonzalez et al., 2012).

4.4. Towards the assessment of GDEs contributions to people in drylands

Nature contributions to people are essential for human wellbeing (IPBES, 2019). However, anthropogenic activities have led to rapid alterations in ecosystems' composition, structure and function (Vitousek et al., 1997), hence in their capacity to provide services (Daily, 1997). Ecosystem services (ES) have been widely used as indicators of ecosystem resilience to local and global pressures since they link the social and ecological components (Millennium Ecosystem Assessment, 2005; Reyers et al., 2013). Although significant improvements have been made to assess ES, predicting how much change in a system component will result in a change in service provision remains challenging (Hough et al., 2018).

The ES supply depends on the biodiversity functional traits (Kremen, 2005; De Bello et al., 2010; Cernansky, 2017). These traits are ecological attributes by which species influence ecosystem services through their effects on underlying processes (Lavorel and Garnier, 2002). Whereas specific ecological processes are affected by the combination of key traits, particular traits concurrently control several processes (de Bello et al., 2010). Nevertheless,

dominant plant traits strongly influence ecosystem functioning (Díaz et al., 1998), following the mass ratio hypothesis (Grime, 1998). Therefore, understanding such traits at different biological levels contributes to upscale single plant processes to ecosystem-level functions (Mori and Niinemets, 2010) and, ultimately, to ecosystem services (de Bello et al., 2010) (ES cascade, Fig. 1 of the General introduction). In this sense, a first step in the assessment of nature's contributions to people is to understand the extent to which functional traits, and the related ecological process (e.g., nutrient mineralization, C balance), are affected by abiotic/biotic perturbations (e.g., land-use changes, groundwater drawdown). Throughout this PhD thesis and its Chapters, I have assessed the response of functional traits to environmental factors, not only incorporating the functional characteristics of plants but also those of other organisms that interact with plants for the supply of ES (de Deyn et al., 2008; de Bello et al., 2010) (Fig. 3).
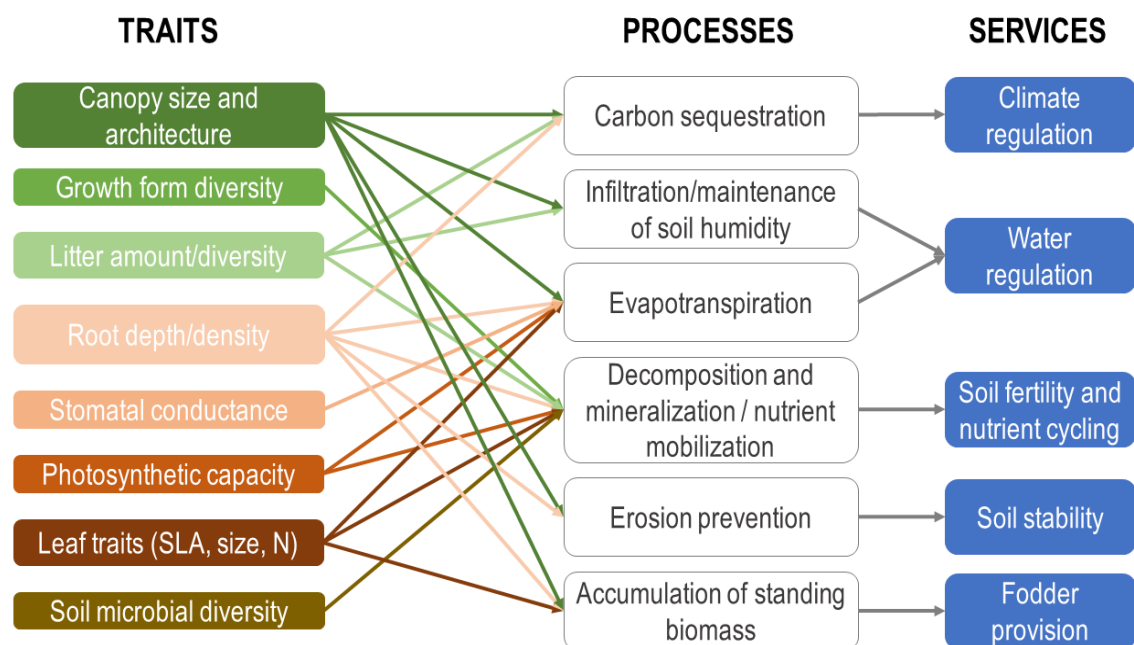
Figure 3. Relationships of some functional traits addressed through this PhD thesis with ecosystem services and their underlying ecological processes (Modified from de Bello et al., 2010).

The presence of phreatophytic species and GDEs is of paramount importance to ensure, or even increase ES supply in drylands (Murray et al., 2006). The primary productivity, i.e., the balance between carbon assimilation through photosynthesis and carbon loss through autotrophic respiration (de Deyn et al., 2008), is the principal regulator of all ecological

processes and the foundation for all terrestrial ES (Eamus et al., 2005). Our results suggest the capacity of phreatophytes to enhance the primary productivity with the use of groundwater and the anisohydric stomatal regulation. Therefore, it contributes to processes such as carbon sequestration (previous section), evapotranspiration, erosion prevention or accumulation of standing biomass, which are the foundations of climate and water regulation, soil stability, and fodder provision (Fig. 3).

Phreatophytic and anisohydric shrubs like *Z. lotus* can move a vast amount of water from soil/groundwater upwards into the atmosphere, promote evapotranspiration processes, and minimise groundwater recharge and salinity in drylands (Eamus et al., 2005). Additionally, when located in intermittent or ephemeral streams, sizable phreatophytes can dampen the water flow, reducing the impact of floods, soil erosion, and sediment accumulation. Furthermore, GDEs provide other valuable ES in drylands, such as habitats for biodiversity (Eamus et al., 2006). Finally, patches of *Z. lotus* may act as a service-providing unit (SPUs) (sensu Luck et al., 2003) with different structure and functions in the arid landscape matrix. Therefore, by removing a single plant of *Z. lotus*, an SPU will disappear in a territory where climatic drivers already jeopardize the ES supply.

Expected changes in temperature and precipitation regimes will likely reduce the productivity of these ecosystems in drylands, which will have critical implications for climate regulation and soil conservation, due to the strong impact of phreatophytes on processes such as carbon sequestration, water run-off and infiltration, soil erosion and nutrient cycling (Maestre et al., 2012). In addition to the effective management of GDEs, the ES framework provides scientific evidence that targets ecological restoration and conservation efforts towards the most vulnerable ecosystems (Murray et al., 2006).

4.5. Final remarks: scientific evidence for the management of *Ziziphus lotus* shrublands in the face of global change

In this PhD thesis I have addressed the main ecophysiological mechanisms of *Z. lotus* underling the functioning of the GDE that this species drives. Such mechanisms can be altered by climate change or groundwater depletion, risking the whole ecosystem. At higher temperatures, *Z. lotus* increases its transpiration rate, especially in conditions with better access to groundwater (Chapter III). However, if precipitation decreases and

becomes more extreme, recharge of the aquifers on which *Z. lotus* depends will also decrease, which added to the increase in transpiration, would produce a synergistic effect that would increase aquifer discharge and the consequent decrease in the water table (Eamus et al., 2006).

The functioning of *Z. lotus* is impaired by deeper water tables, up to a threshold of 14 meters where such functioning stabilizes (Chapter II and III). Thus, individuals that have available water at depths of up to 14 meters will show higher transpiration and carbon assimilation rates than those that have to take up water at greater depths. Therefore, the lowering of the water table could be detrimental to the functioning of the species.

Changes in the precipitation regime could also affect nutrient uptake by *Z. lotus* (Querejeta et al., 2021; Chapter IV). Its dimorphic root system allows groundwater uptake by deep roots and nutrient absorption by shallow ones. Accordingly, decreasing rainfall and rising temperatures could reduce soil moisture, which is necessary for the plants to obtain nutrients available in the shallower layers through the decomposition processes of organic matter (Jobbagy and Jackson, 2000). These nutrients are essential for photosynthesis, so a decrease in their uptake would affect the species´s growth, reproduction, and CO_2 uptake, i.e., its ability to fix atmospheric carbon (Chapter I). In addition, since the decomposition of organic matter, and therefore the release of nutrients is highly dependent on the activation of soil microbiota by precipitation, a decrease in precipitation and an increase in its torrential nature under a climate change scenario would decrease soil quality and the nutrients available for *Z. lotus*.

An additional problem to the changes in precipitation patterns and seasonality in nutrient uptake is the decoupling of plant functioning from precipitation (Querejeta et al., 2021). For example, decreasing spring precipitation could reduce the mineralization of nutrients by soil microorganisms and, therefore, the uptake of these nutrients by *Z. lotus* at the beginning of its vegetative and reproductive cycle. All these may drive changes in GDEs functioning, even the mortality of *Z. lotus* plants that already suffer from physiological limitations, which could diminish the contributions of this GDE to people.

The scientific evidence provided in this PhD thesis can directly impact policies and management strategies that contribute to the conservation of the GDE dominated by *Z.*

lotus. However, this knowledge hardly permeates society, which might limit the success of these strategies for the conservation of GDEs. This limitation can be approached from the implementation of transdisciplinary working schemes integrated by researchers, managers, and social actors to promote the transfer of scientific, technical, and local knowledge about the GDE and its phreatophytic vegetation and to design collaborative strategies that foster its conservation (López-Rodríguez et al., 2020).

References

Arquero O, Barranco D, Benlloch M (2006) Potassium Starvation Increases Stomatal Conductance in Olive Trees. *HortScience* 41:433–436.

Austin AT, Yahdjian L, Stark JM, et al (2004) Water pulses and biogeochemical cycles in arid and semiarid ecosystems. *Oecologia,* 141:221–235.

de Bello F, Lavorel S, Díaz S, et al (2010) Towards an assessment of multiple ecosystem processes and services via functional traits. *Biodivers Conserv,* 19:2873–2893.

Butterfield BJ, Palmquist EC, Hultine KR (2021) Regional coordination between riparian dependence and atmospheric demand in willows (S*alix* L.) of western North America. *Divers Distrib,* 27:377–388.

Cernansky R (2017) The biodiversity revolution. *Nature,* 546, 22-24.

Chen J, Stark JM (2000) Plant species effects and carbon and nitrogen cycling in a sagebrush-crested wheatgrass soil. *Soil Biol Biochem,* 32:47–57.

Cleveland CC, Reed SC, Keller AB, et al (2014) Litter quality versus soil microbial community controls over decomposition: a quantitative analysis. *Oecologia,* 174:283–294.

Cortez J, Garnier E, Pérez-Harguindeguy N, et al (2007) Plant traits, litter quality and decomposition in a Mediterranean old-field succession. *Plant Soil,* 296:19–34

Dai A (2013) Increasing drought under global warming in observations and models. *Nature Clim Change,* 3, 52–58.

Daily GC (1997) *Nature's Services: Societal Dependence on Natural Ecosystems*. Island Press, Washington

Dawson TE, Mambelli S, Plamboeck AH, et al (2002) Stable Isotopes in Plant Ecology. *Annu Rev Ecol Syst,* 33:507–559.

De Deyn, G.B., Cornelissen, J.H.C. and Bardgett, R.D. (2008), Plant functional traits and soil carbon sequestration in contrasting biomes. *Ecol Lett,* 11: 516-531.

Delgado-Baquerizo M, Maestre FT, Gallardo A, et al (2013) Decoupling of soil nutrient cycles as a function of aridity in global drylands. *Nature,* 502:672–676.

Diaz S, Cabido M, Casanoves F (1998) Plant functional traits and environmental filters at a regional scale. *J Veg Sci* 9:113–122.

Eamus D, Froend R (2006) Groundwater-dependent ecosystems: the where, what and why of GDEs. *Aust J Bot* 54:91.

Eamus D, Froend R, Loomes R, et al (2006) A functional methodology for determining the groundwater regime needed to maintain the health of groundwater-dependent vegetation. *Aust J Bot,* 54:97.

Eamus D, Macinnis-Ng CMO, Hose GC, et al (2005) Ecosystem services: an ecophysiological examination. *Aust J Bot,* 53:1.

Feng X, Ackerly DD, Dawson TE, et al (2019) Beyond isohydricity: The role of environmental variability in determining plant drought responses. *Plant Cell Environ,* 42:1104–1111.

Fenner M (1998) The phenology of growth and reproduction in plants. *Perspect Plant Ecol Evol Syst,* 1:78–91.

Fisher JB, Badgley G, Blyth E (2012) Global nutrient limitation in terrestrial vegetation. *Glob Biogeoch Cycl,* 26: GB3007.

Fontaine S. and Barot S. (2005) Size and functional diversity of microbe populations control plant persistence and long-term soil carbon accumulation. *Ecol. Lett.,* 8, 1075–1087.

Froend RH, Drake PL (2006) Defining phreatophyte response to reduced water availability: preliminary investigations on the use of xylem cavitation vulnerability in Banksia woodland species. *Aust J Bot,* 54:173.

Giorgi F, Lionello P (2008) Climate change projections for the Mediterranean region. *Glob Planet Change* 63: 90–104

González E, González-Sanchis M, Comín FA, Muller E (2012) Hydrologic thresholds for riparian forest conservation in a regulated large Mediterranean river: Hydrologic thresholds for mediterranean riparian forest conservation. *River Res Applic,* 28:71–80.

Grime JP (1998) Benefits of plant diversity to ecosystems: immediate, filter and founder effects. *J Ecol,* 86:902–910.

Guiot J, Cramer W (2016) Climate change: The 2015 Paris Agreement thresholds and Mediterranean basin ecosystems. *Science,* 354: 4528–4532.

Guo JS, Hultine KR, Koch GW, et al (2020) Temporal shifts in iso/anisohydry revealed from daily observations of plant water potential in a dominant desert shrub. *New Phytol,* 225:713–726.

Hortal S, Lozano YM, Bastida F, et al (2017) Plant-plant competition outcomes are modulated by plant effects on the soil bacterial community. *Sci Rep,* 7:17756.

Hough M, Pavao-Zuckerman MA, Scott CA (2018) Connecting plant traits and social perceptions in riparian systems: Ecosystem services as indicators of thresholds in social-ecohydrological systems. *J Hydrol,* 566:860–871.

IPBES (2019): Summary for policymakers of the global assessment report on biodiversity and ecosystem services of the Intergovernmental Science-Policy Platform on Biodiversity and Ecosystem Service. *IPBES secretariat,* Bonn, Germany. 56pp.

Jackson RB, Sperry JS, Dawson TE (2000) Root water uptake and transport: using physiological processes in global predictions. *Trends Plant Sci,* 5:482–488.

Jobbágy EG, Jackson RB (2000) The vertical distribution of soil organic carbon and its relation to climate and vegetation. *Ecol Appl,* 10:423–436.

Kath J, Powell S, Reardon-Smith K, et al (2015) Groundwater salinization intensifies drought impacts in forests and reduces refuge capacity. *J Applied Ecol,* 52:1116–1125

Klein T (2014) The variability of stomatal sensitivity to leaf water potential across tree species indicates a continuum between isohydric and anisohydric behaviours. *Funct Ecol,* 28:1313–1320.

Kremen C (2005) Managing ecosystem services: what do we need to know about their ecology?: Ecology of ecosystem services. *Ecol Lett,* 8:468–479.

Lang P, Ahlborn J, Schäfer P, et al (2016) Growth and water use of Populus euphratica trees and stands with different water supply along the Tarim River, NW China. *For Ecol, Manag,* 380:139–148.

Lavorel S, Garnier E (2002) Predicting changes in community composition and ecosystem functioning from plant traits: revisiting the Holy Grail: Plant response and effect groups. *Funct Ecol,* 16:545–556.

Le Houérou, H. N. (2006) Agroforestry and silvopastoralism: The role of trees and shrubs (Trubs) in range rehabilitation and development. *Science et changements planétaires/Sécheresse* 17:343–348

Leigh A, Zwieniecki MA, Rockwell FE, et al (2011) Structural and hydraulic correlates of heterophylly in *Ginkgo biloba*. *New Phytol,* 189:459–470.

Linton MJ, Sperry JS, Williams DG (1998) Limits to water transport in *Juniperus osteosperma* and *Pinus edulis*: implications for drought tolerance and regulation of transpiration: Limits to water transport in Juniper and Pinyon. *Funct Ecol*, 12:906–911.

Liu B, Guan H, Zhao W, et al (2017) Groundwater facilitated water-use efficiency along a gradient of groundwater depth in arid northwestern China. *Agric For Meteorol* 233:235–241.

López-Ballesteros A, Serrano-Ortiz P, Sánchez-Cañete EP, et al (2016) Enhancement of the net CO_2 release of a semiarid grassland in SE Spain by rain pulses: Rain Pulses Enhance Net CO_2 Release. *J Geophys Res Biogeosci*, 121:52–66.

Lorenz K, Lal R (2005) The Depth Distribution of Soil Organic Carbon in Relation to Land Use and Management and the Potential of Carbon Sequestration in Subsoil Horizons. *Adv Agron*, 88: 35–66

Luck GW, Daily GC and Ehrlich PR (2003) Population diversity and ecosystem services. *Trends in Ecol Evol*, 18: 331-336.

Maestre FT, Salguero-Gómez R, Quero JL (2012) It is getting hotter in here: determining and projecting the impacts of global environmental change on drylands. *Phil Trans R Soc B*, 367:3062–3075.

Manzoni S, Vico G, Katul G, et al (2013) Hydraulic limits on maximum plant transpiration and the emergence of the safety–efficiency trade-off. *New Phytol*, 198:169–178.

Maraghni M, Gorai M, Neffati M The Influence of Water-Deficit Stress on Growth, Water Relations and Solute Accumulation in Wild Jujube (*Ziziphus lotus*). 10

Maraghni M, Gorai M, Neffati M, Van Labeke MC (2014) Differential responses to drought stress in leaves and roots of wild jujube, *Ziziphus lotus*. *Acta Physiol Plant*, 36:945–953.

Maraghni M, Gorai M, Steppe K, et al (2019) Coordinated changes in photosynthetic machinery performance and water relations of the xerophytic shrub Ziziphus lotus (L.) Lam. (Rhamnaceae) following soil drying. *Photosynt*, 57:113–120.

Markesteijn L, Poorter L (2009) Seedling root morphology and biomass allocation of 62 tropical tree species in relation to drought- and shadetolerance. *J Ecol*, 97:311–325.

Maseda PH, Fernandez RJ (2006) Stay wet or else: three ways in which plants can adjust hydraulically to their environment. *J Exp Bot*, 57: 3963–3977.

Millennium Ecosystem Assessment, 2005. Ecosystems and Human Well-being. Synthesis.Island Press, Washington D.C.

Moore PD (1992) A leaf for all seasons. *Nature* 360:110–111.

Moreno-Gutiérrez C, Dawson TE, Nicolás E, Querejeta JI (2012) Isotopes reveal contrasting water use strategies among coexisting plant species in a Mediterranean ecosystem. *New Phytol,* 196:489–496.

Mori A, Niinemets Ü (2010) Plant responses to heterogeneous environments: scaling from shoot modules and whole-plant functions to ecosystem processes. *Ecol Res,* 25:691–692.

Morillas L, Roales J, Portillo-Estrada M, Gallardo A (2017) Wetting-drying cycles influence on soil respiration in two Mediterranean ecosystems. *Eur J Soil Biol,* 82:10–16.

Murray BR, Hose GC, Eamus D, Licari D (2006) Valuation of groundwater-dependent ecosystems: a functional methodology incorporating ecosystem services. *Aust J Bot,* 54:221.

Naumburg E, Mata-Gonzalez R, Hunter RG, et al (2005) Phreatophytic Vegetation and Groundwater Fluctuations: A Review of Current Research and Application of Ecosystem Response Modeling with an Emphasis on Great Basin Vegetation. *Environ Manage,* 35:726–740.

Nippert JB, Holdo RM (2015) Challenging the maximum rooting depth paradigm in grasslands and savannas. *Funct Ecol,* 29:739–745.

Ochoa-Hueso R, Eldridge DJ, Delgado-Baquerizo M, et al (2018) Soil fungal abundance and plant functional traits drive fertile island formation in global drylands. *J Ecol,* 106:242–253.

O'Grady AP, Eamus D, Hutley LB (1999) Transpiration increases during the dry season: patterns of tree water use in eucalypt open-forests of northern Australia. *Tree Physiol,* 19:591–597.

Orellana F, Verma P, Loheide SP, Daly E (2012) Monitoring and modeling water-vegetation interactions in groundwater-dependent ecosystems: groundwater-dependent ecosystems. *Rev Geophys,* 50.

Peguero-Pina JJ, Vilagrosa A, Alonso-Forn D, et al (2020) Living in Drylands: Functional Adaptations of Trees and Shrubs to Cope with High Temperatures and Water Scarcity. *Forests,* 11:1028.

Peñuelas J, Sardans J, Filella I, et al (2018) Assessment of the impacts of climate change on Mediterranean terrestrial ecosystems based on data from field experiments and long-term monitored field gradients in Catalonia. *Environ Exp Bot,* 152:49–59.

Pérez-Harguindeguy N, Díaz S, Garnier E, et al (2013) New handbook for standardised measurement of plant functional traits worldwide. *Aust J Bot,* 61:167.

Poulter B, Frank D, Ciais P, et al (2014) Contribution of semi-arid ecosystems to interannual variability of the global carbon cycle. *Nature,* 509:600–603.

Prieto I, Querejeta JI, Segrestin J, et al (2018) Leaf carbon and oxygen isotopes are coordinated with the leaf economics spectrum in Mediterranean rangeland species. *Funct Ecol,* 32:612–625.

Querejeta JI, Estrada-Medina H, Allen MF, Jimenez-Osornio JJ (2007) Water source partitioning among trees growing on shallow karst soils in a seasonally dry tropical climate. *Oecologia,* 152: 26–36.

Querejeta JI, Ren W, Prieto I (2021) Vertical decoupling of soil nutrients and water under climate warming reduces plant cumulative nutrient uptake, water-use efficiency and productivity. *New Phytol,* 230:1378–1393.

Rey PJ, Cancio I, Manzaneda AJ, et al (2018) Regeneration of a keystone semiarid shrub over its range in Spain: habitat degradation overrides the positive effects of plant–animal mutualisms. *Plant Biol,* 20:1083-1092.

Rey A, Carrascal LM, Báez CG-G, et al (2021) Impact of climate and land degradation on soil carbon fluxes in dry semiarid grasslands in SE Spain. *Plant Soil,* 461:323–339.

Reyers B, Biggs R, Cumming GS, et al (2013) Getting the measure of ecosystem services: a social–ecological approach. *Front Ecol Environ,* 11, 268–273.

Reynolds James F., Smith D. Mark Stafford, Lambin Eric F., et al (2007) Global Desertification: Building a Science for Dryland Development. *Science,* 316:847–851.

Reynolds JF, Virginia RA, Kemp PR, et al (1999) Impact of drought on desert shrubs: effects of seasonality and degree of resource island development. *Ecol Monog,* 69:69–106.

de la Riva EG, Prieto I, Villar R (2019) The leaf economic spectrum drives leaf litter decomposition in Mediterranean forests. *Plant Soil,* 435:353–366.

Ryel RJ, Leffler AJ, Ivans C, et al (2010) Functional differences in water-use patterns of contrasting life forms in great basin Steppelands. *Vadose Zone J,* 9: 548–560.

Sardans J, Peñuelas J (2015) Potassium stoichiometry and global change. Global Ecology and *Biogeography,* 24: 261-275.

Sardans J, Peñuelas J, Prieto P, Estiarte M (2008) Drought and warming induced changes in P and K concentration and accumulation in plant biomass and soil in a Mediterranean shrubland. *Plant Soil,* 306:261–271.

Schlesinger WH, Bernhardt ES (2020) Biogeochemistry (Fourth Edition). Academic Press.

Sponseller RA (2007) Precipitation pulses and soil CO $_2$ flux in a Sonoran Desert ecosystem. *Glob Change Biol*, 13:426–436.

Tyree MT, Ewers FW (1991) The hydraulic architecture of trees and other woody plants. *New Phytol*, 119:345–360.

Valencia E, Maestre FT, Bagousse-Pinguet YLe, et al (2015) Functional diversity enhances the resistance of ecosystem multifunctionality to aridity in Mediterranean drylands. *New Phytol*, 206, 660–671.

Vargas R, Sánchez-Cañete P. E, Serrano-Ortiz P, et al (2018) Hot-Moments of Soil CO2 Efflux in a Water-Limited Grassland. *Soil Syst*, 2:47.

Vitousek PM, Mooney HA, Lubchenco J, Melillo JM (1997) Human domination of Earth's ecosystems. *Science*, 277, 494–499.

Voltas J, Lucabaugh D, Chambel MR, Ferrio JP (2015) Intraspecific variation in the use of water sources by the circum-Mediterranean conifer Pinus halepensis. *New Phytol*, 208: 1031–1041.

Whitford WG, Duval BD (2002) *Ecology of Desert Systems* (Second Edition). Academic Press, pp 343.

Zeppel M, Eamus D (2008) Coordination of leaf area, sapwood area and canopy conductance leads to species convergence of tree water use in a remnant evergreen woodland. *Aust J Bot*, 56:97.

Zeppel MJB, Murray BR, Barton C, Eamus D (2004) Seasonal responses of xylem sap velocity to VPD and solar radiation during drought in a stand of native trees in temperate Australia. *Funct Plant Biol*, 31, 461–470.

Zolfaghar S, Villalobos-Vega R, Cleverly J, et al (2014) The influence of depth-to-groundwater on structure and productivity of Eucalyptus woodlands. *Aust J Bot*, 62:428.

Zolfaghar S, Villalobos-Vega R, Zeppel M, et al (2017) Transpiration of Eucalyptus woodlands across a natural gradient of depth-to-groundwater. *Tree Physiol*, 37:961–975.

5. GENERAL CONCLUSIONS

Groundwater-dependent ecosystems and their phreatophytic vegetation are highly valuable in drylands because of its access to groundwater sources. However, these ecosystems, their structure and function, and the contributions they provide to people are at risk. Climate change effects (temperature rises and precipitation reductions) and anthropogenic activities such as groundwater drawdown and contamination will alter the level and quality of groundwater reservoirs, threatening the functioning of the phreatophytic vegetation that depends on these water sources. Additionally, not only do these drivers alter groundwater characteristics, but also land-use changes in favor of agriculture or urbanization, diminishing aquifer recharge and increasing ecosystem fragmentation.

Taking the phreatophytic shrub *Ziziphus lotus* and the GDE it constitute as a case study, this PhD thesis provides: (1) insights on the processes related to water, carbon, and nutrient cycles in terrestrial GDEs of drylands, and (2) scientific evidence to managers and policymakers who have to deal with the preservation of these ecosystems and the sustainable use of groundwater on which they depend. The main conclusions of this thesis are:

1 Trait-based analysis allowed us to gain insight into the functioning of *Z. lotus* and their strategies to persist in drylands. I identified the species growth pattern, based on the development of modular units that produced morpho-functionally distinct leaves (i.e., heterophylly). Both modular differentiation and heterophylly might promote resource investment for particular functions throughout the growing season, either for growth or for reproduction.

2 Morpho-functional and physiological traits such as rooting depth, hydraulic architecture and leaf area can explain spatial and temporal variations in plant water-use patterns. I demonstrated that *Z. lotus* is a facultative phreatophyte that partially uses groundwater. As depth-to-groundwater (DTGW) increases, plants found difficulties to uptake groundwater, hence diminished aboveground biomass investment (i.e., leaf area) to reduce hydraulic demand, but increased sapwood area to enhance water supply. The reduction of soil moisture during the growing season might increase *Z. lotus* dependence

on groundwater and diminish plant's ability to obtain nutrients from the topsoil layers. A poor nutritional status might have contributed to lower photosynthetic rates in summer.

3 The decrease of soil water availability, together with higher atmospheric evaporative demands foster more negative water potential to *Z. lotus* water uptake. This behavior indicates an extreme anisohydric stomatal regulation of this phreatophyte altough with spatiotemporal variations in response to water availability. *Z. lotus* plants showed extreme anisohydry during the wet spring and partial isohydry during the dry hot summer, indicating some stomatal regulation under water stress but not stomatal closure.

4 Assessing the expression of multiple traits contributed to predicting patterns of change in the GDE and thresholds in *Z. lotus* response to groundwater variability across seasons. I identified an ecophysiological threshold at 12-14 m of DTGW, which differentiates plants according to their water relations. Plants accessing deep water tables (DTGW > 14m) had more difficulties obtaining groundwater, which was also saltier, and showed lower anisohydric stomatal regulation and gas exchange rates than plants at shallow sites (DTGW < 12m). Moreover, Mediterranean summer conditions, which increased water stress, promoted water loss more intensively at shallow water tables.

5 Soil moisture was essential for stimulating soil biological activity in this GDE. Particularly, soil respiration and mineralization processes were coupled to precipitation pulses typical of drylands. However, this soil biological activity was decoupled to the functioning of *Z. lotus*, since the activity of this species depends on groundwater availability. Despite this fact, soil activity ultimately depended on *Z. lotus* (and to a lesser extent, on its companion species) for litter inputs and the enhancement of soil quality.

6 The amount of plant litter that *Z. lotus* provides, and its mineralization rate by soil microbial community promoted the accumulation of organic matter and nutrients under large canopies, hence the development of fertile islands. Although precipitation and temperature stimulates soil activity, increasing the decomposition of the available carbon that accumulated under canopies, landscape patches with this shrub largely contributed to the formation of fertile islands by enhancing soil biological activity, soil quality and nutrient content.

7 Groundwater-dependent ecosystems ensure, or even increase the supply of ecosystem services in drylands. Species like *Z. lotus* contribute to enhancing primary productivity with the use of groundwater and the anisohydric behavior. The primary productivity, together with the efficient feedback between plant and soil biota for carbon and nutrient cycling, might foster carbon sequestration in this dryland GDE. Whereas the deep-root system of *Z. lotus* can contribute to the vertical allocation of C in the soil, its significant biomass and litter quality enhance carbon and nutrient cycling. Moreover, it contributes to evapotranspiration, erosion prevention or accumulation of standing biomass, which are the foundations of climate and water regulation, soil stabilization and fodder provision.

8 Expected changes in temperature and precipitation regimes will likely reduce the recharge of groundwater reservoirs, the soil moisture and nutrient mineralization, and the productivity of dryland ecosystems. All these can trigger changes in the functioning of GDEs, even the mortality of plants that already suffer from physiological limitations to obtain water at great depths, which could diminish the contributions of this GDE to people.

SCIENTIFIC PUBLICATIONS DERIVED FROM THIS THESIS

Torres-García MT, Salinas-Bonillo MJ, Cleverly JR, et al (2021a) A multiple-trait analysis of ecohydrological acclimatisation in a dryland phreatophytic shrub. *Oecologia*, 196, 1179–1193.

Torres-García MT, Salinas-Bonillo MJ, Gázquez-Sánchez F, et al (2021b) Squandering water in drylands: the water-use strategy of the phreatophyte *Ziziphus lotus* in a groundwater-dependent ecosystem. *Ame J Bot*, 108, 236–248.

Torres-García MT, Salinas-Bonillo MJ, Pacheco-Romero M, Cabello J (2021c) Modular growth and functional heterophylly of the phreatophyte *Ziziphus lotus*. A trait-based study. *Plant Species Biol*, 1442-1984.12343.

Torres-García MT, Oyonarte C, Cabello J, Guirado E, Rodríguez-Lozano B, Salinas-Bonillo MJ. Decoupled soil biological activity and vegetation dynamics in a groundwater-dependent ecosystem in drylands. *Sci tot environ* (under review).

OTHER PUBLICATIONS

López-Rodríguez MD, Salinas-Bonillo MJ, Torres MT, et al (2020) Impulsando estrategias colectivas ciencia-gestión-sociedad para conservar el hábitat de *Ziziphus lotus* (Hábitat Prioritario 5220). *Revista Ecosistemas* 29(1):1890.

Cabello J, López-Rodríguez MD, Pacheco M, Torres MT, Reyes A (2019) Valores y argumentos para la conservación de la diversidad vegetal de Sierra Nevada. En: Peñas, J. y Lorite, J. (eds.), *Biología de la Conservación de plantas en Sierra Nevada. Principios y retos para su preservación*. Editorial Universidad de Granada, Granada, pp. 345-363. ISBN 9788433865120.

Pacheco-Romero M, Vallejos M, Paruelo J, Alcaraz-Segura D, Torres-García MT, Salinas-Bonillo MJ, Cabello J. A data-driven methodological routine to identify key indicators for social-ecological system archetype mapping. *Environ Res Lett* (under review)

Groundwater-dependent ecosystems (GDEs) and their phreatophytic vegetation are highly valuable in drylands because of its access to groundwater sources. However, these ecosystems, their structure and function, and the contributions they provide to people are at risk. This PhD thesis provides knowledge of the functioning of a terrestrial GDE of Mediterranean Basin drylands dominated by *Ziziphus lotus* shrubs to: (1) understand its contribution to the water, carbon, and nutrient cycles, and (2) provide scientific evidence to managers and policymakers who must deal with the sustainable management of groundwater and ensure GDEs contributions to people in the face of global change.

CAESCG

CENTRO ANDALUZ PARA LA EVALUACIÓN
Y SEGUIMIENTO DEL CAMBIO GLOBAL